
Diatom analysis as a tool for reconstructing limnological
features and its application to the Late Quaternary
sediments from Lake Palaeo-Makgadikgadi (northern
Botswana) and Lake Kushu (northern Japan)

DISSERTATION

Submitted to the
Department of Earth Sciences of the
FREIE UNIVERSITÄT BERLIN

In fulfillment of the requirements for the
Degree of
Doctor rerum naturalium
(Dr. rer. nat.)

by

M. Sc.
Mareike Schmidt

Berlin, June 2018

1st Reviewer: **Prof. Dr. Pavel E. Tarasov**
Freie Universität Berlin

2nd Reviewer: **Prof. Dr. Frank Riedel**
Freie Universität Berlin

Date of Disputation: 17 July 2018

Abstract

Diatoms are unicellular, eukaryotic microalgae that form two valves made of silica. After death, these frustules accumulate at the bottom of lake basins. The persistent diatom valves mirror valuable information about water parameters through the lifetime of the organism. The high diversity and the specific ecological requirements allow diatoms to grow in almost all kind of waters and the assemblages accurately identify the limnology. That makes diatoms excellent bioindicators for palaeolimnological reconstructions. In this doctoral thesis, diatoms are used as a tool to study two different lake systems, in different time periods and different hemispheres.

The first object is an ancient mega-lake phase of the Lake Palaeo-Makgadikgadi in the Makgadikgadi-Okavango-Zambezi Basin (MOZB) in northern Botswana. The MOZB is a structural depression consisting of five sub-basins, which feature palaeo-lacustrine structures indicative for past humid conditions that resulted in huge lakes (*c.* 37,000 km²) in the nowadays semi-arid Middle Kalahari. Environmental and climatic implications and fluctuations of the Late Quaternary highstands are controversial and poorly constrained. In this work, a 30 cm thick lacustrine deposit close to the western palaeo-shoreline of the Makgadikgadi Basin was analyzed to obtain a high-resolution diatom record to infer first palaeolimnological parameters such as salinity, pH and trophic level. 60 diatom samples (0.5 cm steps) and 30 samples (each 1 cm) for oxygen isotope analysis ($\delta^{18}\text{O}$) were analyzed for a high-resolution reconstruction of the Late Pleistocene lake phase. Optically stimulated luminescence (OSL) dating suggests that the highstand existed during Marine Isotope Stage (MIS) 5d-b (*c.* 100 kyr BP). The diatom assemblages and $\delta^{18}\text{O}$ values indicate a shallow oligohaline lake with alkaline conditions and subsequent changes in the hydrologic balance (evaporation / precipitation) that implies variability between warm-wet and cold-arid climate. For the first time, palaeolimnological features of a Lake Palaeo-Makgadikgadi lake phase have been identified. The existence of such a large lake during MIS 5 provides evidence that at least one short-term anomaly of higher humidity occurred during a period that was long thought to be very dry in southern Africa. These findings contribute to the hypothesis that Late Pleistocene hunter-gatherers (Khoisan) have lived permanently in the arid to semi-arid Middle Kalahari at least since MIS 5.

In the second part of the thesis, the focus lies on the coastal Lake Kushu on the small Rebun Island (82 km²) in northern Japan. Rebun Island is a key research area of the interdisciplinary Baikal-Hokkaido Archaeology Project (BHAP) to understand population changes and pathways of Holocene hunter-gatherers (Okhotsk, Jomon) from East Siberia towards the Japanese Archipelago and focusses on human-environmental interactions. 43 archaeological sites show the occupation of Rebun Island since the last 6000 years. Records of past climate variabilities and environmental changes in this region are sparse. The need for a nearby archive resulted in the recovery of the 19.5 m sediment core from Lake Kushu, the only freshwater lake on Rebun Island. The obtained sediments covering the last *c.* 16,600 years (AMS dated) provide the chance to reconstruct climate

and environmental changes since the evolution of Lake Kushu in the Late Glacial and to detect human-environmental interactions, when first Holocene hunter-gatherers occupied the island. It also helps to decode the requirements for incipient habitability of Rebus Island.

In a first step, it was tested whether the RK12 sediment core represents a continuous palaeoenvironmental archive suitable for multi-proxy analyses. Therefore, 10 diatom and 20 geochemical samples were analyzed. Radiocarbon dating was obtained from a set of 57 bulk samples. In addition, a modern set of 15 diatom and water samples from Lake Kushu and the surrounding area were used to characterize the lake and to develop an overview about the salinity, pH and trophic of the modern situation. This knowledge was used to interpret the fossil diatom assemblages.

In a second step, a high-resolution analysis was performed with a set of 210 diatom and pollen and non-pollen palynomorph analysis (each 8 cm) and p-ED-XRF analysis (each 1 cm). Micro-facies analysis of a 90 cm section (848-938 cm) provides in-situ insights into 400 years of Mid-Holocene lake deposits.

The successfully tested RK12 sediments core represents a good archive covering the last 16,600 years. The multi-proxy approach combined of diatom, aquatic plant, p-ED-XRF and micro-facies analyses and delimits three main lake phases during the Late Glacial / Holocene with the help of the age model. An early marshy phase (16.6-9.3 cal. kyr BP) reflects a riverine depositional environment shown by sandy clays with pebbles and highest Ti-Si contents in the sediments. A lagoon phase (9.3-5.9 cal. kyr BP) represents first marine influence (Chaetocerotaceae, dinoflagellate cysts, highest Ca-Cl content) onto the current lake basin in the course of the Holocene relative sea level rise. A freshwater lake phase (5.9-0.3 cal. kyr BP) is characterized by highest percentages of freshwater Aulacoseiraceae valves and green algae implying a meso- to eutrophic, alkaline lake. Eutrophication is suggested by the modern diatom assemblages that represent a hypereutrophic dimictic lake that possibly reflects a mature lake phase. The annual- to seasonal-scale micro-facies analysis improves our understanding of the lake that is characterized by a sensitive interplay of marine and terrestrial impact factors during the Mid-Holocene and short-term climatic variations (e.g. 5.5 kyr climate deterioration event). The existence of the freshwater lake since c. 5.9 cal. kyr BP possibly plays a major role for permanent human occupation on Rebus Island because it serves potable water.

The results show that the diatom content of both lakes differs in diversity and concentration. Nevertheless, the limnology of both lakes has been successfully reconstructed. This shows that diatom analysis is a valuable and successful method, which can be applied to differently sediments and archives. Our new insights into Late Quaternary palaeolimnology contribute to the understanding of the habitability for local hunter-gatherers. The results point out the need for further palaeoenvironmental records to improve the spatiotemporal understanding of the complex systems and to increase the knowledge about human-environmental interactions in both regions.

Kurzfassung

Diatomeen sind einzellige, eukaryotische Mikroalgen, die zwei Schalen aus Siliziumdioxid ausbilden. Nach dem Absterben akkumulieren die Frusteln auf dem Seeboden. Die witterungsbeständigen Schalen enthalten wertvolle Informationen der Wasserparameter, die zu Lebzeiten der Organismen vorherrschten. Die hohe Diversität und die spezifischen ökologischen Anforderungen erlauben es ihnen in sämtlichen Gewässern zu wachsen und die Diatomeengesellschaftung kann die Limnologie detailliert rekonstruieren. Diese Eigenschaften führten dazu, dass sich die Diatomeen zu exzellenten Bioindikatoren für paläolimnologische Rekonstruktionen etablierten. In der vorliegenden Doktorarbeit werden Diatomeen als Werkzeug benutzt, um zwei verschiedene Seesysteme zu verschiedenen Zeiten auf verschiedenen Hemisphären zu studieren.

Das erste Forschungsobjekt ist eine ehemalige Seephase des Megasees Paläo-Makgadikgadi im Makgadikgadi-Okavango-Sambesi Becken (MOZB) im Norden Botsuanas. Das MOZB ist eine geotektonische Senke bestehend aus fünf Teilbecken, welche paläolakustrine Strukturen aufweisen, die auf ehemals feuchtere Bedingungen in der heutzutage (semi-)ariden Mittleren Kalahari deuten. Diese vergangenen humiden Perioden ließen riesige Seen entstehen (ca. 37.000 km²). Umwelt- und klimatisch bedingte Veränderungen und Schwankungen der spätquartären Hochstände sind kontrovers diskutiert und noch nicht vollständig verstanden. In dieser Arbeit wird ein 30 cm mächtiges lakustrines Schichtpaket von der westlichen ehemaligen Strandlinie des Makgadikgadi Beckens analysiert, um ein hochauflösendes Archiv zu erhalten, welches erste paläolimnologische Parameter wie Salinität, pH und Trophiestufe einer ehemaligen Seephase identifiziert.

60 Proben zur Diatomeenanalyse (in 0,5 cm Abständen) und 30 Proben (in 1 cm Abständen) zur Analyse der Sauerstoffisotopenverhältnisse ($\delta^{18}\text{O}$) wurden für die hochauflösende Rekonstruktion der spätpleistozänen Seephase ausgewertet. Optisch stimulierte Lumineszenz (OSL) Datierungen zeigen, dass die Seephase während des marinen Isotopenstadiums (MIS) 5d-b (ca. 100,000 tausend Jahre vor heute) existierte. Die Diatomeengesellschaftungen und die $\delta^{18}\text{O}$ Werte zeigen einen flachen, oligohalinen See mit alkalinen Bedingungen an, der subsequeute Veränderungen in der Wasserbilanz (Evaporation / Niederschlag) aufweist und einen Übergang von warm-feuchten zu kalt-trockenen Klimaten andeutet. Zum ersten Mal konnten so paläolimnologische Merkmale einer Seephase des Megasees Paläo-Makgadikgadi bewiesen werden. Die Existenz eines solch großen Sees während des MIS 5 liefert den Beweis, dass es zumindest eine kurzzeitige Klimaanomalie gab, die zu einer höheren Feuchtigkeit in der Region führte, obwohl davon ausgegangen wurde, dass während des MIS 5 im südlichen Afrika eine große Dürreperiode herrschte. Diese Erkenntnisse tragen zur Debatte bei, ob die spätpleistozänen Jäger und Sammler (Khoisan) durchgehend in der ariden bis semi-ariden Mittleren Kalahari seit dem MIS 5 lebten.

Im zweiten Teil der Arbeit lag der Fokus auf dem küstennahen Kushu-See auf der kleinen Insel Rebun (82 km²) im Norden Japans. Rebun nimmt eine Schlüsselrolle für das interdisziplinäre “Baikal-Hokkaido Archaeology Project” (BHAP) ein, welches die Besiedlungsgeschichte und die Wanderrouten der holozänen Jäger und Sammler (Okhotsk, Jomon) von Ostsibirien bis zum japanischen Archipel rekonstruieren möchte und sich auf die Interaktionen von Mensch und Umwelt fokussiert. 43 archäologische Fundstätten deuten eine Besiedlung Rebuns seit etwa 6000 Jahren an. Daten zur Rekonstruktion von klimatischen Schwankungen und Umweltveränderungen sind aus dieser Region wenig bekannt. Die Notwendigkeit eines nahegelegenen Archivs führte zur Bohrung des 19,5 m langen Sedimentkerns auf dem Kushu-See, dem einzigen Süßwasserkörper auf der Insel Rebun. Die gewonnenen Sedimente decken die letzten 16,600 Jahre (AMS datiert) ab und bieten die Möglichkeit klimatische Schwankungen und Umweltveränderungen seit dem Entstehen des Kushu-Sees im Spätglazial zu rekonstruieren und die Wechselbeziehung zwischen Mensch und Umwelt seit der Besiedlung durch holozäne Jäger und Sammler in dieser Region zu erfassen. Die notwendigen Bedingungen für eine Bewohnbarkeit von Rebun Island sollen so entschlüsselt werden.

Im ersten Schritt wurde getestet, ob der Sedimentkern RK12 für ein kontinuierliches Paläoumweltarchiv geeignet ist und für multi-proxy Analysen möglich sind. Daher wurden zunächst 10 Diatomeen- und 20 geochemische Proben analysiert. Radiokarbondatierungen wurden anhand von 57 Mischproben durchgeführt. Zusätzlich konnten 15 Diatomeenproben aus den rezenten Seesedimenten sowie von Wasserproben gewonnen werden, um den See limnologisch zu klassifizieren (Salinität, pH-Wert, Trophiestufe) und einen Überblick über die heutige Situation zu erhalten. Dies wurde für die Interpretation der fossilen Vergesellschaftungen genutzt.

Im zweiten Schritt wurde ein hochauflösender Datensatz mit 210 Diatomeen- und Pollenproben (alle 8 cm) sowie p-ED-XRF-Elementanalysen (je 1 cm) ausgewertet. Mikrofaziesanalysen eines 90 cm langen Abschnitts (848-938 cm) bieten in-situ Einblicke in zirka 400 Jahre mittelholozäner Seeablagerungen.

Der erfolgreich getestete Sedimentkern RK12 hält ein gutes Archiv über die letzten 16,600 Jahre bereit. Der einzigartige multi-proxy Ansatz kombiniert aus Diatomeen-, Pollen-, p-ED-XRF- und Mikrofaziesanalysen zusammen mit dem präzisen Altersmodell grenzen drei Seephasen seit dem Spätglazial ab. Die Sumpfhase (16.6-9.3 kal. tausend Jahre vor heute) deutet anhand der sandigen Tone mit eingeschalteten Kieseln und erhöhten Titan und Silizium Gehalten in den Sedimenten auf fluviatil beeinflusste Ablagerungsbedingungen hin. Die Lagunphase (9.3-5.9 kal. tausend Jahre vor heute) spiegelt erste marine Einflüsse (Chaetocerotaceae, Dinoflagellat-Zysten, höchste gemessene Ca-Cl Werte) nach dem holozänen Meeresspiegelanstieg wider. Die Süßwasserphase (5.9-0.3 kal. tausend Jahre vor heute) ist charakterisiert durch den höchsten prozentualen Anteil der Süßwasserdiatomeen Aulacoseiraceae sowie Grünalgen, die einen meso- bis eutrophen, alkalinen See repräsentieren. Die rezenten Diatomeenvergesellschaftungen

reflektieren einen hypereutrophen dimiktischen See im Endstadium gekennzeichnet durch Eutrophierung und Verflachung (hoher Sedimenteintrag). Die jährlichen bis saisonal aufgelösten Mirofaziesanalysen tragen zu einem besseren Verständnis bezüglich der Umwelteinflüsse während des Mittelholozäns bei. Kurzzeitige marine sowie terrestrische Events prägen die Seegeschichte und die Diatomeen spiegeln klimatische Schwankungen wider (z.B. die Klimaverschlechterung vor 5,500 Jahren). Der seit ca. 5900 Jahren vor heute existierende Süßwassersee fungierte womöglich als Trinkwasserquelle für Jäger und Sammler. Dies stellt eine wichtige Voraussetzung für eine dauerhafte Besiedlung der auf der Insel Rebus dar.

Die Ergebnisse zeigen, dass sich die Diatomeen aus den Sedimenten beider Seen sowohl in der Diversität als auch in der Konzentration stark unterschieden. Dennoch ist es gelungen, die jeweilige Seegeschichte erfolgreich zu rekonstruieren. Dies zeigt, dass die Diatomeenanalyse als eine wertvolle und erfolgreiche Methode auf unterschiedliche Sedimente und Archive angewandt werden kann. Es konnten neue Einblicke in die spätquartäre Paläolimnologie beider Seesysteme gewährt werden, die zum Verständnis über die Bewohnbarkeit der Regionen für lokale Jäger und Sammler beitragen. Weitere Paläoumweltrekonstruktionen zur Verbesserung des raumzeitlichen Verständnisses der komplexen Systeme werden benötigt, um auch das Wissen der Mensch-Umwelt-Wechselbeziehungen zu erweitern.

Acknowledgements

I would like to express my gratitude to several people who supported me to write this dissertation.

First of all, my very special thanks go to my supervisor Prof. Dr. Pavel E. Tarasov (FU Berlin) who gave me the opportunity to prepare the thesis. He constantly supported and helped me over the years. I appreciated his constructive criticism to improve my skills, his encouragement and his patience.

I would like to acknowledge my second reviewer Prof. Dr. Frank Riedel (FU Berlin) for his endless support, encouragement, the constructive discussions and helpful advices. It has been a pleasure to work and to travel with him.

I wish to thank the project director of the Baikal-Hokkaido Archaeology Project (BHAP), Prof. Dr. Andrzej W. Weber (University of Alberta) who provided me a three-year PhD stipend (University of Alberta, 0424634401), the field trip to Rebun Island (Japan) and the conference participation in Lanzhou (China). Without the generous financial support of the BHAP the work would not have been possible. I acknowledge Prof. Dr. Hirofumi Kato (Hokkaido University) and the Japanese field team for invitation and company during Lake Kushu field trip.

PD Dr. Annette Kossler (FU Berlin) introduced me to the diatom analysis, and supported me whenever it was needed. Thanks for the chat, laughs and the great field trip to Japan.

Many thanks go to Dr. Christian Leipe (FU Berlin) for reading carefully and improving the thesis, for many talks, his helpful support, and the great field trip to Rebun Island (Japan).

I appreciate the Kalahari (Botswana) field trip assistance of Prof. Dr. Elisha Shemang (BIUST), Franziska Slotta (FU Berlin), Linda Taft (Universität Bonn), Michael Taft (Abenden), Karl Uwe Heußner and Alexander Janus (both Deutsches Archäologisches Institut).

It was always a pleasure to work with Jan Evers (FU Berlin) who helped me with technical issues, Maike Glos and Marc Barlage (both FU Berlin) who supported me in the laboratory. Many thanks for all the coffee and lunch breaks, conversations and sports!

I would like to acknowledge Philipp Hoelzmann (FU Berlin) for his help and support and Frank Kutz (FU Berlin) for his assistance during geochemical analyses.

I thank Andrea Hiob (BHAP) for organizing the paperwork and for her easy-going mentality and for the monthly BHAP newsletter.

Many thanks go to all the other friends and colleagues of the institute, especially my (next door-) roommates Carolina Müller, Caroline Seidig, Gregor Radtke, Manja Hethke, Stefanie Müller for their company, their help, the chats, laughs and parties.

Finally and most important, I would like to thank my family, my parents who allowed me to follow my interests and supported me at all points, Sven for his stunning optimism, endless happiness, encouragement and unlimited love and our son Finnley who suddenly appeared to my life and brought along so much cuteness, happiness and love!

Table of contents

Abstract	i
Kurzfassung	iii
Acknowledgements	vii
List of Figures	xii
List of Tables	xiv
1. Introduction	1
1.1 Preface	1
1.2 Diatoms as bioindicators in palaeolimnological research	2
1.3 Scientific background	3
1.3.1 Regional setting of Lake Palaeo-Makgadikgadi in southern Africa	3
1.3.2 Palaeo-lacustrine approach in the Middle Kalahari	5
1.3.3 Regional setting of Lake Kushu in Northern Japan	7
1.3.4 Archaeological approach in the Hokkaido region	8
1.4 Aims of the thesis	9
1.5 Material and methods	11
1.5.1 Fieldwork	11
1.5.2 Diatom analysis	11
1.5.3 OSL and radiocarbon dating	12
1.5.4 Isotope analyses from diatom silica and surface water samples	13
1.5.5 Pollen and non-pollen palynomorphs (NPP) analysis	14
1.5.6 Micro-facies analysis	14
1.5.7 XRF analyses	15
1.6 Overview of the integrated manuscripts	17
1.7 Contribution to the individual manuscripts	18
2. Manuscript I - Palaeolimnological features of a mega lake phase in the Makgadikgadi Basin during MIS 5 inferred from diatoms	19
2.1 Abstract	19
2.2 Introduction	20
2.3 Study site	24
2.4 Materials and methods	25
2.4.1 Sediment samples	25
2.4.2 OSL dating	25
2.4.3 Diatom assemblages	26
2.4.4 Diatom oxygen isotope analysis	27
2.5 Results	27
2.5.1 OSL dating	27

2.5.2 Diatom assemblages and $\delta^{18}\text{O}_{\text{diatom}}$	28
2.6 Discussion.....	29
2.6.1 Dating.....	29
2.6.2 Diatom assemblages and $\delta^{18}\text{O}_{\text{diatom}}$	31
2.7 Conclusions.....	37
2.8 Acknowledgements.....	38
3. Manuscript II - Palaeobotanical records from Rebun I. and their potential for improving the chronological control & understanding human environmental interactions.....	39
3.1 Abstract.....	39
3.2 Introduction.....	40
3.3 Study area.....	42
3.3.1 Site and regional settings.....	42
3.3.2 Climate.....	43
3.3.3 Vegetation.....	43
3.3.4 Archaeology.....	44
3.4 Data and methods.....	46
3.4.1 Lake Kushu core RK12.....	46
3.4.2 The Hamanaka 2 archaeological site.....	47
3.5 Results.....	48
3.5.1 RK12 core chronology.....	48
3.5.2 RK12 coarse-resolution pollen record.....	48
3.5.3 Diatom analysis.....	50
3.5.4 Plant macrofossil analysis.....	54
3.6 Interpretation and discussion.....	55
3.7 Conclusion.....	60
3.8 Acknowledgements.....	61
3.8.1 Funding.....	61
4. Manuscript III - Diatoms from Lake Kushu: A pilot study to test the potential of a late Quaternary palaeoenvironmental archive from Rebun Island.....	63
4.1 Abstract.....	63
4.2 Introduction.....	64
4.3 Study area.....	66
4.3.1 Environments.....	66
4.3.2 Hydrology.....	67
4.4 Material and methods.....	69
4.4.1 Modern diatom samples.....	69
4.4.2 Water chemistry analysis.....	69

Table of contents

4.4.3 Fossil samples from Lake Kushu sediment: Choice and chronology.....	71
4.4.4 Diatom analysis	72
4.4.5 Geochemical analyses of core sediments	74
4.4.5.1 X-Ray fluorescence analysis (XRF).....	74
4.4.5.2 ICP-OES analysis.....	74
4.5 Results	75
4.5.1 Modern diatom assemblages.....	75
4.5.2 Water analysis.....	77
4.5.3 Fossil diatom assemblages.....	78
4.5.4 Geochemical (P-ED-XRF and ICP-OES) analysis of the core sediment	80
4.6 Interpretation and discussion	82
4.6.1 Modern lake basin.....	82
4.6.2 Comparison to Kushu core diatom assemblages	86
4.6.3 Correlation to past climate and sea level changes	87
4.6.4 Marshy phase 16.6–10 cal. kyr BP	88
4.6.5 Brackish water lagoon phase 10–6.6 cal. kyr BP	88
4.6.6 Freshwater lake phase since 6.6 cal. kyr BP.....	89
4.7 Conclusions	90
4.8 Acknowledgements.....	91
5. Manuscript IV - Multi-proxy palaeoenvironmental record of the last 16,600 years derived from coastal Lake Kushu.....	92
5.1 Abstract	92
5.2 Introduction.....	93
5.3 Regional settings	94
5.4 Material and methods.....	95
5.4.1 Core RK12 and chronology	95
5.4.2 Diatom analysis	96
5.4.3 Analysis of pollen and non-pollen palynomorphs (NPP).....	96
5.4.4 Semi-continuous X-Ray Fluorescence (XRF) analysis	97
5.4.5 Micro-facies analysis	98
5.5 Results	98
5.5.1 Diatoms.....	98
5.5.1.1 The RK12 core (1932-50 cm)	98
5.5.1.2 Detailed analysis of the section 9 (938-848 cm).....	101
5.5.2 Aquatic pollen and algal remains	102
5.5.2.1 The RK12 core (1932-50 cm)	102
5.5.2.2 Detailed analysis of the section 9 (938-848 cm).....	102

5.5.3 XRF analysis.....	102
5.5.4 Micro-facies of section 9 (938-848 cm)	103
5.6 Discussion	105
5.6.1 The Lake Kushu basin evolution since 16.6 cal. kyr BP	107
5.6.2 Insights into the Lake Kushu ecosystem dynamics during the Mid-Holocene (5.6-5.2 cal. kyr BP)	111
5.7 Conclusions.....	113
5.8 Acknowledgements.....	114
6. Conclusions	115
6.1 Outlook	117
7. References	118
8. Appendix	147
8.1 Supplementary material to the manuscripts.....	147
8.1.1 Diatoms from Lake Palaeo-Makgadikgadi.....	147
8.1.2 Diatom taxa list of Lake Kushu sediment core.....	149
8.1.3 Diatom Taxa list of modern Lake Kushu	154
8.2 List of publications	157
8.3 Curriculum Vitae	159
8.4 Declaration of Originality	161

List of Figures

Figure 1.1:	The topographic map shows the location of the Makgadikgadi–Okavango–Zambezi Basin (MOZB) in the Middle Kalahari in southern Africa	4
Figure 1.2	Topographic maps of Hokkaido and Rebun and Rishiri islands	8
Figure 1.3:	Simplified flow chart for diatom preparation.....	12
Figure 1.4:	Simplified flow chart showing the applied methods	16
Figure 2.1:	Overview map of the MOZB with the major subbasins and tributaries and the location of the studied geological section at the western edge of the Makgadikgadi Basin.....	22
Figure 2.2:	Upper part of the Boteti river valley section with the studied 30-cm diatom-rich sediment unit on top (BT) with indicated position of OSL dating.....	24
Figure 2.3:	Scanning electron microscope (SEM) images of the six most abundant diatom species identified in the Boteti section top unit	32
Figure 2.4:	Composite diagram illustrating percentage abundances of most frequent species, P / B ratio, log-centered PCA, $\delta^{18}\text{O}_{\text{diatom}}$ variability, and stack diagrams for salinity, trophy and pH	35
Figure 3.1:	Map compilation showing the location of the study area in northern Japan	41
Figure 3.2:	Archaeological culture sequence of the Hokkaido Region	45
Figure 3.3:	Age–depth model applied to the RK12 sediment core from Lake Kushu	50
Figure 3.4:	Simplified percentage pollen diagram presenting results of the coarse-resolution pollen analysis of the RK12 core	52
Figure 3.5:	Diatom percentage diagram presenting analytical results for 10 selected samples of the RK12 core.	53
Figure 3.6:	Composed imagery of the sedimentary succession of the archaeological site Hamanaka 2 and images of selected plant macro-remains	54
Figure 4.1:	Chart compilation showing the study area in northern Hokkaido, including the sea surface warm and cold currents, the main rivers on Rebun Island and the location of Lake Kushu	66
Figure 4.2:	Diagrams illustrating the meteorological background information, the annual variability of $\delta^{18}\text{O}$ and d excess in precipitation, and the ^{18}O – δD diagram for Lake Kushu setting, Hime-numa Pond, and Terney precipitation.	66

Figure 4.3:	Age-depth model diagram applied to the analyzed RK12 sediment core samples from Lake Kushu.....	73
Figure 4.4:	Overview of the ten samples analyzed for diatoms corresponding to the archaeological time period.	73
Figure 4.5:	Diagram illustrating the percentage abundances of identified diatoms from Lake Kushu and Hime-numa Pond	76
Figure 4.6:	SEM images of the modern diatoms exceeding 5% of the assemblages	79
Figure 4.7:	SEM images continued.	81
Figure 4.8:	Diatom assemblage diagram representing the percentage abundances of identified diatoms for the ten analyzed RK12 core samples.....	83
Figure 4.9:	Diagram compilation showing the percentage stack diagrams of the analyzed water parameters, the No. of taxa and the results of the XRF and ICP – OES analyses	85
Figure 5.1:	Topographic maps showing the location of Rebun Island (Hokkaido Region) in the Sea of Japan	95
Figure 5.2:	The percentage diagram shows the diatom abundances from the Kushu sediment core	97
Figure 5.3:	The diagrams show the reconstructed ecological parameters P/B, salinity, trophy and pH, based on autecology information	100
Figure 5.4:	PCA biplot with polygons that mark the 50% (bold lines) and 95% distribution of observations	103
Figure 5.5:	The geochemical record of RK12 with centered log-ratio (clr) transformed contents of selected elements and the first four principal components (PC)	104
Figure 5.6:	Compilation of the high-resolution analyses of RK12 section 9 with micro-facies, diatom and pollen percentage diagrams, and reconstructed autecology from diatoms	105
Figure 5.7:	Microscopic images of the micro-facies analyses of section 9 showing overview and detailed photographs.....	106

List of Tables

Table 1.1:	Overview of the four manuscripts presented in this thesis.....	17
Table 1.2:	Overview of my own contribution to each manuscript.....	18
Table 2.1:	Analytical data for OSL age calculation	28
Table 3.1:	Summary of the 57 AMS-dated samples of the RK12 core of Lake Kushu	49
Table 3.2:	Summary of radiocarbon dates and calibrated ages for the AMS-dated samples from the Okhotsk and Ainu cultural layers of Hamanaka 2, Rebun Island	55
Table 4.1:	Summary of the sample locations including sample date, geographical position, the on-site measured water parameters and the stable oxygen and hydrogen isotope analyses.....	70
Table 8.1:	Diatom taxa list of Lake Palaeo Makgadikgadi samples with the corresponding autecology	147
Table 8.2:	Diatom taxa list of Lake Kushu core samples with the corresponding autecology ..	149
Table 8.3:	Diatom taxa list of Lake Kushu modern samples with the corresponding autecology	154

1. Introduction

1.1 Preface

This doctoral thesis embraces two case areas across the hemispheres aiming for high-resolution palaeolimnological and palaeoenvironmental reconstructions of (a) a Late Pleistocene lake phase in southern Africa and (b) a Late Glacial - Holocene coastal lake northern Japan to contribute to the understanding of hunter-gatherer cultural dynamics and migration pathways.

The first study presents initial evidence and hydrological parameters of an ancient mega-lake phase called Lake Palaeo-Makgadikgadi located in the semi-arid Makgadikgadi Basin in Botswana, as part of a long-lived lacustrine system during hydrological favorable periods. The semi-arid region is highly controlled by shifts in seasonal rainfall and changes in humidity, which triggered migrations of Kalahari hunter-gatherers (i.e. Khoisan-speaking Bushmen groups). The idea of this project evolved from former investigations (field work by Prof. Dr. Frank Riedel and team in 2007, 2008 and 2010) of the Makgadikgadi Basin to detect past lake highstands and understand hydrological changes in the basin.

The second case study investigates the only freshwater lake on Rebun Island (Japan), which is a key research area for the multi-disciplinary Baikal-Hokkaido Archaeology project (BHAP: <http://bhap.artsmn.ualberta.ca/>). The project follows the objectives to obtain detailed information about the cultural dynamics and variability of Holocene hunter-gatherers and the interplay with changing environments, vegetation and climate. The sediment core from Lake Kushu was obtained to serve as a potential multi-proxy archive to improve the understanding of palaeoenvironmental variations and their potential influence on Holocene hunter-gatherer cultures. For this reason, the thesis was financially supported via a BHAP PhD stipend (University of Alberta, fond number 0424634401).

In both research areas, the focus lies on the study of diatom assemblages to reconstruct the palaeolimnology. Diatom analysis is a well-known and worldwide-established method to classify almost all kind of waterbodies around the world. Whereas in the Lake Palaeo-Makgadikgadi case study exclusively fossil diatoms can be used, in Lake Kushu fossil and modern diatom assemblages can be used to obtain new information. In addition to the diatom analysis, a combination of methods (botanical, hydrological, geochemical and sedimentological analyses) aims to get subsidiary knowledge to gain broad and detailed insights of both lake histories and the (palaeo-) environments. Not only climatic variations, but also tectonically and human-induced changes are possible driving factors for the evolution and existence of the Lake Palaeo-Makgadikgadi phase in Botswana and of Lake Kushu in Japan.

1.2 Diatoms as bioindicators in palaeolimnological research

Diatoms (Greek *diátomos*, from *dia* “apart” and *temnein* “cut, divide”) are eukaryotic, unicellular microalgae with cell walls made of silica. The first discovery of the microorganisms started in 1783 by the Danish naturalist O.F. Müller (Battarbee et al., 2001). C. Agardh introduced the term “diatom” in 1824 (Kalbe, 1980). The mainly photosynthesizing primary producers (size range from few μm to 0.5 mm) grow in almost all kind of water, from fresh via marine to hyper saline waters, from the tropics to the Arctic Ocean (Round et al., 1990). The class Bacillariophyceae comprises *c.* 12,000 approved diatom species (Guiry and Guiry, 2017) with estimated 100,000 existing species (Round et al., 1990). The taxonomic classification is based on the primary existence of two unequal flagella, which are secondary degenerated in diatoms. Their unique feature is the cell structure. The fine silica frustule is composed of two valves (theca). The smaller hypotheca fits exactly into the bigger epitheca like a hatbox. The primary asexual reproduction is processed by binal fission. The parent frustule (hypo- and epitheca) builds two smaller daughter theca in the inside, one for the mother epitheca and one for the mother hypotheca, respectively. Once the daughter cells are formed, the frustule divides into two individuals. This kind of fission leads to a reduction in cell sizes and ends up in a final stage, when further binal fission is impossible. In this case, sexual reproduction is likely. Diatoms can produce male and female gametes, which form the zygote. The spherical initial cell (auxospore) grows to a much larger size and marks the beginning of a new generation (Round et al., 1990; Krammer and Lange-Bertalot, 1997). In unfavorable conditions, diatoms produce resting spores as a long- or short-term survival strategy (McQuoid and Hobson, 1996).

The oldest diatom record from early Jurassic (*c.* 185 Myr) marine deposits shows valves without fine structures (Medlin et al., 1996). High fossil abundance is recorded from shallow water environments from the Lower Cretaceous (115-110 Myr). After a period of poorly preserved records, diatoms are widespread and diverse since the Upper Cretaceous (87-65 Myr; Medlin et al., 1996). The fossil record since the Cretaceous shows the evolution of radial symmetric forms (Centrales) before bilateral (Pennales) valves developed (Medlin et al., 1996). The latter developed a raphe, a thin slit along the valve, which is used to attach to biotic and abiotic substrates and to move with a maximum speed of 20 μm per second (Kalbe, 1980; Round et al., 1990). First freshwater diatoms occurred in the early Eocene (48-40 Myr) and most morphological features of modern-day species exist since the Miocene (20-7 Myr; Medlin et al., 1996; Battarbee et al., 2001).

The valves of diatoms are typically well preserved in the sediments of most lakes, oceans and other environments (Smol and Stoermer, 2010). Thus, the improvement of analytical methods with the help of optical microscopes to identify microfossils increased the scientific meaning of diatoms in the 19th and 20th century (Kalbe, 1980). Early diatomists like Hustedt, Cholnoky and Ehrenberg were pioneers in the studies of aquatic ecology inferred by diatoms (Smol and Stoermer, 2010).

The increasing knowledge of the autecology allows the characterization of the water parameters (e.g. temperature, salinity, pH, trophic). The high number of species within a waterbody (assemblage) describes the aquatic ecology in detail and the resistance of the silica in sedimentary deposits allows diatoms to serve as excellent bioindicators through time and helps to reconstruct palaeolimnological and palaeoenvironmental features (Stoermer and Smol, 1999; Battarbee et al., 2001). The number of studies dealing with modern and ancient lake ecologies exploded in the last decades. Diatoms were used as indicators for eutrophication, pollution and acidification, (e.g. Battarbee et al., 2010; Hall and Smol, 2010), hydrological and climatic changes (e.g. Gasse et al., 1995; Mackay et al., 2012) and as indicators for sea level changes, tsunamis and palaeoceanic events in marine and estuarine environments (e.g. Smol and Stoermer, 2010; Rovira et al., 2012) and as proxies for archaeological studies (Battarbee, 1988).

1.3 Scientific background

1.3.1 Regional setting of Lake Palaeo-Makgadikgadi in southern Africa

The Makgadikgadi-Okavango-Zambezi Basin (MOZB) named after Ringrose et al. (2005) is a structural depression located between 17-22.6°S and 21-27°E in the semi-arid Middle Kalahari in southern Africa (Passarge, 1904) and is characterized by a low topographic relief between 890 and 950 m a.s.l. (Thomas and Shaw, 1991; Riedel et al., 2014). The MOZB spans an area of *c.* 120,000 km² (Thomas and Shaw, 1991) and is composed of five major lacustrine sub-basins (Fig. 1.1). The Makgadikgadi Basin is the largest and deepest depression in the eastern part of the MOZB with an expansion of *c.* 37,000 km² (Ebert and Hitchcock, 1978; Cooke and Verstappen, 1984; Ringrose et al., 1999, 2005). At the western margin the Boteti River Valley connects the Makgadikgadi Basin to the Makalamabedi Basin (*c.* 1,200 km²; Riedel et al., 2014). The Ngami Basin (*c.* 2,600 km²; Burrough et al., 2009b) lies west of the Makalamabedi Basin and the Mababe Basin (*c.* 2,300 km²; Riedel et al., 2014) is located in the north. The shallow Caprivi Depression (*c.* 2,000 km²; Shaw and Thomas, 1988) marks the northernmost edge of the MOZB. Three main rivers drain the MOZB from the northwest (Fig. 1.1). The Okavango River with its catchment area in the Angolan highlands enters the MOZB from the west and forms a large alluvial fan and adjacent fluvio-lacustrine wetlands. The Okavango Delta builds one of the world's largest inland deltas with 22,000 km² (Cooke, 1980; Shaw and Thomas, 1992; Andersson et al., 2003). The Cuando River coming from the Angolan Highlands as well, and the Zambezi River, flowing down through Zambia, both enter the Caprivi Depression and drain the basin as the combined Zambezi River further eastwards via the Victoria Falls to Zimbabwe.

The MOZB is characterized by a complex semi-arid climate setting (Chase et al., 2012; Riedel et al., 2014). The rain season appears from October to April with high variability in precipitation (Batisani and Yarnal, 2010). Precipitation values range from 300 - 650 mm per year with a

1. Introduction - 1.3 Scientific background

precipitation gradient from northeast to southwest (Lancaster, 1978; Cooke, 1979; Thomas et al., 2011) with all-season high evaporation up to 2000 mm (Grey and Cooke, 1977). During austral summer, the moisture is transported from the West and East African monsoons via the Okavango catchment into the MOZB. The southward-shifted intertropical convergence zone lets pour in the east African monsoon towards the Middle Kalahari and therefore leads to rainfall over the MOZB (Verschuren et al., 2009). The moisture thus originates from the Indian Ocean (Riedel et al., 2014). It is still under discussion to which extent the West African Monsoon brings moisture from the Atlantic Ocean into the Middle Kalahari (McHugh and Rogers, 2001; Burrough et al., 2009b, Riedel et al., 2014). During the dry season (May to October), moisture from the South Atlantic and Indian Ocean triggers rainfall mainly over southern Africa (Burrough et al. 2009b; Chase et al. 2012; Urrego et al. 2015).

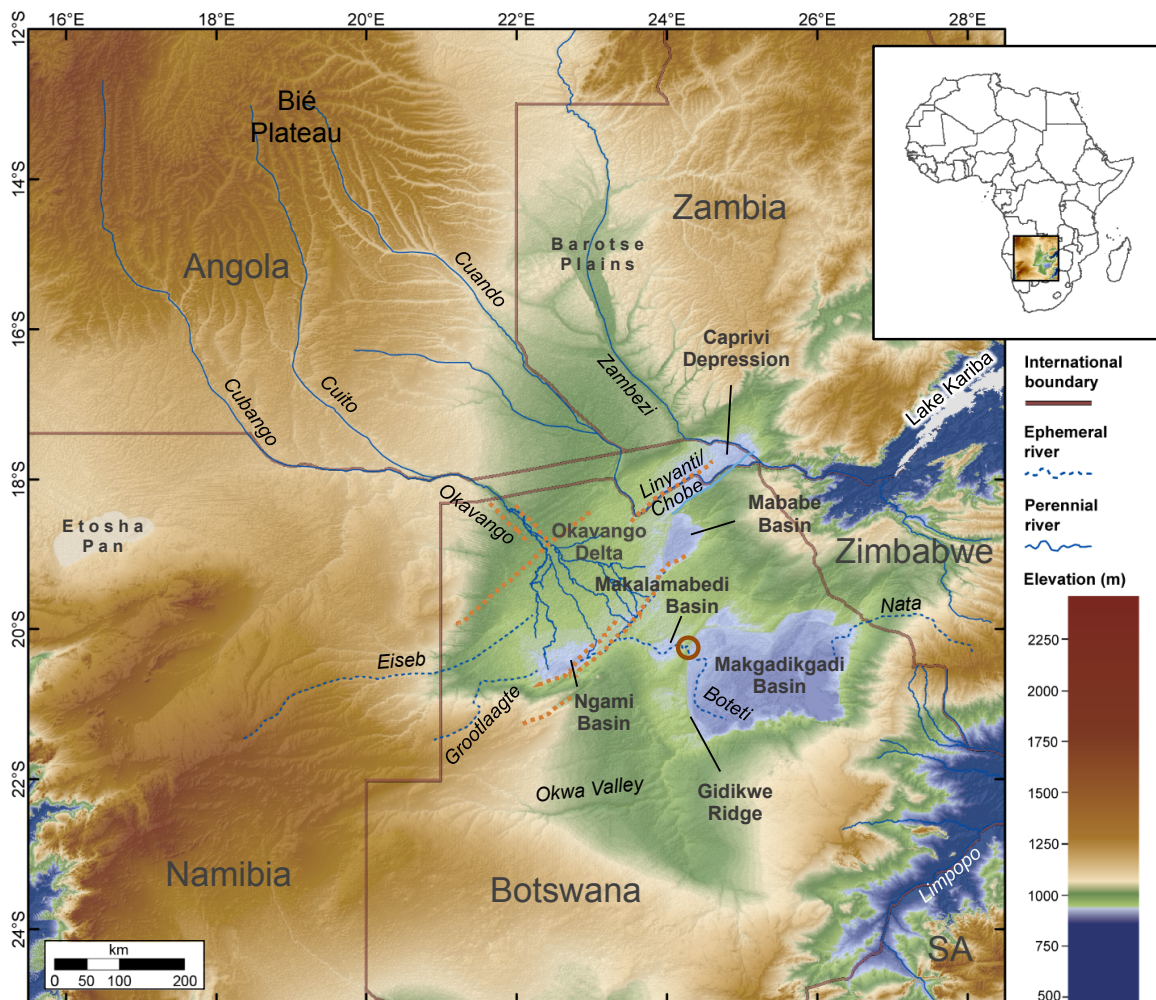


Figure 1.1: The topographic map (after Riedel et al., 2014) shows the location of the Makgadikgadi–Okavango–Zambezi basin (MOZB) in the Middle Kalahari (after Passarge, 1904) in southern Africa and accentuates the flat relief of the depression. Main faults (orange dashed lines) are drawn after Burrough et al. 2009a).

The MOZB is encircled (in the east, south and west) by the southern African mountain chains (Great Escarpments), which result from epeirogenesis in consequence of isostatic uplift after the Gondwana-breakup (Du Toit, 1937; Tankard et al., 1982; Summerfield, 1985a, b). It is suggested, that the Makgadikgadi Basin evolved in the Early Pleistocene (*c.* 1.4 Myr) after the epeirogenetic uplift interrupted the drainage from the west towards the Limpopo River during Late Pliocene / Early Pleistocene and created the internal drainage basin (Du Toit, 1933; Moore et al. 2012).

The MOZB is connected to the southwestern branch of the East African Rift System (EARS; Scholz et al., 1976; Kinabo et al., 2007; Shemang and Molwalefhe, 2011; Riedel et al., 2014). The graben system proceeds southwestwards from Lake Tanganyika via the Luangwa River and Lake Kariba to Botswana (Fairhead and Girdler, 1969). The neo-tectonical influence is visible by a series of northeast-southwest orientated faults within the MOZB (Fig. 1.1; Baillieul, 1979; Cooke, 1980; Nugent, 1990, 1992; Shaw and Thomas, 1992; Haddon and McCarthy, 2005; Ringrose et al., 2005; Kinabo et al., 2008; Burrough et al., 2009a; Shemang and Molwalefhe, 2011). The influence of the EARS changed the water dispersal in the MOZB. It has been discussed whether the Zambezi River in the past changed its course after tectonic disruption (Du Toit, 1933; Lister, 1979; Cooke, 1980; Shaw and Thomas, 1988, 1992; Nugent, 1990, 1992; Moore and Cotterill, 2010).

Also, the incipient rifting influenced the water dispersal of the Okavango wetlands. The initiation of the Thamalakane fault defines the southeastern limit of the Okavango Delta (McCarthy et al., 1993) and the water coming from the Okavango Delta is redirected northeast-southwestwards alongside the Thamalakane fault into the Ngami and Mababe Basin (Burrough et al., 2007). The interconnection to the Makalamabedi and Makgadikgadi Basin has been mainly blocked except of the ephemeral Boteti River, which drains water into the Makgadikgadi Basin from the west (Fig. 1.1).

Further water fed in the past is suggested from e.g. the fossil Okwa River (southwest of Makgadikgadi Basin), which likely was a major contributor to the water budget of the Makgadikgadi Basin in the Late Quaternary (Breyer, 1982; Shaw et al., 1992; Nash et al., 1994; Nash and McLaren, 2003; Riedel et al., 2014) and the ephemeral Nata River (northeast of Makgadikgadi Basin), which fills the Sua Pan, located in the eastern part of the Makgadikgadi Basin, periodically (Riedel et al., 2011; Riedel et al., 2014).

1.3.2 Palaeo-lacustrine approach in the Middle Kalahari

Since the first discovery of an ancient vast freshwater lake by David Livingstone in middle of the nineteenth century, the Kalahari attracted numerous researchers and scientists to study and identify several geomorphological features (e.g. palaeo-shorelines, ridges) of a complex Quaternary lacustrine system (e.g. Livingstone, 1857; Passarge, 1904; Cooke, 1979; Cooke and Verstappen,

1984; Thomas and Shaw, 1991; Ringrose et al., 2005; Burrough et al., 2009a, 2009b; Riedel et al., 2014).

Numerous palaeo-shorelines as remains of former lake phases have been identified in the nowadays very dry Makgadikgadi Basin. The most prominent is the Gidikwe Ridge at the western margin of the Makgadikgadi Basin (Fig. 1.1), which was created by aeolian sands during palaeolake lowstands and was shaped by water activity during palaeolake highstands (Cooke and Verstappen, 1984; Thomas and Shaw, 1991; Burrough et al., 2009a, b; Riedel et al., 2014). The suggested lake highstands have been termed Lake Palaeo-Makgadikgadi (Grey and Cooke, 1977). Burrough et al. (2009a) identified seven so-called mega-lake phases OSL (optically stimulated luminescence) dated to the last *c.* 100 kyr. Several mega-lake scenarios have been modeled based on palaeo-shoreline evidence to 908 m, 912 m, 920 m, 936 m and 945 m a.s.l. (above sea level) for the Late Pleistocene and Holocene time period (White and Eckardt, 2006; Riedel et al., 2014). The identified lake phases since *c.* 100 kyr BP indicate several relatively more humid periods in southern Africa. Carto et al. (2009) showed that Heinrich events, short-term climate anomalies triggered by North Atlantic iceberg discharges, lead to aridification in northern Africa but to increased humidity in southern Africa.

Archaeological and genetic studies identified Africa to be the continent of origin of modern human populations (e.g. Wallace et al., 1999). However, it is still arguable whether the origin of humans lies in eastern or southern Africa (Henn et al., 2011). It is suggested that Kalahari hunter-gatherers are genetically the most divers of all human populations (Henn, et al. 2011), which implies a high adaptation potential (Charlesworth, 2009) due to dramatic changes in environmental changes and habitability.

The environmental and climatic implications for the rise and fall of such a large-scale lake system and the consequences for the Kalahari hunter-gatherers remain ambiguous and the timing and fluctuations are still poorly understood. There is a need for a palaeoenvironmental archive to reconstruct and characterize former lake phases and to improve the understanding of the Lake Palaeo-Makgadikgadi driving factors and the human occupation history of the last 100,000 years.

The Boteti River Valley exposed two diatom rich sediment units at the Gidikwe Ridge between *c.* 936-945 m a.s.l. (Fig. 1.1) revealing an excellent archive for high-resolution diatom analysis to - for the first time - characterize a Lake Palaeo-Makgadikgadi phase. The elevation (945 m a.s.l.) of the deposits indicates that the Makgadikgadi Basin possibly was completely filled by a vast lake spanning an area of *c.* 37,000 km² and potentially reached the adjacent sub-basins in the MOZB. The hydrological conditions are still unknown. For this reason, the lake sediments were diatom-analyzed to reconstruct the water quality of the Lake Palaeo-Makgadikgadi. In addition, OSL dating is used to relate the deposits to one of the previously identified mega-lake phases by Burrough et al. (2009a). This new information contributes to the understanding of the complex lacustrine system. The oxygen isotope analysis from diatom valves provides further information of

the hydrologic balance between the sensitive interaction of precipitation and evaporation, that decides on the evolution and decline of a Lake Palaeo-Makgadikgadi lake phase.

1.3.3 Regional setting of Lake Kushu in Northern Japan

Rebun Island and neighboring Rishiri Island, both are situated in the northernmost tip of the Japanese Archipelago in the Sea of Japan *c.* 45 km and 30 km, respectively, west of NW Hokkaido and *c.* 9 km apart from each other (Fig. 1.2). About 100 km separate Rebun Island from southern Sakhalin in the north and 240 km from continental Asia. Both islands are of volcanic origin, whereas Rebun Island results from Cretaceous subaqueous dome growth (Hashimoto, 1991; Kimura, 1997; Goto and McPhie, 1998; Mandal et al., 2011), Rishiri Island is built from a strato-volcano, whose activity started *c.* 200 kyr BP (Kuritani and Nakamura, 2006; Mandal et al., 2011).

Rebun Island occupies an area of about 82 km² spanning *c.* 20 km from north to south, and *c.* 6 km from east to west. Mount Rebun (Rebun-dake) marks the highest point with 490 m a.s.l. (Geospatial Information Authority of Japan, 2012). Steep cliffs on the west coast contrary to gentle hills that slope to the eastern shoreline characterize the island.

Lake Kushu (45°25'58"N, 141°02'05"E) is the only freshwater body located in the northern part of Rebun Island. The lake is separated from the Funadomari Bay by a sand dune reaching up to 15 m a.s.l. (Fig. 1.2). The shortest distance to the modern seacoast is *c.* 270 m. The maximum water depth reaches *c.* 6 m in the eastern part of the lake with average depths of about 3–5 m (bathymetry data provided by T. Haraguchi, Osaka City University). The lake surface covers 0.53 km² with a shoreline of 3.5 m. The Oshonnai River enters the lake in the south and a small, canalized outflow drains through Funadomari Town into the Bay.

The East Asian Monsoon (EAWM) and sea currents in the Sea of Japan and northwestern Pacific affect the climate in the Hokkaido region (Igarashi, 2013, 2016; Leipe et al., 2013). In winter (November to May) the EAWM brings cold and dry air masses from continental Siberia towards Hokkaido and collects ascending moisture and heat over the warm Tsushima Warm Current (TWC; Fig. 1.2) and leads to high amount of snowfall on Rebun Island and western Hokkaido (Leipe et al., 2013). In summer, the Okhotsk High over the Sea of Okhotsk and the Ogasawara High in the northwestern subtropical Pacific control the climate and result in high precipitation in the Hokkaido region (Ogi et al., 2004; Igarashi et al., 2011; Igarashi, 2013). The mean monthly air temperature on Rebun Island varies from -6.4 °C in January to 19.4 °C in August with a mean annual precipitation of 1102 mm, with highest amounts falling from September (131 mm) to December (106 mm).

Rebun and neighboring Rishiri Island build the Rishiri Rebun Sarobetsu National Park, where vegetation consists of cool mixed and cool conifer forest (Nakagawa et al., 2002; Tarasov et al. 2011, Leipe et al., 2013).

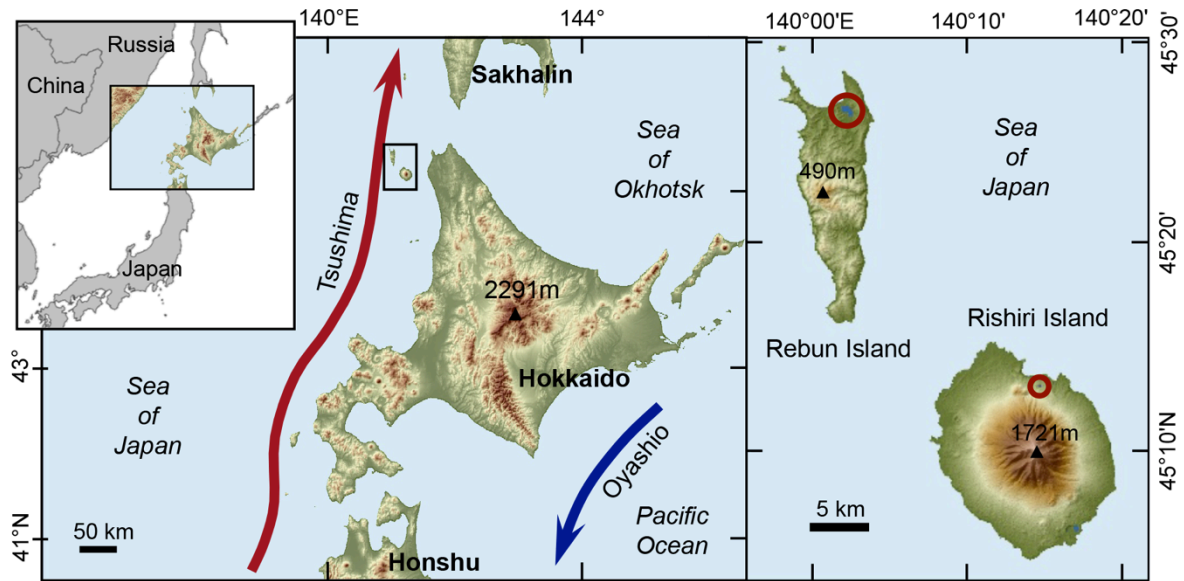


Figure 1.2: Topographic map of Hokkaido (left) and Rebus and Rishiri islands (right). Red circles show the study areas of Lake Kushu on Rebus Island and Hime-numa Pond on Rishiri Island. Topographic maps are based on elevation Shuttle Radar Topography Mission (SRTM) V4.1 data (Reuter et al., 2007; Jarvis et al., 2008) and Geospatial Information Authority of Japan (2012); modified after Müller et al., 2016.

1.3.4 Archaeological approach in the Hokkaido region

The study of human history and ancient pathways of Holocene hunter-gatherers is of high interest for archaeologists. The hunter-gatherer research has focused on the evolution of the foraging life style in the Pleistocene, the transition from foraging to farming during the Holocene and the impact of modern world hunter-gatherers (e.g. Lee and Daly, 1999; Fuentes, 2009; Weber et al., 2013). Since the beginning of successful archaeological excavations on Rebus Island in the 20th century (Sakaguchi, 2007a), the island appeared in the spotlight to help for the understanding of Holocene hunter-gatherers and their route from east Siberia to Japan (Tarasov et al., 2013; Weber et al., 2013). It is still debated, whether the Neolithic Japanese Jomon culture originated from the migration via the northern or southern route from the Asian mainland (Hanihara, 1991; Omoto and Saitou, 1997; Hudson, 1999; Tanaka et al., 2004; Adachi et al., 2009; Hanihara and Ishida, 2009). The southward movement of hunter-gatherers is supported by the existence of a land bridge that connected Sakhalin with Hokkaido and adjacent islands during the relative low sea level during the Last Glacial Maximum (LGM; Kuzmin et al., 2002, 2013; Taruno, 2010; Igarashi, 2016).

So far, 43 archaeologically excavated sites on Rebus Island span an interval of 6000 years continuous human history covering an interval from the Paleolithic to historic Ainu (Inui, 2000). A test survey undertaken by H. Kato (BHAP member, Hokkaido University) in 1996 identified sites of multi-component usage and multi-period located in Hamanaka and Funadomari on the northern part of Rebus Island (Fig. 1.2).

In 2011, the multi-disciplinary Baikal-Hokkaido Archaeology Project (BHAP) started to investigate Holocene hunter-gatherers in the Lake Baikal region of Siberia and in the Hokkaido Region in Japan. Because of the geographical location and abundant archaeological finds, Rebun Island was selected as one of the key research areas to study Holocene hunter-gatherer dynamics, migration pathways and cultural changes and the influence of climatic and environmental factors. First BHAP excavations established the high research potential of Hamanaka and Funadomari sites since the Mid-Holocene. The need for a high-resolution multi-proxy archive arose to derive detailed information about local and regional climate and environmental changes during the entire Holocene.

Kumano et al. (1990a) presented diatom studies from Lake Kushu. The diatom analysis from a 16.2 m core recovered from the marshy floodplain at the southern margin of the lake, which covers the last *c.* 9000 yr BP, revealed that marine and brackish-water taxa were very abundant in the sediment prior to *c.* 6000 cal. yr BP. Afterwards, freshwater taxa prevailed with several brackish / marine peaks, which suggest short marine influence likely associated with palaeo-tsunami events. However, the coarse-resolution analysis and the age-depth model with only four radiocarbon dates calls for further investigation to improve the palaeolimnological understanding of Lake Kushu. Local pollen and other palaeoenvironmental records are still unknown.

For this reason, a *c.* 20 m long, continuous sediment core was recovered from Lake Kushu in February 2012. The intention was to reach the Late Glacial / Holocene transition to recover a detailed and continuous archive to perform environmental reconstructions, to explore regional postglacial climate variations, sea level changes, marine influence (e.g. storm waves, tsunamis) and to link this new information to the hunter-gatherer population dynamics.

1.4 Aims of the thesis

The main goal of this doctoral thesis is to provide new insights into the palaeolimnology of two different lakes and to link these findings to the regional evolution of hunter-gatherer cultures. Diatoms are used as a key proxy to precisely reconstruct selected water parameters (pH, salinity, trophic) of fossil Lake Palaeo-Makgadikgadi in southern Africa and modern Lake Kushu in northern Japan.

On the one hand, it is intended to reconstruct for the first time the palaeohydrological status of a Late Pleistocene (MIS 5) mega-lake phase in the MOZB. The analysis of diatom assemblages and their oxygen isotope composition ($\delta^{18}\text{O}$) contributes to the understanding of the Kalahari hunter-gatherer occupation history, phylogeographical patterns and climate evolution in southern Africa.

On the other hand, high-resolution diatom analysis aims to improve the understanding of the environmental history of Lake Kushu (Rebun Island) in northern Japan and its catchment area. For the first time, modern diatom assemblages from Rebun Island and neighboring Rishiri Island are

analyzed to understand the modern situation and are then compared with the fossil assemblages. The multi-proxy analysis of the extracted sediments from Lake Kushu (past *c.* 16,6000 years) aims to provide a detailed palaeolimnological record to facilitate regional palaeoclimatic and palaeoenvironmental interpretations for the Late Glacial and Holocene time period in the Hokkaido Region to link the results to the archaeological findings and to contribute to the knowledge of the Holocene hunter-gatherer spread into northern Japan, which have been dependant on potable water.

The main objectives of this thesis are:

- palaeoenvironmental reconstructions of lacustrine systems across the hemispheres as a tool to improve the understanding of human-environmental interactions and habitability of the Middle Kalahari for hunter-gatherers
- first diatom-inferred palaeolimnological features of Lake Palaeo-Makgadikgadi in the MOZB (Botswana) and chronological correlation to previously suggested lake phases in the MOZB
- reconstruction of hydrological changes and climate driven environmental changes in southern Africa
- verification of fossil diatom assemblages with modern analogue data sets and testing the potential of the Kushu core (Japan) to serve as a suitable archive for palaeoenvironmental reconstructions
- multi-proxy study to provide first continuous high-resolution reconstruction of lacustrine evolution of Lake Kushu (Hokkaido Region) and to identify short-term events (e.g. storm waves, typhoons) that affected the coastal lacustrine system after Holocene transgression
- obtain new information about the Late Quaternary climate and relative sea level changes as main impact factors for the Lake Kushu system and
- Late Glacial and Holocene environmental and climate reconstruction to infer possible driving factors for favorable conditions for incipient permanent habitability for Holocene hunter-gatherers on Rebun Island and the Hokkaido Region

1.5 Material and methods

1.5.1 Fieldwork

During field campaigns to the Gidikwe Ridge near Moremaoto in May 2011 and 2013, the 30 cm thick lake deposits have been sampled each 0.5 cm gaining 60 samples (each 50-70 g) for high-resolution diatom analysis. In addition, a sediment block (15x15x30 cm) has been cut out of the section for optically stimulated luminescence (OSL) dating. Differential global positioning system (GPS) was used to measure the exact elevation of the deposits.

The analytical work of Lake Kushu on Rebus Island started with the coring of RK12 core by the commercial company Dokon Co. (Sapporo) equipped with professional facilities. The 19 1-meter segments (86-mm diameter) have been transported to the Graduate School of Environmental Science, Hokkaido University (Sapporo) and opened in April 2012. After description and documentation, the core has been subsampled for multi-proxy analyses by using the non-destructive double L channel technique (Nakagawa et al., 2012).

The field campaign to Rebus and Rishiri Islands was undertaken in August 2014. Modern surface water, surface sediments and water plant samples have been collected from Lake Kushu and Hime-numa pond. Furthermore, we measured pH, temperature, conductivity and oxygen saturation of the water to characterize the modern habitats.

1.5.2 Diatom analysis

Diatoms are primary producers in lakes, rivers and oceans. The high number of species allows the diatoms to grow in almost every kind of waterbody. The essential nutrients silica (Si), nitrogen (N) and phosphorus (P) and temperature regulate the growth (Leng and Barker, 2006). The increasing knowledge of the autecology allows researchers to define the water parameters in which the individuals live in (e.g. Van Dam et al., 1994). Due to the resistant silica frustules, the information is saved in lake sediments. The analysis of the fossil diatom assemblages throughout the last several thousand years reveals changes in water parameters (e.g. salinity, temperature, pH, trophic), which can be extrapolated to environmental (e.g. climate) variations.

The lake deposits from Lake Palaeo-Makgadikgadi and Lake Kushu were prepared after standard techniques for diatom preparation (Battarbee et al., 2001, Kossler et al., 2011) in the laboratories of the Paleontology Branch at the Institute of Geological Sciences at the Freie Universität Berlin. Chapters 2.4.3, 4.4.4 and 5.4.2 reveal further information. The taxa lists and information about the preferred mode of living (benthic / planktonic) and the specific optima for salinity, pH and trophic, which were used to calculate the stack diagrams to illustrate the reconstructed ecology (e.g. Fig. 2.4), are given in the tables 8.1-8.6 in the supplementary material (chapter 8.1).

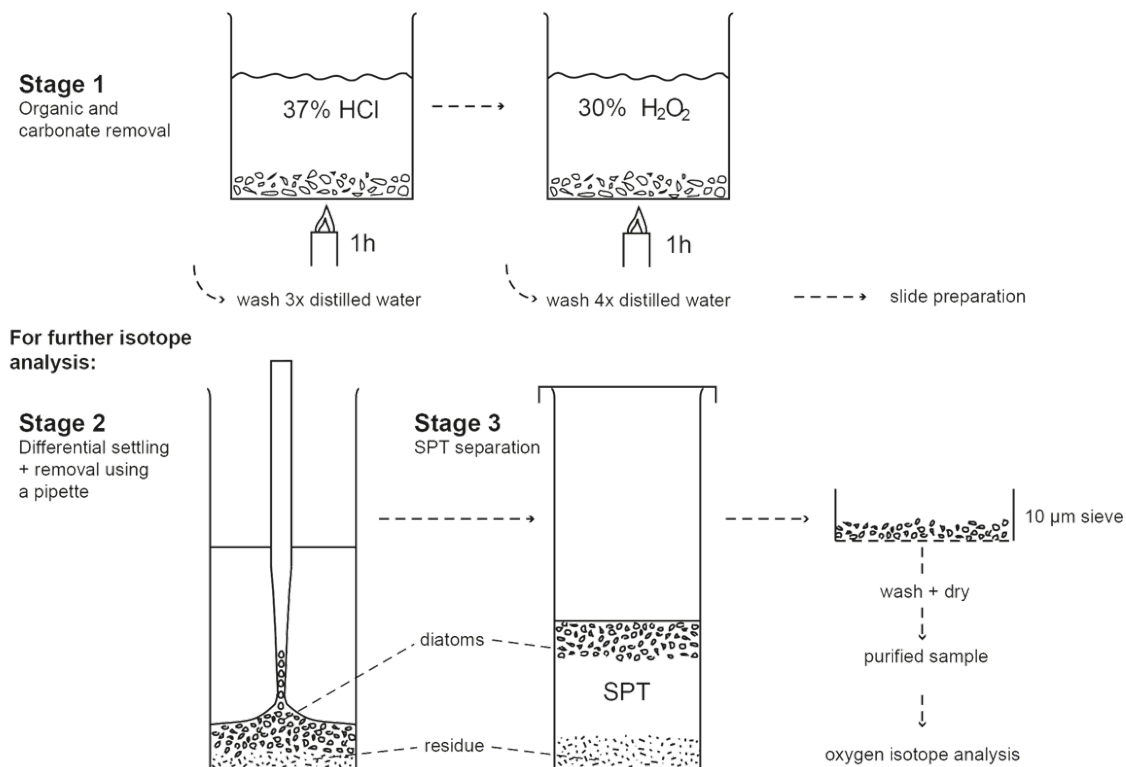


Figure 1.3: Simplified flow chart for diatom preparation, modified after Morley et al. (2004). Stage 1 implies the standard preparation techniques after Battarbee et al. (2001) and Stage 2 is necessary to purify the sediment samples for isotope analysis.

The main purpose of this thesis is to reconstruct the lake history of both lake systems with diatom analysis, the focus lies on the results and interpretation of the microalgae. However, the combination of diatom analyses with palynological, geochemical, sedimentological and isotopic methods is used to obtain as much information as possible. The combination of the methods is illustrated in figure 1.4. All applied methods are explained in detail in the corresponding paragraph in the integrated manuscripts (chapter 2-5). To reduce repetition, the used analyses are explained briefly in the following chapters (1.5.3-1.5.7), and are concentrated to basic (biological, physical and chemical) processes of each approved method.

1.5.3 OSL and radiocarbon dating

For each case study the most adapted dating method was used. Optical stimulated luminescence (OSL) dating was chosen to determine the age of the Lake Palaeo-Makgadikgadi deposits. Here, sedimentary minerals (quartz or feldspar) serve as dosimeters. The method measures the time since the last exposure to daylight prior to deposition (Stokes, 1999). Due to inhomogeneity in the mineral crystal structure, the electrons can be relocated by adding (thermal or

optical) energy to the mineral. While the minerals are uncovered, the daylight and cosmic rays constantly relocates the electrons at defects in the mineral structure (Aitken, 1998; Stokes, 1999). Once the mineral is covered with sediments, energy radiation stops and the electrons are fixed. This state keeps the mineral stable until a further amount of (optical) energy is introduced to the system. To determine the sample age, the aliquots are heated and optically stimulated to determine the natural OSL rate. The aliquot is then heated and stimulated several times with increasing dose. The dose plotted against OSL calculates the equivalent dose that is necessary to produce the natural OSL signal. To determine the sediment age, the equivalent dose rate is divided by the environmental dose rate (Bøtter-Jensen, 1997; Aitken, 1998; Bøtter-Jensen et al., 2003). For this purpose, a sediment block (15x15x30 cm) was removed from the Lake Palaeo-Makgadikgadi sediments and covered with a black plastic foil to avoid resetting prior dating. Three measurements were undertaken from the top, middle and bottom of the section. A former sample from a field excavation in 2009 was added to the current age modeling. The samples were transported to the OSL laboratory of Bayreuth University, Germany. The detailed operation method is described in chapter 2.4.2.

Accelerator mass spectrometry (AMS) was used to determine the age of the sediments from the Lake Kushu core. The method allows the measurement of very small samples (<0.5 mg C) with a high precision on 0.3% (Jull, 2007). The principle is to measure the ratio of ^{14}C and ^{12}C that changes after the organism died. After deposit, the carbon decay starts to count with initially *c.* 226 Bq kg⁻¹ C in modern samples, to less than 1 Bq kg⁻¹ C in old samples (Cook and van der Plicht, 2007). Therefore, radiocarbon dating is practical limited to the last 50,000 years (Cook and van der Plicht, 2007). In contrast to the conventional counter tube measurements (Cook and van der Plicht, 2007) the ultra sensitive mass spectrometry isolates the carbon ions from the molecules by acceleration and is able to measure ^{14}C directly without waiting for its radioactive decay (Jull, 2007). As this is not the focus of the thesis detailed operational information is provided by e.g. Jull (2007).

To achieve an appropriate age model for the Lake Kushu setting, 57 bulk samples were sent to the Poznan Radiocarbon Laboratory of the Adam Mickiewicz University (international cooperation partner T. Goslar; see chapter 2.4.2).

1.5.4 Isotope analyses from diatom silica and surface water samples

The diatom valves from the Lake Palaeo-Makgadikgadi sediments have been analyzed for oxygen isotopes composition ($\delta^{18}\text{O}_{\text{diatom}}$). The idea of this method is based on the natural fractionation processes of most abundant (lighter) ^{16}O and a small percentage of (heavier) ^{18}O isotopes, which alternate depending on the aggregate state of water (fluid, gaseous, solid) and per material (shells, plants; Plessen and Helle, 2017). Basically, the temperature plays a major role

during precipitation and evaporation processes and leads to variations in the $\delta^{18}\text{O}$ composition (Leng and Barker, 2006; Leng and Henderson, 2013; Sharp, 2007). The changes of ^{18}O in lacustrine systems is commonly attributed to changes in the precipitation / evaporation ratio and temperature during this processes (Leng and Marshall, 2004). However, a wide range of environmental processes influence the $\delta^{18}\text{O}$ (Leng and Marshall, 2004). The oxygen isotope composition in open (outflow) lakes reflects the $\delta^{18}\text{O}$ in precipitation. Closed (no outflow) lakes tend to have $\delta^{18}\text{O}$ that responds predominantly to the balance of precipitation and evaporation (Leng and Barker, 2006). The oxygen isotope composition of diatom silica is dependent from the water temperature and the isotopic composition of the lake water from which the frustule is formed (Leng and Barker, 2006). Nevertheless, culture experiments have proofed that no “vital effects” exist in diatoms (Binz, 1987, Swann et al., 2007).

From the 60 diatom samples of the Lake Palaeo-Makgadikgadi deposits alternate samples have been analyzed with a mass spectrometer (detailed information provided in chapter 2.4.4) at the stable isotope facility of the Natural Environment Research Council (NERC) in Nottingham.

Similar processes are valid for oxygen and hydrogen (δD) isotopes in lake water. Isotopes of water samples from modern Lake Kushu and surrounding area and Hime-numa Pond on Rishiri Island have been analyzed for isotopic composition ($\delta^{18}\text{O}$, δD). The stable oxygen and hydrogen isotope compositions were measured with a Finnigan MAT Delta-S mass spectrometer at the stable isotope laboratory of the Alfred Wegener Institute Helmholtz Centre for Polar and Marine Research, Research Unit Potsdam (detailed information in chapter 4.4.2).

1.5.5 Pollen and non-pollen palynomorphs (NPP) analysis

Pollen and NPP analysis is highly interlinked with palaeoclimatic reconstruction, since the plant remains reflect the local to regional temperature and moisture during growing interval (Velichko and Nechaev, 2005). The method provides information of climatic changes in the Quaternary period and traces early human-environmental interactions (Leipe et al., 2014a, b; Tarasov et al., 2018). Pollen and spores have resistant exines that protect them from weathering and allow the preservation in sediments. The preparation of sediment samples for pollen analysis involved standard techniques of chemical treatment. Preparation and counting (Cwynar et al., 1979; Fægri et al., 1989) was undertaken in the pollen laboratory at the Paleontology Branch of the Institute of Geoscience at the Freie Universität Berlin. Chapter 5.3.3 includes a detailed description of pollen analysis.

1.5.6 Micro-facies analysis

The counting of laminations of varved lake sediments provides a high-resolution technique for annual to seasonal climate and environmental reconstructions (Zolitschka et al., 2015). In dimictic

lakes (like Lake Kushu) the overturn periods in spring and autumn lead to massive diatom blooms, parts of it settle down and build a layer of valves in the sediments. Lakes with ice cover in winter can preserve typical snowmelt layers in early spring sometimes containing dropstones from the ice cover. Clastic varves derive from heavy rain or monsoonal events of marine impacts and show a gradation (Zolitschka et al., 2015). Here, the frequency and duration of marine impacts, diatom blooms, snowmelts and dropstone events can be tracked on a very short time interval by examine the layers under the microscope.

Slides (each 10 cm) from the sediment core have been prepared by first, adding epoxy resin to stabilize the core material (Brauer and Casanova, 2001) and second, thin sectioned to *c.* 20-30 μm in the laboratory of the GeoForschungsZentrum in Potsdam (for details see chapter 5.3.4).

1.5.7 XRF analyses

X-ray fluorescence analysis (XRF) is a non-destructive method, which was used to analyze the Lake Kushu sediments for its elemental composition. Variations in elemental composition provide information of the sediment provenience, for example marine influence in coastal lakes (e.g. Goff and Chagué-Goff, 2001; Hürkamp et al., 2009). X-rays were pointed to the sample and thus stimulate electrons at low energy orbitals of the atom. Hence, the electrons have been stroked out, they leave a hole and that leads to an unstable atom structure. As a result, electrons from higher energy orbitals fall back to the lower orbital to fill the hole left behind. At this “falling”-process energy is released and emits an atom specific light radiation. The so-called fluorescence is then detectable by a sensor (Jenkins, 1999; De Vries and Vebros, 2002; Beckhoff et al., 2006). The measured XRF resolution of the 19 m core is 1 cm. Exact operational information is given in chapter 4.4.5.1. XRF measurements have been undertaken in the laboratories of the Institute of Physical Geography at the Freie Universität Berlin.

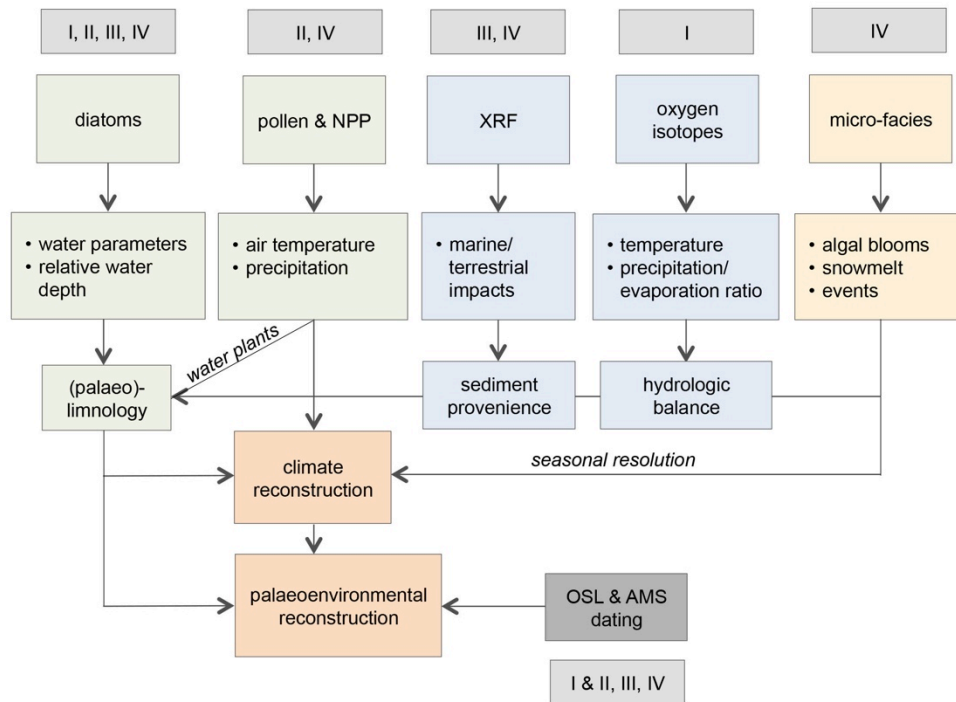


Figure 1.4: Simplified flow chart showing the applied biological (green), geo-/ biochemical (blue) and sedimentological (yellow) methods to reconstruct the palaeolimnology of Lake Palaeo Makgadikgadi and Lake Kushu. The light grey boxes contain the manuscript numbers where the methods were used in.

1.6 Overview of the integrated manuscripts

This dissertation is written in a cumulative form and consists of four separate manuscripts (Chapters 2-5), which have been published in (manuscript I to III) or “prepared-for-submission” to (manuscript IV) international peer-reviewed scientific journals. The following Table 1.1 gives an overview about the title and authorship of each manuscript and the selected scientific journal with the actual publication status. Each individual manuscript represents a self-contained research part, so that repetitions in the regional settings and method chapters are unavoidable.

Table 1.1: Overview of the four manuscripts presented in this thesis.

Chapter	Title <i>Authorship</i>	Journal <i>Status</i>
2	Paleolimnological features of a mega-lake phase in the Makgadikgadi Basin (Kalahari, Botswana) during Marine Isotope Stage 5 inferred from diatoms <i>Mareike Schmidt, Markus Fuchs, Andrew C.G. Henderson, Annette Kossler, Melanie J. Leng, Anson W. Mackay, Elisha Shemang, Frank Riedel</i>	Journal of Paleolimnology, Volume 58, Issue 3, pp. 373–390 <i>published: October 2017</i>
3	Palaeobotanical records from Rebun Island and their potential for improving the chronological control and understanding human–environment interactions in the Hokkaido Region, Japan <i>Stefanie Müller, Mareike Schmidt, Annette Kossler, Christian Leipe, Tomohisa Irino, Masanobu Yamamotu, Hitoshi Yonenobu, Tomasz Goslar, Hirofumi Kato, Mayke Wagner, Andrzej W. Weber, Pavel E. Tarasov</i>	The Holocene, Volume 26, Issue 10, pp. 1646–1660 <i>published: 1 October 2016</i>
4	Diatoms from Lake Kushu: A pilot study to test the potential of a Late Quaternary palaeoenvironmental archive from Rebun Island (Hokkaido Region, Japan) <i>Mareike Schmidt, Pavel E. Tarasov, Philipp Hoelzmann, Hanno Meyer, Christian Leipe</i>	Journal of Asian Earth Sciences, Volume 122, pp. 106–122 <i>published: 15 May 2016</i>
5	Multi-proxy palaeolimnological record of the last 16,600 years derived from coastal Lake Kushu in the Hokkaido Region of Japan <i>Mareike Schmidt, Fabian Becker, Philipp Hoelzmann, Christian Leipe, Jens Mingram, Stefanie Müller, Rik Tjallingii, Pavel E. Tarasov</i>	ready for submission to: Palaeogeography Palaeoclimatology Palaeoecology

1.7 Contribution to the individual manuscripts

Mareike Schmidt is the main author of three of the individual manuscripts (chapters 2, 4 and 5) and predominantly planned, wrote and accomplished them. She collected all modern samples from the Lake Kushu area (Japan) and fossil diatom samples from the Boteti River Valley (Botswana). She treated all diatom samples in the laboratory, identified the taxa, analyzed and interpreted the diatom assemblages, drew most of the images and finalized the manuscripts (except of manuscript II).

As the second author of the manuscript II Mareike Schmidt was responsible for all points relating to diatoms (methods, images, results, interpretation). The contribution of Mareike Schmidt to each manuscript is given in Table 1.2.

Table 1.2: Overview of the author's contribution to each manuscript.

Chapter/ Manuscript	Contribution of Mareike Schmidt [%]		
	conception	accomplishment	publication
2. / I	80	70	60
3. / II	30	20	20
4. / III	90	80	90
5. / IV	90	90	100

2. Manuscript I

Paleolimnological features of a mega-lake phase in the Makgadikgadi Basin (Kalahari, Botswana) during Marine Isotope Stage 5 inferred from diatoms

Mareike Schmidt,¹ Markus Fuchs,² Andrew C. G. Henderson,³ Annette Kossler,¹
Melanie J. Leng,^{4,5} Anson W. Mackay,⁶ Elisha Shemang⁷ and Frank Riedel¹

¹*Institute of Geological Sciences, Freie Universität Berlin, Malteserstr. 74-100, 12249 Berlin, Germany, e-mail: paleobio@zedat.fu-berlin.de*

²*Department of Geography, Universität Gießen, Senckenbergstr. 1, 35390 Giessen, Germany*

³*School of Geography, Politics and Sociology, Newcastle University, Newcastle upon Tyne NE1 7RU, UK*

⁴*NERC Isotope Geosciences Facility, British Geological Survey, Nottingham NG12 5GG, UK*

⁵*Centre for Environmental Geochemistry, University of Nottingham, Nottingham NG7 2RD, UK*

⁶*Department of Geography, Environmental Change Research Centre, UCL, Gower Street, London WC1E 6BT, UK*

⁷*Department of Earth and Environmental Sciences, Botswana International University of Science and Technology, P. Bag 16, Palapye, Botswana*

published in: Journal of Paleolimnology, Volume 58, Issue 3, pp. 373-390
accepted: 17 June 2017, published: October 2017

This is a post-peer-review, pre-copyedit version of an article published in Journal of Palaeolimnology. The final authenticated version is available online at: <http://dx.doi.org/10.1007/s10933-017-9984-9>.

2.1 Abstract

The Makgadikgadi–Okavango–Zambezi Basin (MOZB) is a structural depression in the southwestern branch of the East African Rift System of the Northern and Middle Kalahari, central southern Africa. In the present day, the mainly dry subbasins of the MOZB are part of a long-lived lacustrine system that has likely existed since Early Pleistocene and from which an extant freshwater fish radiation emerged seeding all major river systems of southern Africa. During hydrologically favorable periods the subbasins were connected as a single mega-lake termed Lake Palaeo-Makgadikgadi. Previous geomorphological studies and OSL dates have provided evidence for repeated mega-lake periods since approximately 300 kyr. The environmental and climatic implications of such large-scale Late Quaternary lake-level fluctuations are controversial, with the duration of mega-lake phases poorly constrained. Here, we present the first evidence for a Marine Isotope Stage (MIS) 5 mega-lake period (about 935–940 m a.s.l.) reconstructed from a diatom-rich, 30-cm-thick lacustrine sediment section, exposed close to a palaeo-shoreline of the

Makgadikgadi Basin. Based upon the environmental setting and in comparison with sedimentation rates of other similar lake environments, we tentatively estimated that the highstand lasted approximately 1 kyr during MIS 5d–b. The 30-cm section was sampled in 0.5-cm steps. Diatom species diversity ranges from 19 to 30 through the section. The dominant species are *Pseudostaurosira brevistriata*, *Rhopalodia gibberula*, *Cyclotella meneghiniana* and *Epithemia sorex*. The total of 60 sediment samples provide us with a record at decadal to bi-decadal resolution. Based on diatom assemblages and their oxygen isotope composition ($\delta^{18}\text{O}$) we infer an alkaline and mostly oligohaline lake with shallow water conditions prevailing in MIS 5, and is potentially analogous to a Heinrich event. The climate over southern Africa during MIS 5 has been considered very arid but the hydromorphological context of our sediment section indicates that we captured a mega-lake period providing evidence that short-term excursions to significantly higher humidity existed. A hydrologically more favorable environment during MIS 5 than formerly presumed is in line with the early human occupation of the Kalahari.

2.2 Introduction

Geomorphological studies of the northern and Middle Kalahari in northern Botswana have provided evidence of a former mega-lake system (Passarge, 1904; Grove, 1969; Ebert and Hitchcock, 1978; Cooke, 1979; Heine, 1982; Thomas and Shaw, 1991; Burrough et al., 2009a; Podgorski et al., 2013; Riedel et al., 2014; Fig. 2.1), which developed within the Makgadikgadi–Okavango–Zambezi Basin (MOZB). The structural depression of the MOZB belongs to the southwestern branch of the East African Rift System (Ringrose et al., 2005; Kinabo et al., 2007; Shemang and Molwalefhe, 2011; Riedel et al., 2014). Grey and Cooke (1977) termed highstands in this lacustrine system Lake Palaeo-Makgadikgadi (referring to the Makgadikgadi Basin, the largest and deepest of the depressions), which likely comprised of several lacustrine basins (Fig. 2.1) and exhibited a maximum expansion of about 66,000–90,000 km² (Eckardt et al., 2008; Podgorski et al., 2013). There is geological and phylogeographical evidence that the mega-lake system may have existed since the Early Pleistocene (Genner et al., 2007; Moore et al., 2012; Riedel et al., 2014; Schultheiß et al., 2014). An OSL (optical stimulated luminescence) date of c. 290 kyr (Burrough et al., 2009a) provides only a minimum age of the palaeolake system as this is at the limit of the OSL dating technique (Cordier et al., 2012).

Burrough et al. (2009a) presented a large number of OSL dates in order to illuminate the chronology of mega-lake periods. Apart from two dates that fall within MIS 8 (c. 290 and c. 270 kyr) they dated highstands during MIS 5–MIS 1. Their OSL samples were taken from palaeo-shorelines of the Makgadikgadi Basin, which represents the dominant water body during Lake Palaeo-Makgadikgadi highstands. Burrough et al. (2009a) inferred seven periods of lake highstands in the Makgadikgadi Basin during the past approximately 105 kyr. Two of these

occurred during MIS 5 (104.6 ± 3.1 and 92.2 ± 1.5 kyr) and the next youngest one is of MIS 4 age (64.2 ± 2.0 kyr).

Today, the Makgadikgadi Basin (Fig. 2.1) is characterized by several salt pans. The largest are the central Ntwetwe Pan (about 4700 km²) and the eastern Sua Pan (about 3000 km²), which are occasionally filled with water in modern times, but these temporary infills are not high enough to link the pans together (Riedel et al., 2011). The bottoms of the pans lie generally below an altitude of 950 m a.s.l. (Grove, 1969; Grey and Cooke, 1977; Cooke, 1980; Mallick et al., 1981), with the deepest point (also of the MOZB) located in the northern part of the Sua Pan at an altitude of 890 m a.s.l. (Cooke, 1980; Thomas and Shaw, 1991; Eckardt et al., 2008).

The western margin of the Makgadikgadi Basin is sharply bordered by the prominent Gidikwe Ridge (Fig. 2.1), which stretches about 250 km from north to south and exhibits a series of palaeo-shorelines. Here, two distinct palaeo-shorelines were determined at an altitude of 945 and 936 m a.s.l. (Cooke and Verstappen, 1984; Thomas and Shaw, 1991; Burrough et al., 2009a, b). Lacustrine sediments recorded west to the Gidikwe Ridge (Fig. 2.1) were interpreted to be of lagoon origin (Cooke, 1980; Thomas and Shaw, 1991). The backside of the Gidikwe Ridge, however, was considered a second ridge (Moremaoto) by Gumbrecht et al. (2001; personal observations FR), delimiting the Makalamabedi Basin (Fig. 2.1) to the east, which exhibits a curvilinear morphology interpreted as palaeo-shorelines at approximately 930–940 m a.s.l. (Gumbrecht et al., 2001; Riedel et al., 2014). Near the Moremaoto Ridge about 2-m-thick diatom-rich sediments (personal observation MS and FR) are exposed, which were originally described in Passarge (1904) who considered an Eemian (MIS 5e) lake period. Shaw et al. (1997) re-studied the diatom-rich sediments, established a MIS 3 age and related them to a lake highstand of the Makgadikgadi Basin. These sediments however are located in the Makalamabedi Basin (Riedel et al., 2014).

There are currently no paleontological records from lacustrine sediments in the MOZB older than MIS 3 (Riedel et al., 2014) that could be used to characterize mega-lake periods. Joyce et al. (2005) concluded an extant cichlid radiation emerged from Lake Palaeo-Makgadikgadi during the Middle Pleistocene seeding all major river systems of southern Africa. These fish require freshwater habitats, which could be sustained over longer periods only when the lake had an outlet (Riedel et al., 2014). The Zambezi, which transverses the northern extension of the lacustrine system, could have acted as an outflow during highstands when all basins were connected into a single mega-lake. It has been suggested that the inflow of the Okavango River, and possibly of the Zambezi, controlled mega-lake periods (Nugent, 1990). There are, however, several fossil river systems entering the Makgadikgadi Basin (Riedel et al., 2014) of which the Okwa Valley is the largest (Fig. 2.1). Riedel et al. (2014) suggested that the Okwa River was fully active for the last time during the Last Glacial Maximum and ceased flowing during Heinrich event 1. So far it can only be speculated whether during periods of enhanced Okwa River inflow the Makgadikgadi

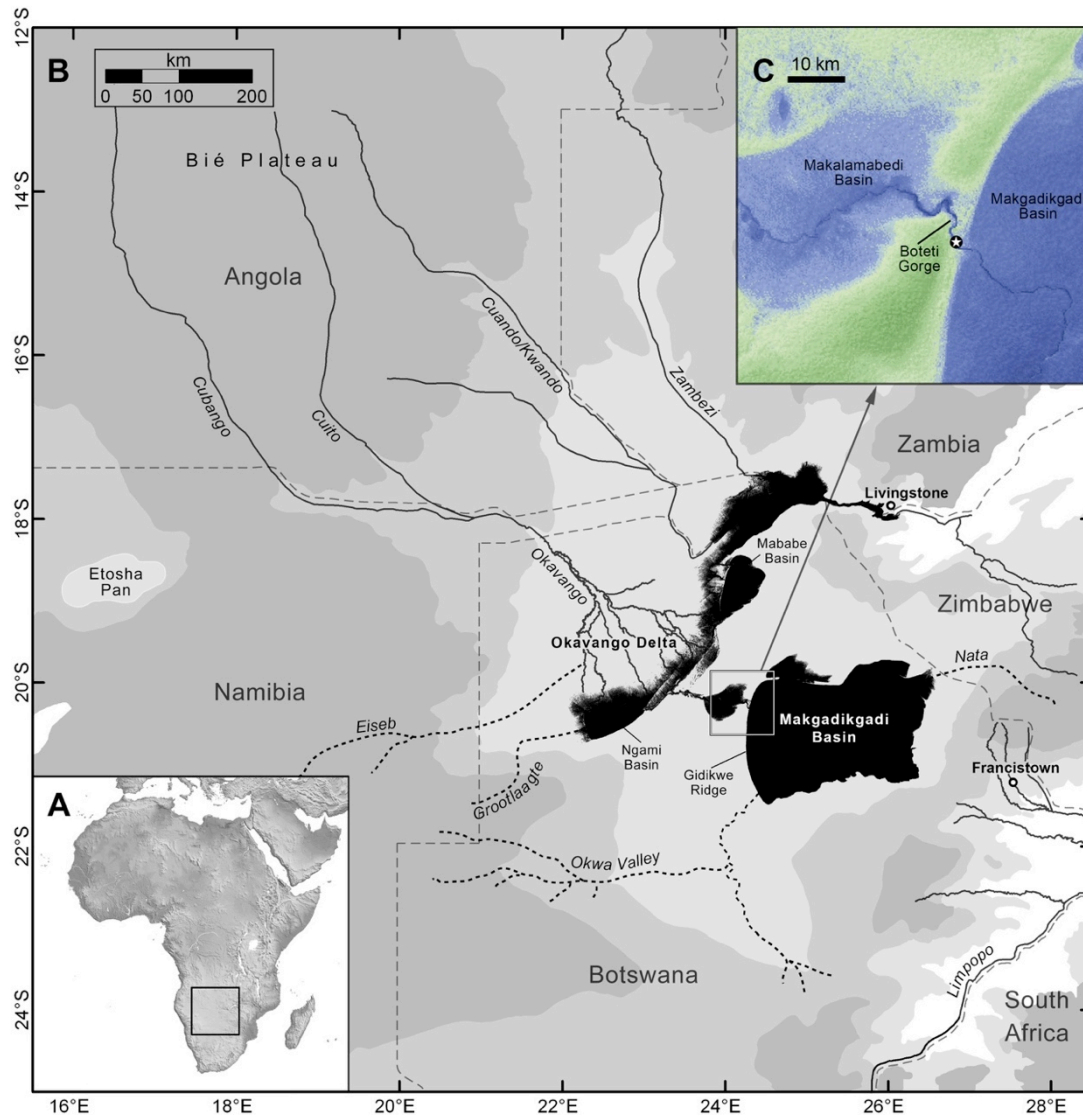


Figure 2.1: (A) General location of study area. (B) Map of Makgadikgadi–Okavango–Zambezi Basin (MOZB) of the south-western branch of the East African Rift System and the major tributaries. Black dashed lines indicate valleys of palaeo-rivers. Major subbasins of MOZB shaded black. During late Quaternary hydrologically favourable periods these subbasins may have been part of a mega-lake. Due to tectonics and hydromorphological processes the modern setting can be used only tentatively for simulating past mega-lake sizes and shapes. (C) A digital elevation model (modified from Riedel et al., 2014) exhibits the location of the studied geological section at the western edge of the Makgadikgadi Basin where palaeoshorelines can be found on the structural Gidikwe Ridge.

Basin became exoreic, with an outflow to the west, and freshwater conditions prevailed (Riedel et al., 2014).

On the one hand the environmental and climatic implications of such large scale Late Quaternary lake-level fluctuations and the dynamics of aeolian activity are mainly controversial and on the other hand the discussion has focused especially on the period MIS 3–MIS 1 (Street and Grove, 1976; Van Zinderen Bakker, 1976; Heine, 1981, 1987, 1988; Stokes et al., 1997;

Gasse et al., 2008; Burrough and Thomas, 2009; Burrough et al., 2009a, b; Hürkamp et al., 2011; Riedel et al., 2014). There has been limited work on MIS 5 sediments, and some climate interpretations do exist although these rely heavily on marine sediments (from off Namibia: Shi et al., 2001; Stuut et al., 2002) at a low temporal resolution (Urrego et al., 2015). It is noteworthy that Urrego et al. (2015) reported increased aridity in southwestern Africa (neighboring our study area) during the warmest periods of MIS 5 (5e, 5c, 5a), but they also identified short increases in humidity during warm-cold and cold-warm transitions. Geyh and Heine (2014) reported MIS 5 speleothem growth from the Namib Desert. In southeastern Africa, MIS 5 was characterized by episodes of extremely arid conditions leading to dramatic low-stands of Lake Malawi (Cohen et al., 2007; Scholz et al., 2007).

These tropical African MIS 5 “megadroughts” (Scholz et al., 2007) are discussed to have facilitated human expansions across Africa and ultimately out of Africa (Rito et al., 2013). Genetic data suggest that anatomically modern humans (Balter, 2002) originated in Africa during MIS 6 (Ingman et al., 2000) and there is archaeological evidence that they populated the southern tip of Africa as early as ~165 kyr (Marean et al., 2007). Genomic diversity of extant hunter-gatherer populations is in agreement with this early occupation of southern Africa and tentatively suggests even the origin of modern humans from this region (Henn et al., 2011). Symbolic and thus modern behavior of such southern African human populations may have first appeared during MIS 5a (Henshilwood et al., 2002) or early MIS 4 (Jacobs and Roberts, 2009). In the Kalahari, archaeological sites at the Tsodilo Hills indicate human occupation since at least 90 kyr (Robbins et al., 2016). Burrough (2016) discussed the environmental contributions to early human dispersal in the Kalahari and emphasized the contrast between MIS 5 lake highstands in the Makgadikgadi Basin and extreme lowstands of Lake Malawi.

The modern climate setting over semi-arid southern Africa is complex (Peel et al., 2007; Gasse et al., 2008; Chase et al., 2012; Riedel et al., 2014) and comprises moisture transport from the West and East African monsoons (including convective moisture from the Congo Basin) to the Okavango catchment and the Kalahari during austral summer. Rainfall variability in Botswana is described by Batisani and Yarnal (2010). During austral winter, moisture from the southeastern Atlantic triggers rainfall (mainly) over the Western Cape Province. Southwestern Indian Ocean (Agulhas Current) derived moisture triggers rainfall over southern Africa mainly during austral summer but also during winter (Chase and Meadows, 2007; Gasse et al., 2008; Burrough et al., 2009b; Chase et al., 2012; Urrego et al., 2015).

The aim of our study is to reconstruct for the first time the palaeohydrological status of a mega-lake phase (about 66,000–90,000 km²) in the MOZB, which corresponds to a highstand of at least 936–945 m a.s.l. of Lake Palaeo-Makgadikgadi, by analyzing diatom assemblages and their oxygen isotope composition ($\delta^{18}\text{O}_{\text{diatom}}$). The mega-lake phase addressed here occurred during MIS 5 and is the first attempt to infer the duration of a mega-lake phase in this region. Our

findings contribute to the understanding of phylogeographical patterns and climate evolution of southern Africa.

2.3 Study site

Our study site (Fig. 2.1) is located at the Gidikwe Ridge where the ridge is cut by the Boteti River valley forming a 20–22 m deep gorge. Here, a 10-m-thick sedimentary succession was exposed (S 20.28672°, E 24.26822°), which exhibited 40 cm consolidated, heavily diagenetically altered lacustrine deposits at the base, followed by 9.3 m unfossiliferous, silcrete- and calcrete-rich playa sediments (Riedel et al., 2014). On the top of the succession of sediments, at about 935 m a.s.l., the playa sediments are overlain by a 30-cm-thick unit (Fig. 2.2), which consists of consolidated, fine-laminated to thin-bedded, finely clastic, light-grey to whitish lacustrine sediments rich in diatoms and deposited during MIS 5 (Riedel et al., 2014). Lithological hiatuses were not identified in the 30-cm unit, suggesting sedimentation was continuous. This sediment unit thins out a few hundred meters west of the section where sandy palaeo-beach features can be found indicating that the former shore was relatively close.

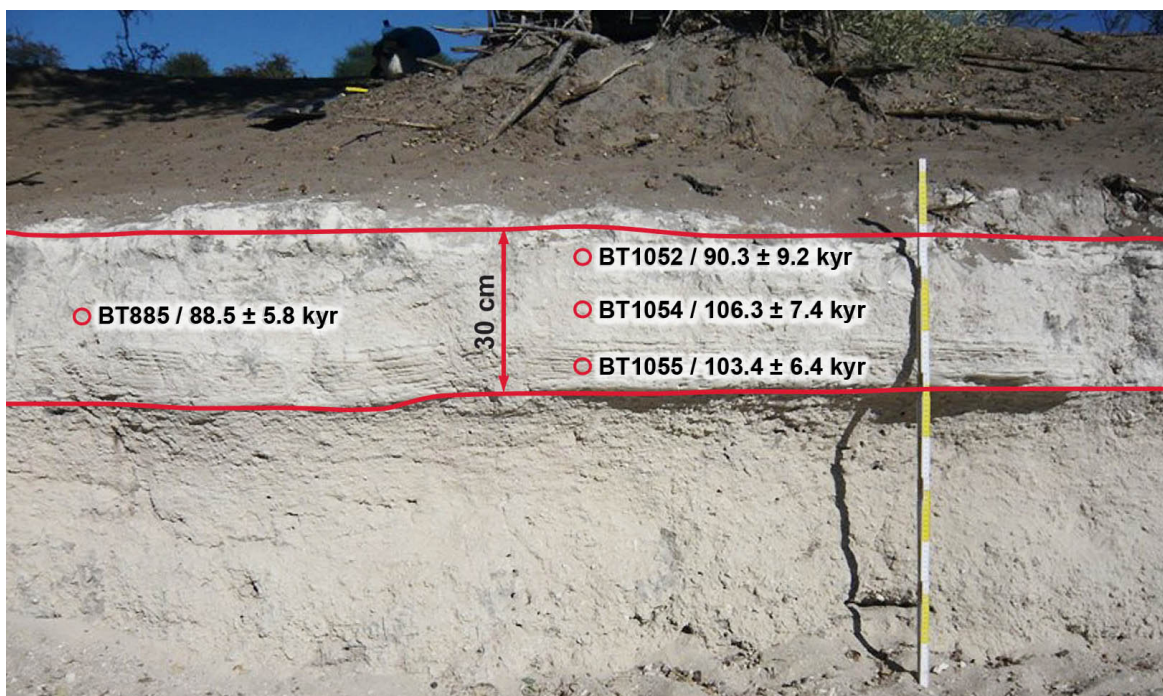


Figure 2.2: Upper part of the Boteti river valley section with studied 30-cm diatom-rich sediment unit on top (BT). Position of samples for OSL dating and OSL dates are indicated.

2.4 Materials and methods

2.4.1 Sediment samples

The 10-m sediment outcrop within the Boteti Gorge at the western margin of the Makgadikgadi Basin (Figs. 2.1, 2.2) was first visited by AK and FR in 2007 and a small number of samples were taken. Samples from a 40-cm-thick unit of white and pale-gray lacustrine sediments at the base of the profile has been strongly affected by diagenesis, and contains only few broken valves of diatoms, while the light-grey to whitish 30-cm-thick deposits at the top of the section (Boteti Top = BT) have abundant diatoms. Although carbonate is contained in BT, remains of ostracod valves were only exceptionally preserved. Except for a few pollen grains, no other fossil remains were identified. When revisiting the section in 2009 samples for OSL dating were taken from the two lacustrine sediment units. MF provided an OSL date suggesting MIS 5 age for BT. OSL dating of the 40-cm unit at the base of the Boteti section failed because the OSL signal was close to saturation and therefore at its upper limit.

In 2011 the outcrop was revisited for high-resolution sampling and a fresh surface was exposed and thoroughly cleaned using spade, saw, knife and brush. The sampling of the relatively hard sediments was done in 0.5-cm increments with a knife from the base to the top of the BT unit. 60 sediment samples of about 60 grams each were taken, sample BT_{diatom}-1 corresponding to the lowermost and sample BT_{diatom}-60 to the uppermost layer. In addition, using a saw, a 30 × 15 × 15-cm-sediment block was removed covering the complete BT unit in order to obtain suitable material for optical dating. The sawed surfaces did not exhibit cracks through which light could have penetrated into the internal sediments. The block was immediately wrapped with thick black plastic foil and stored in a sealed box.

2.4.2 OSL dating

Samples were taken from the lower (BT 1055), middle (BT 1054) and upper part (BT 1052) of the sediment block in the OSL lab of Bayreuth University, Germany. A further sample (BT 885) from the middle part of the BT section had been already obtained during fieldwork in 2009 (Fig. 2.2).

The coarse grain quartz fraction (90–200 µm) of the sediment samples was used for OSL dating. Luminescence measurements were carried out using a Risø-Reader TL / OSL-DA-15 (Bøtter-Jensen, 1997), equipped with blue LEDs (470 ± 30 nm) for stimulation, a Thorn-EMI 9235QA photomultiplier combined with one 7.5 mm U-340 Hoya filter (transmission 290–370 nm) for detection and a ⁹⁰Y / ⁹⁰Sr β-source (8.1 ± 0.6 Gy / min) for artificial irradiation.

The equivalent dose (D_e) was determined by applying a single aliquot regenerative (SAR) dose protocol (Murray and Wintle, 2000). Shine-down curves were measured for 20 s at elevated temperatures (125 °C) after preheats for 10 s at 220 and 240 °C respectively for the natural

and regenerated signals and a cut-heat of 160 °C for the test doses. The preheat temperatures were chosen after a preheat plateau test, which indicated that the given dose could be reproduced within a temperature range of 220–240 °C.

Finally, the D_e was calculated from the integral of the first 0.4 s from the shine-down curves after subtracting the mean background (16–20 s) signal. For each sample, up to 28 small aliquots (steal cups) were measured with 200–500 grains per aliquot. Possible feldspar contamination of the aliquots was checked by stimulating the artificially irradiated samples with infrared (IR-OSL) and detecting in the UV range (290–370 nm). For D_e determination, only those aliquots of a sample were used, which passed the criteria of a recycling ratio of 1 ± 0.1 and a recuperation value of <5% (Murray and Wintle, 2000). The standard error was used as D_e error.

The dose rate (\dot{D}) for OSL age calculation was determined by thick source α -counting and ICP-MS. Cosmic-ray dose rates were calculated according to Prescott and Hutton (1994). The water content of the samples was determined using the average value of the possible water content range, based on the porosity of the samples. An error for the water content value was chosen, which included the possible water content range. The values used for the water content were checked by measuring the in situ water contents of the samples, showing conformity within errors.

2.4.3 Diatom assemblages

Diatom extraction and slide preparation for microscopic analyses were carried out following Battarbee et al. (2001). Diatom identification and counting were performed using a Meiji Techno 4000 microscope at 1000 \times magnification with an oil immersion objective. Approximately 500 diatom valves were counted per sample to ensure that effective numbers of taxa were counted. Diatom relative abundances were plotted using Tilia® (Grimm, 1991–2011), and planktonic to benthic ratios calculated according to the formula: $\Sigma_{(\text{planktonic})} / \Sigma_{(\text{planktonic} + \text{benthic})}$.

For precise identification of the diatom taxa, a Zeiss Supra 40 VP scanning electron microscope (SEM) was additionally used. Diatoms for the SEM analyses were prepared by drying 0.5 ml of the treated sample suspension on a cover slip fixed on a stub. After drying, the diatoms were coated with gold in a sputter coater and then examined with the SEM. Diatom species were identified using, amongst other keys, Krammer (2002), Krammer and Lange-Bertalot (1997, 1999, 2000, 2004), Levkov (2009) and Kusber and Cocquyt (2012). A list of species and their authorities is provided in ESM 2.1.

The ecological preferences of identified diatoms concerning salinity, pH and trophic level were taken from the literature (ESM 2.2), but are unknown in some taxa. The salinity classification follows Schlunbaum and Baudler (2001): freshwater = <0.5 psu; oligohaline = 0.5 to <5 psu; mesohaline = 5–18 psu; euryhaline = fresh to saltwater, indifferent or non- significant.

Ordination analyses were undertaken using Canoco 4.5 (ter Braak and Šmilauer, 2002) to reveal major trends in the diatom data. An initial detrended correspondence analysis (DCA) gave an axis 1 gradient of only 0.734, revealing a dataset with very little species turnover, so principal components analysis (PCA) was used instead. Scaling for both samples and species was optimized through symmetric scaling of the ordination scores (Gabriel, 2002). Because we have closed relative abundance data, species data were $\log(x + 1)$ transformed and both species and samples were centered to give a log-linear contrast PCA (Lotter and Birks, 1993). To determine if any of the PCA axes were in themselves significant in explaining variation in the diatom data, a broken stick analyses was undertaken (Jolliffe, 1986). The diatom stratigraphy was zoned using - (CONISS) according to Grimm (1991–2011).

2.4.4 Diatom oxygen isotope analysis

From the 60 BT samples studied in respect of diatom assemblages, alternate samples were analyzed for their oxygen isotope composition. Following the protocol established by Morley et al. (2004) the 30 sediment samples for $\delta^{18}\text{O}_{\text{diatom}}$ analysis underwent chemical digestion using 30% H_2O_2 and 5% HCl followed by sieving of samples at 74 and 10 μm . Diatoms were then isolated using a combination of differential settling and heavy liquid separation using sodium polytungstate (SPT). The SPT was then washed out of the purified sample using multiple rinses of deionized distilled water, and dried down prior to analysis. Samples were measured using a step-wise fluorination procedure using 6 mg of sample (Leng and Sloane, 2008) and a Finnigan MAT 253 isotope ratio mass spectrometer. $\delta^{18}\text{O}_{\text{diatom}}$ were converted to the Vienna Standard Mean Ocean Water (VSMOW) scale using an international laboratory diatom standard (BFC_{mod}) calibrated against NBS28. The methodology has been verified through an inter-laboratory calibration exercise (Chapligin et al., 2011). Replicate analyses of sample material from this current study indicating an analytical reproducibility (mean difference) of 0.2% ($1\sigma = 0.5$, $n = 9$).

2.5 Results

2.5.1 OSL dating

The suitability of the quartz extracts for OSL dating was evaluated using a combined preheat plateau and dose-recovery test. In ESM 2.3c, the result of this test is shown, indicating the given dose of 70.2 Gy could be reproduced within a temperature range of 220–260 °C. In addition, ESM 2.3a shows a typical OSL shine-down curve, displaying a bright OSL signal that is quickly bleached to measurement background. Growth curves could be established with high precision, with recycling ratios of 0.9–1.1 (ESM 2.3b). Thus, the OSL quartz behavior, the preheat plateau and the dose-recovery tests demonstrate the suitability of the applied SAR protocol.

2. Manuscript I - 2.5 Results

In Table 2.1, the analytical data for OSL age calculation, including the data for dose rate determination are given. The results of the OSL age calculation ranging from 106.3 ± 7.4 to 88.5 ± 5.8 kyr indicate the studied section can be assigned to MIS 5. The sample BT 1055 from the lower part of the studied sediment unit (Fig. 2.2) has an OSL age of 103.4 ± 6.4 kyr, the following sample BT 1054 from the middle part of the 30-cm unit (Fig. 2.2) shows an age of 106.3 ± 7.4 kyr, which is within errors still consistent with the stratigraphic order. Sample BT 1052 from the upper part (Fig. 2.2) reveals an age of 90.3 ± 9.2 kyr. The sample BT 885, which was previously taken in 2009, shows an age of 88.5 ± 5.8 kyr and correlates with the result of BT1052 (Table 2.1).

Table 2.1: Analytical data for OSL age calculation: sample code, ^{238}U , ^{232}Th and 40K-concentrations, total dose rate, equivalent dose and OSL age.

Sample	U [ppm]	Th [ppm]	K [%]	D [Gy/kyr]	D_e [Gy]	OSL Age [kyr]
BT 885	1.14 ± 0.08	2.20 ± 0.05	0.41 ± 0.01	0.88 ± 0.04	77.6 ± 3.8	88.5 ± 5.8
BT 1052	0.97 ± 0.10	2.02 ± 0.04	0.32 ± 0.01	0.66 ± 0.03	59.7 ± 5.2	90.3 ± 9.2
BT 1054	0.91 ± 0.07	2.38 ± 0.05	0.34 ± 0.01	0.69 ± 0.33	72.9 ± 3.7	106.3 ± 7.4
BT 1055	0.93 ± 0.09	2.42 ± 0.05	0.33 ± 0.01	0.68 ± 0.33	70.7 ± 2.8	103.4 ± 6.4

2.5.2 Diatom assemblages and $\delta^{18}\text{O}_{\text{diatom}}$

The microscopic analyses of the samples reveal the sediments are rich in well-preserved diatom valves (Fig. 2.3). In total, 50 species could be identified of which 44 species are benthic, that is they prefer littoral rather than planktonic habitats (ESM 2.1, ESM 2.2). The number of species per sample ranges from 19 to 30. Generally, most species are represented by a few valves only. Benthic diatoms dominate the whole sequence (70–95%), especially in the uppermost sediments, resulting in very low planktonic / benthic ratios (Fig. 2.4).

Using broken stick, only PCA axis 1 showed significant variation. PCA axis 1 sample scores are therefore also plotted against depth in Fig. 2.4. These data show considerable variation, superimposed on a strong directional change from the base of the sediment unit to about 25 cm, before sample scores decline to the top of the profile. A moderate but significant Pearson product moment correlation coefficient exists between PCA axis 1 sample scores and the P/B ratio ($r = -0.618$; $p = 0.0001$). CONISS has delimited 3 zones (Kala-1 to Kala-3), with major divisions at 13.75 and 23.25 cm (Fig. 2.4).

Kala-1: This zone is dominated by *Pseudostaurosira brevistriata* and *Rhopalodia gibberula*, although the planktonic *Cyclotella meneghiniana* is also abundant, resulting in highest P/B ratios for the sequence and lowest PCA axis 1 samples scores. *Halamphora thermalis* is also relatively common. At this time, $\delta^{18}\text{O}_{\text{diatom}}$ values increase steadily to their highest values of +34.2‰ at 11.5 cm.

Kala-2: This zone is delimited by a small peak in *P. brevistriata*, a P/B minimum and declining $\delta^{18}\text{O}_{\text{diatom}}$ values. Within this zone, the most notable changes include declining *C. meneghiniana* values and increases in *Epithemia sorex*.

Kala-3: This zone is delimited by very low P/B ratio values and high PCA axis 1 samples, and lowest $\delta^{18}\text{O}_{\text{diatom}}$ values (+28.2‰ at 23.5 cm). During this zone, *C. meneghiniana* values are generally at their lowest, while *E. sorex* values are at their highest. Towards the top of this zone, P/B ratio values increase slightly, concomitant with declining PCA axis 1 sample scores and increasing $\delta^{18}\text{O}_{\text{diatom}}$ values to about +31‰.

The inferred hydrological parameters (salinity, trophic status, pH) show little variation throughout the palaeolake-phase. Most diatoms are tolerant to salinity fluctuations but about 15% of the species of the assemblages reflect oligohaline conditions in zones Kala-1 and -2 with an increase to 20% in Kala-3. About 60% of the diatom species indicate eutrophic conditions and 20–30% are nutrient-tolerant. The pH reconstruction indicates alkaline conditions (>7). Approximately 30–40% of the diatom species require pH values of 7–8 and 50–80% of 8–9 with slight decrease of alkalinity during zone Kala-3.

2.6 Discussion

2.6.1 Dating

Age calculation of mega-lake phases in the MOZB (Fig. 2.1) has previously been established using a large set of OSL dates from palaeo-shoreline features (Burrough and Thomas, 2009; Burrough et al., 2009a, b). In respect of MIS 5, Burrough et al. (2009a) identified two highstands of Lake Palaeo-Makgadikgadi centered at *c.* 105 and *c.* 92 kyr respectively, analyzed as “events of unknown duration” (Burrough et al., 2009b). In contrast to samples obtained from shoreline sediments (Burrough et al., 2009a), which may have been reworked by waves, we dated quartz grains from a low energy aquatic milieu. The fine lamination of the sediments indicates still water conditions below the wave-line and reworking of the sediments can likely be ruled out. The range of our dates, however, shows large uncertainty remains. Considering the uncertainties of the oldest (106.3 ± 7.4 kyr) and the youngest age (88.5 ± 5.8 kyr), the max. range is 113.7–82.7 kyr, a period of 31 kyr covering roughly MIS 5d–b, and the min. range is 98.9–94.3 kyr, a period of 4.6 kyr.

The range has to be considered in the context of the duration of continuous deposition of 30 cm of lacustrine sediments. In comparison with lake systems showing at least partly similar (palaeo-) environmental settings (Aral Sea: 30 cm ~650 years, Filippov and Riedel, 2009; Lake Titicaca: 30 cm ~900–1200 years, Fornace et al., 2014; Tso Moriri, Ladakh, India: 30 cm ~1100 years, Leipe et al., 2014a; Lake Kotokel, Buryatia, Russia: 30 cm ~700 years, Kostrova et al., 2016; Lake Teletskoye, Russian Altai: 30 cm ~600 years, Mitrofanova et al., 2016; Lake Van, Turkey: 30 cm ~1000 years, North et al., unpublished data) it can be roughly estimated that the 30-cm sediment unit of the Boteti section had been deposited during a period of approximately 1 kyr.

It is possible, but not likely that the terminal highstand is not archived in the 30-cm unit. This could be because of potential deflation processes after the lake level had decreased. Once exposed, sediments of such composition usually harden quickly under a (semi-) arid climate and subsequent weathering and erosion processes are limited. This is also due to the fact that under retreating lake levels, aeolian activity is increasing and consolidated lacustrine sediment sequences are often, instead of being deflated, covered by sand (as can be observed across the MOZB), which protects them from erosion. Moreover, the 40-cm-lacustrine-sediment unit at the base of the Boteti section, which is overlain by playa sediments, appears to be complete and provides an independent example of a relatively short lake highstand. We thus can provide at least a first idea how long so-called mega-lake phases may have lasted.

The estimation that the 30-cm-sediment unit covers a period of not more than approximately 1 kyr allows us to infer a temporal resolution of the analyzed samples of 1–2 decades. Dating uncertainties remains a major challenge for an accurate reconstruction of environmental dynamics in the Kalahari, and is probably responsible for most of the controversial discussions related to (Street and Grove, 1976; Heine, 1981, 1987, 1988; Stokes et al., 1997; Gasse et al., 2008; Burrough and Thomas, 2009; Burrough et al., 2009a, b; Chase and Brewer, 2009; Hürkamp et al., 2011; Riedel et al., 2014; Burrough, 2016).

Significant uncertainties also exist with respect to measured palaeo-shoreline altitudes. In a number of studies the uncertainty is as high or even higher as the 9 m difference between the 936 and 945 m a.s.l. palaeo-shorelines (Riedel et al., 2014). On the other hand, it is unlikely mega-lake highstands reached the same elevation repeatedly, except in exceptional circumstances. The two different lacustrine sediment units of the Boteti section indicate two lake periods at the same position, which means they are of likely similar extension, although the older highstand is about 9.3 m lower than the younger one. The amount of available water during these two periods may have been similar, pointing at comparable climate settings, but with increased accumulation of sediments in the MOZB raising the lake floor (Haddon and McCarthy, 2005). Thus a higher lake level of significant younger age than an earlier lower lake level could have potentially been reached even with less hydrological input.

2.6.2 Diatom assemblages and $\delta^{18}\text{O}_{\text{diatom}}$

The diatom assemblage presented here is very different from contemporary flora found in the fresh, shallow waters of the Okavango Delta (Mackay et al., 2012). The dominance of benthic taxa (Fig. 2.4) in the BT unit indicates the persistence of shallow water conditions and extensive littoral regions, especially during the terminal stages of sediment accumulation (zone Kala-3). Patrick (1977) described *E. sorex* as an aerophilous species that can persist in environments characterized by desiccation. Therefore, an increase of the abundance of *E. sorex* within the sediments at this time potentially shows a stronger proximity to the shoreline caused by a drop in lake level during this period of inferred lake level decline. The maximum water depth can be calculated in the hydromorphological context to have been a few meters only (max. depth of palaeolake ~50 m). The diatom assemblages reveal changes in lake water depth throughout the record. The significant correlation between PCA axis 1 sample scores and P/B ratio suggests varying water levels influenced diatom composition in the shallow lake waters. What is notable is the period of highest P/B ratio is coincident with increasing $\delta^{18}\text{O}_{\text{diatom}}$ values (increasing effective moisture), indicative of increasing planktonic habitats in this part of the lake (Fig. 2.4).

These shallow waters were likely freshwater to brackish; qualitative salinity reconstruction indicate oligohaline conditions (0.5 to <5 psu) persisted during the whole period (Fig. 2.4). For example, the dominant species *P. brevistriata*, *R. gibberula* and *M. elliptica* have wide salinity tolerances (Caljon and Cocquyt, 1992; Krammer and Lange-Bertalot, 1999; Van Dam et al., 1994; Stachura-Suchoples, 2001). *E. sorex* is also described from oligohaline waters (Cholnoky, 1968; Patrick, 1977; Krammer and Lange-Bertalot, 1999; Kelly et al., 2005), while *C. meneghiniana* is often found in brackish water (Hecky and Kilham, 1973).

The qualitative oligohaline salinity reconstruction at the study site does not mean that Lake Palaeo-Makgadikgadi was oligohaline in general but exhibited salinity gradients. Filling up and interconnecting the lacustrine basins to a single lake (Fig. 2.1) required significant inflow from at least one of the major river systems, either from the Okavango River in the (north-) west or from the Okwa River in the southwest. It also cannot be ruled out that both river systems were active simultaneously. If the Okavango was the main source of hydrological input, the main lacustrine depression of the palaeolake-system, the Makgadikgadi Basin, would have acted as a terminal lake with increasing salinity to the east (Fig. 2.1). The likely outflow in this scenario would be through the Zambezi valley. Therefore, western lake areas between major inflow and outflow would have been under freshwater conditions. An example of a comparator to this behavior can be found at extant Bosten Lake, Xinjiang, China, where inflow and outflow are located at the western side of the lake and freshwater conditions prevail only there, while the largest part of the water body is oligohaline (Mischke and Wünnemann, 2006; Wufuer et al., 2014; personal observation FR). A second scenario considers the Okwa River the main source of water inflow

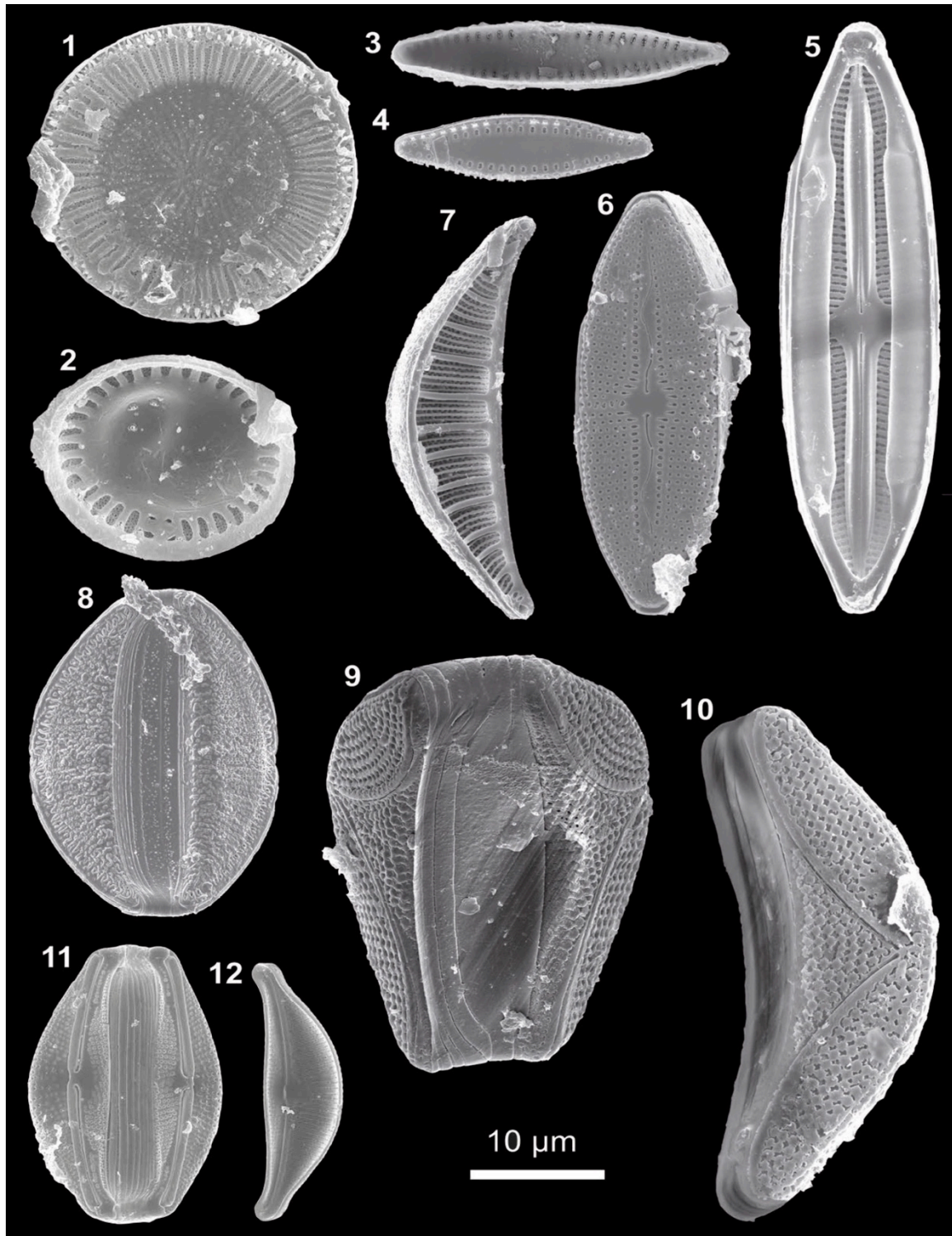


Figure 2.3: Scanning electron microscope images of the six most abundant diatom species identified in the Boteti section top unit (BT). 1–2 *Cyclotella meneghiniana*, 3–4 *Pseudostaurosira brevistriata*, 5–6 *Mastogloia elliptica*, 7–8 *Rhopalodia gibberula*, 9–10 *Epithemia sorex*, 11–12 *Halamphora thermalis*.

during the highstand. In this case the Makgadikgadi Basin was exoreic and the study site would have been in proximity to the outflow. In both scenarios freshwater areas are limited, and

considering the relatively short period of approximately 1 kyr, the mega-lake phase likely did not foster evolutionary radiations of freshwater fish or gastropods. This is in agreement with the phylogeographic studies of Joyce et al. (2005) and Schultheiß et al. (2014) who considered Early to Middle Pleistocene age of Lake Palaeo-Makgadikgadi evolutionary radiations, indicating palaeohydrology and hydromorphology differed significantly from our observed MIS 5 setting.

In respect of pH, it can be inferred from the diatoms that the lake was always alkaline (pH ~8). Whereas *C. meneghiniana*, *E. sorex*, *H. thermalis* and *R. gibberula* occur preferentially in waters with the pH greater than 8 (Cholnoky, 1968; Gasse, 1986; Gasse et al., 1995; Van Dam et al., 1994), *M. elliptica* and *P. brevistriata* predominantly occur in circumneutral to low alkaline waters (pH = 7–8; Cholnoky, 1968; Gasse, 1986; Van Dam et al., 1994; Stachura-Suchoples, 2001; Fig. 2.4). In addition, *P. brevistriata*, *C. meneghiniana*, and *E. sorex* indicate elevated trophic levels throughout the record (Cholnoky, 1968; Van Dam et al., 1994; Gasse et al. 1995; Krammer and Lange-Bertalot, 2000; Stachura-Suchoples, 2001; Kelly et al., 2005).

The $\delta^{18}\text{O}_{\text{diatom}}$ data reflects the oxygen isotope composition of lake water ($\delta^{18}\text{O}_{\text{lake}}$), and the water temperature at the time of frustule formation (Leng and Barker 2006; Leng and Henderson, 2013). In turn, $\delta^{18}\text{O}_{\text{lake}}$ is controlled by the isotopic composition of precipitation ($\delta^{18}\text{O}_{\text{p}}$) recharging the lake and the balance of evaporation over precipitation on the lake. Open lake systems that have permanent river inflow and outflow have short residence times, and as a result $\delta^{18}\text{O}_{\text{diatom}}$ tends to reflect changes in $\delta^{18}\text{O}_{\text{p}}$. Whereas in closed lakes that have no discernable outflow, $\delta^{18}\text{O}_{\text{lake}}$ is usually influenced by evaporation of surface waters, and as a result $\delta^{18}\text{O}_{\text{diatom}}$ reflects the moisture balance (precipitation over evaporation) of the region (Leng and Marshall, 2004; Leng and Barker, 2006; Leng and Henderson, 2013).

There is scant information about the isotope composition of precipitation ($\delta^{18}\text{O}_{\text{p}}$) in Botswana, and southern Africa in general, with much of our understanding of isotope dynamics linked to changes in Late Pleistocene groundwater and speleothem $\delta^{18}\text{O}$ records (de Vries et al., 2000; Lee-Thorp et al., 2001; Holmgren et al., 2003; Kulongoski et al., 2004). The ^{18}O enrichment of older groundwaters in Uitenhage, South Africa, have previously been interpreted in terms of a change in moisture source, with a northeastward incursion of South Atlantic winter precipitation, which displaces or mixes with monsoonal precipitation from the Indian Ocean in southwestern Africa (Stute and Talma, 1998). By comparison, a more recent study from Letlhakeng, southern Botswana, suggests there was no role for Atlantic-sourced moisture and that the Indian Ocean has been the dominant moisture source over the southern Kalahari since the Late Pleistocene through to the present day (Kulongoski et al., 2004). The influence of the ‘amount effect’ on $\delta^{18}\text{O}_{\text{p}}$ has also been discounted, as modern $\delta^{18}\text{O}_{\text{p}}$ values for the region range from 0 to –5‰, but the most depleted $\delta^{18}\text{O}_{\text{p}}$ values occur during months with the most amount of rainfall (de Vries et al., 2000). As a result, Kulongoski et al. (2004) concluded that Late Pleistocene groundwater $\delta^{18}\text{O}$

variability is caused by changes in atmosphere- $\delta^{18}\text{O}_p$ dynamics driven by changing sea surface temperatures.

A $\delta^{18}\text{O}$ speleothem record from Cold Air Cave in the Makapansgat Valley, northern South Africa, was interpreted in terms of $\delta^{18}\text{O}_p$ variability caused by changes in the frequency of intense convective storm events during the dry season that bring depleted $\delta^{18}\text{O}_p$ (Rozanski et al., 1993), against a background of persistent mid-latitude rain during the wet season (Holmgren et al., 2003). As a result, higher or more positive $\delta^{18}\text{O}_p$ values reflect generally warmer, wetter conditions while lower values suggest cooler, drier conditions. This interpretation is supported by a 100-year data set from the region, which demonstrates a positive correlation between measured regional temperatures and speleothem $\delta^{18}\text{O}$ (Lee-Thorp et al., 2001). In addition, an observed correlation between regional temperature and precipitation and speleothem color, layer thickness and $\delta^{18}\text{O}$ further supports the interpretation that lighter $\delta^{18}\text{O}_p$ is representative of drier, colder conditions over southern Africa (Holmgren et al., 1999).

The $\delta^{18}\text{O}_{\text{diatom}}$ record from the BT unit spans approximately 1 kyr sometime during MIS 5d–b and shows decadal to bi-decadal variability. Based on the interpretative framework for changes in $\delta^{18}\text{O}_p$ during the Late Pleistocene set out above, the shift in $\delta^{18}\text{O}_{\text{diatom}}$ from +30.5‰ at the base of the sediment unit to higher values of +34.2‰ at 11.5 cm would indicate increasingly warmer and wetter conditions during this period (Fig. 2.4). The lower $\delta^{18}\text{O}_{\text{diatom}}$ values would be driven by the enhancement of a wet season over the Kalahari and a subsequent increase in lake level. This observation is consistent with the increase in P/B ratio (Fig. 2.4), suggesting an increase in planktonic habitats associated with greater lake levels. Moreover, on top of an increasing lake level, the lake water would also be undergoing enhanced evaporation because of the generally warmer conditions, and therefore lake waters would also become further enriched in ^{18}O . Taken together, the shift to a dominant wet season and greater evaporation would both drive $\delta^{18}\text{O}_{\text{diatom}}$ to the more positive values observed in our record (Fig. 2.4). However, it is difficult to tease out which would be the dominant mechanism, and the $\delta^{18}\text{O}_{\text{diatom}}$ record is likely to reflect a combination of both.

After the initial increase there are a number of significant fluctuations in $\delta^{18}\text{O}_{\text{diatom}}$ from +34 to +30.5‰ between 11.5 and 19.5 cm (Fig. 2.4), which broadly mirror changes in P/B, and could reflect variability between warm-wet and cold-arid climate, as well as the subsequent changes in evaporative concentration of Lake Palaeo-Makgadikgadi. Following this, the shift to the lowest $\delta^{18}\text{O}_{\text{diatom}}$ values in our record occurs at 23.5 cm (Fig. 2.4), which we interpret as a shift to colder and more arid conditions, as well as a lowering of lake level as indicated by the P/B ratio from the diatom assemblages. The return to more positive $\delta^{18}\text{O}_{\text{diatom}}$ values after this event (Fig. 2.4) could reflect a shift back to a warm, wet environment, but as the P/B ratios show, lake levels remain low and so could reflect enhanced evaporation of lake water during this arid stage in climate.

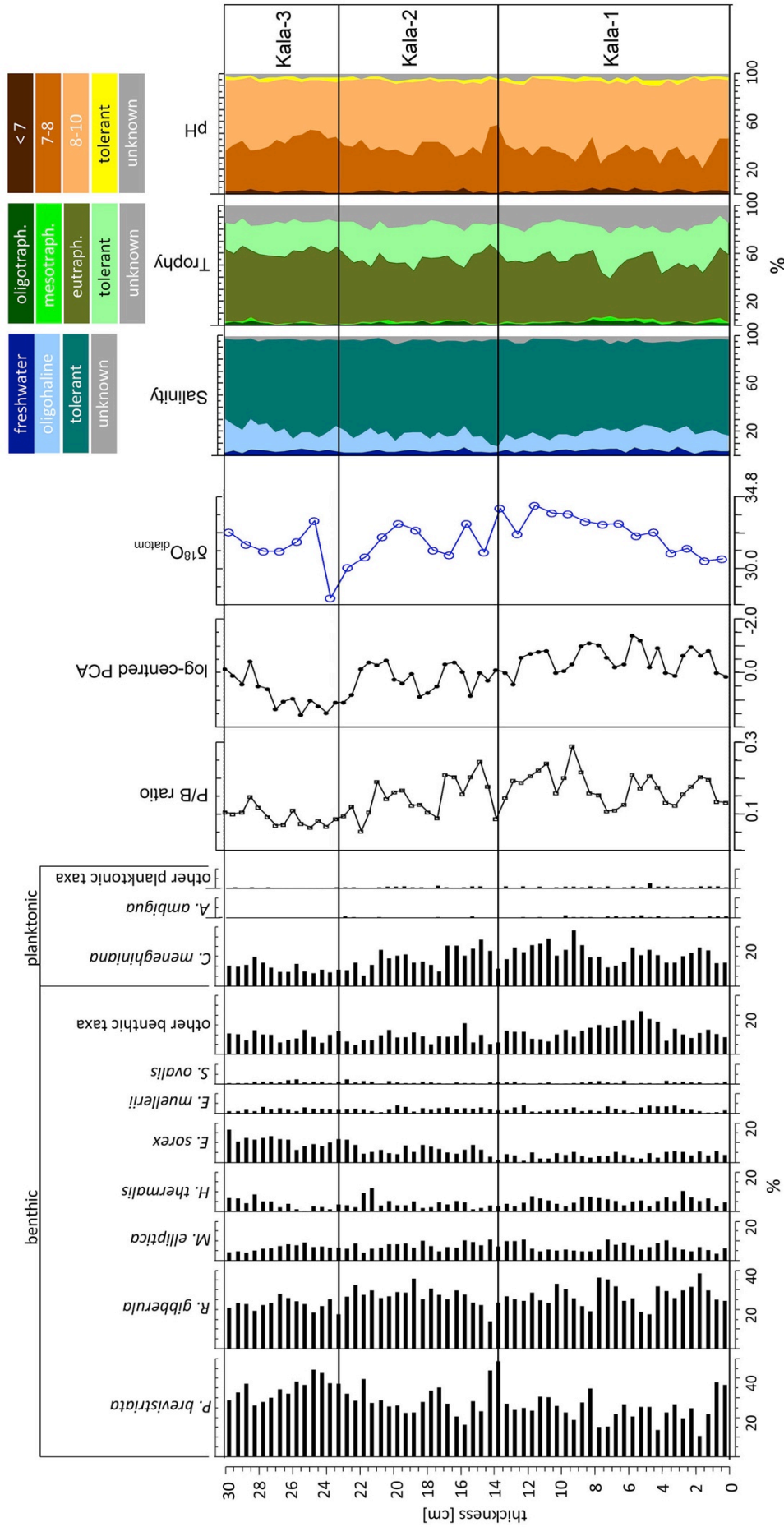


Figure 2.4: Composite diagram illustrating percentage abundances of most frequent species separated into benthic and planktonic forms, P/B ratio, log-centred PCA, $\delta^{18}\text{O}_{\text{diatom}}$ variability, and stack diagrams for salinity, trophic and pH inferred from the autecology of the diatom species.

The relatively short duration of the mega-lake phase of approximately 1 kyr under a generally arid climate over large parts of southern Africa during MIS 5 (Scholz et al., 2007; Urrego et al., 2015) suggests we may have captured a climate event at the scale of a Heinrich event (Bond and Lotti, 1995; Broecker, 2002). Previous studies have modeled the impact of Heinrich events on South Atlantic sea surface temperatures, which increase abruptly (“Atlantic Heat Piracy Model”, Ganopolski and Rahmstorf, 2001; Seidov and Maslin, 2001). The climatic effect of northern hemisphere triggered Heinrich events on the southern hemisphere has also been identified in Antarctica ice cores (Jouzel et al., 2007). The observation of Urrego et al. (2015) that during climate transitions between warm and cold or cold and warm, humidity during arid MIS 5 temporarily increased, supports the idea of a Heinrich event-like climate period. Our record thus demonstrates the decadal to bi-decadal climate variability during such an event.

Our data cannot contribute to the discussion whether the MIS 5 climate extremes triggered large-scale early human migration across and ultimately out of Africa (Carto et al., 2009; Rito et al., 2013). The data, however, can contribute to the discussion why the Kalahari hunter-gatherers, i.e. the Khoisan-speaking Bushmen groups, represent the genetically most divergent population in the world (Tishkoff et al., 2007; Li et al., 2008; Henn et al., 2011). High genetic variation means high adaptation potential (Charlesworth, 2009). Semi-arid areas such as the Kalahari are particularly vulnerable because small negative changes in precipitation amount or in rainfall seasonality may trigger major changes in the environment and thus largely control the habitability. Even under the assumption of large dating uncertainties, it is clear that anatomically modern humans have lived in the Kalahari during MIS 5 and the climate extremes likely triggered migration to environmentally more favorable regions. On the other hand it is evident that Khoisan-speaking groups have adapted to arid climate, exhibiting traits, which are absent in other human groups such as the ability to store water and lipid metabolites in body tissues (Schuster et al., 2010). Considering these adaptations in the context of archaeological findings (Robbins et al., 2016), it can be assumed that Khoisan-speaking groups have lived permanently in (semi-)arid environments since MIS 5, that is they probably never left the Kalahari as other human groups did. The environmental history of the Kalahari since MIS 5 appears to be a highly dynamic and thus often fragmented ecosystem; habitat fragmentation leads to human population fragmentation. Small populations however are prone to genetic drift, which results in loss of genetic variation (Charlesworth, 2009). Against this background it can be suggested that the Khoisan-speaking groups have not been fragmented into small populations but represented a relatively large human population all over the Kalahari. This was possible only if these humans and the animals they hunted had access to potable water.

The here studied MIS 5 lake highstand in the MOZB of approximately 1 kyr appears to be a relatively short period, which however, can be compared with the tip of an iceberg. We do not know how far the lake regressed after the highstand. We do not know how the seasonality of MIS

5 rainfall was. We do not know which rivers were active during which period of supposedly extra-arid MIS 5, except that we can assume from the geographical settings of headwaters that Okavango, Orange and Zambezi rivers were likely perennial even during megadroughts. These river systems however cannot have been the only sources of potable water because otherwise the Khoisan-speaking population would have been fragmented, which evidently was not the case. The idea that the Kalahari was even drier than present day during much of the last approximately 100 kyr as was postulated for MIS 5 (Urrego et al., 2015) or for the Last Glacial Maximum (LGM; Riedel et al., 2014) must be questioned. Gasse et al. (2008) saw evidence for enhanced humidity over parts of southwestern Africa during LGM. Hürkamp et al. (2011) proposed winter rainfall in addition to summer rainfall over the southern Kalahari during this period and Riedel et al. (2014) suggested that the Okwa River (Fig. 2.1) was fully active during the LGM. It thus can be speculated that future studies of MIS 5 climate over the Kalahari may exhibit the environment was more favorable for humans than supposed.

2.7 Conclusions

OSL ages suggest the identified mega-lake phase in the Kalahari occurred during a period of MIS 5d–b. The climate over southern Africa during MIS 5 was considered to have been (extremely) arid (Scholz et al., 2007; Urrego et al., 2015), although Urrego et al. (2015) identified short excursions to more humid conditions during cold-warm and warm-cold transitions. One of these humid periods triggered a highstand at Lake Palaeo-Makgadikgadi of about 935–940 m a.s.l. for approximately 1 kyr, as is tentatively estimated here based on the potential sedimentation rate of the studied section. This short-term hydrologically favorable phase is at the scale of a North Atlantic-driven Heinrich event, and we speculate whether rapid increases of southern Atlantic SSTs could have triggered significantly increased moisture supply over the Kalahari and/or the Bié Plateau (Angola) where the (nowadays) active catchment of the Okavango river system is located (Fig. 2.1).

The studied section is in close proximity to the palaeo-shore of the mega-lake and based on the P/B ratio of diatom assemblages we infer shallow water conditions prevailed at the site. The analyzed diatom assemblages indicate an alkaline and oligohaline lake, although the reconstructed salinity is not representative of the whole mega-lake because the studied section is located about 100–150 km away from the two major inflow systems, the Okavango River in the (north-) west and the Okwa River in the southwest of the lacustrine basins (Fig. 2.1). As we could not infer which of the inflow systems was active during the highstand, a salinity gradient from freshwater to oligohaline either existed off the Okavango or Okwa river mouths.

Considering the role Pleistocene Lake Palaeo-Makgadikgadi is likely to have played in the phylogeography of freshwater fish (Joyce et al., 2005) or freshwater gastropods (Schultheiß et

al., 2014), we suggest the mega-lake phase in this study is too short a duration that is dominated by oligohaline conditions, and therefore it was not a suitable trigger for evolutionary radiations of freshwater taxa. The comparatively high temporal resolution of 1–2 decades of our studied samples provides valuable insights of climate variability during a mega-lake phase. Albeit significant changes in $\delta^{18}\text{O}_{\text{diatom}}$ values occurred (Fig. 2.4), the highstand is considered a hydrologically stable period.

Although the studied mega-lake period was likely a short-term climate anomaly possibly triggered by North Atlantic iceberg discharges, it is challenging the view that MIS 5 was mostly extremely dry. That the environment may have hydrologically been more favorable, is supported by archaeological and genetic data suggesting permanent human occupation of the Kalahari since MIS 5.

2.8 Acknowledgements

We appreciate the field assistance of Franziska Slotta (FU Berlin, Germany), Linda Taft (University of Bonn, Germany), Michael Taft (Abenden, Germany), Karl-Uwe Heußner and Alexander Janus (both German Archaeological Institute, Berlin). Maike Glos (FU Berlin) helped processing samples and Jan Evers (FU Berlin) designed Fig. 2.1 and helped improving further figures. Many thanks to Manfred Fischer (University of Bayreuth, Germany) for dose rate determination. We also like to thank the reviewers for constructive criticism. The Ministry of Minerals, Energy and Water Resources of Botswana kindly granted a research permit. FR is grateful to the Deutsche Forschungsgemeinschaft for financial support.

3. Manuscript II

Palaeobotanical records from Rebun Island and their potential for improving the chronological control and understanding human–environment interactions in the Hokkaido Region, Japan

Stefanie Müller,^{1,2} Mareike Schmidt,¹ Annette Kossler,¹ Christian Leipe,^{1,3} Tomohisa Irino,⁴ Masanobu Yamamoto,⁴ Hitoshi Yonenobu,⁵ Tomasz Goslar,^{6,7} Hirofumi Kato,² Mayke Wagner,³ Andrzej W. Weber⁸ and Pavel E. Tarasov¹

¹*Section Paleontology, Institute of Geological Sciences, Free University of Berlin, Germany*

²*Center for Ainu and Indigenous Studies, Hokkaido University, Japan*

³*Eurasia Department and Beijing Branch Office, German Archaeological Institute, Germany*

⁴*Faculty of Environmental Earth Science, Hokkaido University, Japan*

⁵*College of Education, Naruto University of Education, Japan*

⁶*Faculty of Physics, Adam Mickiewicz University in Poznań, Poland*

⁷*Poznan Radiocarbon Laboratory, Foundation of the A. Mickiewicz University, Poland*

⁸*Department of Anthropology, University of Alberta, Canada*

published in: The Holocene, Volume 26, Issue 10, pp. 1646-1660

accepted: 26 November 2015, published: 1 October 2016

This is a post-peer-review version of an article published in *The Holocene*. The final authenticated version is available online at: <https://doi.org/10.1177/0959683616641738>.

3.1 Abstract

Rebun Island with Hamanaka and Funadomari among the 43 documented archaeological sites and the environmental archive stored in the Lake Kushu sediment proves to be one of the key areas to study the interplay between ecology, climate and human activities. This paper focuses on the potential of palaeobotanical records from Rebun Island for improving the chronological control and understanding of Late Quaternary climate changes and habitation environments of northern hunter-gatherers in the Hokkaido Region of Japan. A set of 57 radiocarbon dates of the RK12 core (Lake Kushu) demonstrates that it represents a continuous environmental archive covering the last *c.* 17,000 years. The RK12 pollen record reflects distinct vegetation changes associated with the onset of the Late Glacial warming about 15,000 cal. yr BP and the cold climate reversal after *c.* 13,000 cal. yr BP. The onset of the current Holocene Interglacial *c.* 11,700 cal. yr BP is marked by a major spread of trees. The Middle Holocene (*c.* 8000–4000 cal. yr BP) is characterized by a major spread of deciduous oak in the vegetation cover reflecting a temperature increase. A decline of oak and spread of fir and pine is recorded at *c.* 2000 cal. yr BP. After *c.* 1100 cal. yr BP, arboreal pollen

percentages decrease, possibly linked to intensified usage of wood during the Okhotsk and Ainu culture periods. The results of diatom analysis suggest marshy or deltaic environments at the RK12 coring site prior to *c.* 10,500 cal. yr BP and a brackish lagoon between *c.* 10,500 and 7000 cal. yr BP. A freshwater lake developed after 6500 cal. yr BP, likely reflecting sea level stabilization and formation of the sand bar separating the Kushu depression from the sea. Plant macrofossil analysis shows use of various wild plants and also domesticated barley during the Okhotsk and Ainu periods.

3.2 Introduction

The Baikal–Hokkaido Archaeology Project (BHAP: <http://bhap.artsrn.ualberta.ca/>) gathered together a multi-disciplinary team of scholars investigating Holocene hunter-gatherer cultural dynamics and environmental and climate changes in the Lake Baikal Region of Russia and the Hokkaido Region of Japan (Tarasov et al., 2013; Weber et al., 2013). In contrast to the much more recently developed farming and pastoral economies, the hunter-gatherer lifestyle, in its various modes, has sustained humankind during most of its history (Fuentes, 2009; Kelly, 1995). In some places (e.g. the Near East and eastern China), the shift to food production in the Early Holocene was followed by farming dispersals and the eventual rise of villages, towns and eventually states. However, in many other areas, prehistoric groups did not switch to farming but first intensified foraging (hunting, fishing and gathering) and only much later adopted agriculture (e.g. central and southern Japan), while other groups (e.g. in Hokkaido, Greenland and most of northern Eurasia) remained hunter-gatherers well into the historic period (e.g. Weber et al., 2010, 2013).

Weber et al. (2013), summarizing the substantial progress achieved in hunter-gatherer research during the past few decades and defining the BHAP rationales, noted that ‘the understanding of the cultural dynamism, variability, and resilience of Holocene hunter-gatherers in many regions remains rather impoverished’. The Holocene cultural sequence of the Hokkaido Region is characterized by a series of hunter-gatherer populations.

Through this time, it represented a cultural and ecological junction between the Neolithic and post-Neolithic populations of warmer latitudes of mainland Asia and central Japan and foragers of the colder regions of Northeast Asia. Recent investigations brought to light that Hokkaido’s prehistoric hunter-gatherers (long time regarded as ‘static’ and ‘primitive’, e.g. Kobayashi, 1992; Watanabe, 1986) are marked by a complex pattern of inter-regional variability with a number of demographic and cultural transitions distinguished by changes in population size, distribution, organization, socio-political differentiation and degrees of sedentism and mobility (e.g. Habu, 2004; Nomura and Udagawa, 2006a, 2006b, 2006c; Underhill and Habu, 2006). What role unstable environments and climate played in the local and regional cultural dynamics remains an extremely important, although an empirically challenging question (e.g. Weber et al., 2013). Thus, in the northern part of the Japanese Archipelago including Hokkaido and adjacent islands (Fig. 3.1a and

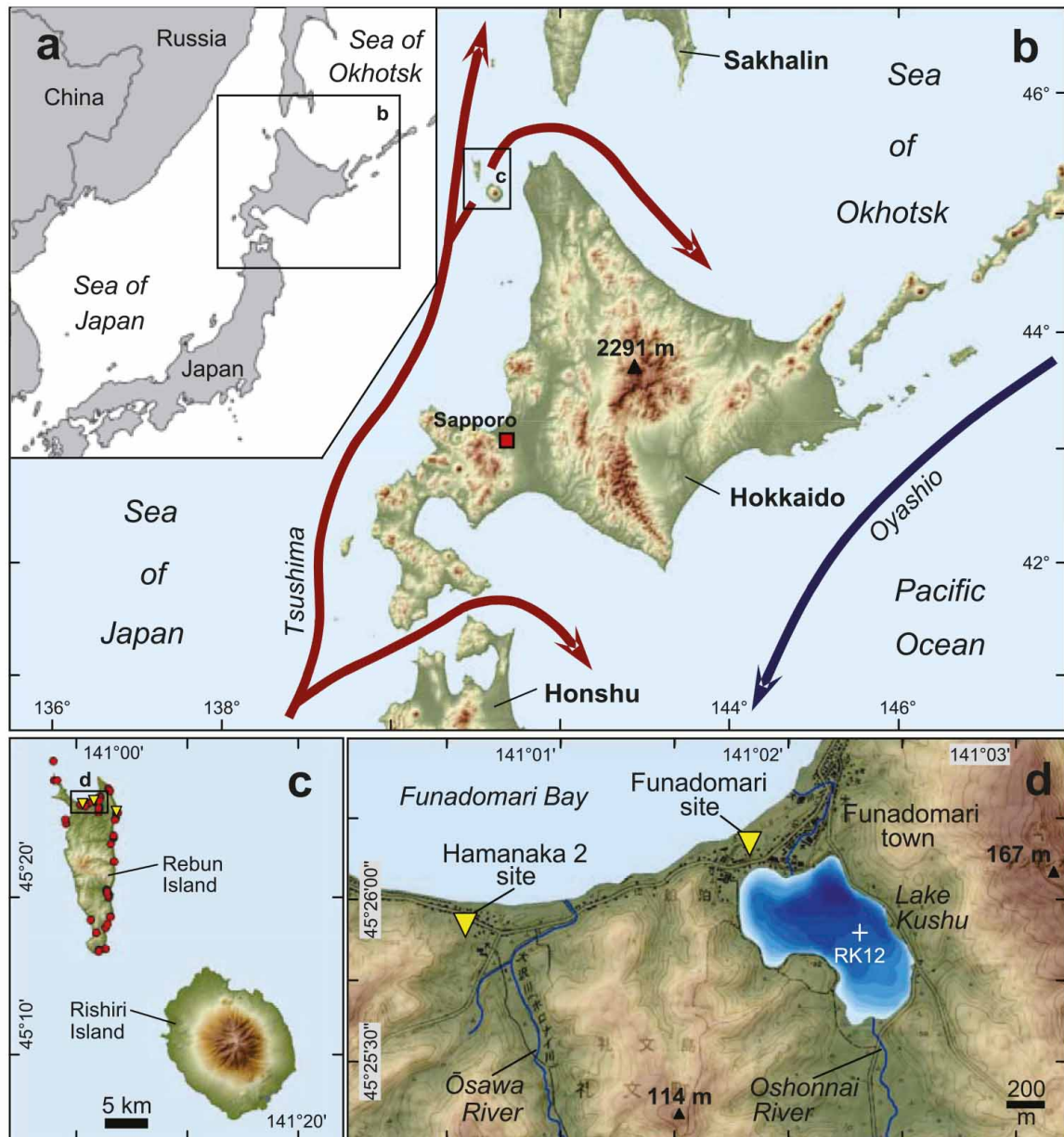


Figure 3.1: Map compilation showing (a) the northwest Pacific and (b) the Hokkaido Region including the Tsushima warm current (red) and the Oyashio cold current (blue); (c) Rebun and Rishiri islands; and (d) the northern part of Rebun with Lake Kushu (white cross indicates location of the RK12 cores) and Hamanaka 2 and Funadomari archaeological sites (yellow triangles). In (c), yellow triangles indicate locations of the Hamanaka 2, Funadomari and Uedomari archaeological sites and red dots indicate locations of the remaining 40 archaeological sites documented so far on Rebun. Topographic maps are based on elevation Shuttle Radar Topography Mission (SRTM) V4.1 data (Jarvis et al., 2008). Isolines for terrestrial area are drawn from a topographic map (Geospatial Information Authority of Japan, 2012). Bathymetry of Lake Kushu (0.5 m isolines) is based on survey data provided by T. Haraguchi (Osaka City University).

b), potentially rich in archaeological and environmental archives, the main challenge remains the scarcity of published environmental and archaeological records with high temporal resolution and adequate dating control (see Igarashi (2013) and Habu (2004) for details and references). These

common problems hinder direct correlation between the individual archives and make discussion of regional environmental and societal responses extremely difficult, thus preventing inter-regional comparison and identification of leads and lags in reconstructed changes. A multi-disciplinary research started in 2011 on Rebun Island in the northwestern Hokkaido Region (Fig. 3.1c), under the umbrella of the BHAP, aiming to fill the existing gap in the current knowledge and to address the causal factors driving cultural processes, including the role of climate and environment (Weber et al., 2013).

The geographic location of Rebun Island at the border between the cool temperate zone and boreal zone makes its vegetation and environments very sensitive to climatic change. The bottom sediment of Lake Kushu (Fig. 3.1d) is a valuable natural archive which stores detailed and high-resolution information about past environmental changes and, possibly, human–environment interactions. As indicated in the title, the aim of this paper is to emphasize the potential of palaeobotanical (i.e. pollen, plant macrofossil and diatom) records from Rebun Island for better understanding environmental and human histories of the study region and for improving the chronological control of the reconstructed changes. Furthermore, the discussion and publication of the first results are of importance for planning future archaeological and environmental research and for selecting priority research questions.

3.3 Study area

3.3.1 Site and regional settings

Rebun is located in the northern part of the Sea of Japan (Fig. 3.1a), *c.* 45 km west of Hokkaido (Fig. 3.1b) and *c.* 10 km northwest of volcanic Rishiri Island (highest point at 1721 m a.s.l.). Both islands (Fig. 3.1c) are part of the Rishiri Rebun Sarobetsu National Park, where natural vegetation consists of cool mixed and cool conifer forest associations, shrubs, grasslands and meadows. About 100 km of open seawater separates Rebun from southern Sakhalin and the direct waterway to continental Asia exceeds 240 km.

Rebun Island occupies an area of about 82 km² (Schmidt et al., 2016). It extends for over 20 km from north to south and for up to 6–8 km from east to west. Steep slopes characterize the hilly landscape. The highest point (490 m a.s.l.) is situated in the western part of the island (Fig. 3.1c).

Lake Kushu (Fig. 3.1d) is the only freshwater lake on Rebun (Fig. 3.1c). Located in the northern part of the island (45°25'58"N, 141°02'05"E), about 230–400 m from the modern sea coast, the lake has a kidney bean shape and a maximum length of *c.* 1100 m. The maximum water depth reaches *c.* 6 m in the eastern part of the lake with average depths of about 3–5 m.

3.3.2 Climate

The climate conditions of Rebus and Rishiri islands are mainly controlled by the East Asian monsoon system. The East Asian summer monsoon (EASM) circulation, which is formed by the pressure gradient between the Asiatic Low over Siberia and the Hawaiian High over the northern Pacific Ocean, transports warm and moist air from southern to southeastern directions. The formation of the Aleutian Low and the Siberian High during autumn is paralleled by the reversal of the ocean–continent pressure gradient that culminates in winter. During this time, the islands are mainly influenced by cold continental airflow from northern to northwestern directions controlled by the East Asian winter monsoon (EAWM) circulation.

Another important climatic control in the study region is the Tsushima warm current (TWC), which flows as a branch of the Kuroshio warm current northwards along the eastern margin of the Sea of Japan (Fig. 3.1b). Especially during winter, the TWC promotes moisture uptake by the predominant winter monsoon winds, which results in enhanced snow fall and prevents sea ice formation in the region (Nikolaeva and Shcherbakova, 1990).

A global high-resolution (30 arc seconds) dataset of surface climate variables averaged over the years from 1950 to 2000 (Hijmans et al., 2005) reveals year-round moist conditions around Lake Kushu and on Rebus Island with mean monthly precipitation values reaching ~90–130 mm from July to January. The driest month (March) is still reasonably wet (~55 mm). The mean annual precipitation is ~1100 mm. The summers are relatively mild and winters are cool. The annual mean temperature is 6.1°C. During the warmest month (August) mean temperature reaches 19.4°C. In winter (December–March), mean temperatures drop below 0°C, with the mean temperature of the coldest month (January) as low as –6.4°C.

3.3.3 Vegetation

The combination of cool temperatures and abundant all-year-round precipitation results in dense vegetation cover and predominance of cool temperate and boreal woody plants. Rebus and Rishiri islands are situated within the cool mixed forest biome zone (Nakagawa et al., 2002), which roughly stretches between 48° and 42°30' N, that is, from southwestern Sakhalin (Bukhteeva and Reimers, 1967) to the northern limit of the temperate deciduous forest biome (known as Kuromatsunai line) in southwestern Hokkaido (Itoh, 1987). The natural forest vegetation is dominated by boreal evergreen conifers including *Abies sachalinensis* (Sakhalin fir), *Picea jezoensis* (Jezo spruce) and boreal and temperate deciduous broadleaf trees including several *Betula* (birch) and *Alnus* (alder) spp., *Salix* (willow) spp., *Quercus crispula* (Mongolian oak), *Sorbus commixta* (Japanese rowan), *Sorbus sambucifolia* var. *pseudogracilis* (Siberian mountain ash), *Acer pictum* subsp. *mono* (painted maple), *Fraxinus* (ash) spp., *Juglans ailantifolia* (Japanese walnut), *Morus australis* (Chinese mulberry), *Phellodendron amurense* (Amur cork tree) and woody vine *Toxicodendron orientale* (syn. *Rhus ambigua*, Asian poison ivy). Japanese botanical

literature (Haruki et al., 2004) also reports *Ulmus davidiana* var. *japonica* (Japanese elm), *Ulmus laciniata* (Manchurian elm), *Tilia japonica* (Japanese lime) and *Fraxinus mandschurica* (Manchurian ash). Mild maritime climate and deep snow cover might explain the presence of some warm-temperate taxa such as *Ilex* (holly) spp., *Aralia* (spikenard) spp., *Skimmia japonica* (Japanese skimmia) and *Kalopanax septemlobus* (prickly castor oil tree) on the islands.

Today, large parts of Rebun Island are deforested and mostly covered by dense *Sasa kurilensis* (dwarf bamboo) stands or *Reynoutria sachalinensis* (Sakhalin knotweed), likely hindering the re-establishment of arboreal taxa. Although arboreal plants are less common on Rebun today, occupying mainly valleys in the central and eastern part of the island, interviews with the local villagers in August 2014 suggest that forests played a greater role in the vegetation cover in the first half of the 20th century. Rishiri Island reveals a much better preserved well-developed natural forest belt (e.g. Igarashi, 2008; Sawada et al., 2015). On exposed elevated sites on Rebun Island and above c. 400–600 m a.s.l. on Rishiri Island, *Pinus pumila* (Siberian dwarf pine), *Sasa kurilensis* and shrubby forms of *Betula* and *Alnus* are common. *Empetrum nigrum* (black crowberry), *Juniperus chinensis* (Chinese juniper) and *Taxus cuspidata* var. *nana* (dwarf Japanese yew) also grow at these higher elevations.

3.3.4 Archaeology

Within the prehistory of the Japanese Archipelago, the Hokkaido Region played a specific role as a cultural crossroad between mainland Japan and northern territories (i.e. Russian Far East and Siberia). A diverse pattern of cultural shifts is displayed by regional archaeological studies (Fig. 3.2). The oldest traces of human presence in Hokkaido are stone artifacts which date to c. 30,000 cal. yr BP (i.e. calibrated or calendar years before present, where ‘present’ is conventionally taken as 1950) as suggested by Izuho and Sato (2007). Some authors argue that Upper Paleolithic groups migrated from Siberia (Izuho et al., 2014 and references therein) via a land bridge, which connected Hokkaido with Sakhalin and the northeast Asian mainland during most of the Last Glacial period (Kuzmin et al., 2002). Paleolithic exchange networks extended at least as far as southern Sakhalin / Hokkaido (Kuzmin et al., 2013). The origin of the Neolithic Japanese Jomon culture is still debated (Adachi et al., 2009). In addition to the traditional view of a southern origin (e.g. Hanihara, 1991; Hudson, 1999), a growing number of anthropological studies stress the role of immigration from northern regions via Hokkaido (e.g. Hanihara and Ishida, 2009; Omoto and Saitou, 1997; Tanaka et al., 2004). Widely accepted is another southward movement of hunter-gatherer populations around the Last Glacial Maximum (c. 20,000 cal. yr BP) into Hokkaido. These groups later (c. 15,000 cal. yr BP) introduced microblade tools on Honshu Island (e.g. Imamura, 1996) and likely mixed with local communities (Matsumura and Oxenham, 2013).

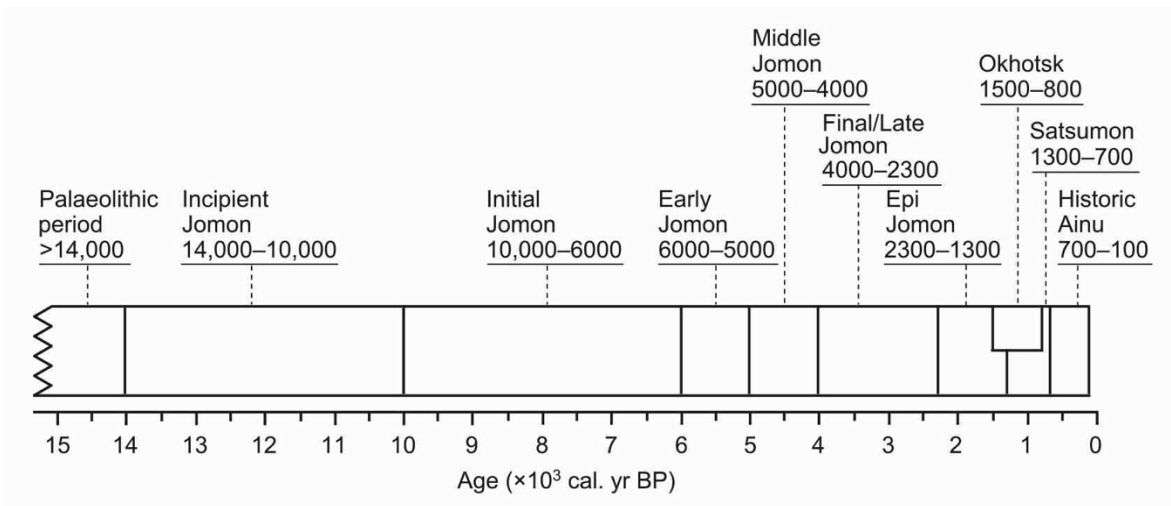


Figure 3.2: Archaeological culture sequence of the Hokkaido Region (according to Hanihara et al., 2008; Weber et al., 2013).

In most of mainland Japan, foraging became much less important at the end of the Jomon period, during the 3rd millennium BP, when farming was continuously introduced from the Korean Peninsula (Hudson, 2013). In Hokkaido, however, foraging remained fundamental subsistence strategy from the Upper Paleolithic (*c.* 30,000 cal. yr BP) through to the historic Ainu (*c.* 800–100 cal. yr BP). Also, the Jomon cultural sequence in Hokkaido (*c.* 14,000–1300 cal. yr BP) was extended compared with mainland Japan with the Epi Jomon period dated to *c.* 2300–1300 cal. yr BP. The Epi Jomon communities, who are believed to be direct descendants of the Jomon people, first started to incorporate rice cultivation as an additional food source (e.g. Habu, 2004). However, only insignificant quantities of rice remains are reported from Epi Jomon sites (Crawford, 2011). After the Jomon era, Hokkaido experienced a number of cultural transitions and migrations from the north. People of the Okhotsk culture, probably originating from the lower Amur Region, spread from Sakhalin into the region and occupied Rebun and Rishiri islands and the northeastern coastline of Hokkaido between *c.* 1500 and 800 cal. yr BP. This culture was highly specialized in marine fishing and hunting sea mammals including *Phoca vitulina* (harbor seal), *Callorhinus ursinus* (fur seal), *Zalophus japonicus* (Japanese sea lion, extinct species), *Eumetopias jubatus* (Steller's sea lion) and whale species (Sato et al., 2007). The Satsumon culture (*c.* 1300–700 cal. yr BP), more or less contemporarily established in the southern and inner parts of Hokkaido, is believed to have developed from the Epi Jomon (Adachi et al., 2009). This culture is marked by plant cultivation (e.g. barley, wheat and millets) at least in the southwestern part of Hokkaido (Crawford, 2011). The historical Ainu culture (*c.* 700–100 cal. yr BP) incorporates characteristics of the Okhotsk (e.g. bear cult and marine mammal hunting) and Satsumon (e.g. dry-farming crop cultivation) cultures. Utagawa (2002) and Sato et al. (2007) suggest that the Ainu emerged from the merging of both cultures.

It is plausible that Rebun and Rishiri islands represent an important link in terms of prehistoric human migrations and cultural exchanges between Hokkaido and adjacent regions. A short summary of Rebun archaeology provided by Sakaguchi (2007a, b) points out that the oldest remains of human activities on Rebun Island are Paleolithic microblades, microcores and tanged projectile points dating to *c.* 22,000–13,000 cal. yr BP. Residential sites cover the period from Middle Jomon to modern Ainu. Most of these sites are concentrated on marine terraces and sand dunes around the Funadomari (Fig. 3. 1d) and Kafukai bays. Inui (2000) registered 43 sites on the island. The oldest (so far reported) residential site is Uedomari located on the northeastern coast of Rebun Island (Fig. 3.1c), which dates to *c.* 4900–4400 cal. yr BP (Middle Jomon period). The number of sites increased during the period *c.* 4400–3200 cal. yr BP. After a decrease in the Final Jomon period, the number of sites increased again during the Epi Jomon, Okhotsk and Ainu periods (Inui, 2000).

3.4 Data and methods

3.4.1 Lake Kushu core RK12

Lake Kushu was chosen as a key site for palaeoenvironmental research. It is located in a climatically sensitive region (i.e. the boreal–temperate transition), about 1.5 km east of the Hamanaka 2 site (Fig. 3.1d), and contains a thick sedimentary succession storing diverse palaeoenvironmental information (Kumano et al., 1990a). A preliminary survey of the lake to determine the best coring point and to obtain necessary permits from the Wakkanai Nature Conservation Bureau, the Rebun Forest Service, the Rebun Town administration and the local fisherman’s union was accomplished by H. Yonenobu (Naruto University of Education) and his team in November–December 2011.

In February 2012, when a thick ice layer covered the lake, coring was performed in the central part of the lake (Fig. 3.1d) by the commercial company Dokon Co. (Sapporo) using professional equipment for scientific lake coring (e.g. Nakagawa et al., 2012). The composite core RK12 was recovered from two boreholes (i.e. RK12-1 and RK12-2) located within a few meters from each other (Fig. 3.1d). Once coring was completed, the core segments (in thin-wall tubes of 86 mm diameter) were transported to the Graduate School of Environmental Science, Hokkaido University (Sapporo), and stored under cool temperature. In April 2012, the tubes were opened by cutting in two halves, the sediments were photographed, described, documented and sub-sampled for multi-proxy analyses using the double-L channel (LL-channel) technique (Nakagawa, 2007; Nakagawa et al., 2012) by a team led by T. Irino and M. Yamamoto (Hokkaido University).

The composite core revealed a continuous, partly laminated, organic-rich *c.* 19.5-m-long sediment column. The basal unit contains sandy clay with pebbles, likely indicating stronger river influence. Peat (1925–1935 and 1905–1915 cm) and organic-rich clay (1915–1925 and 1895–1905 cm) layers appear in the lower part of the core, suggesting shallow water or marshy environments.

The interval between 1895 and 1390 cm is generally characterized by homogeneous, relatively organic-poor clay, which is only interrupted by two short intervals (1790–1815 and 1765–1780 cm) showing a higher amount of coarser grains (i.e. sand). Between 1390 and 850 cm, the clayey material is mostly finely laminated with sections of relatively low to high organic matter concentration. The upper 850 cm of the sediment column consists of homogeneous organic-rich clayey material. The sedimentological comparison with the 16.2-m core (Kumano et al., 1990a) recovered from the marshy floodplain at the southern coast of the lake (Fig. 3.1d) and spanning the last *c.* 9000 cal. yr BP, suggests it may represent the entire Late Glacial and Holocene time interval at very high temporal resolution.

A subset of the RK12 core material has been shipped to Free University of Berlin where a range of pilot analyses was performed. A total of 57 bulk samples, each representing 1 cm of core material, were sent to the Poznan Radiocarbon Laboratory for age determination. For pollen analysis, sub-samples (each representing 1 cm of core sediment) were processed in the chemical laboratory of the Paleontology Section at FU Berlin and microscopically analyzed (see Demske et al., 2013; Müller et al., 2014 for technical details and references). Fossil samples for diatom analysis have been processed using standard procedures (see Battarbee et al., 2001; Kossler et al., 2011 for details and references). Microscopic analyses revealed high contents and good preservation of diatoms, pollen and spores along the RK12 core.

3.4.2 The Hamanaka 2 archaeological site

Rebun Island is one of the key areas selected for the BHAP research, not least because of its location and the high number of archaeological hunter-gatherer sites spanning an interval from the Paleolithic to historic Ainu (Inui, 2000). A test survey undertaken by H. Kato (Hokkaido University) in 1996 helped to identify Hamanaka and Funadomari as multi-component (habitation and mortuary) and multi-period archaeological sites. Both are located in the northern part of the island close to Lake Kushu (Fig. 3.1d). Sakaguchi (2007b) has suggested that the Hamanaka 2 site was first used by the Late Jomon maritime hunter-gatherers as a campsite for intensive hunting and processing, while it was used as a human burial area and dog butchering site during the Okhotsk period. The first BHAP excavations in summer 2011 confirmed the high research potential of the Hamanaka 2 site. Sediment samples representing different cultural layers (e.g. Epi Jomon, Okhotsk / Satsumon and Ainu) and archaeological features (e.g. refuse areas, pits, fire places, and graves) were treated in the field laboratory organized in the old school building in Uedomari. A flotation machine (see Crawford, 1983) was used to isolate the light material (seeds, charcoal etc.) from the sediments. Selected flotation samples from the set obtained during the 2013 campaign were analyzed for plant macro-remains. In this paper, we show the analytical results representing the Okhotsk and Ainu cultural layers. Terrestrial plant material of the most representative samples was submitted to Poznan Radiocarbon Laboratory for AMS ^{14}C dating.

3.5 Results

3.5.1 RK12 core chronology

Table 3.1 presents the results of the AMS radiocarbon dating of the RK12 core samples and their calibration to cal. yr BP. The age model (Fig. 3.3a) suggests that the RK12 core sedimentation continued since *c.* 17,000 cal. yr BP. Fig. 3.3a shows rather unambiguous age–depth relation in the upper half of the core accumulated during the past *c.* 6000 years. The accumulation rate is very high, that is, about 1 cm of sediment in *c.* 6 years. In the bottom half of the core, the radiocarbon dates demonstrate several well distinguishable reversals, suggesting contamination of the respective samples by older material. Reversed dates were consistently excluded when constructing the age model for the RK12 core (Fig. 3.3a). The age–depth model also suggests greater variations in sedimentation rates in the lower half of the core and substantially slower sedimentation (i.e. 1 cm in *c.* 20 years) prior to *c.* 9500 cal. yr BP.

3.5.2 RK12 coarse-resolution pollen record

For the purpose of this study, 28 samples have been microscopically analyzed in which about 90 different plant taxa could be distinguished. Besides higher plant species of trees, shrubs and herbaceous plants, 15 different species of mosses and ferns were identified. The pollen and spore content of the samples was sufficiently high to allow the counting of a minimum of 400 terrestrial pollen grains per sample. Bisaccate pollen grains of *Abies* and *Pinus* were frequently broken and hampered identification. These counts were grouped to Pinaceae. In addition to pollen, vascular cryptogam spores and green algae colonies (*Pediastrum*, *Botryococcus*) were identified and counted. The preliminary results are summarized in the pollen percentage diagram (Fig. 3.4). For description of the results, we subdivided the diagram into seven chrono-stratigraphic units (i.e. zones Ku-7 to Ku-1) on the basis of the RK12 core chronology and observed changes in plant taxa composition and relative abundance.

The lowermost part of the core (Ku-7) is characterized by high amounts of sedges (Cyperaceae) which form up to 60% of the total pollen sum. *Sphagnum* is present with highest values (about 5%) in this zone. Arboreal pollen taxa increase to up to 50% in the following zones (Ku-6 and Ku-5) together with increasing amounts of spores of Lycopodiales and Polypodiales. The percentages of sedges drastically decrease (to 15%) while Poaceae amounts slightly increase (up to 20%). Aquatic plant taxa are rather abundant in zone Ku-5.

However, temperate deciduous tree taxa, like *Fraxinus*, *Quercus* and *Ulmus*, which appear in zone Ku-6, disappear again. The following zone Ku-4 is characterized by higher amounts of arboreal pollen taxa (especially Pinaceae, *Alnus*, *Betula* and *Quercus*), which from now on dominate the pollen spectra (up to 90%). Poaceae pollen and spore percentages reach their maxima in this zone. Zone Ku-3 is characterized by high taxonomic diversity and rather stable abundances of arboreal and non-arboreal taxa. In zone Ku-2, *Abies* pollen percentages reach maximum values

about 20%). Noticeably decreasing percentages of arboreal pollen taxa and increasing percentages of Poaceae, *Artemisia*, *Lysichiton camtschatcensis* and spores of Lycopodiales are characteristic for zone Ku-1.

Table 3.1: Summary of radiocarbon dates, and calibrated and modelled ages for the set of 57 AMS-dated samples from the RK12 core of Lake Kushu. Dates shown in cursive font are regarded as being too old.

Laboratory number	Composite depth, cm	AMS ¹⁴ C date, uncal. yr BP	Calendar age (OxCal v4.2.3 Bronk Ramsey, 2013), 95% range		Calendar age (best-fit model)	
			From, cal. yr BP	To, cal. yr BP	Cal. yr BP	Cal. yr AD/BC
Poz-51689	64.5	470 ± 25	535	499	350	1600
Poz-51700	96.5	415 ± 30	521	331	499	1451
Poz-51713	126.5	510 ± 35	627	502	615	1335
Poz-51721	164.5	1065 ± 25	1051	929	962	988
Poz-51731	196.5	1290 ± 30	1286	1180	1194	756
Poz-51735	226.5	1445 ± 30	1386	1297	1315	635
Poz-51736	264.5	1520 ± 35	1523	1340	1405	545
Poz-51737	296.5	1745 ± 30	1719	1565	1622	328
Poz-51770	326.5	1765 ± 30	1808	1571	1704	246
Poz-51690	364.5	2070 ± 30	2124	1951	2003	-53
Poz-51691	396.5	2160 ± 30	2308	2058	2149	-199
Poz-51692	426.5	2270 ± 30	2350	2160	2320	-370
Poz-51694	464.5	2420 ± 30	2698	2352	2457	-507
Poz-51695	496.5	2635 ± 30	2837	2730	2753	-803
Poz-51696	527.5	2930 ± 30	3170	2975	3009	-1059
Poz-51697	564.5	2915 ± 35	3166	2958	3134	-1184
Poz-51698	596.5	3190 ± 35	3480	3353	3391	-1441
Poz-51699	626.5	3250 ± 30	3563	3401	3540	-1590
Poz-51703	664.5	3505 ± 35	3876	3651	3774	-1824
Poz-51704	696.5	3670 ± 35	4140	3896	3982	-2032
Poz-51705	726.5	3790 ± 40	4351	3996	4215	-2265
Poz-51706	764.5	4185 ± 30	4839	4619	4660	-2710
Poz-51707	796.5	4300 ± 35	4962	4830	4853	-2903
Poz-51709	826.5	4495 ± 35	5302	4987	5066	-3116
Poz-51710	864.5	4730 ± 35	5585	5327	5340	-3390
Poz-51816	896.5	4735 ± 35	5586	5327	5539	-3589
Poz-51817	926.5	4885 ± 30	5660	5587	5603	-3653
Poz-51711	969.5	5045 ± 35	5906	5665	5749	-3799
Poz-51837	996.5	5770 ± 40	6667	6476	5846	-3896
Poz-51714	1028.5	6840 ± 40	7758	7574	5958	-4008
Poz-51838	1064.5	12,050 ± 70	14,089	13,750	6084	-4134
Poz-51840	1098.5	13,030 ± 70	15,852	15,311	6218	-4268
Poz-51715	1126.5	14,650 ± 70	18,027	17,624	6359	-4409
Poz-51716	1165.5	5820 ± 40	6731	6506	6652	-4702
Poz-51717	1196.5	6850 ± 40	7787	7609	7072	-5122
Poz-51718	1226.5	6550 ± 40	7565	7418	7435	-5485
Poz-51719	1264.5	6870 ± 50	7827	7611	7686	-5736
Poz-51720	1296.5	7670 ± 50	8555	8386	8064	-6114
Poz-51841	1330.5	7660 ± 50	8549	8383	8296	-6346
Poz-51723	1364.5	7610 ± 50	8538	8346	8396	-6446
Poz-51724	1397.5	9080 ± 40	10,369	10,183	8437	-6487
Poz-51725	1426.5	8560 ± 50	9626	9471	8465	-6515
Poz-51726	1464.5	8180 ± 40	9263	9021	8520	-6570
Poz-51727	1496.5	7820 ± 50	8766	8456	8594	-6644
Poz-51842	1526.5	8260 ± 50	9422	9041	8736	-6786
Poz-51728	1564.5	8070 ± 50	9131	8769	9007	-7057
Poz-51729	1599.5	8300 ± 50	9442	9134	9394	-7444
Poz-51730	1625.5	10,610 ± 80	12,718	12,402	10,255	-8305
Poz-51843	1664.5	11,170 ± 60	13,146	12,849	11,318	-9368
Poz-51844	1696.5	10,510 ± 60	12,650	12,147	12,250	-10,300
Poz-51733	1726.5	13,600 ± 80	16,697	16,133	13,150	-11,200
Poz-51734	1764.5	15,030 ± 80	18,491	18,011	14,161	-12,211
Poz-51765	1814.5	13,220 ± 80	16,155	15,598	15,215	-13,265
Poz-51766	1832.5	14,270 ± 90	17,636	17,096	15,518	-13,568
Poz-51767	1864.5	14,330 ± 90	17,722	17,149	15,963	-14,013
Poz-51768	1889.5	13,490 ± 70	16,512	16,012	16,236	-14,286
Poz-51769	1930.5	13,740 ± 100	16,958	16,280	16,591	-14,641

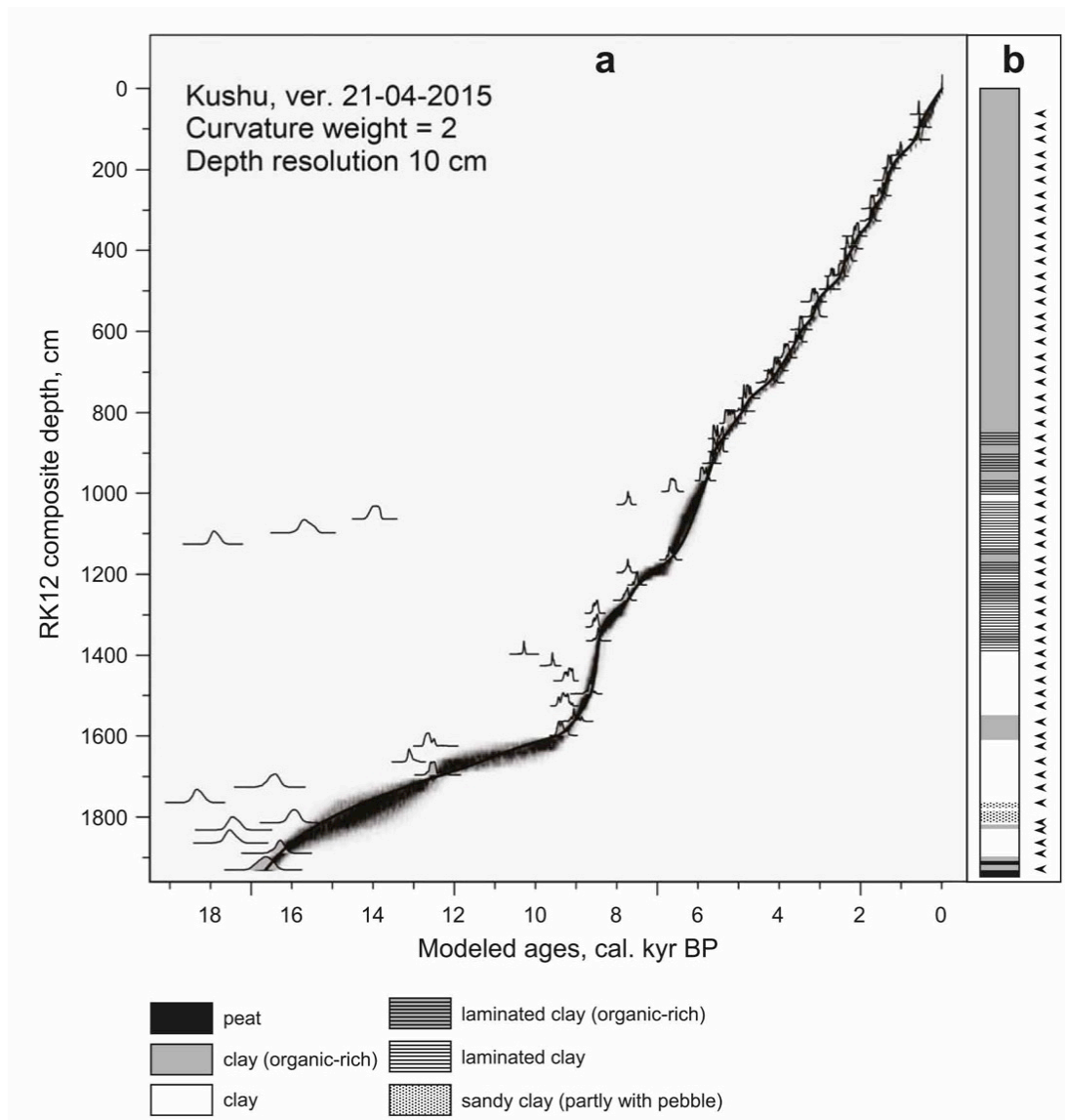


Figure 3.3: (a) The age–depth model (best-fit line with uncertainty ranges) applied to the RK12 sediment core (b) from Lake Kushu. Radiocarbon dates (dated levels are indicated by the horizontal arrows in b) were calibrated against the calibration curve Intcal13 (Reimer et al., 2013), and the model was constructed using the free-shape algorithm (Goslar et al., 2009). The grey silhouettes along the best-fit line (a) represent calibrated ^{14}C dates taken into account by the model, while the non-filled silhouettes left of the best-fit line represent older ^{14}C dates rejected by the model.

3.5.3 Diatom analysis

A total of 10 selected samples have been analyzed (Fig. 3.5) to check the potential of the RK12 core for diatom-based reconstructions. Eight samples show sufficient well-preserved valves allowing for counting of at least 500 valves. Two samples, that is, RK12-02-02_7-8 with 331 counted valves and RK12-02-19_82-83 with 444 counted valves, reveal lower diatom concentrations.

The lowermost analyzed sample (RK12-02-19_82-83) shows dominance of benthic *Diploneis subovalis* Cleve 1894 (78%) and *Pinnularia viridis* (Nitzsch) Ehrenberg 1843 (15%) and low taxonomic diversity. No diatoms have been detected between 19 and 16.5 m composite depth. The sample RK12-02-16_16-17 shows high abundance of benthic freshwater *Pseudostaurosira brevistriata* (Grunow) Williams and Round 1987 (31%) and *Pseudostaurosira elliptica* (Schuhmann) Edlund, Morales and Spaulding 2006 (30%). Benthic brackish / marine taxa are represented by *Pinnunavis yarrensensis* (Grunow) Okuno 1975 (3.8%), *Rhopalodia acuminata* Krammer 1987 (3.3%) and *Mastogloia elliptica* (Agardh) Cleve 1893 (0.3%). Some planktonic marine *Chaetoceros* spp. appear with less than 5%. The following sample (RK12-02-14_7-8) contains freshwater benthic *Epithemia sorex* Kützing 1844 and *Cocconeis placentula* Ehrenberg 1838 (each 12%) and highest recorded percentages of marine taxa, including *Chaetoceros seiracanthus* Gran 1897 (23%), *Chaetoceros radicans* Schütt 1895 (7.3%), *Chaetoceros diadema* (Ehrenberg) Gran 1897 (0.7%) and *Cyclotella choctawhatcheeana* Prasad 1990 (6.2%). The sample RK12-02-12_9-10 reveals re-increased percentage of benthic freshwater *P. brevistriata* (27%). The proportion of marine taxa decreased related to the previous sample RK12-02-14_7-8. Thus, *C. choctawhatcheeana* reaches 5.2% and brackish benthic *M. elliptica* 6.5% of the assemblage.

In the middle part of the RK12 core (sample RK12-02-10_40-41), the ratio of planktonic to benthic taxa (P/B-ratio) shifts significantly, reflecting the dominance of planktonic *Stephanodiscus hantzschii* Grunow 1880 (53%), *Aulacoseira ambigua* (Grunow) Simonsen 1979 (15%), *Aulacoseira granulata* (Ehrenberg) Simonsen 1979 (11%) and *Asterionella formosa* Hassall 1850 (8.6%). The overlying sample (RK12-02-07_9-10) is also mainly composed of planktonic diatoms including *A. ambigua* (16%), *A. granulata* (16%), *Aulacoseira islandica* (Müller) Simonsen 1979 (18%) and *S. hantzschii* (18%). The sample RK12-02-06_21-22 shows the dominance of *A. ambigua* (33%) and *A. granulata* (31%), whereas *A. islandica* still accounts for 18%. Marine taxa are represented by *Cyclotella choctawhatcheeana* (5.4%).

In the upper part of the core, the sample RK12-02-03_73-74 is dominated by *Aulacoseira granulata* (65%), *Aulacoseira ambigua* (19%) and *Aulacoseira islandica* (9.7%). In the sample RK12-02-02_7-8, *A. islandica* becomes the dominant taxa reaching 56% of the assemblage. A noticeable increase in benthic freshwater diatoms, including *Gomphonema grovei* var. *lingulatum* (Hustedt) Lange-Bertalot 1985 (6.9%), *Pseudostaurosira elliptica* (9.3%) and other minor taxa (i.e. other benthic <5%) is recorded in this sample. The uppermost analyzed sample RK12-02-01_1-2 is dominated by planktonic freshwater diatoms including *A. ambigua* (64%), *A. granulata* (15%) and *A. islandica* (7.8%). *P. elliptica* (Schuhmann) Edlund, Morales and Spaulding 2006 accounts for 9.3%.

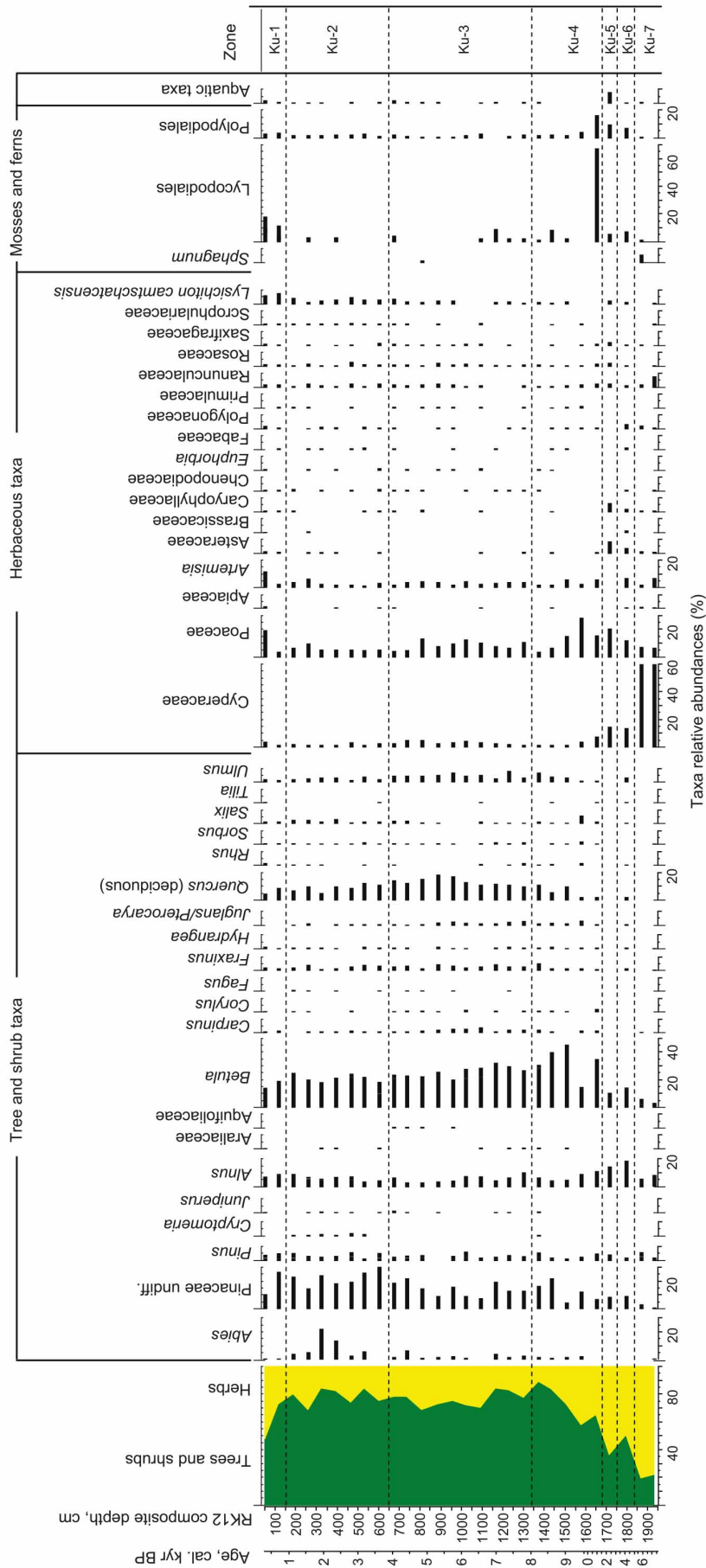


Figure 3.4: Simplified percentage pollen diagram presenting results of the coarse-resolution pollen analysis of the RK12 core from Lake Kushu along the composite depth and age axes.

3.5.4 Plant macrofossil analysis

Our results demonstrate that all 30 flotation samples from the sediment layers I, IIa–c, IIIa–c and VII of the Hamanaka 2 site (Fig. 3.6) contain plant macrofossils, but abundance and diversity of remains vary between the samples. Dark, organic-rich cultural layers (i.e. I and IIIb) contain generally more abundant and diverse plant material than the less organic-rich, sandy layers IIa–c, IIIc, VII and the pure shell midden layers IIIa, IIIc. Seeds from wild plants such as *Rumex*, *Aralia*, *Sonchus*, *Chenopodium* and other Caryophyllales were found in all studied layers. In this study, we focus on the cultural layers I and IIIb (both are characterized by greater amounts of identifiable plant material) to demonstrate the potential for the plant macrofossil analysis.

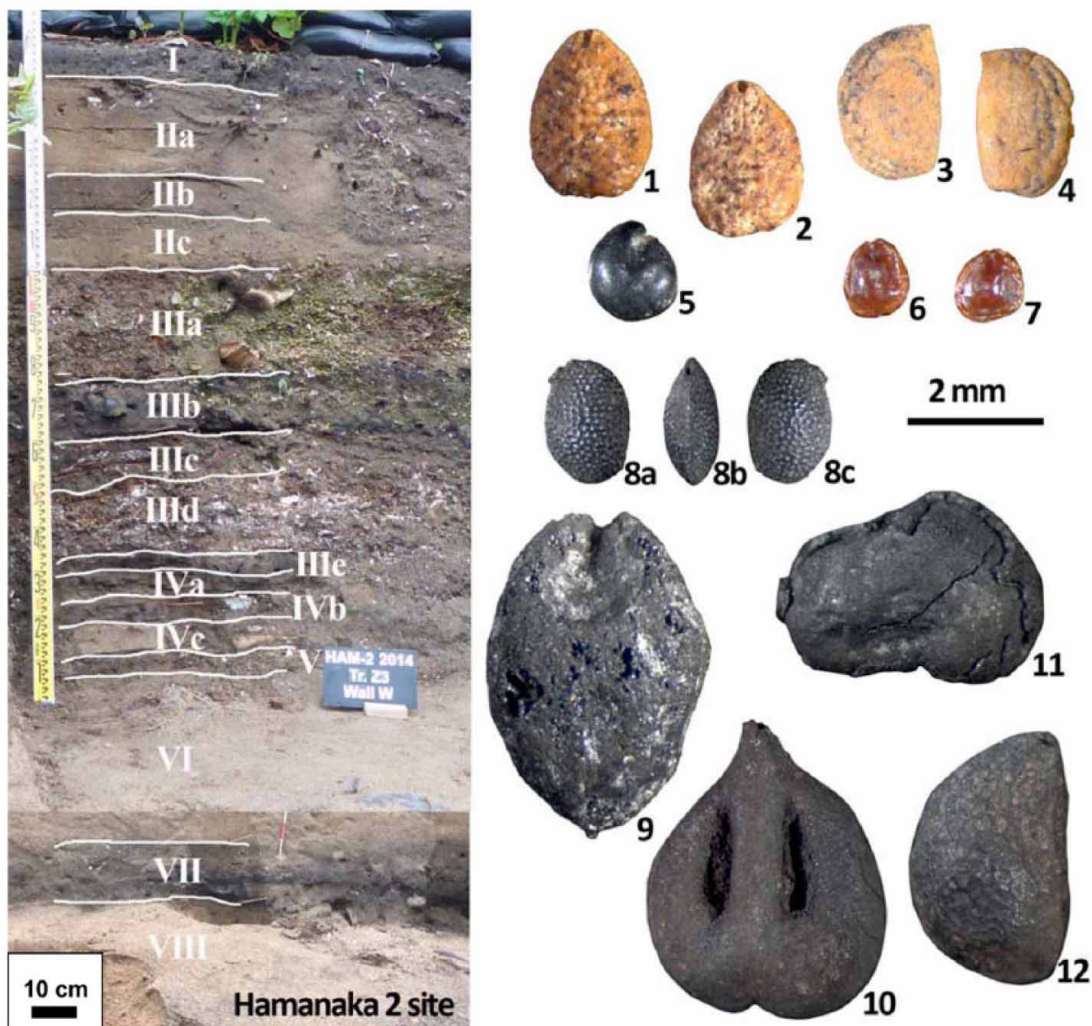


Figure 3.6: Composed photo of the sedimentary succession (left) of the archaeological site Hamanaka 2 with cultural layers I–VIII (August 2014). Images of selected plant macro-remains (right) representing the cultural layer I (1–7: non-charred seeds): *Sambucus sieboldiana* (1, 2), *Aralia cordata* (3, 4), *Chenopodium album* (5), *Amaranthus* sp. (6, 7) and cultural layer IIIb (8–12: charred seeds): *Actinidia arguta* (8a–c), *Hordeum vulgare* (9), *Vitis coignetiae* (10), *Toxicodendron* sp. (11) and *Phellodendron amurense* (12).

The layer IIIb is rich in charred seeds of wild plants (Fig. 3.6), although a few charred *Hordeum vulgare* (barley) grains were also identified. AMS ^{14}C dating performed on charred seeds from three different samples of the cultural layer IIIb shows similar ages (Table 3.2) ranging between *c.* 1150 and 1250 cal. yr BP (i.e. *c.* AD 700–800). Based on typological characteristics of stone tools and pottery, the cultural layer IIIb is assigned to the Okhotsk period. The radiocarbon dating results confirm the archaeological classification, but allow narrowing down the deposition time of the layer IIIb.

The uppermost cultural layer I is characterized by mainly noncharred and few charred macroremains (including barley and some unidentified plant material). The composition of plant remains differs significantly from layer IIIb. Especially seeds of *Sambucus sieboldiana* (elderberry, ‘ezoniwatoko’), *Aralia cordata* (‘udo’) and *Chenopodium album* occur in greater quantities. Additional identified herbs are edible *Amaranthus* (amaranth), *Anthriscus cf. sylvestris* and *Solanum sp.* (nightshade). Three samples from this layer sent for AMS ^{14}C dating also show compatible ages (Table 3.2) ranging between *c.* 50 and 250 cal. yr BP (i.e. *c.* AD 1700–1900). All three dates confirm archaeological attribution of cultural layer I to the historical Ainu period.

Table 3.2: Summary of radiocarbon dates and calibrated ages for the set of AMS-dated samples from the Okhotsk and Ainu cultural layers of Hamanaka 2, Rebun Island.

Laboratory number	Sample number	Dated material	AMS radiocarbon date, uncal. yr BP	Calendar age (OxCal v4.2.3 Bronk Ramsey, 2013), 95% range		Best-fit date (http://www.calpal-online.de/), 68% range	
				From, cal. yr BP	To, cal. yr BP	Cal. yr BP	Cal. yr AD
Poz-60766	F2013/129	<i>Toxicodendron</i> seeds	1305 ± 30	1292	1181	1240 ± 40	710 ± 40
Poz-60767	F2013/147	<i>Vitis coignetiae</i> seeds	1265 ± 30	1284	1087	1221 ± 36	729 ± 36
Poz-60768	F2013/145	<i>Toxicodendron</i> seeds	1215 ± 30	1256	1061	1151 ± 56	799 ± 56
Poz-60760	F2013/31	<i>Sambucus</i> seeds	165 ± 30	288	1	146 ± 117	1804 ± 117
Poz-60761	F2013/39a	<i>Aralia</i> seeds	115 ± 30	270	11	142 ± 97	1808 ± 97
Poz-60762	F2013/39b	Charred twig piece	210 ± 30	304	1	221 ± 69	1729 ± 69

3.6 Interpretation and discussion

Since the introduction of pollen analysis by Lennart von Post in 1916, pollen records serve as a valuable proxy for reconstruction and interpretation of postglacial vegetation, climate change and human activities (e.g. Dolukhanov et al., 2002; Litt et al., 2009; Tarasov et al., 2007) and, more recently, for data–model comparison aiming in improving climate predictability (e.g. Kageyama et al., 2001; Kleinen et al., 2011; Wanner et al., 2008; White and Bush, 2010).

Particularly in situations when archaeological data suggest that major changes in population size and distribution, subsistence strategy, and social complexity were rapid rather than gradual, high-resolution pollen and diatom records may provide detailed information about gradual and short-term changes in the local to regional environments and help improve interpretation and better

understanding of the archaeological results. Such environmental archives are rare and seldom occur in combination with archaeological material from the boreal forest zone of eastern Eurasia (e.g. Weber et al., 2013). The most recent synthesis of available pollen records from the Hokkaido Region (Igarashi, 2013 and references therein) shows a good number of pollen diagrams representing (entirely or partly) the postglacial time interval at centennial- to millennial-scale temporal resolution. However, none of them could serve for decadal-scale reconstructions of climate and vegetation of the entire Holocene.

The intensive radiocarbon dating and coarse-resolution pollen and diatom analyses of the RK12 core demonstrate that it represents a continuous environmental archive covering the last *c.* 17,000 years. Due to the changes in sedimentation rate, temporal resolution of this sedimentary archive may vary along the record, that is, from about 20 yr/cm in the lower part to about 6 yr/cm in the upper part of the core. However, the overall potential of the Lake Kushu sediment for high-resolution environmental reconstructions over the entire postglacial period remains very high. The RK12 record could serve as a link between the high-resolution and accurately dated records from central (i.e. Lake Suigetsu: Nakagawa et al., 2012) and northern Honshu (i.e. Lake Megata: Yamada et al., 2010; Lake Ogawara: Ikeda et al., 1998), on one hand, and the decadal resolution pollen records from China (i.e. Sihailongwan Maar Lake: Stebich et al., 2009, 2015) on the other hand.

The pilot results of pollen analysis presented here (Fig. 3.4) clearly demonstrate changes in vegetation and climate, such as the onset of the Late Glacial warming around 15,000 cal. yr BP, the cold climate reversal after *c.* 13,000 cal. yr BP and the Late Glacial / Holocene transition around 11,650 cal. yr BP. This result is consistent with a formal definition and dating of the base of the Holocene Interglacial obtained from an array of physical and chemical parameters within the Greenland ice cores, including an abrupt shift in deuterium excess values, accompanied by more gradual changes in $\delta^{18}\text{O}$, dust concentration and annual layer thickness (Walker et al., 2009).

The transition from the Glacial (Ku-7 in Fig. 3.4) to the Late Glacial (Ku-6) environments on Rebun is characterized by a shift from herbaceous (predominantly sedge) to tree and shrub (pine, alder and birch) dominated vegetation. Spread of woody vegetation interrupted by the Late Glacial cold reversal (Ku-5) continues during the Early Holocene phase (Ku-4). The observed transition to colder (and more open) vegetation communities during the Late Glacial cold reversal – commonly referred to as Younger Dryas / Greenland Stadial 1 cold phase in the European and North Atlantic records (Walker et al., 2009) and Pollen Stadial 1 in the Lake Suigetsu record from central Japan (Nakagawa et al., 2005) – is not pronounced in the RK12 sediment column characterized by relatively organic-poor, homogeneous clay (Fig. 3.3b). However, a higher amount of sand grains in the layers dated to *c.* 15,200–14,750 and *c.* 14,500–14,150 cal. yr BP likely reflects intensified fluvial erosion activity during the Late Glacial climate amelioration phase. The pollen-based climate reconstruction from Lake Suigetsu (Nakagawa et al., 2005) suggests a pronounced increase

in the mean annual temperature from *c.* 4–8°C prior to *c.* 15,000 years ago to *c.* 8–12°C after this time. This deglacial warming accompanied by more gradual increase in atmospheric precipitation (Nakagawa et al., 2002) led to a replacement of the cool mixed forest vegetation that consisted of coniferous and deciduous broadleaf trees, such as *Picea*, *Abies*, *Tsuga*, *Betula*, *Quercus* and *Fagus crenata*, by *Fagus*-dominated temperate deciduous forest in the region of Lake Suigetsu (Gotanda et al., 2002; Nakagawa et al., 2005), *c.* 1175 km south of Lake Kushu.

The Middle Holocene phase (between *c.* 8000 and 4000 cal. yr BP) is well distinguishable in the composite core sediment characterized by mostly organic-rich and finely laminated clayey material after *c.* 8430 cal. yr BP and in the pollen record (Ku-5) suggesting a major spread of deciduous oak trees in the vegetation, with the highest percentages of oak pollen registered between 6000 and 5000 cal. yr BP. A noticeable increase in *Quercus* pollen percentages occurred in many regions of Hokkaido by about 8000 cal. yr BP, when cold-tolerant *Larix* disappeared from the pollen records (Igarashi, 2013), indicating Middle Holocene climatic optimum with slightly increased precipitation and improved thermal conditions. This is well in line with a major spread of cool mixed and cool conifer forests in the Hokkaido Region and in the southern part of Sakhalin which is reflected by maximum pollen percentages for *Ulmus*, *Quercus*, *Fraxinus*, *Juglans*, *Corylus* and *Acer* (Igarashi, 2013 and references therein). Middle Holocene optimum climate conditions are also reported for the lower Amur River region (Mokhova et al., 2009) and for the Kuril Archipelago (Razjigaeva et al., 2013).

The Khoe pollen record from Sakhalin Island, *c.* 650 km north of Lake Kushu (Igarashi and Zharov, 2011), and the pollen-based climate reconstruction (Leipe et al., 2015) demonstrate most favorable climate conditions on the island between *c.* 8700 and 5200 cal. yr BP. Compared with the Early Holocene part of the Khoe record, the reconstructed mean January and July temperature and mean annual precipitation values were higher by about 2.5°C, 0.5°C and 70 mm, respectively, during the Middle Holocene interval (Leipe et al., 2015).

The Late Holocene part of the RK12 record demonstrates homogeneous organic-rich clay sedimentation and reveals highest percentages of fir and pine pollen by *c.* 2000 cal. yr BP (Ku-2), suggesting an increase in coniferous forest cover in the regional vegetation. In the topmost part of the Khoe record, from *c.* 5200 cal. yr BP to present, the pollen analysis also shows a dominance of coniferous (e.g. *Picea* and *Abies*) pollen, whereas percentages of temperate woody taxa decrease (Igarashi and Zharov, 2011), suggesting a slight deterioration of the climate conditions on Sakhalin Island (Leipe et al., 2015). Analogous Late Holocene climate trends are inferred on the basis of palynological investigations from the wider study region including the lower Amur River basin (Mokhova et al., 2009) and the Kuril Islands (Razjigaeva et al., 2013). However, Late Holocene climate deterioration is less obvious in the fossil pollen records from Hokkaido, as suggested by the migration history of *Fagus crenata* (Igarashi, 2013) and a recent quantitative climate reconstruction derived from a *c.* 5500-year-old pollen record from southwest Hokkaido (Leipe et al., 2013). These

results and the Holocene vegetation and climate reconstruction based on the pollen record from Sihailongwan Maar Lake in northeast China (Stebich et al., 2015) suggest that hydrology of the Sea of Japan, particularly the re-intensified TWC, had a stronger influence on the regional and local climate conditions during the Late Holocene than the progressively weakening summer insolation. Forthcoming high-resolution pollen and sedimentary analyses of the RK12 core from Rebus will provide missing information helping to address this problem.

The uppermost zone of the RK12 pollen record (Ku-1) shows decrease in arboreal pollen after *c.* 1100 cal. yr BP, but more pronouncedly after *c.* 750 cal. yr BP. If the older part of the record primarily reflects natural, that is, climatically driven, changes in vegetation, this upper zone most likely reflects human activities, that is, intensive use of wood during the Okhotsk and particularly during the Ainu period. The pollen diagram (Fig. 3.4) also reveals several troughs in the arboreal pollen curve dated to around *c.* 1500, 2800, 3600, 4800 and 6600 cal. yr BP. However, an important task of the further in-depth environmental (including high-resolution pollen analysis) and archaeological research on Rebus would be to establish whether these and earlier drops in the arboreal pollen percentages reflect human presence on the island or natural climate variability or both. Another important question to be addressed by the continued archaeological excavations is whether consecutive peaks in the arboreal pollen curve correspond to the intervals with limited human activities or even absence of human settlements on Rebus Island during the earlier Jomon interval. In answering these questions and searching for possible connections between Holocene hunter-gatherer culture change and environmental / climatic conditions, high-resolution pollen and other palaeorecords (including diatoms and plant macrofossils) will play an important role.

Supporting the first results of diatom analysis obtained from the Lake Kusu basin (Kumano et al., 1990a), our pilot results (Fig. 3.5) also demonstrate that marine / brackish-water diatom taxa were abundant in the sediment between *c.* 10,500 and 7000 cal. yr BP, and freshwater taxa became dominant after that time. Presence of exclusively benthic freshwater diatom taxa near the core base is in line with the shallow water, marshy or deltaic environments suggested by the sedimentological (Fig. 3.3b) and pollen (Fig. 3.4) records. Both, the proxy-based reconstructions (Waelbroeck et al., 2002) and ICE-5G (VM2) model simulations (Peltier and Fairbanks, 2006) indicate that relative global sea level was about 110–115 m below present level at that time (i.e. around 17,000 cal. yr BP). Since then, global sea level rose steadily and reached *c.* 40 m below modern level *c.* 10,500 years ago. The diatom record (Fig. 3.5) suggests that marine water penetrated into the Kusu depression at about this time and turned it to a brackish-water lagoon, which existed until about 7000–6500 cal. yr BP. The diatom assemblage composition indicates that Kusu became a freshwater lake between *c.* 6500 and 6000 cal. yr BP, when global seas basically reached modern levels (Peltier and Fairbanks, 2006; Waelbroeck et al., 2002) and the sand bar separating Kusu lagoon from the sea has been formed. Greater environmental stability over the last 6000 years (in

comparison with the Early Holocene interval) is also supported by the results of radiocarbon dating of the RK12 core, stable sedimentation rates, and pollen composition.

However, four peaks in brackish / marine diatoms registered in the upper freshwater part of the floodplain core (Kumano et al., 1990a) may indicate short-term transgressions of seawater into the lake, which could be associated with catastrophic storms or palaeo-tsunami events. The diatom analysis of the RK12 core supports findings of earlier investigations demonstrating small but variable presence of marine taxa in the freshwater lake diatom assemblage. The diatom and sedimentary records from the Kiritappu marsh in eastern Hokkaido helped to identify 13 tsunami sands. Two of these lie within a peat bed above a historical tephra dated to AD 1739, and underlying are 11 prehistoric tsunami sand beds deposited during the past 4000 years (Nanayama et al., 2007). Ongoing high-resolution diatom and geochemical analyses of the upper RK12 core sediment accumulated during the last 6000–7000 years will help in deciphering the interactions within the lake–sea system on Rebun and contribute to the regional discussion of tsunamis and their possible impact on the prehistoric populations.

Complementing the pollen and diatom data, the analysis of plant macro-remains from the archaeological layers of Hamanaka 2 provides more detailed information about the plants used by ancient hunter-gatherers. The first results demonstrate that most of the identified remains belong to edible plants. The Okhotsk culture layer contains seeds of wild ruderal herbs and a great quantity of charred seeds of edible plants that is, *Actinidia arguta* (kiwi berry, ‘sarunashi’), *Vitis coignetiae* (grape, ‘yama-budō’) and *Empetrum nigrum* (black crowberry, ‘gankouran’). Few charred grains of *Hordeum vulgare* (barley) give evidence for the usage of this cereal. The presence of several charred seeds of *Toxicodendron* (sumac) and *Phellodendron amurense* (‘karafutokihada’) requires more attention. Sun et al. (2014) reported seeds of *P. amurense* from an Early Neolithic cave site in Shandong, China. Medicinal qualities of this plant and its edible bast were mentioned by Sun et al. (2014), and Crawford (1983) reported that the Ainu used its berries for food. The sumac seeds are well known from the older Jomon archaeological sites on Hokkaido (Crawford, 2011; Noshiro et al., 2007), but no use of sumac by the Ainu people has been reported so far (Crawford, 1983). The woody vine *Toxicodendron orientale* found in the modern vegetation on Rebun is a toxic plant. Other *Toxicodendron* (‘Rhus’) species from Japan are known to be used for wax and lacquer production (Wan et al., 2007). However, species-level identification of the Rebun seeds requires more work.

Our results indicate that the Hamanaka 2 site was not only used during summertime but during autumn as well, because fruits of *Vitis* and *Actinidia* become ripe on Rebun not until October. Edible plants such as *Vitis coignetiae*, *Sambucus sieboldiana*, *Actinidia arguta*, *Aralia cordata* and *Empetrum nigrum* are abundant in the natural vegetation on Rebun and the fossil record suggests their use in the past, as has been shown by the records from Neolithic sites in China (e.g. Wu et al., 2014). Despite some differences between the examined layers, our results suggest that plants could

have played an important supplementary role in the diet of the local inhabitants during the Okhotsk and Ainu periods. Particularly for the Okhotsk culture, highly specialized in marine fishing and hunting (e.g. Sato et al., 2007), our results from Rebus indicate a more complex subsistence. The roughly contemporaneous Satsumon culture (Fig. 3.2) identified in the southern and inner parts of Hokkaido had a stronger focus on plant cultivation (Adachi et al., 2009).

The utilization of barley has been proven for different Satsumon sites (Crawford, 2011). There is also evidence that the Okhotsk people cultivated barley, which was probably mainly used for rituals (Yamada, 1996). Barley remains associated with Okhotsk sites exhibit a different morphology compared with barley grown by the Satsumon, who introduced this crop from mainland Japan. It is believed that the barley cultivated by the Okhotsk was brought from the lower Amur Region (Yamada and Tsubakisaka, 1995). The barley grains currently recovered from the Okhotsk cultural layers of the Hamanaka 2 site open a new page in the study of agriculture spread across Eurasia.

While there is a long history of debate over the origin of barley and the possibility of an East Asian domestication (see Dai et al., 2012 for reasons why the Tibetan origin theory has recently been rejected), it is generally accepted that the crop originated from a wild progenitor in the Fertile Crescent about 10,000 years ago (Harlan and Zohary, 1966). A rapidly growing body of data from across Asia is illustrating how this crop, in unison with free threshing wheat, traversed the entire continent and became established as an important cultigen in East Asia (for a discussion, see Spengler, 2015). Crawford (1992) noted that East Asian archaeobotanical finds of hexaploid wheat and barley from Korea date to *c.* 3000 cal. BP and Japanese finds date to the beginning of the 1st millennium AD (see also Crawford and Lee, 2003). Crawford et al. (2005) further noted the importance of wheat in the economy of peoples in northeastern China, specifically discussing finds of wheat from the Liangchengzhen site in Rizhao City, Shandong. They were also quick to point out that rice and millet (broomcorn and foxtail) were the main crops throughout the archaeological record of northeast Asia, with barley playing a minor role. Crop cultivation was known in Japan at least as far back as the Late Jomon period (Fig. 3.2) (D'Andrea et al., 1995). Crawford (1992) also pointed out that, historically speaking, both hulled and naked forms of barley were traditionally grown in the warmer zones of southern Korea and southern Japan as a winter crop and in northern Japan as a summer crop. However, as long as the morphotype of the barley from the Okhotsk layers on Rebus is not further distinguished, trade with people from southern Hokkaido or other regions cannot be excluded.

3.7 Conclusion

The BHAP research strategy successfully introduced in the Lake Baikal Region strongly relies on the individual life history approach and multi-proxy environmental and climatic reconstructions for better understanding Neolithic and Bronze Age hunter-gatherer life ways (see Bezrukova et al.,

2013; Weber et al., 2013 and references therein). However, compatible (both bioarchaeological and palaeoenvironmental) datasets are still to be generated for the Hokkaido Region in order to revisit its past from this new evolutionary perspective. The pilot results from Rebun Island, northwest Hokkaido, presented in the current work demonstrate that forthcoming high-resolution pollen and diatom analyses of the Lake Kushu sedimentary archive are able to provide environmental records of high quality and temporal resolution required to address three main scientific goals: (1) generating objective environmental reconstructions of the shifts in climate, vegetation, ocean currents and sea levels; (2) validating regional proxy- and model-based climatic scenarios; and (3) evaluating their potential effects on the Hokkaido cultural sequence, including resource availability and foraging strategies, settlement and population dynamics. The third goal, however, requires strong contribution from the archaeological research in the region and implies interdisciplinary cooperation. Examples of detailed analysis of plant macro-remains preserved in the cultural layers of the Hamanaka 2 site emphasize the benefits of such cooperation. On one hand, the AMS ^{14}C dating of the identified terrestrial plant remains allows a well-founded age determination of the excavated cultural layers and improved correlation between the environmental and archaeological datasets. The latter often becomes a serious problem in coastal environments, where the ages of excavated animal and human bones are affected to varying degrees by the marine reservoir effect. On the other hand, identification of plant remains allows detailed insights into the living condition and use of plant resources by ancient human populations. Recent discovery of cultivated barley grains in the cultural layers of the Hamanaka 2 site provides new information for discussion of spread of agriculture (or agricultural products) into northern Japan during the Okhotsk and Ainu periods.

3.8 Acknowledgements

We greatly acknowledge various help and support of the project from local Ainu and fishermen communities and local governmental organizations. We thank Dr. T. Haraguchi (Osaka City University) for providing the bathymetry data of Lake Kushu, Dr. Y. Igarashi for useful consultations. Last but not least, we would like to thank Dr. R. Spengler for editorial corrections and valuable suggestions concerning barley agriculture, and two anonymous reviewers for their helpful comments on an earlier version of this manuscript.

3.8.1 Funding

Coring of Lake Kushu and core transportation costs were covered by the Japanese MEXT-Japan Kakenhi research grant no. 21101002 held by Dr. H. Yonenobu. The Baikal–Hokkaido Archaeology Project (BHAP) and BHAP-related research activities on Rebun Island presented in this paper are supported by the Major Collaborative Research Initiative (MCRI) program of the Social Sciences and Humanities Research Council of Canada, and collaborating institutions,

3. Manuscript II - 3.8 Acknowledgements

including University of Alberta, German Archaeological Institute (DAI), Free University of Berlin and German Science Foundation (DFG TA 540/5), Hokkaido University, and Japan Society for the Promotion of Science.

4. Manuscript III

Diatoms from Lake Kushu: A pilot study to test the potential of a Late Quaternary palaeoenvironmental archive from Rebun Island (Hokkaido Region, Japan)

Mareike Schmidt,¹ Pavel E. Tarasov,¹ Philipp Hoelzmann,² Hanno Meyer,³ Christian Leipe¹

¹ *Institute of Geological Sciences, Paleontology, Freie Universität Berlin, Malteserstrasse 74-100, Building D, 12249 Berlin, Germany*

² *Institute of Geographical Sciences, Physical Geography, Freie Universität Berlin, Malteserstrasse 74-100, Building B, 12249 Berlin, Germany*

³ *Alfred Wegener Institute Helmholtz Centre for Polar and Marine Research, Research Unit Potsdam, Telegrafenberg A43, 14473 Potsdam, Germany*

*published in Journal of Asian Earth Sciences, Volume 122, pp. 106-122
accepted: 4 March 2016, published: 15 May 2016*

This is a post-peer-review version of an article published in Journal of Asian Earth Sciences. The final authenticated version is available online at: <https://doi.org/10.1016/j.jseaes.2016.03.005>.

4.1 Abstract

Rebun Island is a key research area for the Baikal-Hokkaido Archaeology Project to better understand the dynamics of the Neolithic hunter–gatherers in the NW Pacific region. Hence, the *c.* 19.5 m sediment core RK12 spanning the last *c.* 16.6 cal. kyr BP was obtained from Lake Kushu. Our aim is to test its potential as a high-resolution multi-proxy archive. Here, we used diatoms to investigate the modern ecosystem of Lake Kushu and its surrounding area on Rebun Island and of Hime-numa Pond on Rishiri Island and selected core samples for comparison. Modern diatom and stable isotope analyses show well-mixed freshwater bodies with eutrophic, alkaline conditions. The fossil diatom and geochemical sediment analyses display three phases that represent major changes in the lake development: (i) a marshy phase (*c.* 16.6–10 cal. kyr BP); (ii) a brackish water lagoon phase (*c.* 10–6.6 cal. kyr BP); and (iii) a freshwater lake phase (since *c.* 6.6 cal. kyr BP). This shows the major role of the postglacial climate amelioration, global sea-level rise and marine transgression in the development of this landscape. Further analyses will provide a palaeolimnological record at (sub-) decadal resolution that will facilitate the interpretation of the hunter–gatherer dynamics.

4.2 Introduction

An increasing number of archaeological sites of the hunter–gatherer cultures in the Hokkaido Region are being investigated (Weber et al., 2013 and references therein). Main research foci are to outline the differences between the Japanese and Okhotsk civilizations and the origin and geographical distribution of the Okhotsk people (Ohyi, 1975) that led to cultural heterogeneity (Moiseyev, 2008), which is also reported in characteristic pottery types (Deryugin, 2008).

The Baikal-Hokkaido Archaeology Project (BHAP) enlarged its study area from the Baikal Region (Siberia) towards the Hokkaido Region to improve the understanding of Holocene hunter–gatherers, their cultural dynamism, variability and lifestyle (Weber et al., 2013). In fact, the driving factors for cultural changes, e.g. environmental and climate changes or epidemic diseases, are not fully understood. Because numerous remains of the Middle Jomon (5–4 cal. kyr BP), Late to Final Jomon (4–2.3 cal. kyr BP), Epi Jomon (2.3–1.3 cal. kyr BP), Okhotsk (1.5–0.8 cal. kyr BP), and Historic Ainu (0.7–0.1 cal. kyr BP; Müller et al., 2016) cultures that were recently found on Rebun Island, this area is of special interest for the BHAP research. So far there are 43 sites on Rebun Island, with the oldest residential sites dated to *c.* 4.9–4.4 cal. kyr BP (see Müller et al., 2016 and references therein).

The need for a nearby high-resolution archive for reconstructing local and regional climate as well as environmental changes resulted in the Lake Kushu coring campaign in February 2012. Two parallel, overlapping sediment cores (RK12-01 and RK12-02) were taken in the central part of the ice-covered lake. The obtained *c.* 19.5 m composite sediment core is a potentially high-resolution environmental archive, which will be investigated using a multi-proxy approach that includes a ¹⁴C-inferred chronology, pollen, tephra, and geochemical analyses.

Various proxies have been used to reconstruct the Holocene climate and vegetation of Hokkaido and central Japan. Pollen-based reconstructions are among the most numerous during the last few decades, resulting in a number of articles concerning past vegetation or biome dynamics and its climatic and human-impact implications (e.g. Nakagawa et al., 2002, 2005; Gotanda et al., 2002, 2008; Igarashi et al., 2011; Tarasov et al., 2011; Hase et al., 2012; Igarashi, 2013; Leipe et al., 2013; Kigoshi et al., 2014).

Like terrestrial pollen, diatoms have been successfully used as a palaeoenvironmental proxy in Europe, North America and Africa (e.g. Gasse, 1986; Round et al., 1990; Smol and Stoermer, 2010). A considerable amount of studies has been published in local journals and in the Japanese language. Nevertheless, an increasing number of internationally accessible studies describing taxonomy, geographical distribution, and ecology of lacustrine, riverine, and coastal marine diatom taxa appeared during the last two decades. In Hokkaido, several water bodies have been analyzed including Lake Akan (Tuji et al., 2003), Hii River (Ohtsuka, 2002), and Lake Tokotan (Sawai, 2002). Diatom-inferred environmental reconstructions for the Holocene were obtained from coastal plains including the Tokoro Region (Hamano et al., 1985), Akkeshi Estuary (Kumano et al.,

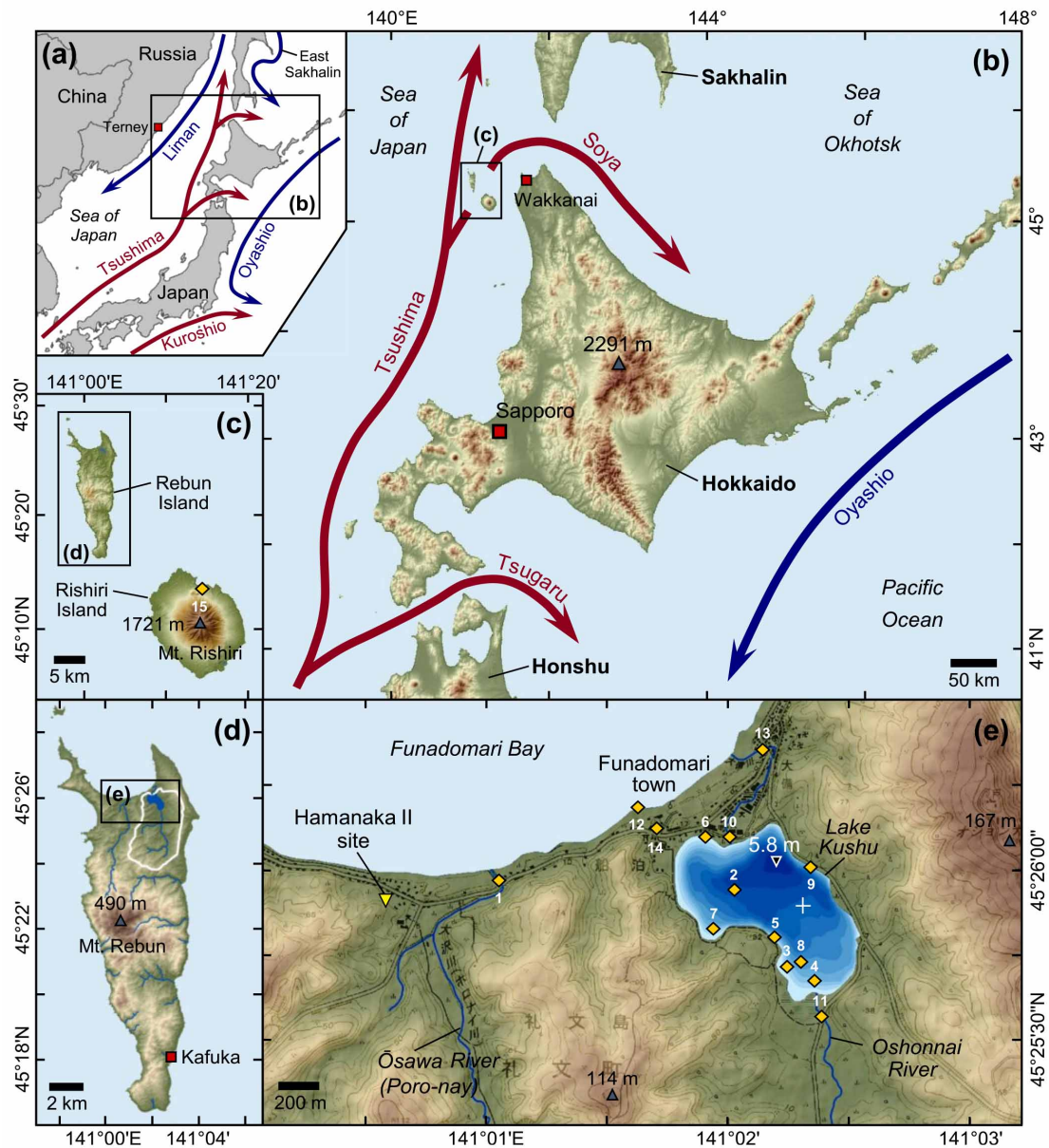


Figure 4.1: Chart compilation showing (a) Japan and the location of Terney Climate Station; (b) Hokkaido, including the Tsushima, Tsugaru and Soya sea surface warm currents (red) and Oyashio cold current (blue); (c) outline of Rebun and Rishiri islands; (d) Rebun Island, including main rivers and location of Lake Kushu; (e) Lake Kushu. Isolines represent water depth in 0.5 m steps. Yellow triangle marks the archaeological Hamanaka 2 site, orange rhombuses indicate the sampling sites on Rebun and Rishiri islands (see Table 4.1 for details), white cross marks the location of the Kushu core RK12. Topographic maps are based on elevation Shuttle Radar Topography Mission (SRTM) V4.1 data (Reuter et al., 2007; Jarvis et al., 2008). Isolines for terrestrial area are drawn from a topographic map (Geospatial Information Authority of Japan, 2012). Bathymetry of Lake Kushu is based on survey data provided by T. Haraguchi (Osaka City University); a, b, c and e, modified after Müller et al., 2016.

1990a), Kushiro Moor (Ihira et al., 1985; Kumano et al., 1990b), and Kutcharo Lake (Kumano et al., 1984).

On Rebun Island, Kumano et al. (1990a) and Sato et al. (1998) analyzed a 16.25 m sediment core spanning the last *c.* 9000 years as suggested by the four ^{14}C dates given in their studies. Their core was obtained from the peat moor on the southern margin of Lake Kushu. These papers provide a relatively coarse-resolution diatom record with repeated occurrences of brackish-water

environments, suggesting multiple phases of marine influence on Lake Kushu during the Holocene. Sato et al. (1998) mention taxonomic problems, which could be addressed by a high-resolution diatom analysis and would improve the understanding of the environmental history of Lake Kushu and its catchment. Until now, no study has focused on the modern diatom assemblages of Rebun Island and neighboring Rishiri Island. Our paper is a pilot study and presents the first results on modern diatom assemblages from the Rebun and Rishiri islands in order to discuss the potential of fossil diatom assemblages as regional palaeoenvironmental indicators in a new sediment core from Lake Kushu representing the last 16,600 years.

4.3 Study area

4.3.1 Environments

Rebun and Rishiri islands are located 45 km and 19 km, respectively, northwest off the coast of Hokkaido in the northeastern part of the Sea of Japan (Fig. 4.1a and b). The islands are – as with the entire Japanese Archipelago – located in a tectonically active zone with volcanism, earthquake and tsunami activities (e.g. Hashimoto, 1991; Kimura, 1997; Mandal et al., 2011). The formation of Rebun Island started with the subaqueous volcanic dome growth in the Cretaceous (Kimura, 1997; Goto and McPhie, 1998). Accordingly, the main units on Rebun Island exhibit Cretaceous volcanic rocks of the Rebun Group overlain by Late Miocene sedimentary formations with several basaltic to dacitic intrusions (Goto and McPhie, 1998). The highest point of the island is named Mount Rebun and reaches 490 m a.s.l. (Geospatial Information Authority of Japan, 2012). Rebun Island has an elongated shape and extends for *c.* 20 km along the north–south axis and *c.* 6 km along the east–west axis, spanning an area of *c.* 82 km² (Fig. 4.1d).

Rishiri Island, situated *c.* 9 km southeast of Rebun Island (Fig. 4.1c), is composed of the main strato-volcano called Mount Rishiri, reaching 1721 m a.s.l. (Kuritani and Nakamura, 2006), and several small surrounding volcanoes attached to the main volcano (Mandal et al., 2011). Volcanic activity started *c.* 200 kyr BP and deformed the Tertiary basement rocks (Mandal et al., 2011). The island has a more or less circular shape, measures *c.* 14–18 km in diameter and spans an area of *c.* 183 km². Distance and area calculations for Rebun and Rishiri islands were performed based on ASTER GDEM 2 data (METI and NASA, 2011) applying a projected coordinate system (EPSG projection 2623) using ArcGIS v10.2 (ESRI, 2014).

The Tsushima Warm Current (TWC) flowing along the west coast of Hokkaido also influences Rebun and Rishiri islands. Its one branch, called the Soya Warm Current, flows through the Soya (or La Perouse) Strait and into the Sea of Okhotsk (Fig. 4.1a and b). The TWC affects the regional climate significantly (Igarashi, 2013), particularly during the cold season (November to May; see Leipe et al., 2013 for details and references therein) when the region is strongly influenced by the East Asian Winter Monsoon. Cold and dry air masses from Siberia passing over the relatively warm Sea of Japan collect its ascending moisture and heat resulting in heavy

snowfalls in the western Hokkaido Region from November to April with highest amounts recorded in December (Igarashi, 2013; Leipe et al., 2013 and references therein). The Okhotsk High over the Sea of Okhotsk and the Ogasawara High in the northwestern subtropical Pacific control climatic conditions of the warm season. In years with a strong Okhotsk High, linked to the positive mode of the Winter North Atlantic Oscillation, summers are cool; by contrast, the Ogasawara High is connected to La Niña and results in relatively warm summers (Ogi et al., 2004; Igarashi et al., 2011; Igarashi, 2013). The following climatic data for Rebun and Rishiri islands were derived from a global high-resolution interpolated (30 arc seconds or 1-km spatial resolution) climate surface dataset for land areas (Hijmans et al., 2005) averaged over a fifty-year (1950–2000) period and based on meteorological station data (Fig. 4.2a). The mean monthly air temperature on Rebun Island varies from -6.4°C in January to 19.4°C in August with a mean annual precipitation of 1102 mm, with highest amounts falling from September (131 mm) to December (106 mm).

Nakagawa et al. (2002) and Leipe et al. (2013) described the predominant natural vegetation type (biome) of Rebun and Rishiri islands (as well as most of Hokkaido) as cool mixed forest. The vegetation on Rebun Island was severely impacted by human activities during the last century. The modern landscape is considerably deforested and *Sasa* spp. (bamboo grass from the Poaceae family) became widespread on the entire island (Müller et al., 2016). Patchy forests and shrubs occupy the river and spring valleys. The vegetation on Rishiri Island consists of a mixture of boreal conifers and cool-temperate broad-leaved trees (Igarashi, 2013). In the volcanic deposition area below 400 m a.s.l., *Sasa* spp. are very frequent as well, but their distribution decreases with higher altitude and under the forest cover.

4.3.2 Hydrology

Lake Kushu (45°25'58"N, 141°02'05"E, 4 m a.s.l.) is a relatively shallow coastal freshwater lake in the northern part of Rebun Island. The distance to Funadomari Bay is about 200 m (Fig. 4.1e). The lake is separated from the sea by sand barriers with dune ridges reaching up to 15 m a.s.l. that was formed by strong winter winds (Sato et al., 1998). The lake catchment spans an area of *c.* 10 km². The lake surface area covers about 0.53 km² with a total shoreline length of 3.4 km. The maximum water depth of 5.8 m occurs in the northern part of the lake and the average water depth is *c.* 3.5 m (bathymetry data provided by T. Haraguchi, Osaka City University). Lake Kushu has two inflows and one outflow that connects with the sea. The major inflow, called Oshonnai River, enters the lake from the south. The second inflow is a small stream that reaches Lake Kushu from the southeast. The outflow in the north is canalized and flows through Funadomari town and into Funadomari Bay. The lake is surrounded by a ring of dense aquatic vegetation (mainly *Phragmites* and *Typha*) followed by a ring of trees and shrubs, and extensive grasslands and meadows. The absence of large-scale agricultural activity and the dense vegetation cover substantially reduce soil erosion so that the accumulation in the lake reflects mainly lake

4. Manuscript III - 4.3 Study area

bioproductivity and aeolian influx, with a minor impact from the inflowing rivers. The lake freezes from December to April (Sato et al., 1998). The Ōsawa River flows west of the Lake Kushu catchment. It originates at Mt. Rebun and enters Funadomari Bay *c.* 1.45 km west of the Lake Kushu outflow.

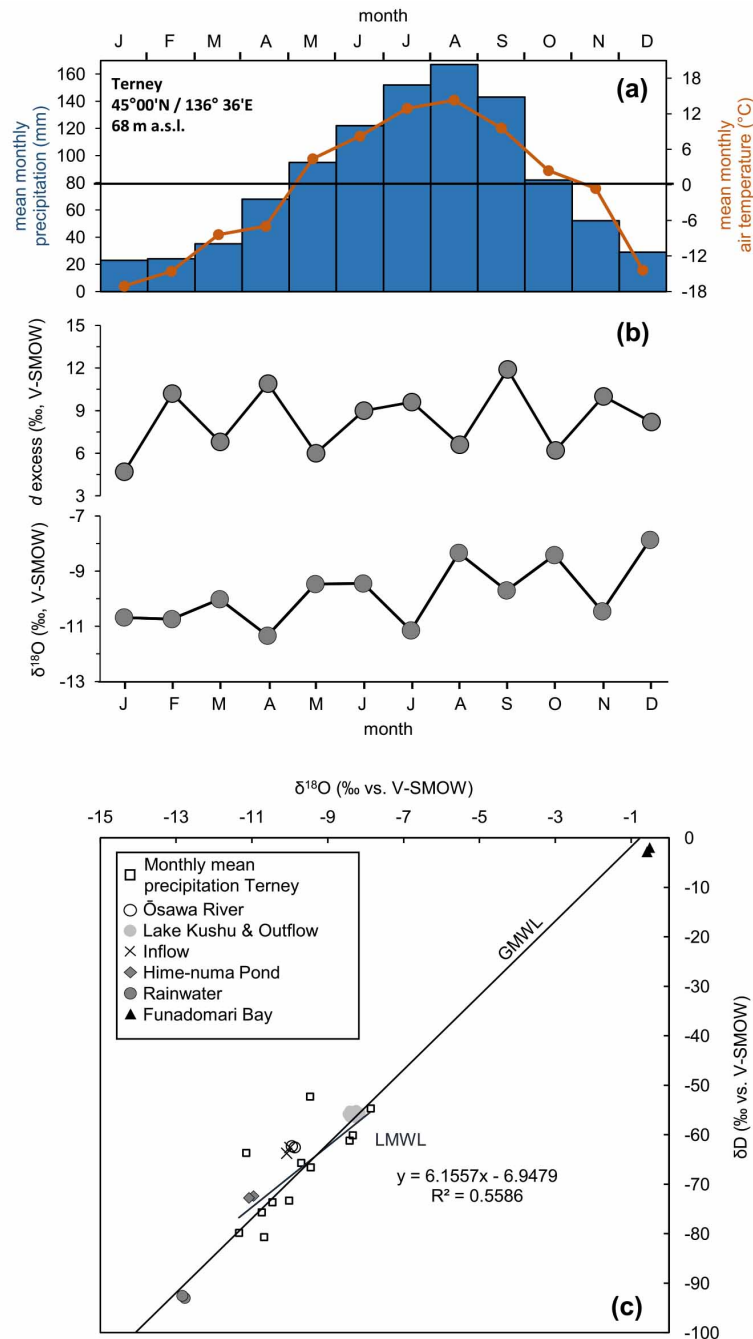


Figure 4.2: Diagrams illustrating meteorological background information including (a) mean monthly precipitation (blue) and temperature (orange) data derived from interpolated climate surface dataset for global land areas from Hijmans et al. (2005); (b) plotted annual variability of $\delta^{18}\text{O}$ and d excess in precipitation, based on the data from the GNIP Station in Terney; and (c) $\delta^{18}\text{O}$ - δD diagram for Lake Kushu setting, Hime-numa Pond, and Terney precipitation. The Local Meteoric Water Line (LMWL) given by the monthly mean isotopic composition in precipitation from the Terney dataset (blank black rectangles) and the Global Meteoric Water Line (GMWL) are included.

Hime-numa Pond (45°13'36"N, 141°14'43"E, 129 m a.s.l.) is a shallow circular artificial pond located in the northern part of Rishiri Island. The pond was created in 1917, when small swamps and springs were combined to form one larger waterbody. The freshwater pond has a shoreline of *c.* 0.7 km (estimated during fieldwork), which corresponds, to a surface area of 0.03 km². The pond is fed by atmospheric precipitation (i.e. rain and snow) falling within its catchment area on the northern flanks of Mt. Rishiri. It has no major permanent surface inflow or outflow. The shore and lake bottom are partly stabilized with cement to control the shore, since the pond functions as a tourist site with a wooden trail constructed around it. The surrounding area is vegetated with trees and shrubs protecting the soil from erosion.

Unless otherwise stated, all given distances and areas in this chapter were calculated based on ASTER GDEM 2 data (METI and NASA, 2011) and a digitized and georeferenced topographic map (Geospatial Information Authority of Japan, 2012) applying a projected coordinate system (EPSG projection 2623) using ArcGIS v10.2 (ESRI, 2014).

4.4 Material and methods

4.4.1 Modern diatom samples

In August 2014, 15 modern diatom samples were collected. Most samples originate from Lake Kushu on Rebun Island (Fig. 4.1e, Table 4.1) and one sample represents Hime-numa Pond on Rishiri Island (Fig. 4.1c).

For a comprehensive overview of the diatom species living in Lake Kushu (including the inflow and outflow) we aimed at sampling different habitats. Therefore, surface lake sediments, surface waters and aquatic plants were collected. The surface lake sediments (1–2.4 m water depths) were collected in the near-shore area using a plastic cup fixed on a scaled telescope bar. Approximately, 30 ml of material was taken from each location. The planktonic diatoms were sampled using a 65- μ m-mesh size plankton net with a 100 ml plastic tube mounted (Kalbe, 1980; Göke, 1993). The plankton net was hauled several times through the uppermost 10–20 cm of the water column. In total, *c.* 250 ml of each surface water sample was preserved in wide mouthed sterile plastic tubes with a screw top. To collect the epiphytic diatoms, the uppermost aquatic plant parts were removed and stored in a 500 ml sterile wide mouthed plastic tube with a screw top. Following Battarbee et al. (2001), all samples were preserved with a few drops of Lugol's Iodine and stored in a cool and dark place.

4.4.2 Water chemistry analysis

Water variables such as surface water temperature, pH, oxygen saturation, and electrical conductivity were measured with a WTW 340i portable meter. The samples for stable water isotope analysis – 11 surface water samples and one precipitation sample – were stored in 30 ml

Table 4.1: Summary of the sample locations including sample date and geographical position together with the on-site measured water parameters pH, surface oxygen saturation, water temperature, and electrical conductivity. The last five columns contain the results of the stable oxygen and hydrogen isotope analyses.

ID	RI-14- Samples	Location name	Date [2014]	Longitude [N]	Latitude [E]	Altitude [m a.s.l.]	Water Depth [m]	pH	Oxygen [%]	Temp. [°C]	Cond. [S/m]	$\delta^{18}\text{O}$ [‰ vs. SMOW]	δD [‰ vs. SMOW]	1σ	1σ	d excess
01a	Surface water	Ōsawa River	Aug-16	45.4330	141.0175	1	0.1	8.2	80	16.0	0.02	-9.9	-62.5	0.05	0.3	16.9
01b	Water plant	Ōsawa River	Aug-16	45.4330	141.0175	1										
02a	Surface water	Kushu Lake	Aug-19	45.4322	141.0343	4	0.1	10.7	180	23.6	0.023	-8.2	-55.4	0.02	0.2	10.3
03a	Surface water	Kushu Lake	Aug-19	45.4287	141.0378	4	0.1					-8.4	-55.9	0.05	0.3	11.5
03b	Water plant	Kushu Lake	Aug-19	45.4287	141.0378	4										
04a	Surface water	Kushu Lake	Aug-19	45.4277	141.0395	4	0.1	10.4	104	23.6	0.021	-8.3	-55.9	0.03	0.4	10.3
05a	Sediments	Kushu Lake	Aug-19	45.4302	141.0362	4	1.7									
06a	Sediments	Kushu Lake	Aug-19	45.4351	141.0318	4	0.1									
07a	Surface water	Kushu Lake	Aug-21	45.4303	141.0325	4	0.1	9.2	78	22.6	0.02	-8.3	-56.1	0.03	0.3	10.3
07b	Sediments	Kushu Lake	Aug-21	45.4303	141.0325	4	2.0									
07c	Water plant	Kushu Lake	Aug-21	45.4303	141.0325	4										
08a	Sediments	Kushu Lake	Aug-21	45.4289	141.0378	4	2.4									
09a	Surface water	Kushu Lake	Aug-21	45.4335	141.0389	4	0.1	10.7	160	23.7	0.021	-8.3	-56.1	0.03	0.3	10.3
09b	Sediments	Kushu Lake	Aug-21	45.4335	141.0389	4	2.0									
10a	Surface water	Kushu Lake	Aug-21	45.4350	141.0335	4	0.1					-8.4	-55.7	0.02	0.3	11.2
11a	Surface water	Oshonnai River	Aug-21	45.4261	141.0398	4	0.1	8.0	106	17.7	0.024	-10.0	-63.2	0.02	0.3	17.2
12a	Surface water	Funadomari Bay	Aug-22	45.4364	141.0271	0	0.1	8.6	90	24.3	4.93	-0.5	-2.4	0.02	0.3	2.0
12b	Sediments	Funadomari Bay	Aug-22	45.4364	141.0271	0	0.4									
12c	Water plant	Funadomari Bay	Aug-22	45.4364	141.0271	0										
13a	Surface water	Kushu Outflow	Aug-22	45.4392	141.0357	3	0.1	9.6	63	24.4	0.02	-8.4	-56.1	0.04	0.4	11.4
13b	Water plant	Kushu Outflow	Aug-22	45.4392	141.0357	3										
14a	Water	Rain water	Aug-24	45.4354	141.0280	8						-12.8	-92.8	0.03	0.3	9.9
15a	Surface water	Hime-numa Pond	Aug-25	45.2269	141.2472	129	0.1	9.3	76	16.1	0.007	-11.0	-72.6	0.03	0.4	15.6
15b	Sediments	Hime-numa Pond	Aug-25	45.2269	141.2472	129	1.0									

narrow mouthed sterile plastic tubes, closed tightly with a screw top and stored in a cool and dark place. The stable oxygen and hydrogen isotope compositions were measured with a Finnigan MAT Delta-S mass spectrometer at the stable isotope laboratory of the Alfred Wegener Institute Helmholtz Centre for Polar and Marine Research, Research Unit Potsdam, Germany (see Meyer et al., 2000 for detailed explanation). The values are given as δ -values in per mil difference to V-SMOW (Vienna Standard Mean Ocean Water). The standard deviation (1σ) is better than $\pm 0.8\%$ and $\pm 0.1\%$ for δD and $\delta^{18}O$, respectively.

4.4.3 Fossil samples from Lake Kushu sediment: Choice and chronology

Lake Kushu coring was performed on the ice-cover, in the central part of the lake at a water depth of *c.* 4.5 m (the location is indicated with a white cross in Fig. 4.1e). Two parallel sediment cores RK12-01 and RK12-02 were drilled within a couple of meters distance using a hydro-pressure thin-walled piston corer. The overlap of the parallel cores allows for the sampling of a continuous *c.* 19.5 m long composite sequence. The cores were transported to the Graduate School of Environmental Science at Hokkaido University in Sapporo and opened in April 2012 by splitting the core into two identical halves. Both cores were described and photographed in the laboratory and subsampled using the double L-channel (written as LL-channel) method (Nakagawa, 2007). The complete set of the plastic wrap-packed 1 m long LL-channel segments was sent to the Institute of Geological Sciences at the Freie Universität Berlin.

A set of 57 bulk samples (each representing 1 cm of the sediment core) was sent to the Poznan Radiocarbon Dating Laboratory for AMS dating. The obtained results of the ^{14}C dating allow the construction of an accurate age model, suggesting continuous sedimentation through the last *c.* 16.6 kyr (calibrated calendar ages before present, cal. yr BP are consistently used throughout the manuscript, unless specified otherwise, Fig. 4.3).

A detailed description of the ^{14}C data and discussion of the calibration issues and age-depth model for the RK12 core will be presented in a separate paper (Müller et al., 2016).

On the material of the RK12 composite core from Lake Kushu a continuous diatom analysis at 1 cm intervals is planned. Before starting this time and labor consuming analysis the potential of the core's diatom assemblages for addressing different research questions such as marine impact and climate changes should be tested. Therefore, we selected and analyzed ten fossil samples from throughout the core. Sample details such as corresponding ages and selected research foci that could be potentially addressed are presented in Fig. 4.4. To support interpretations made from the diatom record, sediment samples from selected depths were also geochemically analyzed.

4.4.4 Diatom analysis

To remove the organic matter from the samples, 100 ml of 10% hydrogen peroxide (H₂O₂) were added and the beakers were placed on a hot plate at 80°C to accelerate the chemical reaction. After reaction had ceased, the chemical was washed out four times with 800 ml distilled water.

The fossil sediment samples were treated using the standard techniques for diatom preparation according to Battarbee et al. (2001). First, 37% hydrochloric acid (HCl) was added to the dried, weighted samples to remove the carbonates. Afterwards, 10% H₂O₂ was added to remove the organic residual. After each step, the chemicals were washed out with distilled water. After treatment, one drop of the solution (both for modern and fossil samples) was placed onto a cover slip, air-dried at room temperature and embedded into NaphraxTM (refractive index = 1.67). The valves were counted using a Meiji Techno 4000 microscope, at 1000x magnification with immersion oil. When possible, 500 valves were counted in each sample. To avoid double counting, only fragments exceeding 50% of the total valve area were counted. To help with the identification of difficult taxa, photographs were taken with a Zeiss Supra 40VP scanning electron microscope (SEM).

Diatom identification was performed using the floras of Krammer and Lange-Bertalot (1997, 1999, 2000, 2004), Ohtsuka (2002), Kobayasi et al. (2006), Levkov (2009), Houk et al. (2010), Lee (2011, 2012) and Tanaka (2014). The taxonomical names follow the system on the website AlgaeBase (Guiry and Guiry, 2017). Bar diagrams of diatom percentages were plotted using Tilia[®] software (Grimm, 1991–2011).

For each sample, the individual taxon percentages were calculated based upon the total sum of counted valves taken as 100%. Both, modern and fossil assemblage diagrams show taxa exceeding 5% individually. They are classified to pennate (mostly benthic) and centric (mostly planktonic) forms and further subdivided into freshwater and brackish / marine taxa. Species not exceeding 5% of the assemblages are summed up in the following groups: other benthic freshwater taxa, other benthic brackish / marine taxa, other planktonic freshwater taxa, and other planktonic brackish / marine taxa. The stack diagrams for B/P (relationship of benthic to planktonic species, defined as $B/P = \frac{\sum_{\text{benthic taxa}}}{\sum_{\text{benthic+planktonic taxa}}}$), salinity, trophic and pH illustrate the sums of the ecological optima for each taxon based on data from the literature. The specific optima were coded with letters from A to E for the pH, from A to F for the trophic, from A to D for the salinity, and with B or P for the B / P, and added to the taxa information column in the Tilia[®] spreadsheet for calculation.

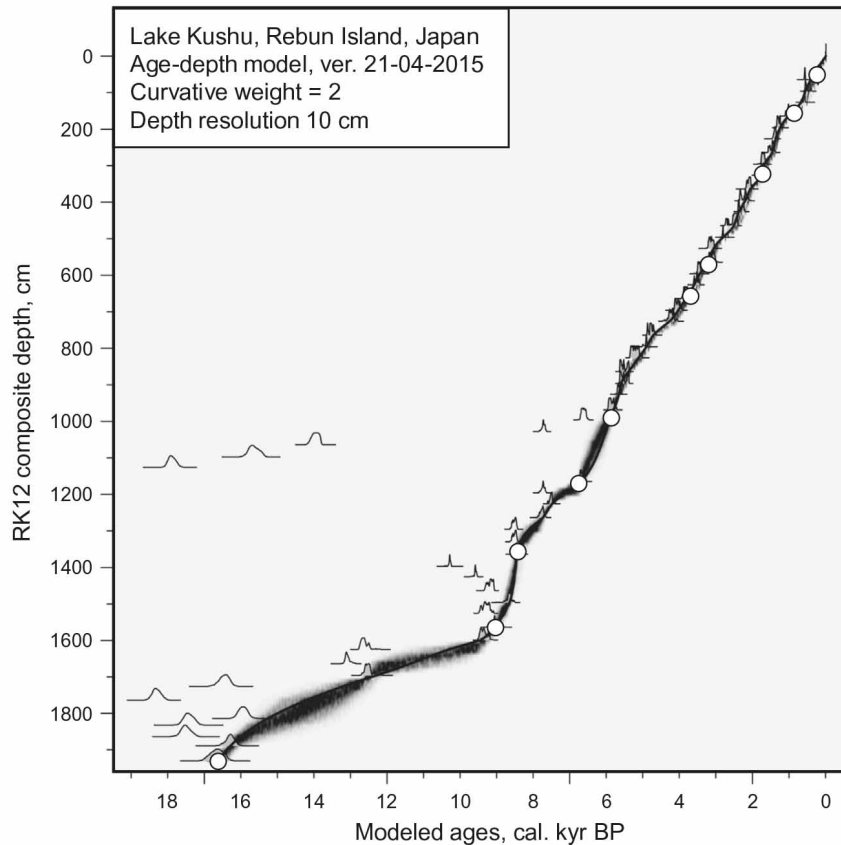


Figure 4.3: Age-depth model diagram (best-fit line with uncertainty ranges) applied to the analysed RK12 sediment core samples (white dots) from Lake Kushu. Radiocarbon dates were calibrated against the calibration curve Intcal13 (Reimer et al., 2013), and the model was constructed using the free-shape algorithm (Goslar et al., 2009). The grey silhouettes along the best-fit line represent calibrated ¹⁴C dates taken into account by the model, while the not-filled silhouettes left of the best-fit line represent older ¹⁴C dates rejected by the model (redrawn after Müller et al., 2016).

Sample ID RK12-02-	Composite depth [cm]	Cal ¹⁴ C age [cal. kyr BP]	Geological epoch [kyr BP]	Cultures in Hokkaido [kyr BP]	Research question
01_1-2	51.5	0.3	Late Holocene (4 - 0)	Historic Ainu* (0.7 - 0.1)	Are there dramatic environmental changes, e.g. marine transgression, since the first settlement on Rebus I. 5000 years ago?
02_7-8	157.5	0.9		Okhotsk* (1.5 - 0.8)	
03_73-74	323.5	1.7		Epi Jomon* (2.3 - 1.3)	
06_21-22	571.5	3.2	Middle Holocene (8 - 4)	Late to Final Jomon* (4 - 2.3)	Does RK12 show maximum lacustrine extent between 4.9 and 3.1 ka as suggested by Sato et al. (1998)?
07_9-10	659.5	3.7		Middle Jomon* (5 - 4)	
10_40-41	990.5	5.8		Early Jomon (6 - 5)	
12_19-20	1169.5	6.7			
14_7-8	1357.5	8.4	Early Holocene (11.7 - 8)	Inical Jomon (10 - 6)	Does the archive provide information about the transition from late-glacial to early Holocene?
16_16-17	1566.5	9.0		Incipient Jomon (14 - 10)	
19_82-83	1932.5	16.6	Late Pleistocene (126 - 11.7)		

Figure 4.4: Listing of the ten samples analysed for diatoms with their composite depth, cal. age BP and placement in the geological and archaeological time period. Asterisks mark cultures of which remains were found on Rebus Island. Archaeological dates from Müller et al. (2016).

4.4.5 Geochemical analyses of core sediments

4.4.5.1 X-Ray fluorescence analysis (XRF)

For elemental analyses of the bulk sediment a portable energy dispersive X-Ray fluorescence spectrometer (P-ED-XRF) Analyticon NITON XL3t equipped with a CCD-camera and a semiconductor detector was used. The samples were grinded and homogenized with a vibrating cup mill. The resulting powder was dried for 2 h at 105°C and kept in a desiccator at room temperature. C. 4 g of the powdered samples were placed in plastic cups and sealed with Mylar foil (0.4 µm). The prepared sample cups were placed on the P-ED-XRF and measured for 120 sec with different filters for the detection of specific elements with specifications (X-Ray source and Ag-anode) of $U_{\max} \cdot I_{\max} = 2 \text{ W}$, $U_{\max} = 40 \text{ kV}$ and $I_{\max} = 100 \text{ µA}$. Four filters were used with the following adjustments: (i) main measuring 30 sec at 50 kV with 40 µA, (ii) low measuring 30 sec at 20 kV with 100 µA, (iii) light measuring 30 sec at 8 kV with 250 µA, and (iv) high measuring 30 sec at 50 kV with 40 µA. Before analyzing the prepared samples the P-ED-XRF was calibrated using two lacustrine sediments (Lynch, 1990) as certified reference material (CRM) LKSD-2 (lake sediment; Lot. Nr. 688) and LKSD-4 (lake sediment; Lot. No. 897). Only elements that show mean values larger than four times the 2σ error of the measurements, i.e. aluminum (Al), calcium (Ca), iron (Fe), potassium (K), rubidium (Rb), sulphur (S), silicon (Si), strontium (Sr), titanium (Ti), and zinc (Zn) were taken into account for the analyses (for further information see: Jenkins, 1999; De Vries and Vrebos, 2002). The calibration with the CRM was checked after every fifth sample measurement.

4.4.5.2 ICP-OES analysis

Sediment samples were analyzed for major elements (Ca, Fe, K, magnesium (Mg), manganese (Mn), sodium (Na), phosphorus (P), S, and Sr) using an inductively coupled plasma optical emission spectrometer (ICP-OES Perkin Elmer Optima 2100DV) on the base of DIN EN 1346 (Anonymous, 2001). Dilutions of 0.5 up to 3.0 g of dry sediment were produced with aqua regia (1.2 ml of 65% nitric acid, 3.6 ml of 3% HCl and 0.5 ml of water) in a microwave furnace (microwave digestion unit MLS-MEGA 90).

The solution was filtered into volumetric flasks (50 ml) using glass funnels, fluted filters (particle retention 5–8 µm, size 150 mm), and bi-distilled water. The solution was kept in polyethylene (PE) flasks of 50 ml. For data quality control, blank reagents, duplicate dilutions and certified reference materials such as soils (NCS DC 73387, NCS 73325; with grain sizes of <0.074 mm), harbor sediment (LGC6156; with grain size <200 µm), or lake sediments (LKSD-2; LKSD-4; with grain size <80 µm; Lynch, 1990) were used. Relative standard deviations are as following: Ca = 7%, Fe = 6%, K = 7%, Mg = 5%, Mn = 6%, Na = 5%, P = 6%, S = 7%, Sr = 6%.

4.5 Results

4.5.1 Modern diatom assemblages

The results for the set of modern diatom samples are shown in Fig. 4.5. The analyzed samples were rich in diatom valves. In total, 94 taxa could be identified of which eight species are planktonic and 86 are benthic. The species richness varies between 6 and 44 species per sample. The surface sediment samples from Lake Kushu being most diverse and the surface water samples from the inflow and Hime-numa Pond the least diverse. The most abundant taxa are illustrated with SEM photographs in Figs. 4.6 and 4.7.

The epiphytic diatom sample, taken from the Ōsawa River, consists of 84% monoraphid *Cocconeis pediculus* Ehrenberg. Lake Kushu samples are mainly composed of benthic species. The two planktonic species are *Aulacoseira granulata* (Ehrenberg) Simonsen reaching 31% of the assemblage in a surface sediment sample and *Belonastrum berolinense* (Lemmermann) Round and Maidana with up to 19% in surface water and sediment samples from Lake Kushu. Dominant benthic species are *Staurosirella pinnata* (Ehrenberg) Williams and Round reaching 79% in a surface sediment sample from Lake Kushu and *Nitzschia palea* (Kützing) Smith with a maximum frequency of 46% in surface water samples. *Amphora* cf. *indistincta* Levkov reaches 25% in one surface sediment sample, whereas *Epithemia adnata* (Kützing) Brébisson reaches 25% in one plant sample. *Pseudostaurosira brevistriata* (Grunow) Williams and Round is abundant in a surface sediment sample with 22% and in one plant sample with 15%.

The Lake Kushu inflow surface water sample contains the following seven species: *Melosira varians* Agardh (41%), *Navicula lanceolata* Ehrenberg (19%), *Cocconeis neothumensis* Krammer (13%), *Surirella brebissonii* Krammer and Lange-Bertalot (9.4%), *Meridion circulare* var. *constrictum* (Ralfs) Van Heurck (9.4%), *Frustulia vulgaris* (Thwaites) De Toni (3.1%), and *B. berolinensis* (6.3%). However, this sample shows a low valve concentration (32 valves) and must be excluded from the interpretation.

In the Lake Kushu outflow, the plant sample is dominated by *Cocconeis placentula* Ehrenberg attaining 46%. The surface water sample is predominated by *B. berolinensis* (16%), *S. pinnata* (20%), and *Fragilaria capucina* var. *vaucheriae* (Kützing) Lange-Bertalot (14%).

Regarding Hime-numa Pond, the surface water sample consists of 97% planktonic *Aulacoseira ambigua* (Grunow) Simonsen. The most frequent taxa in the surface sediment sample are *A. ambigua* (24%), *Stephanodiscus hantzschii* Grunow (21%) and *A. cf. indistincta* (23%).

The valve concentration in the sediment, plant, and surface water samples from Funadomari Bay is too low (<50 valve per sample) to obtain statistically reliable data. A few valves of *Navicula directa* (Smith) Ralfs, *Proschkinia* cf. *bulnheimii* (Grunow) Karayeva, *Cocconeis* sp., *Amphora* sp., and *Psammodictyon* sp. were observed. Therefore, the marine samples must be excluded from the discussion.

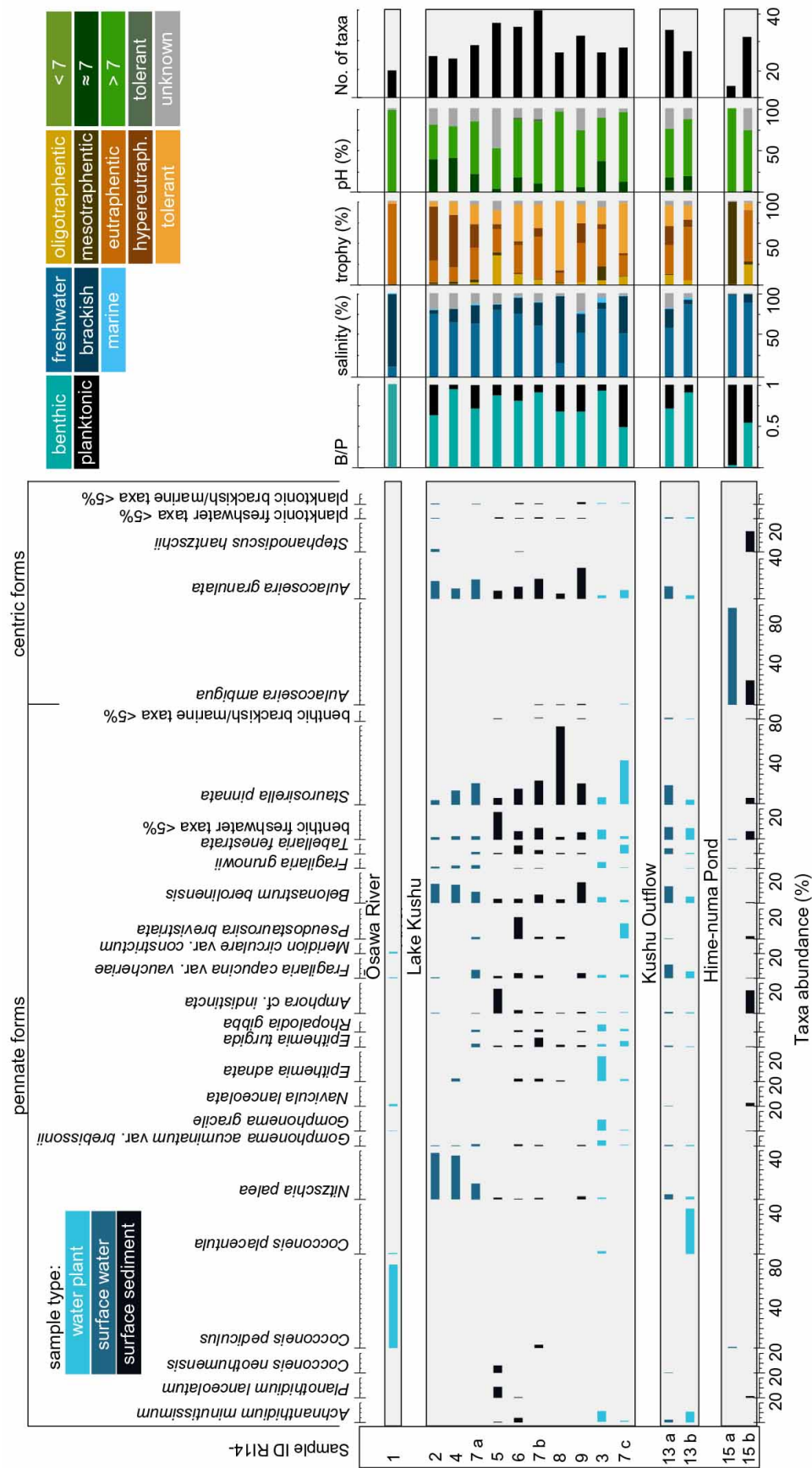


Figure 4.5: Diagram illustrating the percentage abundances of identified diatoms for the analysed set of 16 modern diatom samples from Lake Kushu and its surrounding area, and from Hime-numa Pond (see Fig. 4.1c and d for locations). The diatom taxa are grouped into pennate and centric forms. Samples from top to bottom are from the Osawa River, Lake Kushu, Kushu Outflow, and Hime-numa Pond. Taxa not exceeding 5% of the assemblage are combined to benthic freshwater taxa <5%, benthic brackish/marine taxa <5%, planktonic freshwater taxa <5%, and planktonic brackish/marine taxa <5%. Percentage stack diagrams based on the autecology of each taxon illustrate B/P, salinity, trophicity, pH, and No. of taxa.

4.5.2 Water analysis

The results of the hydrochemical and stable oxygen and hydrogen isotope analyses are summarized in Table 4.1. In total, nine samples recording the pH, surface oxygen saturation, temperature and electrical conductivity of the water were measured at different locations within Lake Kushu and once in the Ōsawa River, Oshonnai River, Lake Kushu outflow, Funadomari Bay, and Hime-numa Pond. Hydrogen and oxygen isotope analyses were performed on water samples from each water body and one precipitation sample. The water temperatures varied between 16.1 and 24.4°C showing lowest values in the Ōsawa River and Hime-numa Pond and highest values in the Kushu outflow. The pH varies between 8.0 in the Oshonnai River and 10.7 in Lake Kushu. All measured water bodies (excluding Funadomari Bay with 4.93 S/m) show freshwater conditions with a low to moderate conductivity (70–240 $\mu\text{S}/\text{cm}$). The lowest oxygen saturation of 63% was measured in the Lake Kushu outflow; highest values of 180% in the Lake Kushu surface water.

Fig. 4.2c presents a $\delta^{18}\text{O}$ – δD plot of all samples, related to the Global Meteoric Water Line (GMWL) which is defined as $\delta\text{D} = 8 \cdot \delta^{18}\text{O} + 10$, valid on a global scale for surface fresh water of non-closed basins without significant evaporation (Craig, 1961), as well as for precipitation (Rozanski et al., 1997). The analyzed rivers and lakes are well separated in the co-isotope diagram, but close to the GMWL (Fig. 4.2c). The samples from Lake Kushu and its outflow show isotopically similar waters with $\delta^{18}\text{O}_{\text{lake}} = -8.2\text{‰}$ to -8.4‰ , $\delta\text{D}_{\text{lake}} = -55.4\text{‰}$ to -56.1‰ and $d \text{ excess}_{\text{lake}} = +10.3\text{‰}$ to $+11.5\text{‰}$. The Ōsawa and Oshonnai rivers both display a similar isotope composition with $\delta^{18}\text{O}_{\text{river}} = -9.9\text{‰}$ to -10.0‰ , $\delta\text{D}_{\text{river}} = -62.5\text{‰}$ to -63.2‰ and $d \text{ excess}_{\text{river}} = +16.9\text{‰}$ to $+17.2\text{‰}$, whereas the stable isotope composition of Hime-numa Pond displays a slightly lighter isotopic composition ($\delta^{18}\text{O}_{\text{pond}} = -11.0\text{‰}$, $\delta\text{D}_{\text{pond}} = -72.6\text{‰}$ and $d \text{ excess}_{\text{pond}} = +15.6\text{‰}$) compared to those of Lake Kushu. During rainfall on 24th August 2014 one precipitation sample was collected yielding $\delta^{18}\text{O}_{\text{rain}} = -12.8\text{‰}$, $\delta\text{D}_{\text{rain}} = -92.8\text{‰}$ and $d \text{ excess}_{\text{rain}} = +9.9\text{‰}$. For comparison, monthly oxygen and hydrogen isotope composition of precipitation from the global network for isotopes in precipitation (GNIP) database (IAEA, 2015) of the nearby Russian meteorological station Terney (WMO code: 3190900, 45°00'N 136°36'E, 68 m a.s.l., Fig. 4.1a) is shown in Fig. 4.2b. The mean annual isotopic precipitation composition in Terney with $\delta^{18}\text{O} = -9.8\text{‰}$ is slightly lower than $\delta^{18}\text{O}_{\text{lake}}$ water of -8.3‰ . The GNIP data are included in the $\delta^{18}\text{O}$ – δD diagram as well and were used to calculate the Terney Local Meteoric Water Line (LMWL) with $\delta\text{D} = 6.15 \cdot \delta^{18}\text{O} - 6.95$ on the base of the mean annual climate data over a five-year period (January 1996 to December 2000). As a consequence of the maritime location of Terney, the isotopic composition in precipitation (Fig. 4.2b) does not correlate with the measured air temperature (Fig. 4.2a).

4.5.3 Fossil diatom assemblages

The ten analyzed fossil samples contain well-preserved diatom valves and in eight samples at least 500 valves were counted. In total, 102 taxa were identified of which 20 are planktonic and 82 benthic. However, most species are represented by low valve concentrations. The fossil assemblages reveal distinct changes along the RK12 core (Fig. 4.8).

The sample RK12-02-19_82-83 (1932.5 cm composite depth; in the following given as cm; 444 counted valves) from the lower part of the core reveals the dominance of benthic *Diploneis subovalis* Cleve (78%) and *Pinnularia viridis* (Nitzsch) Ehrenberg (15%). No diatoms were found in the few samples of the core checked between 19 and 16.5 m. The overlying sample (RK12-02-16_16-17; 1566.5 cm) is dominated by the benthic freshwater species *P. brevistriata* (31%) and *Pseudostaurosira elliptica* (Schumann) Edlund, Morales and Spaulding (30%). Marine *Chaetoceros* species are present with less than 5%. Benthic brackish / marine taxa are represented by *Pinnunavis yarrensii* (Grunow) Okuno (3.8%), *Rhopalodia acuminata* Krammer (3.3%) and *Mastogloia elliptica* (Agardh) Cleve (0.3%). The sample RK12-02-14_7-8 (1357.5 cm) contains the highest observed proportion of marine taxa (37.2%), including *Chaetoceros seiracanthus* Gran (23%), *Chaetoceros radicans* Schütt (7.3%), *Chaetoceros diadema* (Ehrenberg) Gran (0.7%) and *Cyclotella choctawhatcheeana* Prasad (6.2%). Freshwater diatoms are represented by benthic *Epithemia sorex* Kützing and *C. placentula* (each 12%). RK12-02-12_19-20 (1169.5 cm) shows minor percentages of marine taxa (<5%). *Chaetoceros* spp. are absent in this sample, *C. choctawhatcheeana* reaches 5.2%. Brackish *M. elliptica* comprises 6.5% of the assemblage. Benthic freshwater species reoccur with *P. brevistriata* (27%), *Rhopalodia gibba* (Ehrenberg) Müller (14%), *E. sorex* (6%), *Diatoma tenuis* Agardh (5.2%), and several benthic taxa each not exceeding 5% (grouped to other benthic freshwater and brackish / marine taxa <5%) composing in total 22%. The sample of the middle part of the core (RK12-02-10_40-41; 990.5 cm) exhibits a minor amount (<10%) of benthic freshwater diatoms, and a high proportion of planktonic *S. hantzschii* (53%), *A. ambigua* (15%), *A. granulata* (11%), and *Asterionella formosa* Hassall (8.6%). The sample RK12-02-07_9-10 (659.5 cm) is mainly composed of planktonic diatoms (68%) including *A. ambigua* (16%), *A. granulata* (16%), *Aulacoseira islandica* (Müller) Simonsen (18%), and *S. hantzschii* (18%). *P. elliptica* reaches 7.6% in this sample. RK12-02-06_21-22 (571.5 cm) shows almost twice as high abundances of the dominant taxa *A. ambigua* (33%) and *A. granulata* (31%) when compared to RK12-02-07_9-10. *A. islandica* still comprises 18%. Marine *C. choctawhatcheeana* occurs with 5.4%. Benthic freshwater diatoms play a minor role in both samples. RK12-02-03_73-74 (323.5 cm) is dominated by *A. granulata* (65%), *A. ambigua* (19%), and *A. islandica* (9.7%). In sample RK12-02-02_7-8 (157.5 cm) only 331 valves were counted. *A. islandica* is the dominant taxon reaching 56% of the assemblage. The benthic component (18%) is composed of many species occurring at less than 5% of the assemblage which are grouped in the category other benthic freshwater taxa <5%. *Gomphonema grovei* var. *lingulatum* (Hustedt) Lange-



Figure 4.6: SEM images of the modern diatoms exceeding 5% of the assemblage 1 – *Epithemia turgida*, 2 – *E. adnata*, 3 – *Rhopalodia gibba*, 4 – *Amphora* cf. *indistincta*, 5 – *Gomphonema gracile*, 6 – *G. acuminata* var. *brebissonii*, 7 and 8 – *Nitzschia palea*, 9 – *Navicula lanceolata*, 10 – *Stephanodiscus hantzschii*. Scale bar: 1 = 20 μ m, 2–10 = 10 μ m.

Bertalot and *P. elliptica* occur with 6.9% and 9.3%, respectively. RK12-02-01_1-2 (51.5 cm) is also mainly composed of planktonic freshwater diatoms (86.8%). *A. ambigua* reaches 64%, *A. granulata* 15%, and *A. islandica* 7.8%, respectively. *P. elliptica* is the only abundant benthic species in this sample composing 9.3%. Qualitative estimates for water parameters (B/P, salinity, trophy, and pH) based on the autecology of identified diatoms are illustrated in Fig. 4.9a. The salinity stack diagram shows significant abundances of brackish / marine diatoms in sample RK12-02-14_7-8 (1357.5 cm). The B/P diagram displays the shift from a benthos-dominated to a plankton-dominated assemblage in the RK12-02-10_40-41 (990.5 cm) sample. After this, the B/P remains low towards the top.

The trophy diagram shows several changes. The samples from the lower part of the core mainly consist of eutrathentic and trophy-tolerant species. In the sample RK12-02-10_40-41 the proportion of hypereutrathentic taxa increases (50%). Oligotrathentic and mesotrathentic species reach 15% and 5%, respectively. In the samples RK12-02-07_9-10 and RK12-02-06_21-22 mesotrathentic species occur (16% and 35%, respectively) and the proportion of hypereutrathentic species decreases. RK12-02-02_7-8 is characterized by the highest abundance of tolerant diatoms. The uppermost sample (RK12-02-01_1-2) contains 60% mesotrathentic diatoms.

The reconstructed pH indicates alkaline conditions throughout the section. However, the abundance of diatoms preferring lower pH (around 7) represents 25–60% in the samples RK12-02-07_9-10, RK12-02-06_21-22 and RK12-02-02_7-8. Two samples (RK12-02-10_40-41 and RK12-02-03_73-74) contain highest proportions (12–15%) of diatoms, which prefer a pH below 7.

4.5.4 Geochemical (P-ED-XRF and ICP-OES) analysis of the core sediment

20 sediment samples were geochemically analyzed from the RK12 core between 1933.5 and 52.5 cm. For all samples the main components are Si, Fe and Al as the organic fraction has not been determined yet. Si values vary between 14.0% and 29.3% with a mean of 20.7%. Fe values range between 2.3% and 5.3% (mean 3.7%) whereas Al exhibits values between 1.8% and 4.5% (mean 3.4%). However, we focus here on elements and elemental ratios that may reflect marine influences such as K, Na, P, S, Si, Ti, Sr/Ca, and Mg/Ca (Fig. 4.9b).

The basal three samples (1933.5–1701.5 cm) show strong variations in all above listed elements. For example Si (14.3–23.5%), Ti (0.25–0.46%), S (<0.1–2.16%), Na (0.37–0.7%), and P (0.35–1.30%) show heterogenic patterns within this section.

Between 1567.5 and 1170.5 cm seven sediment samples were analyzed. All elements exhibit values within a narrow range. This is most obvious for Na, P and S. Whereas S shows elevated values between 1.7 to 4.2%, lowest and uniform P values (0.25–0.37%; mean 0.32%) represent this section. Also Na exhibits slightly elevated values within a narrow range (0.44–0.55%; mean 0.49%). When the lowermost sample at 1567.5 cm is not considered, the same feature is observed

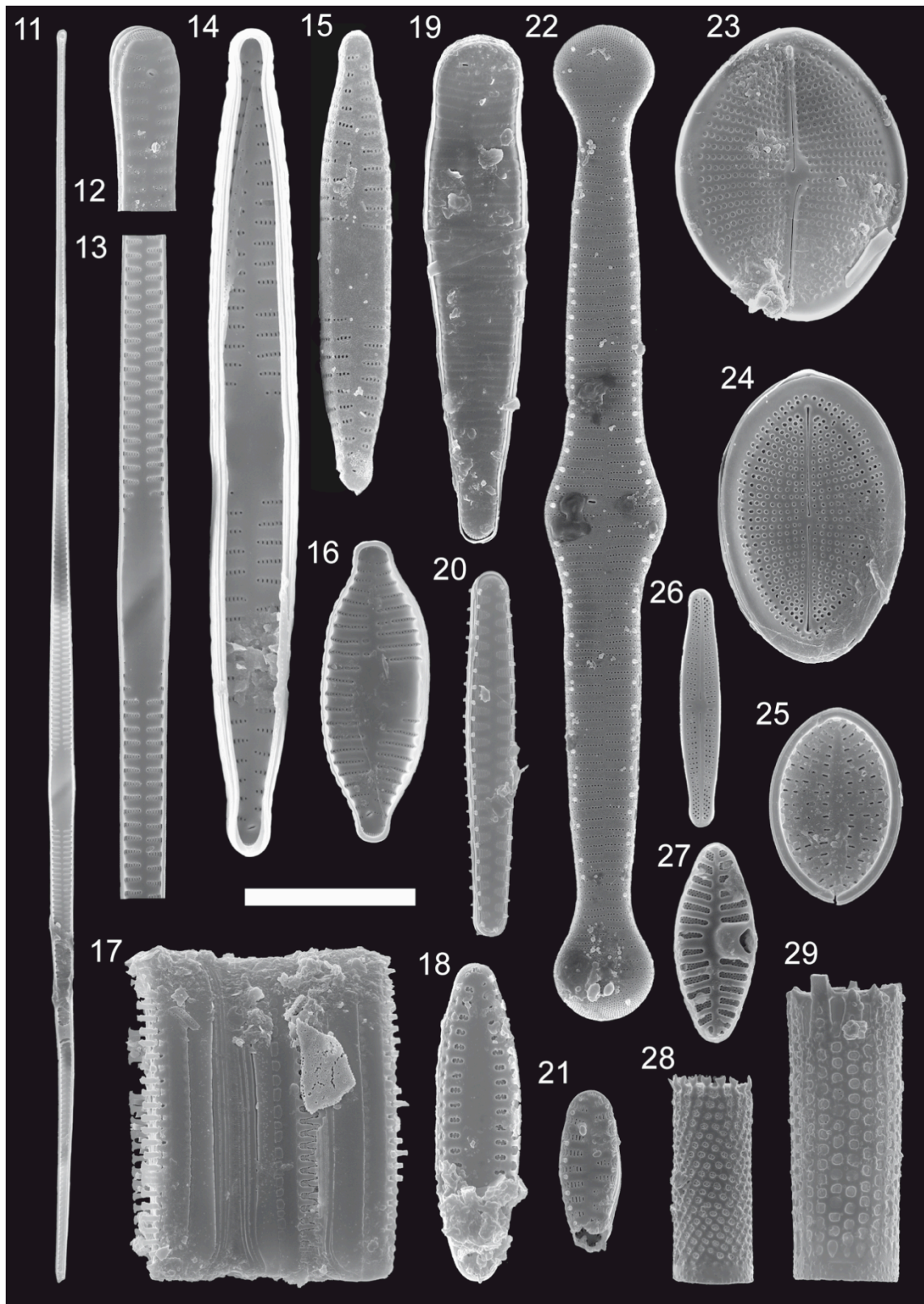


Figure 4.7. SEM images continued. 11–13 – *Fragilaria grunowii*, 14–16 – *Fragilaria capucina* var. *vaucheriae*, 17 and 18 – *Pseudostaurosira brevistriata*, 19 – *Meridion circulare* var. *constrictum*, 20 – *Belonastrum berlinensis*, 21 – *Staurosirella pinnata*, 22 – *Tabellaria fenestrata*, 23 – *Cocconeis pediculus*, 24 – *C. placentula*, 25 – *C. neothumensis*, 26 – *Achnanthyidium minutissimum*, 27 – *Planothyidium lanceolatum*, 28 – *Aulacoseira ambigua*, 29 – *A. granulata*. Scale bar: 11 = 20 μm , 12–29 = 10 μm .

for Si (20.6–23.6%; mean 20.7%) and Ti (0.31–0.37%; mean 0.34%) as well as for the elemental ratios Sr/Ca (0.0063–0.007; mean 0.0066), and Mg/Ca (4.39–5.13; mean 4.67).

Three samples were analyzed from the interval between 1127.5 and 990.5 cm. These samples show slightly different element concentrations, which is most obvious for S, Sr/Ca, Mg/Ca, Si, and Ti. For S (0.84–2.95%), Sr/Ca (0.0048–0.0061) and Mg/Ca (3.33–3.88) the values are lower, whereas Ti (0.33–0.50%) and Si (24.4–29.3%) show higher concentrations.

The interval between 634.5 and 52.5 cm is represented by seven samples that show similar values as the previously described section for the elemental ratios Sr/Ca and Mg/Ca as well as for the elemental concentrations of K, Si, and Ti. However, for this part of the core the S values are low (0.26–0.43%; mean 0.37%) and Na decreases towards the core top (from 0.44% to 0.11%). P also decreases towards the top but shows much higher values (0.45–1.32%) when compared to samples between 1567.5 and 990.5 cm.

4.6 Interpretation and discussion

4.6.1 Modern lake basin

Geographically, Lake Kushu is situated in the temperate climate zone. It is dimictic with a freezing period from December to April (Sato et al., 1998), spring and autumn circulation and summer stagnation (Schönborn and Risse-Buhl, 2013). The shallow basin morphology represents a mature lake stage defined by a high ratio of z_a/z_m (i.e. 0.6; $z_a = 3.5$ m/ $z_m = 5.8$ m), where z_a indicates the average depth of the lake and z_m represents its maximal depth. The low water depth results in the absence of a tropholytic zone that leads to photosynthetic activity in all parts of the lake causing eutrophication (Schönborn and Risse-Buhl, 2013) and massive algal blooms in summer, which we could observe during fieldwork in August 2014. The present influence of human activities on the lake seems minor since there are very limited agricultural activities and cattle breeding on Rebus Island. We observed sewage disposal into the outflow but no drainage directly into Lake Kushu. However, we cannot exclude sewage disposal into the lake. Locals reported that the lake is not being used for any leisure activities like fishing, swimming or other water sports as a result of the eutrophic to hypereutrophic conditions.

Its flat basin topography suggests that Lake Kushu has reached a mature stage. The high bioproductivity in the warm season leads to high accumulation rates of organic-rich sediments. However, the reported deforestation in the first half of the 20th century (see Müller et al., 2016) might have led to soil destabilizations and an increase of the nutrient inflow from the catchment area.

The pH measured near the water surface varied between 9.2 and 10.7 (Table 4.1). The high pH can be explained by the high photosynthetic activity of the algal bloom which consumes the near surface CO₂ causing higher surface water pH during summer stagnation (Schönborn and Risse-Buhl, 2013). Coherently to the photosynthesis-induced decrease of CO₂, the oxygen saturation

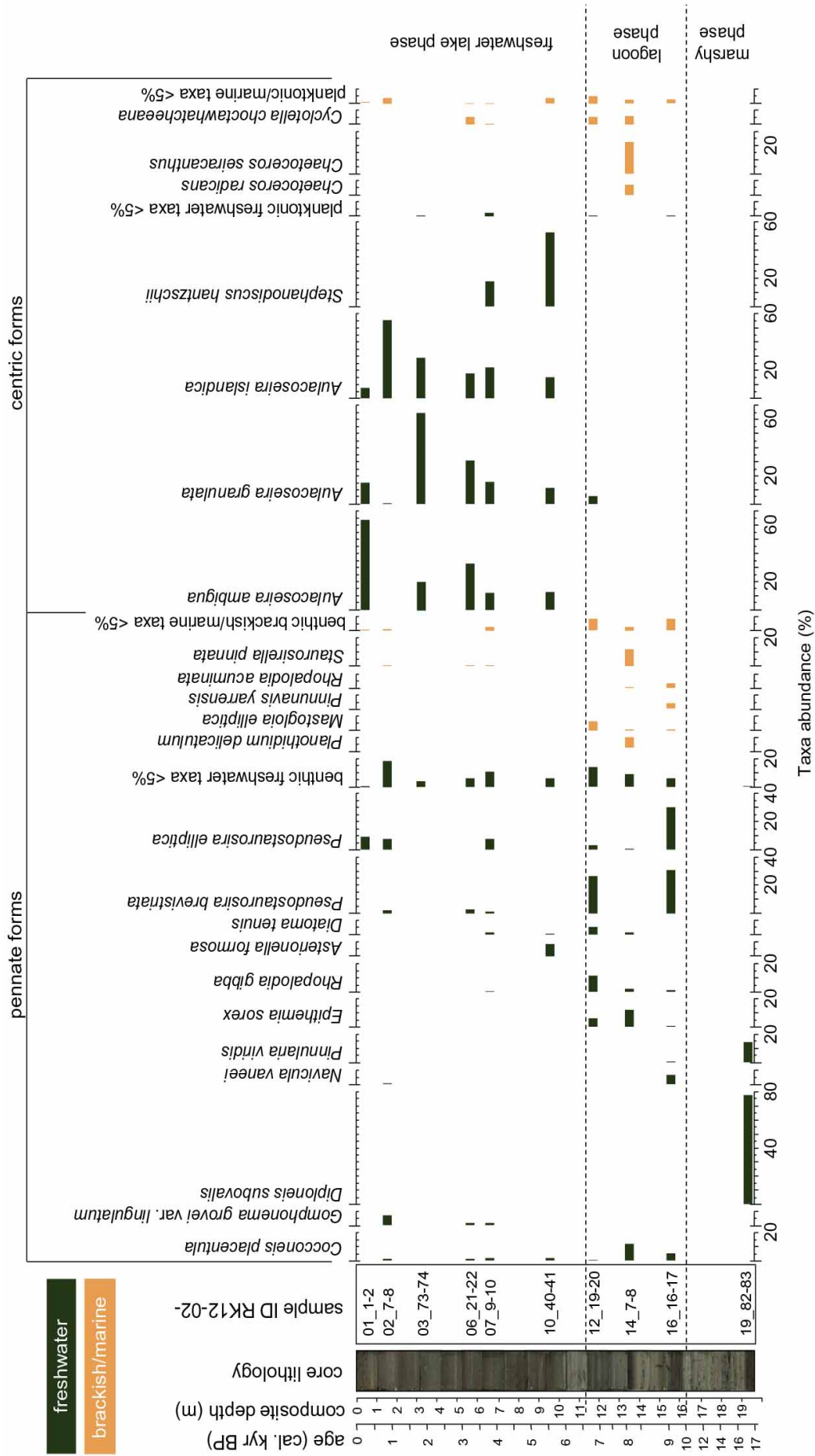


Figure 4.8: Diatom assemblage diagram representing the percentage abundances of identified diatoms for the ten analysed RK12 core samples (location is indicated by a white cross in Fig. 4.1e). The diatom taxa are grouped into pennate and centric forms. Freshwater taxa are coloured in dark green, brackish/marine taxa in orange. Taxa not exceeding 5% of the assemblages are grouped into benthic freshwater taxa <5%, planktonic freshwater taxa <5%, and planktonic brackish/marine taxa <5%.

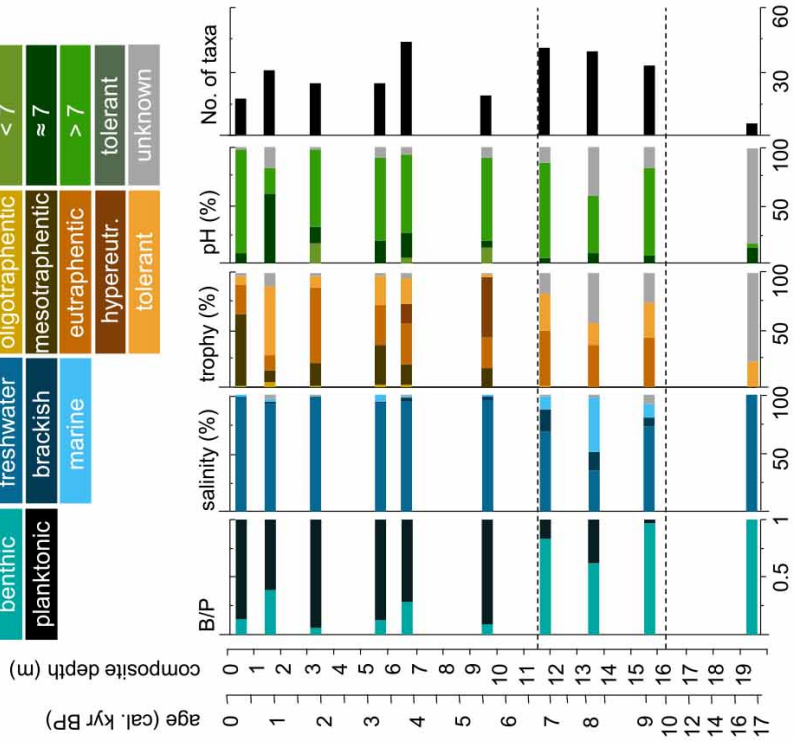
experiences a significant increase resulting in values between 78% and 180%. The measured stable oxygen and hydrogen isotope composition in the surface water samples plot close to the GMWL and LMWL (Fig. 4.2c) indicating the absence of major evaporation processes. The lake samples show very similar stable isotope values and represent a well-mixed water body with an average composition of $\delta^{18}\text{O}_{\text{lake}} = -8.3\text{‰}$, $\delta\text{D}_{\text{lake}} = -55.8\text{‰}$ and $d \text{ excess}_{\text{lake}} = +10.9\text{‰}$. These results correlate with the typhoon season that lasts seven months from May to November. Typhoons bring high amounts of precipitation and storms affecting the studied area regularly (Terry and Feng, 2010). Two weeks prior to our sampling campaign, the typhoon named ‘Halong’ (formed on 27th July 2014, dissipated on 15th August 2014) crossed the Hokkaido Region from south to north, affecting Rebun and Rishiri islands. The isotope composition of Lake Kushu is similar to that of the summer precipitation of the nearby meteorological station Terney (Fig. 4.2b and c) indicating that the shallow lake is completely recharged in summer. However, due to the maritime location of Terney the isotopic composition in precipitation shows minor variations and the absence of annual trends.

During the observation period, the eutrophic, or at time hypereutrophic, lake showed a massive green algal bloom, giving the lake a green color and a low water transparency (<10 cm). The flourishing green algae replace the planktonic diatom species as shown by a very low valve concentration in surface water samples (c. 500 valves per slide, Ø 18 mm).

Within the Lake Kushu samples, *Nitzschia palea* is mainly present in the planktonic samples representing 17–46%. *N. palea* is a widely distributed taxon known from lotic and lentic freshwater habitats, tolerant of heavy organic pollution (Trobajo et al., 2009). Krammer and Lange-Bertalot (1999) described *N. palea* as a common taxon, which occurs frequently within the plankton. Planktonic *Aulacoseira granulata*, which is frequent as well, is described from eutrophic habitats (Van Dam et al., 1994; Gómez et al., 1995; Krammer and Lange-Bertalot, 2000). The presence of *A. granulata*, which needs turbulence of the water (Gómez et al., 1995), can be associated with the typhoon season in summer. *Staurosirella pinnata* and *B. berolinensis* occur in the surface water samples as well as in the surface sediment and plant samples (Fig. 4.8). Van Dam et al. (1994) reported *S. pinnata* as an oligo- to eutraphentic taxon. Krammer and Lange-Bertalot (2000) mentioned the difficulty of the named-by-synonym *Fragilaria pinnata*-taxon (see also Morales et al., 2013) and suggest *S. pinnata* to be a very tolerant species concerning pH (<7 up to 9.3) and trophic level (oligo- to eutrophic; Van Dam et al., 1994). *B. berolinensis* is a planktonic colonial form associated with alkaline, eutrophic (Van Dam et al., 1994) unless hypereutrophic conditions (Bradshaw et al., 2002) which fits very well with the measured water parameters.

Interestingly, the assemblages of the plant, surface water, and sediment samples are much more similar to each other than expected. The B/P values (Fig. 4.9a) display a high similarity between the samples, supporting the assumption of a well-mixed water body.

(b)



(a)

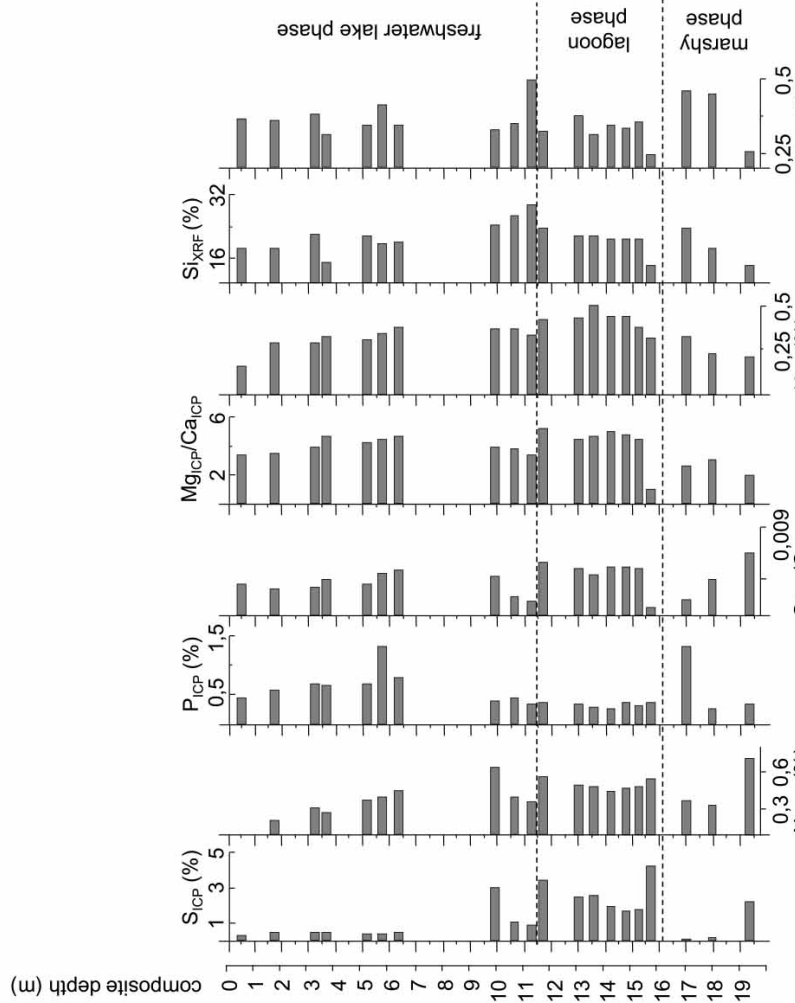


Figure 4.9: (a) percentage stack diagrams illustrating B/P, salinity, trophity, pH, and No. of taxa according to the autecology of the diatoms shown in Fig. 4.8; (b) shows the results of the XRF and ICP – OES analyses.

The analyzed water parameters from Hime-numa Pond show deviating results (compared to Lake Kushu) regarding the lower electrical conductivity (70 $\mu\text{S}/\text{cm}$), temperature (16.1°C), and oxygen saturation (76%). With 9.3, the pH is as high as in Lake Kushu. The isotopic composition of $\delta^{18}\text{O}_{\text{pond}} = -11\text{‰}$, $\delta\text{D}_{\text{pond}} = -72.6\text{‰}$ and $d \text{ excess}_{\text{pond}} = +15.6\text{‰}$ plots above the GMWL which indicates that evaporation is negligible. The isotope composition of Hime-numa Pond is rather low as compared to the Terney mean monthly precipitation and Lake Kushu water (Fig. 4.2c) and therefore indicates that recharge takes place mainly during the cold season. However, an isotope “amount effect” that indicates any dependency of oxygen isotopes from the precipitation amount is not visible in the Terney data. In general, Hime-numa Pond was characterized by a green algal bloom and a water transparency as low as in Lake Kushu (<10 cm). The lower temperature and oxygen saturation in comparison to Lake Kushu can be explained by the permanent cloud cover around Mt. Rishiri (1721 m) as noticed during fieldwork, reducing insolation and photosynthesis-induced bioproductivity. Due to the green algal bloom, the diatom diversity is low (6 taxa in surface water, 32 in surface sediment sample). The assemblage of the surface water sample consists of *A. ambigua*, reaching 97%. *A. ambigua* represents the observed water parameters (pH = 9.32, eutrophic) very well. Further, other occurring taxa (e.g. *C. neothumensis* and *N. lanceolata*) in this assemblage are either trophy-tolerant or prefer eutrophic habitats (Van Dam et al., 1994; Krammer and Lange-Bertalot, 1997, 1999, 2000, 2004). In particular, *S. hantzschii* is associated with highly eutrophic conditions (Bennion et al., 1996). The presence of *S. hantzschii* in the surface sediment sample suggests higher nutrient concentration than in the past. Nevertheless, to provide a more detailed picture about the degree of past human influence further research is needed.

4.6.2 Comparison to Kushu core diatom assemblages

In comparison to the modern record, the fossil diatom assemblage of Lake Kushu is generally different. Only four species (*R. gibba*, *P. brevistriata*, *S. pinnata*, *A. granulata*) exceeding 5% of the assemblage occur both in the modern and fossil assemblages. Most significant changes are traceable in the diagram showing the reconstructed salinity (Fig. 4.9a). Here, the core assemblages between 1566.5 and 1169.5 cm (c. 9–6.7 cal. kyr BP) indicate higher water salinity suggested by the appearance of brackish *M. elliptica* with a highest range in sample RK12-02-12_19-20, *P. yarrensis* and *R. acuminata* in sample RK12-02-16_16-17 and marine *C. choctawhatcheeana*, *C. seiracanthus* and *C. radicans* in sample RK12-02-14_7-8 (8.4 cal. kyr BP). *S. pinnata* reaches its maximum abundance (12%) in sample RK12-02-14_7-8 (1357.5 cm), while *P. brevistriata* is most abundant in samples RK12-02-16_16-17 (1566.5 cm) and RK12-02-12_19-20 (1169.5 cm). *P. brevistriata* prefers weakly brackish conditions (Denys, 1990) and therefore indicates a transition from freshwater to brackish conditions in sample RK12-02 16_16-17 and from brackish to freshwater conditions in sample RK12-02 12_19-20. In contrast, *S. pinnata* is associated with

brackish conditions (Denys, 1990) and shows highest abundance in sample RK12-02 14_7-8 together with the marine taxa. The shift towards freshwater, plankton-dominated assemblages (B/P = 0.1–0.45) starts with sample RK12-02-10_40-41 (990.5 cm) at *c.* 5.8 cal. kyr BP. This could indicate a higher water level. However, the B/P does not only reflect the water level, but also the water transparency and nutrient concentrations and needs to be handled with care. Another main change is indicated in the diagram for trophic conditions (Fig. 4.9a). In comparison to the modern Lake Kushu samples, mesotraphentic *A. ambigua* (Reynolds, 1998; Poister et al., 2012) is replaced by highly eutraphentic *N. palea* and *B. berolinensis* (Bradshaw et al., 2002; Trobajo et al., 2009) indicating an increase in nutrient concentrations within the last 300 yr BP.

The surface water sample from Hime-numa Pond shows highest similarity (high abundance of *A. ambigua*) compared to the sample RK12-02 01_1-2 from the Kushu core. Both samples represent a meso- to eutrophic freshwater lake. This leads to the assumption that the deforestation, sewage or remnants of formerly used fertilizers since the settlement on Rebun Island increased the nutrient inflow to Lake Kushu, resulting in hypereutrophic conditions. On the other hand, the well-preserved natural forest belt on Rishiri Island (Müller et al., 2016) and the location of Hime-numa Pond above the coastal settlement belt have prevented a high level of pollution (as indicated for Lake Kushu) in the pond's catchment. It seems that settlement activities on Rebun Island played an important role in the eutrophication of Lake Kushu. These findings require further high-resolution analyses.

4.6.3 Correlation to past climate and sea level changes

A representative selection of fossil samples has been analyzed to test the potential of using diatom analysis on the RK12 sediment core as a high-resolution archive of the postglacial climate and environments as well as for the reconstruction of possible impact of sea water (long- and short-term events) on the Lake Kushu ecosystem with a special focus on the interval between the onset of the Jomon culture of northern Japan (*c.* 14 kyr BP; Weber et al., 2013) and the present. The results of the pilot analysis presented here indicate significant changes throughout the RK12 core diatom assemblages, which should be correlated in detail with the regional and global-scale environmental changes.

Not only the diatom assemblage was used, but also selected sediment samples were geochemically analyzed to detect potential environmental changes such as a varying impact of seawater throughout the RK12 core. Higher contents of K, Na, and S as well as elevated Sr/Ca and Mg/Ca are regarded as marine markers (Goff et al., 2004; Chagué-Goff, 2010; Chagué-Goff et al., 2012) and represent in the bulk sediment a potential marine influence. Sr/Ca and Mg/Ca ratios are known as salinity indicators from lake sediments (Gasse et al., 1987; Hoelzmann et al., 2010) and increasing salinity is here bound to an increasing marine influence. P is interpreted as an indicator of productivity where higher P values indicate more productive conditions under lacustrine

conditions and diminished seawater influx. Si and Ti in the sediments may result from detrital input originating from suspended matter with higher values suggesting an increasing fluvial (riverine) influence.

4.6.4 Marshy phase 16.6–10 cal. kyr BP

The sample RK12-02-19_82-83 (1932.5 cm) from the lowermost part of the analyzed RK12 core (16.6 cal. kyr BP) represents the final phase of the Last Glacial Maximum (LGM). Studies of diatom-inferred climate reconstructions of the LGM are scarce in the Hokkaido region. However, pollen-based reconstructions dated the end of the LGM and the onset of deglaciation processes to 17 cal. kyr BP for this region (Igarashi et al., 2011). The lowermost sample is dominated by benthic freshwater *D. subovalis* (78%) known as a common species in running waters (Krammer and Lange-Bertalot, 1997). *P. viridis* (15%) is described as frequently occurring in a stream-fed pond at 50 mm water depth (Harper, 1976). Both, *D. subovalis* and *P. viridis*, might indicate a fluvial habitat, which is characterized by ephemeral conditions.

The core sediments change from dark brown, organic-rich, partly laminated clay (1930–1900 cm) to brownish-olive to grey silty clay with intermediate pumiceous sand layers (1900–1650 cm) suggesting a fluvial depositional environment (Einsele, 1992). The sediments show relatively high Si and Ti values that correspond to an increased detrital input under fluvial/deltaic environments. Such unstable environmental conditions for this phase are also reflected by varying values of the other parameters such as Na, P, and K concentrations as well as changing Sr/Ca and Mg/Ca ratios.

Diatom diversity and valve concentration are both relatively low in the lower core part, thus preclude a more detailed interpretation at this stage based on diatoms. However, the pilot results from the pollen analysis presented in Müller et al. (2016) will provide a chronology that shows significant changes, e.g. at the Late Glacial / Holocene transition indicated by the shift from herbaceous to tree and shrub dominated vegetation.

4.6.5 Brackish water lagoon phase 10–6.6 cal. kyr BP

The rapid marine transgression in the Early Holocene 8.5 to 6.5 cal. kyr BP (Omura and Ikehara, 2010) changed the fluvial / deltaic depositional environment and led to the formation of the palaeo-Kushu Bay (Sato et al., 1998). Initial occurrence of benthic brackish *M. elliptica* and *P. yarrensii* as well as the minor abundance of planktonic marine diatoms in RK12-16_16-17 at 9 cal. kyr BP indicate strong marine impact including first tidal influences. Increasing abundance of marine planktonic *Chaetoceros* spp. in RK12-02-14_7-8 suggests maximal marine impact at 8.4 cal. kyr BP (Figs. 4.8 and 4.9a). This corresponds with the geochemical composition of the RK12 core sediments. High Na, K, and S values together with increased Sr/Ca and Mg/Ca element ratios point to increased salinity as a result of the seawater influence. The detrital input of Ti and Si originating from fluvial suspended matter is decreasing and productivity (indicated by P content) is

significantly lower around this time. This might correspond to the pronounced marine transgression associated with the “8.2 k-event”, an abrupt climate change in the northern hemisphere at 8.2 cal. kyr BP, first noted in Greenland ice core records (e.g. Alley and Ágústsdóttir, 2005; Thomas et al., 2007) caused by a meltwater pulse into the North Atlantic Ocean (Hijma and Cohen, 2010).

The diatom assemblage shows a decreasing marine influence in sample RK12-02-12_19-20 at *c.* 6.7 cal. kyr BP with the significant decline in *Chaetoceros* spp., *P. yarrensensis* and *R. acuminata* abundances. There is a time lag between the observed maximal marine impact in the RK12 core (8.4 cal. kyr BP) and that suggested by Sato et al. (1998) between 7.6 and 7 cal. kyr BP. Whether this time difference is due to the extracting location of the peat moor core at the southern margin of the basin (Kumano et al., 1990a) or to an imprecise or incorrect age model (Sato et al., 1998) remains open. Both scenarios seem to be plausible since the marine diatoms documented by Kumano et al. (1990a) are benthic diatoms suggesting that the area in the south was less influenced by marine tides compared to the RK12 core location and the age model published by Kumano et al. (1990a) is based only on four radiocarbon dates representing the *c.* 16 m sediment core.

4.6.6 Freshwater lake phase since 6.6 cal. kyr BP

The transition from the lagoon phase towards a freshwater environment is marked by the decline of brackish / marine species and the occurrence of freshwater *Aulacoseira* spp. (Figs. 4.8 and 4.9a) suggesting a stable freshwater lake phase since 6.6 cal. kyr BP. Isochronously, the geochemical analysis shows lowering Sr/Ca and Mg/Ca ratios along with increasing Si and Ti contents between 1160 and 1050 cm suggesting the decrease of marine influence together with higher detrital input. Further, the low values of S, K, Na, Sr/Ca, and Mg/Ca and the higher P, respectively, indicate reduced ion concentration of the lake water and increased productivity.

Evidence of the Late Holocene marine transgression reconstructed at several sites in eastern Hokkaido shortly before *c.* 3 cal. kyr BP (Kumano et al., 1990b and references therein) was not yet found in the RK12 core. As the sample interval of our pilot study is coarse, this marine transgression affecting Lake Kushu might be detected with high-resolution analysis. At this stage, however, our results are in agreement with the maximum lake extension after the Holocene Climate Optimum (8.7–5.2 kyr BP) as postulated by Sato et al. (1998).

Due to the location of Rebun Island within a tectonically active zone, the question for short-term marine impact on Lake Kushu induced by tsunamis is of high interest. Sawai (2002) discovered dramatic changes in diatom assemblages from Lake Tokotan (Hokkaido) caused by tsunami impacts on Hokkaido. Potentially, tsunami events, which affected the Rebun Island region, should also be detectable in the RK12 core.

The palaeolimnology of Lake Kushu was likely controlled by several environmental factors, e.g. basin morphology, tsunami activities, the East Asian Monsoon system, and the global- and regional-scale sea level fluctuations that also had an influence on changes in the TWC as a main

driver of the regional climate conditions. The TWC started influencing the climate in the southwestern Hokkaido region in the Middle Holocene (Leipe et al., 2013; Nishida and Ikehara, 2013). The planned high-resolution analysis of the RK12 core material will provide an opportunity to get reliable information for reconstructing the palaeolimnology of Lake Kushu in more details.

4.7 Conclusions

In this pilot study the modern and fossil diatom assemblages from Lake Kushu and the surrounding environment have been studied. The samples taken in August 2014 represent a mature shallow freshwater lake, which is characterized by strong eutrophication in summer. This leads to a green algal bloom and to a decreased diversity and concentration of diatoms, especially in the surface water. The nutrient increase was most likely caused by the combination of a natural induced eutrophication process (flat basin topography, high productivity) and human activities (vegetation changes, pollution) during the settlement history of Rebun Island. The high wind energy caused by the East Asian Monsoon (May to November) initiate regular water turnover in the lake. Further sediment and water sampling from Lake Kushu and the surrounding area will facilitate the interpretation of the core diatom assemblages and help in understanding the limnological processes and diatom variability of this lake during the summer and the overturn spring and autumn periods.

We further tested the potential of the RK12 sediment core as a high-resolution archive to reconstruct past environmental and climate changes during the Late Glacial and Holocene interval. The diatom assemblages and the geochemical sediment composition suggest that three substantially different environmental phases took place: (i) the Late Pleistocene marshy phase with unstable environments and higher detrital input (indicated by high Si and Ti values); (ii) the Early Holocene lagoon phase reflecting the postglacial global sea level rise and corresponding marine transgression, as indicated by highest abundances of marine diatoms and increased K, Na, and S contents and corresponding Sr/Ca and Mg/Ca element ratios in the analyzed samples; and (iii) the freshwater lake phase following the Holocene Climate Optimum.

This pilot study clearly shows that further high-resolution diatom and geochemical analyses of the sediments from the Lake Kushu core RK12 will be able to provide a very detailed (subdecadal to decadal) palaeolimnological record with an excellent age-control that will foster regional palaeoclimatic and palaeoenvironmental interpretations for the Late Glacial and Holocene time interval and facilitate interpretation of the hunter-gatherer population dynamics and cultural sequences in the Hokkaido region.

4.8 Acknowledgements

We would like to acknowledge financial support from the Baikal-Hokkaido Archaeology Project (BHAP) founded by the Canadian Social Sciences and Humanities Research Council (SSHRC); project directors Prof. Andrzej Weber (University of Alberta, Canada) and Prof. Hirofumi Kato (Hokkaido University, Japan) for invitation and financial support of the field trip to Rebun Island and immense help during the fieldwork. We are thankful for the helpful comments of the two anonymous reviewers. The research of Mareike Schmidt is financed via a BHAP PhD stipend (University of Alberta, 0424634401). Pavel Tarasov's research is supported by the German Research Foundation (DFG) Heisenberg Program (Grant TA 540/5). We also thank the friendly Rebun islander who provided us with a small boat for water and diatom sampling on Lake Kushu.

5. Manuscript IV

Multi-proxy palaeolimnological record of the last 16,600 years derived from coastal Lake Kushu in the Hokkaido Region of Japan

Mareike Schmidt^{1,*}, Fabian Becker², Philipp Hoelzmann³, Christian Leipe¹, Jens Mingram⁴,
Stefanie Müller⁵, Rik Tjallingii⁴, Pavel E. Tarasov¹

¹ *Institute of Geological Sciences, Paleontology, Freie Universität Berlin, Malteserstr. 74-100, Building D, 12249 Berlin, Germany*

² *Institute of Geographical Sciences, Physical Geography, Freie Universität Berlin, Malteserstr. 74-100, Building H, 12249 Berlin, Germany*

³ *Institute of Geographical Sciences, Physical Geography, Freie Universität Berlin, Malteserstr. 74-100, Building B, 12249 Berlin, Germany*

⁴ *Helmholtz Centre Potsdam, GeoForschungsZentrum, Telegrafenberg, Building C, 14473 Potsdam, Germany*

⁵ *Eurasia Department and Beijing Branch Office, German Archaeological Institute, Im Dol 2-6, 14195 Berlin, Germany*

ready for submission to: Palaeogeography Palaeoclimatology Palaeoecology

5.1 Abstract

Lake Kushu (45°25'58"N, 141°02'05"E) is a small, coastal freshwater body on Rebun Island in the Hokkaido Region in northern Japan. It plays a major role in the Baikal-Hokkaido Archaeology Project (BHAP) to serve as a continuous sediment archive covering the Late Glacial / Holocene time period to better understand the regional hunter-gatherer population changes. The current study uses diatom, aquatic pollen and non-pollen palynomorph (NPP), microfossils, and x-ray fluorescence (XRF) analyses to derive the lake system dynamics from a *c.* 19.5 m sediment core covering the last *c.* 16,600 years. All analyzed proxies play in concert and help in reconstructing three main phases in the lake basin development: (i) a marshy phase (*c.* 16.6–9.3 cal. kyr BP); (ii) a brackish water lagoon phase (*c.* 9.3–5.9 cal. kyr BP) that marks the marine transgression and the postglacial sea level rise; and (iii) a freshwater lake phase with alkaline, meso- to eutrophic conditions that continued since *c.* 5.9 cal. kyr BP, when a sand barrier separated the lake basin from the sea. The lake proximity to the sea resulted (in particular between 5.6–5.2 cal. kyr BP) in irregular marine influences and high variability revealed by the diatom and p-ED-XRF analysis. The high-resolution analyses of section 9 (*c.* 5.6–5.2 cal. kyr BP) of the composite core helped in reconstructing the environmental dynamics during the Mid-Holocene freshwater

lake phase with irregular marine influences in greater details. Fine laminated areas point to marine impacts whereas non-laminated parts represent mesotrophic, circumneutral to alkaline freshwater conditions within a well-mixed water body. Short-time climate variations (e.g. climate deterioration at *c.* 5.5 kyr BP) could be reconstructed by the high-resolution micro-facies and diatom analyses.

5.2 Introduction

Previous studies (Müller et al., 2016; Schmidt et al., 2016) tested the potential of the RK12 sediment core from Lake Kushu at Rebun Island to serve as a high-resolution archive to reconstruct the lake development in response to the changing island environments, sea level and climate fluctuations and human activities during the past *c.* 16.6 cal. kyr BP. The sediment core RK12 was obtained under the framework of the international multi-disciplinary Baikal-Hokkaido Archaeology Project (BHAP: <http://bhap.artsrn.ualberta.ca/>) investigating Holocene hunter-gatherer culture dynamics and its driving factors in two regions of the world: the Lake Baikal region of Siberia, Russia and Hokkaido in Japan (Tarasov et al., 2013; Weber et al., 2013). Rebun Island has been chosen as one of the key study areas in order to reconstruct postglacial climate and environments and to discuss human-environmental interactions. Hence, the reconstruction of the Lake Kushu history is of particular interest, because it is the only freshwater lake on the island and therefore might have played an essential role for the hunter-gatherer populations there. First residential sites of Middle Jomon period occurred *c.* 4.9 cal. kyr BP, but the settlement took place in complex pattern of demographic changes, e.g. population size and distribution (Weber et al., 2013; Müller et al., 2016; Abe et al., 2016). This raised the question if Lake Kushu might have influenced the human occupation history of Rebun Island and, the other way around, if the past human activities could affect the lake system or its components.

First diatom record from Lake Kushu indicated a brackish-water or marine environment around 7000 years ago (Kumano et al., 1990a). However, the age model based on four ¹⁴C dates and resolution of the record did not allow more precise dating of the brackish / marine phase and identification of the short-term marine impacts. The age model of the 19.5 m long composite core RK12 collected from the lake in February 2012 was constructed using 57 AMS dates each representing 1 cm of the core sediment (Müller et al., 2016). The robustness of the age model and rather high sediment accumulation rates (i.e. one cm of sediment represents an interval of *c.* 20 years prior to *c.* 9.5 cal. kyr BP and *c.* 5-6 years after that time) allow tracing environmental variability at very high-resolution, up-to-date non available in the entire region.

In this study we aim to provide a detailed palaeolimnological record to facilitate regional palaeoclimatic and palaeoenvironmental interpretations for the Late Glacial and Holocene time period in the Hokkaido Region. We applied a combination of diatom, pollen, micro-facies and XRF analyses to the fine laminated sediment section of the RK12 core between 838-948 cm to get

insight into the Mid-Holocene interval *c.* 5.6-5.2 cal. kyr BP, conventionally regarded as the interval with most stable and favorable environments promoting spread of the human population in the Hokkaido region (Igarashi et al., 2002; Igarashi, 2013).

5.3 Regional settings

Lake Kushu (45°25'58"N, 141°02'05"E, *c.* 4 m above sea level, a.s.l.) is a coastal freshwater lake in the northern part of the volcanic Rebun Island (Kimura, 1997; Goto and McPhie, 1998, Fig. 5.1). The lake has a maximum depth of 5.8 m and a catchment area of about 10 km² (Müller et al., 2016; Schmidt et al., 2016) and is separated from the Funadomari Bay in the Sea of Japan by a sand dune of ~400 m width and ~15 m height (Sato, 1998; Schmidt et al., 2016). The Oshonnai River enters the lake in the south and a short stream outflow connects it with the Funadomari Bay in the north (Fig. 5.1D).

The modern climate in the study region is mostly controlled by the East Asian Monsoon system and the seasonal migration of the East Asian polar front (Leipe et al., 2013 and references therein). During the cold half of the year (November–April), the northwestern air masses representing the East Asian winter monsoon (EAWM) pass the area of the Sea of Japan, collect the heat and moisture from the Tsushima Warm Current (TWC) (Fig. 5.1B) and bring relatively mild winters with high amount of snow in the western part of the Hokkaido region (Igarashi, 2013). The warm season (May–October) circulation is controlled by southeastern winds of the North Pacific summer monsoon. Depending on the location and strength of the Okhotsk High in the north and the Ogasawara High in the south, the North Pacific summer monsoon results in cool and dry or warm and wet summers (Ogi et al., 2004; Igarashi, 2013; Schmidt et al., 2016). The mean monthly air temperature on Rebun Island varies from -6.4 °C in January to 19.4 °C in August with a mean annual precipitation of 1102 mm, with highest amounts falling from September (131 mm) to December (106 mm, Schmidt et al., 2016). The generally high annual moisture availability promotes a dense vegetation cover with predominantly cool temperate and boreal woody plants (Müller et al., 2016). Human-induced deforestation of Rebun in the early-mid 20th century caused the expansion of the dwarf bamboo *Sasa* spp., which might prevent natural re-growth of local trees (Müller et al., 2016). However, conservation efforts and inclusion of the island in the Rishiri Rebun Sarobetsu National Park helped in re-establishing the natural vegetation and forests during last decades.

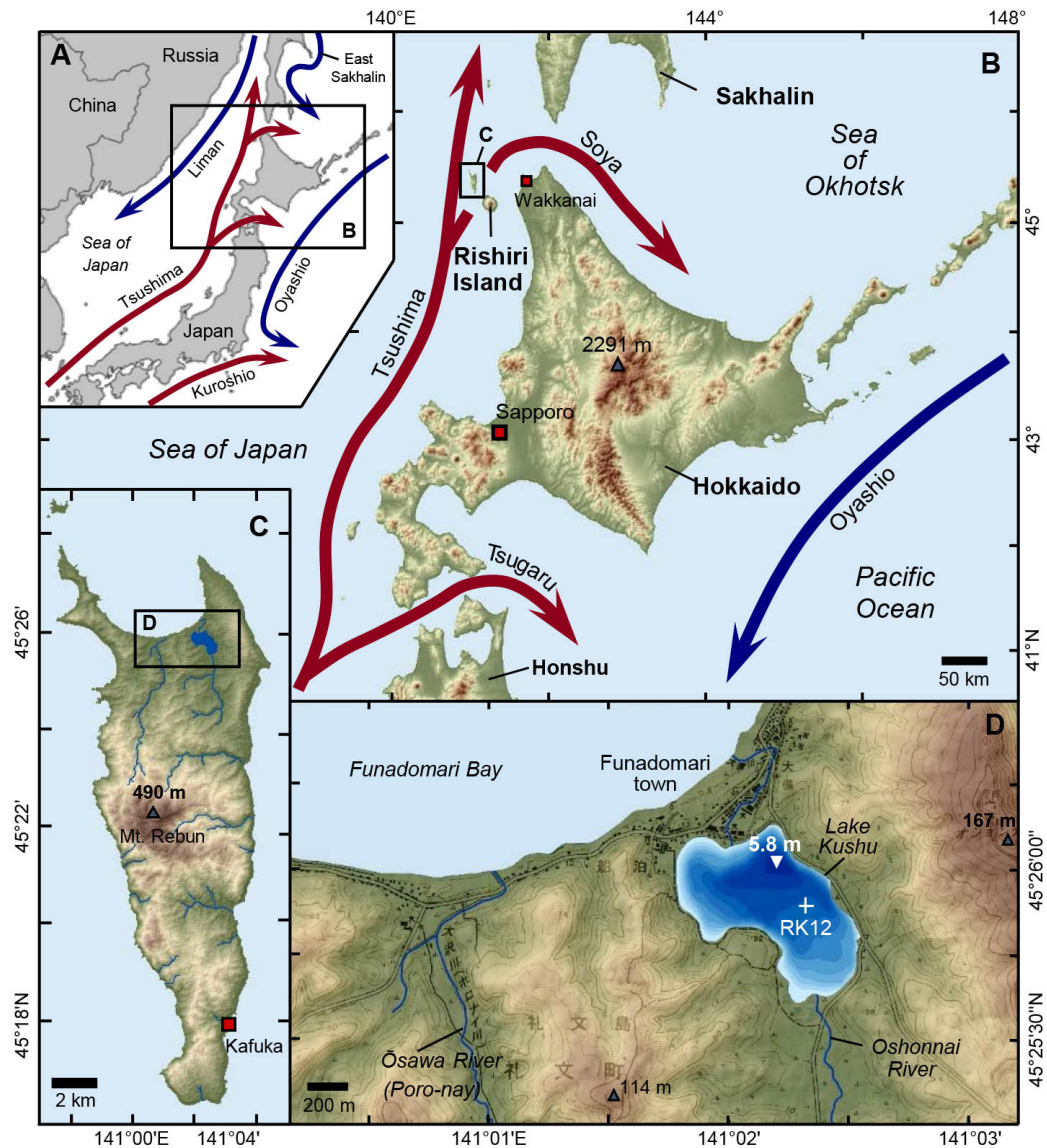


Figure 5.1: Chart compilation showing (A) the location of the Hokkaido Region in Japan; (B) the location of Rebun Island in the Sea of Japan with main cold (blue) and warm (red) sea surface currents around Hokkaido; (C) topographic map and main streams on Rebun I. and (D) outline and bathymetry of Lake Kushu in 0.5 m steps provided by T. Haraguchi (Osaka City University). The white cross marks the location of Kushu Core RK12. The topographic maps are based on elevation Shuttle Radar Topography Mission (SRTM) v4.1 data (Reuter et al., 2007; Jarvis et al., 2008). Isolines in (D) derive from a topographic map (Geospatial Information Authority of Japan, 2012); modified after Müller et al., 2016.

5.4 Material and methods

5.4.1 Core RK12 and chronology

The drilling of the two parallel sediment cores RK12-01 and RK12-02 was performed in the central part of Lake Kushu (at 5.8 m water depth, Fig. 5.1D) in February 2012. The composite core RK12 was assembled of these two overlapping cores providing a 19.5 m long sediment sequence (Müller et al., 2016; Schmidt et al., 2016).

Construction of the age-depth model for the composite record RK12 relies on a set of 57 AMS ^{14}C age determinations (depths indicated with triangles in Fig. 5.2A) obtained in the Poznan Radiocarbon Laboratory (Müller et al., 2016). Although the record does not suggest sedimentary hiatuses throughout the core, the average sedimentation rate increases from *c.* 0.5 mm/yr prior to *c.* 9500 cal. yr BP to *c.* 1.67 mm/yr during the past 6000 years (Müller et al., 2016). Core section RK12-02-9 of the composite record selected for detailed analyses covers the part between 848 and 938 cm (*c.* 5.6-5.2 cal. kyr BP) and shows sedimentation rates of *c.* 1.3-1.4 mm/yr at 848-888 cm, *c.* 2 mm/yr at 878-888 cm and *c.* 5 mm/yr at 888-938 cm.

5.4.2 Diatom analysis

Samples for diatom analysis were extracted every 8 cm (and every 2-3 cm from section 9 respectively) from the sediment core. The 1-cm-thick sediment samples were prepared after the standard preparation method (Battarbee et al., 2001) using 37% HCl and 10% H₂O₂ to remove the carbonates and organic residuals, respectively (see Schmidt et al., 2016 for detailed information). The prepared diatom solutions were embedded in Naphrax™ and counted using a Meiji Techno 4000 microscope at $\times 1000$ magnification with immersion oil. A minimum of 300 counted valves per sample was set due to the partly low valve concentration and small sample size. The taxa were identified with the guides of Krammer and Lange-Bertalot (1997, 1999, 2000, 2004), Ohtsuka (2002), Kobayasi et al. (2006), Levkov (2009), Houk et al. (2010), Lee (2011, 2012), and Tanaka (2014). Taxa names are based on the taxonomy provided on the website AlgaeBase (Guiry and Guiry, 2017). Diatom abundances are presented in percentage diagrams (Fig. 5.2A and 5.6A). The planktonic to benthic ratio (P/B) was calculated by dividing the sum of planktonic valves by the sum of total valves count (see Schmidt et al., 2017). The stack diagrams for the salinity, trophic and pH were plotted with Tilia® software (Grimm, 1991-2011; Fig. 5.3), using the ecological optima for each taxon based on the information from the literature (see Schmidt et al., 2016 for detailed information). The local diatom zones (LDZ) were defined with the CONISS (Constrained Incremental Sum of Squares) in the Tilia® software (Grimm, 1991-2011; Fig. 5.3).

5.4.3 Analysis of pollen and non-pollen palynomorphs (NPP)

Coarse-resolution palynological analysis was applied to the RK12 core sediment as presented in Müller et al. (2016). In this paper the new detailed record of aquatic plant pollen and green algae colonies, commonly named as non-pollen palynomorphs (NPP) are presented to facilitate interpretation and discussion of the aquatic system development. Bulk sediment samples (each representing 1-cm-thick sediment layer) were processed following standard procedures (Cwynar et al., 1979; Fægri et al., 1989), including 7-mm ultrasonic fine sieving, hydrofluoric acid treatment and subsequent acetolysis. Two tablets of *Lycopodium* marker spores, each containing 18,584 spores (batch no. 177745), were added to every sediment sample prior to the chemical treatment for

calculating concentrations of identified palynomorphs (Stockmarr, 1971). Water-free glycerol was used for sample storage and preparation of the microscopic slides. Taxa were counted at magnifications of 400x and 600x, with the aid of published identification keys and atlases (Shimakura, 1973; Nakamura, 1980a, 1980b; Reille, 1992, 1995, 1998; Beug, 2004; Miyoshi et al., 2011; Demske et al., 2013).

For all analyzed fossil pollen samples, calculated percentages of aquatic plants pollen, spores of ferns and mosses and algae percentages were calculated using the total terrestrial pollen sum plus the sum of palynomorphs in the respective group following Müller et al. (2016). The Tilia[®] software (Grimm, 1991-2011) was used for calculating pollen and NPP taxa percentages and drawing the diagrams (Fig. 5.2B and 5.6).

5.4.4 Semi-continuous X-Ray Fluorescence (XRF) analysis

The semi-continuous elemental analysis was performed with a Thermo Scientific Niton XL3t portable energy-dispersive X-ray fluorescence spectrometer (p-ED-XRF) in the ‘mining mode’ for (in-device) fundamental parameter calibration. 19.40 m of split sediment cores in 1-m long core segments were covered with a thin foil and transferred to the ASC[®] manual core track with a mounted sample chamber and analyzed in 1-cm steps for calcium (Ca), chlorine (Cl), iron (Fe), potassium (K), silicon (Si), strontium (Sr), titanium (Ti) and vanadium (V) according to Hoelzmann et al. (2017). Only measurements that show values larger than four times the 1- σ errors were taken into account. The two lacustrine sediments LKSD-2 (lake sediment; Lot. No. 688) and LKSD-4 (lake sediment; Lot. No. 897; Lynch, 1990) were used as certified reference material (CRM) for quality control (Ca, Fe, K, Si, Sr, Ti). Recovery values for both CRMs are shown in the Supplementary Material (ESM 5.1). To assure constant measurement conditions the CRMs were measured at the first and final analyses of each core segment.

Elemental data was analyzed using a compositional data approach to manage the consistent sum-constrained model (Aitchison, 1986). For a more objective interpretation of the multi-variate data and to allow for the comparison of the geochemical data with LDZ, we grouped the data in geochemical units (‘chemofacies’) on the basis of a hierarchical cluster analysis (e.g. Templ et al., 2008; Montero-Serrano et al., 2010 for compositional examples). The procedure is summarized as follows: analysis was performed in R (R Core Team, 2013) using the *compositions* v1.40-1 (Van den Boogaart et al., 2014), the *zCompositions* (Palarea-Albaladejo and Martin-Fernandez, 2015) and the *rioja* v0.9-6 (Juggins, 2015) package. A detailed description of the procedure as well as raw data, interim results, and the computation code is available in the Supplementary Material (ESM 5.2).

In the first step, missing values (values below detection limit) were imputed using multiplicative lognormal replacement (Palarea-Albaladejo and Martin-Fernandez, 2013) to allow for data transformation. With the second step, the data were centered log-ratio (clr) transformed.

The clr is defined as $z = clr(x) = [\ln(\frac{x_1}{g(x)}), \ln(\frac{x_2}{g(x)}), \dots, \ln(\frac{x_D}{g(x)})]$, where $g(x) = [x_1 \cdot x_2 \cdot \dots \cdot x_D]^{1/D}$ is the geometric mean of all parts of the observation $x = [x_1, x_2, \dots, x_D]$. Subsequently, potential outlier (values greater / less than the median $M \pm 3 \times MAD$ (absolute median deviation) of the neighboring observations, $k = 25$ cm) was replaced by a running median ($k = 5$ cm). The third step is used to normalize the variability and value range of major, minor, and trace elements. This includes the standardization of the data using a robust z-transformation (center = M, scale = MAD) or reduction of the dimensionality of the data using a principal component analysis (PCA) of clr-transformed data.

The robust z-transformation is defined as $M - 3 * MAD < x_i < M + 3 * MAD$, where M_j is the median of all parts and $MAD = b M_i(|x_i - M_j(x_j)|)$ the median absolute deviation. x_j is the original observation. We performed the cluster analysis of Manhattan distances applying Ward's method (hierarchical clustering; e.g. Strauss and von Maltitz, 2017) and CONISS (Grimm, 1987) for depth-constrained clustering (Gill et al., 1993). The number of clusters is based on the different lithology and the number of LDZ ($g = 6$). The interpretation of the chemofacies is based upon the LDZ (Fig. 5.4 and 5.5).

5.4.5 Micro-facies analysis

Thin sections for micro-facies analysis from 848-938 cm were prepared from nine 10-cm slices without overlap of fresh core sediments following the standard procedures for soft sediments including freeze-drying and impregnation with epoxy resin (Brauer and Casanova, 2001). Micro-facies analysis was performed with petrographic microscopes with visual light (Nikon SMZ-U at 0.75-7.7 x magnification). The layers were classified after visual description of individual sediment layers and sub-layers as well as careful definition of the layer boundaries. Images (Fig. 5.7) were taken using a digital camera (Olympus DP72) attached to the microscopes and processed with the cellSens Dimension[®] 1.5 software (Olympus Corporation, 2011).

5.5 Results

5.5.1 Diatoms

5.5.1.1 The RK12 core (1932-50 cm)

The results of the diatom analysis are shown in Fig. 5.2A and 5.3. In total, 182 taxa were identified of which 33 species are planktonic and 149 species are benthic. Samples containing at least 300 valves were taken into account. Little to no valves were found between 80 - 150 cm, 180-300 cm, 400-500 cm, 1090-1120 cm, 1410-1500 cm and 1600-1920 cm, which are indicated with blank parts in Fig. 5.2A and 5.3.

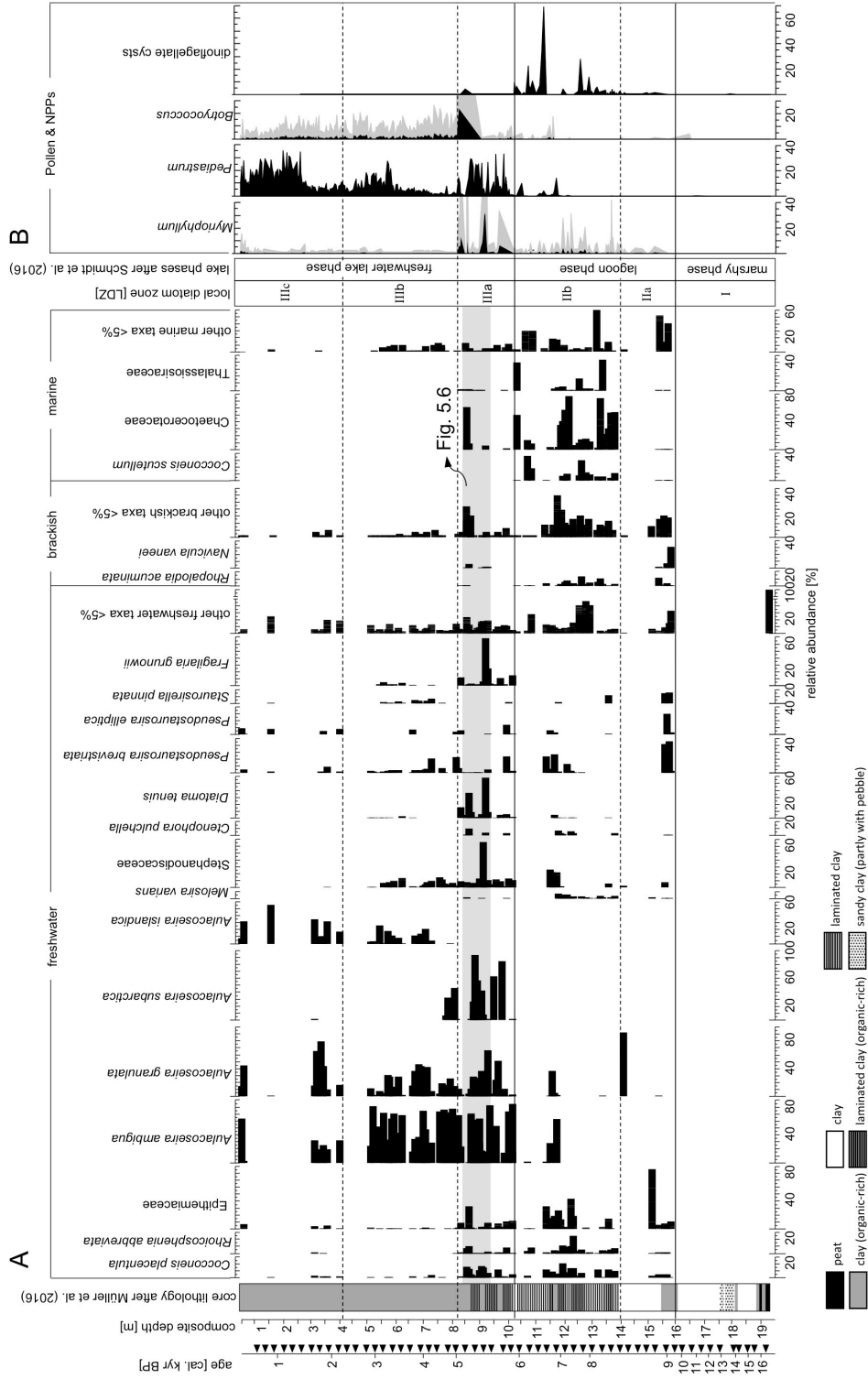


Figure 5.2: The percentage diagram shows (A) the diatom abundances from the Kushu sediment core, grouped into freshwater, brackish, and marine diatoms. Taxa that do not exceed 5% of the assemblages are grouped to ‘other freshwater taxa’, ‘other brackish taxa’, and ‘other marine taxa’. The shadowed part is separately shown in Fig. 5.6. Triangles at the age axis indicate samples for AMS dating and (B) NPPs diagram, the shaded areas show 5-times exaggeration.

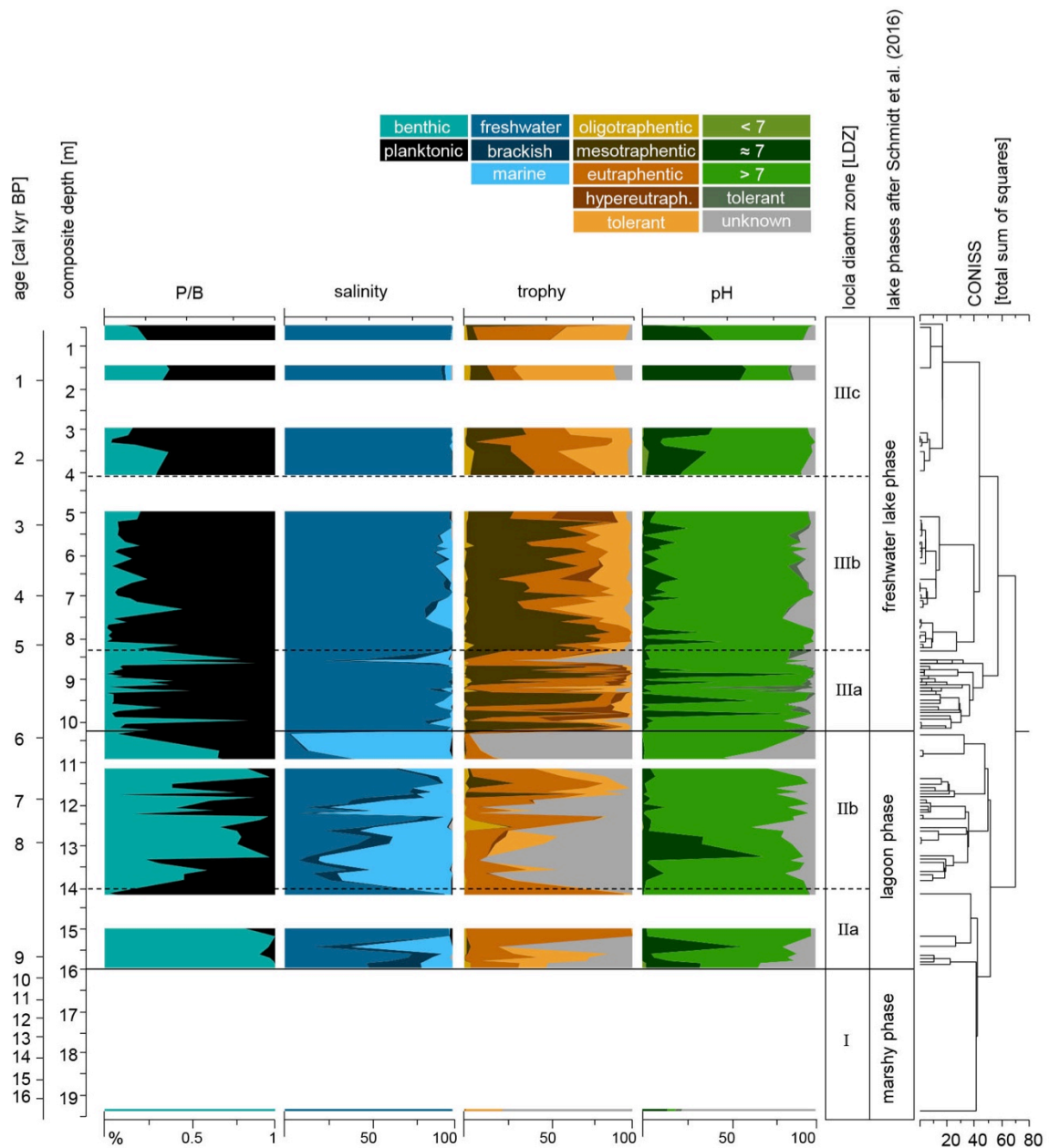


Figure 5.3: The diagrams show the reconstructed ecological parameters P/B, salinity, trophic and pH, based on autecology information calculated with Tilia[®] software (Grimm, 1991-2011). Local diatom zones (LDZ) are delimited with the help of CONISS (Grimm, 1991-2011).

The three lake phases (marshy, lagoon and freshwater lake phase) suggested in the low-resolution pilot study by Schmidt et al. (2016) have been verified using the current high-resolution data. Thus, the transition from the marshy to lagoon phase is now defined at 1600 cm depth (prior study: 1630 cm) and the transition from the lagoon to freshwater lake phase is shifted to 1020 cm (prior study: 1130 cm). The LDZ correlate to the formerly lake phases (Schmidt et al., 2016) and the new high-resolution results allow for subdivisions into subzones. LDZ I (1930-1600 cm) relates to the marshy phase and contains no valves except of freshwater *Diploneis subovalis* Cleve (78%) and *Pinnularia viridis* (Nitzsch) Ehrenberg (15%) in the lowermost sample (see Schmidt et al.,

2016 for detailed information). The core lithology in LDZ I is mostly characterized by clay and sandy clay partly with pebbles. LDZ II (1600-1020 cm) marks the lagoon phase and can be subdivided into two subzones. The organic-rich sediments in LDZ IIa (1600-1400 cm) are mostly composed of benthic freshwater diatoms in the lower part. Clayey sediments with little organic content and absence of valves characterize the upper part of LDZ IIa. LDZ IIb (1400-1020 cm) shows highest percentages of marine Chaetocerotaceae resting spores ($\leq 80\%$). The lithology is characterized by laminated, partly organic-rich clay. A short interval between 1180 and 1130 cm shows freshwater diatoms such as *Aulacoseira ambigua* (Grunow) Simonsen (65%) and *A. granulata* (Ehrenberg) Simonsen (40%), *Pseudostaurosira brevistriata* (Grunow) Williams and Round ($\leq 28\%$), and the absence of marine frustules. LDZ III (1020-50 cm) corresponds to the freshwater lake phase and can be divided into three subzones. The partly laminated organic-rich sediments in LDZ IIIa (1020-830 cm) show a decrease of marine diatoms ($\leq 5\%$) and increase of freshwater *A. ambigua* ($\leq 85\%$), *A. granulata* (Ehrenberg) Simonsen ($\leq 65\%$), *A. subarctica* (Müller) Haworth ($\leq 96\%$), Epithemiaceae ($\leq 35\%$) and Stephanodiscaceae ($\leq 67\%$), and brackish taxa (60%) as well. One peak of marine Chaetocerotaceae resting spores occurs at 850 cm (60%). The lithological analysis in LDZ IIIb (830-410 cm) reveals organic-rich clay without lamination. The diatom assemblages are mainly composed of freshwater *A. ambigua* ($\leq 84\%$), *A. granulata* ($\leq 50\%$), *A. islandica* ($\leq 24\%$), Stephanodiscaceae ($\leq 15\%$), and *P. brevistriata* ($\leq 20\%$). The non-laminated, organic-rich sediments in LDZ IIIc (410-50 cm) are characterized by the absence of diatom valves in most parts. Fewer samples contain valves and consist of planktonic freshwater *A. ambigua* ($\leq 64\%$), *A. granulata* ($\leq 78\%$) and *A. islandica* ($\leq 56\%$, Fig. 5.2A).

5.5.1.2 Detailed analysis of the section 9 (938-848 cm)

The samples from section 9 (848-938 cm) studied in details contain high amounts of well-preserved diatom valves allowing of at least 500 counts per sample. In total, 100 species of 52 genera and 27 families have been identified. The assemblages show the dominance of benthic (84) over planktonic (16) forms. The CONISS analysis delimited five stages, with major divisions at 928 cm, 917 cm, 867 cm, and 864 cm (Fig. 5.6).

The two samples within the *Aulacoseira*-I-stage (A-I, 938-928 cm) show high abundances of planktonic *A. ambigua* ($\leq 82\%$) and *A. granulata* ($\leq 66\%$). The Fragilariaceae-stage (Fr, 928-917 cm, three samples) is characterized by the dominance of freshwater *Fragilaria grunowii* Lange-Bertalot and Ulrich and *Diatoma tenuis* Agardh reaching 68% and 58%, respectively. *Aulacoseira*-II-stage (A-II, 917-867 cm) includes 13 samples that mostly contain the planktonic taxa *A. ambigua*, *A. granulata*, and *A. subarctica*. The lowermost sample of this stage shows a peak of *Cyclotella meneghiniana* Kützing reaching 65% of the assemblage. Increasing abundances of *A. subarctica* are shown at 895-886 cm ranging from 26-93%. Three peaks of *A. ambigua* occur at 895 cm (64%), 880 cm (61%) and 873-868 cm (68-71%). The *Stephanodiscus*-stage (St, 867-864

cm) shows a significant shift from the *Aulacoseira* spp. dominated assemblages in the A-II-stage towards high abundances of *Stephanodiscus hantzschii* Grunow (41%) and *D. tenuis* (36%). The *Chaetoceros*-stage (Ch, 864-848 cm) is marked by the decrease of planktonic freshwater species and the occurrence of the benthic taxa *Cocconeis placentula* Ehrenberg ($\leq 13-15\%$), *Rhopalodia gibba* (Ehrenberg) Müller ($\leq 25\%$), and *Rhoicosphenia abbreviata* (Agardh) Lange-Bertalot ($\leq 10\%$). A significant increase of brackish *Mastogloia elliptica* (Agardh) Cleve 3-4%), *M. pumila* Cleve ($\leq 11\%$) and marine *Chaetoceros* spp. (resting spores) is visible with highest percentages of 61% at 858 cm.

5.5.2 Aquatic pollen and algal remains

5.5.2.1 The RK12 core (1932-50 cm)

Aquatic plants, green algae and dinoflagellates were counted and plotted in figure 5.2B. The water plant *Myriophyllum* (watermilfoil) starts to occur in LDZ IIa and reaches maximum abundance in LDZ IIIa (see also chapter 4.2.2) and decreases in LDZ IIIb to less than 3%. The two green algae *Pediastrum* and *Botryococcus* peak in LDZ IIIa. *Pediastrum* shows highest amounts in LDZ IIIa with several peaks (up to 35%), decreases in LDZ IIIb to 5% and slowly increases to 30% at 550 cm. After a slight reduction towards the termination of LDZ IIIb it increases again in LDZ IIIc with up to 36%. *Botryococcus* occurs with highest abundance at 830 cm (LDZ IIIa) with 24% and decrease in LDZ IIIb and IIIc to 3-5%. Dinoflagellate cysts mainly occur in LDZ IIb with peaks at 1260 cm (30%) and 1130 cm (67%).

5.5.2.2 Detailed analysis of the section 9 (938-848 cm)

A pronounced increase of *Myriophyllum* percentages begins at 930 cm (8%), peaks at 923 cm (33%) and ends at 907 cm (5%). A second peak with 18% is recognized in the uppermost part of the section at 860 cm depth. Freshwater algae colonies of *Pediastrum* reach highest percentages in the lowermost part at 933 cm (36%) and 910 cm (35%), and from 903 to 884 cm (up to 34%). *Pediastrum minima* (less than 1%) are recognized at the lowermost sample (938 cm), at 922 cm and 882 cm (Fig. 5.6). Furthermore, they almost completely disappear in the uppermost three samples of section 9 (860-852 cm). *Botryococcus* occurs in two samples at 928 cm and 910 cm (3% each). Dinoflagellate cysts show a small peak (5%) at 860 cm (Fig. 5.2B).

5.5.3 XRF analysis

The results for Ca, Cl, Fe, K, Si, Sr, Ti, and V from the semi-continuous p-ED-XRF analysis were used to determine and to differentiate the elemental compositions throughout the core. Data are summarized in six different groups by hierarchical cluster analysis and each single observation (n = 1700) analysis is attributed to one of these groups. PC-analysis revealed that 81.4 % of the

geochemical core composition is explained by loadings of PC1 (54.5 %) and PC2 (26.9 %). The compositional biplot of PCs 1 and 2 (Fig. 5.4) shows how specific elements correlate and to which degree the elements contribute to the specific PC. For example, Fe and V as well as Ca and Sr point in similar directions and thus to related characteristics throughout the core. Therefore we abstain to show the plots for Sr and V in figure 5.5. For PC1 Si and Fe are the main drivers, whereas Ca, Sr, and Cl mainly represent variations in PC2. The almost perfect orthogonality between Fe-K-Si (PC1) and Ca-Cl-Sr (PC2) shows that these element combinations represent different chemofacies. The short length of lines representing K and Ti reflects that these elements have only a minor influence on the geochemical variability and thus the formation of the six groups. Therefore, also K is not shown as a plot versus depth in figure 5.5.

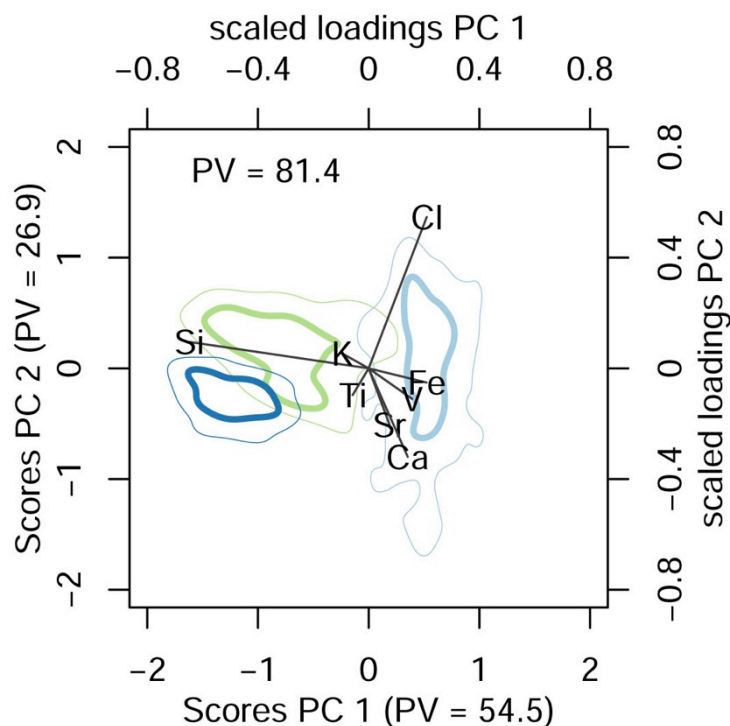


Figure 5.4: PCA biplot with polygons that mark the 50% (bold lines) and 95% distribution of observations. The colors indicate cluster interpretation according to the local diatom zones (LDZ): dark blue = LDZ I; green = LDZ II; light blue = LDZ III, PV = Proportion of Variance [%].

5.5.4 Micro-facies of section 9 (938-848 cm)

Five descriptive types of sediments were identified ranging from well mixed homogenous to finely laminated sediments with visible annual to seasonal layers (Fig. 5.6). Well-laminated areas occur in the lower (926-920 cm) and upper (866-848 cm) parts of the section 9. The sediments in between (920-866 cm) are broad to indistinct broad laminated and show many homogenized areas. The following main layer types were identified: (1) clastic layers with high portions of terrestrial material ('snow'), often containing chrysophyte cysts ('Chry'); (2) diatom bloom layers that consist

entirely of valves i.e. *Aulacoseira* sp. ('Aula'), Fragilariaceae ('Frag'), *Stephanodiscus* sp. ('Steph'); (3) mixed layers with organic residuals and diatom valves ('sum'), sometimes containing *Chaetoceros* spp. resting spores ('Chaet'); (4) well-sorted clastic layers of different thickness ('event') containing glauconitic grains, at times secondary dissolved gypsum crystals and partly with Chaetocerotaceae spp. resting spores and (5) layers with dropstones up to 0.5 mm (Fig. 5.7I).

Relatively thick layers are found at the lowermost part of the section (c. 930-920 cm), which show highest frequencies of freshwater *Aulacoseira* sp. blooms (Fig. 5.7H). Event layers with marine diatoms occur at 926-920 cm and 856-852 cm (red arrows in Fig. 5.6). The laminae in the uppermost part of the analyzed section are very thin and show highest abundances of marine Chaetocerotaceae resting spores.

The micro-facies in this section is characterized by many changes and irregularities regarding occurrence of the lamination, layer thickness, and repetition of similar layers. Here, a typically annual cycle can include a "snow" layer partly accompanied by Chrysophyte cysts ("Chry") or dropstones, a spring diatom bloom layer, followed by a "sum" layer and a fall diatom bloom layer (e.g. "Aula", "Steph", "Frag").

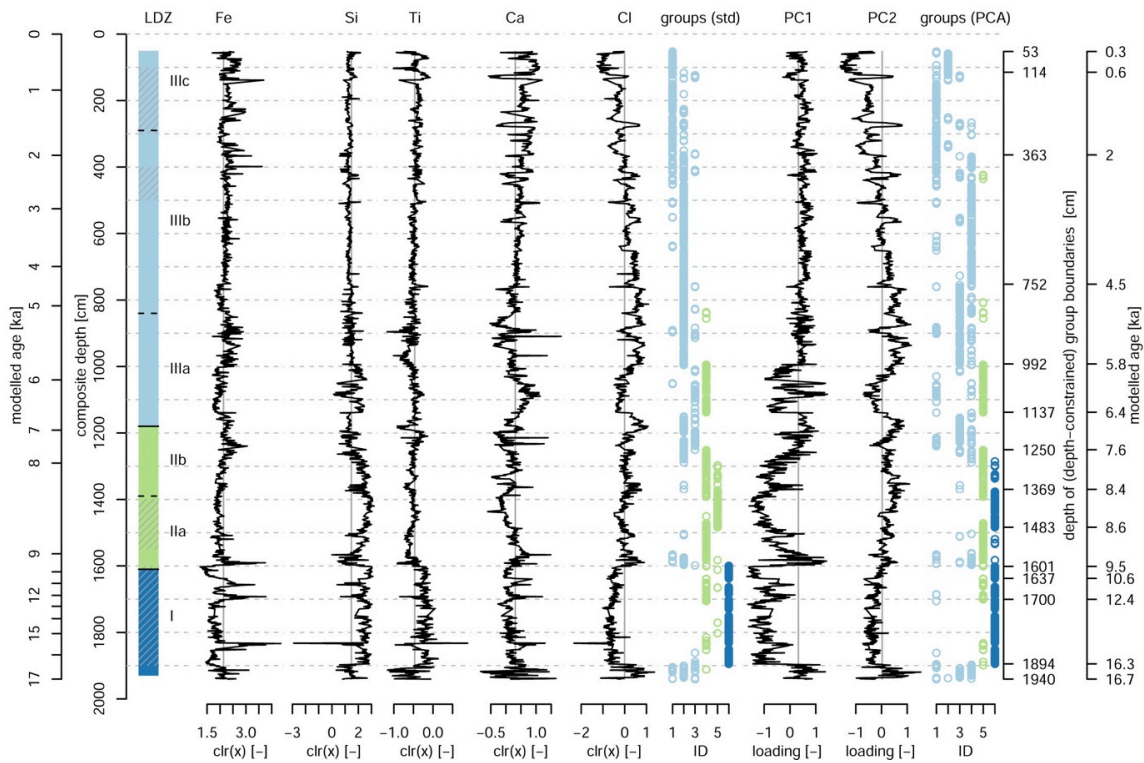


Figure 5.5: The geochemical record of RK12: Age/depth vs. local diatom zones (LDZ), centered log-ratio (clr) transformed contents of selected elements, groups obtained by hierarchical cluster analysis of standardized element contents (std) and the first four principal components (PC). The secondary y-axis shows the boundaries (age/depth) of groups obtained by the depth-constrained cluster analysis of geochemical data. Geochemical groups are in the same color as the most similar LDZ (see Figure 4, PCA). Groups: 1, 2, and 3 = freshwater; 4 = lagoonal (std) or freshwater (PC1–4); 5 = lagoonal; and 6 = marshy.

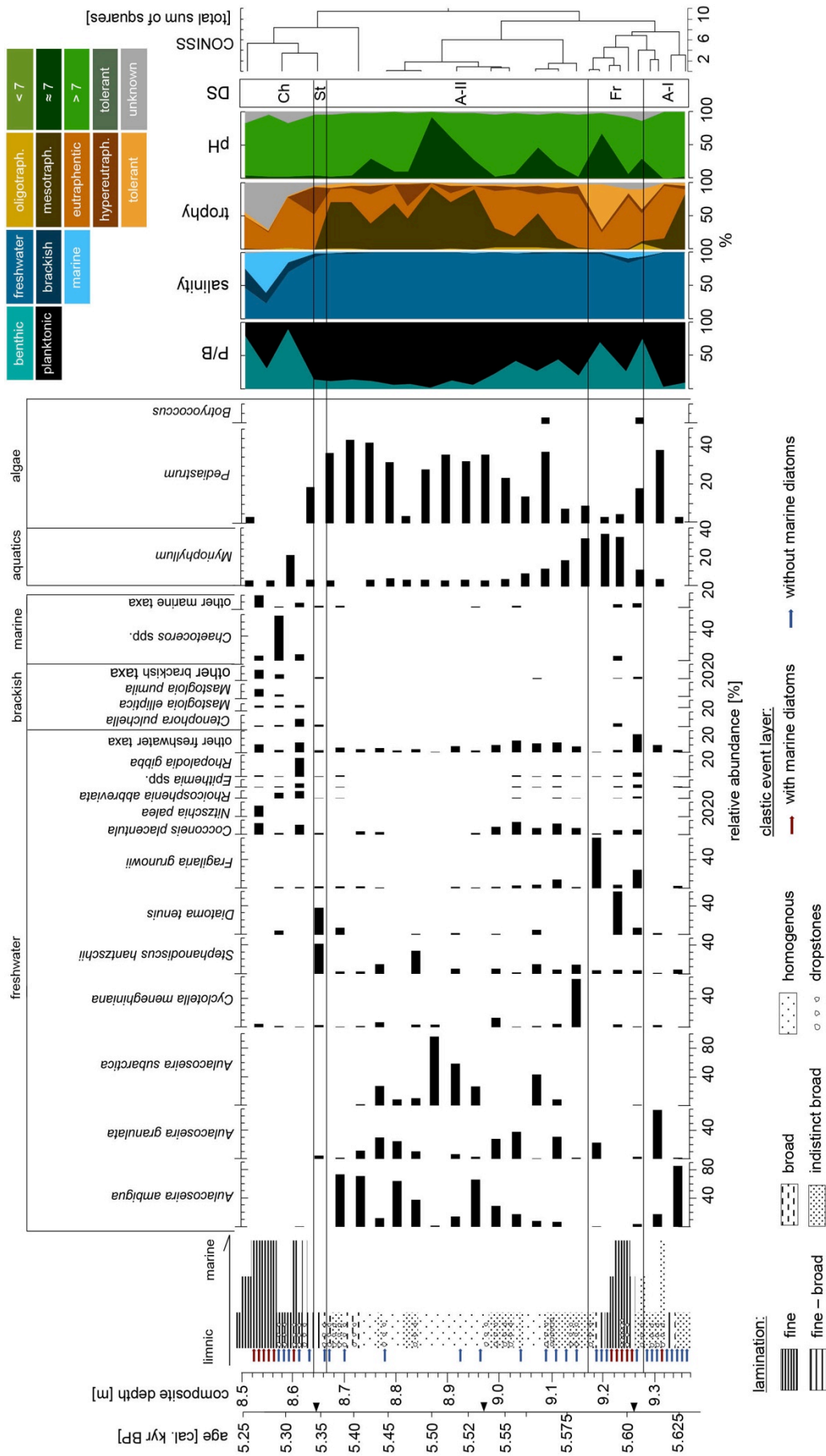


Figure 5.6: Compilation of the high-resolution analyses of section 9 with micro-facies (left) diatom and pollen percentage diagrams (middle) and reconstructed autoecology from diatoms (right). Five diatom stages (DS) are delimited with the help of CONISS (Grimm, 1991-2011) and named after the dominant species: A-I – *Aulacoseira*-I stage, Fr – Fragilariaceae stage, A-II – *Aulacoseira* II stage, St – *Stephanodiscus* stage and Ch – *Chaetoceros* stage.

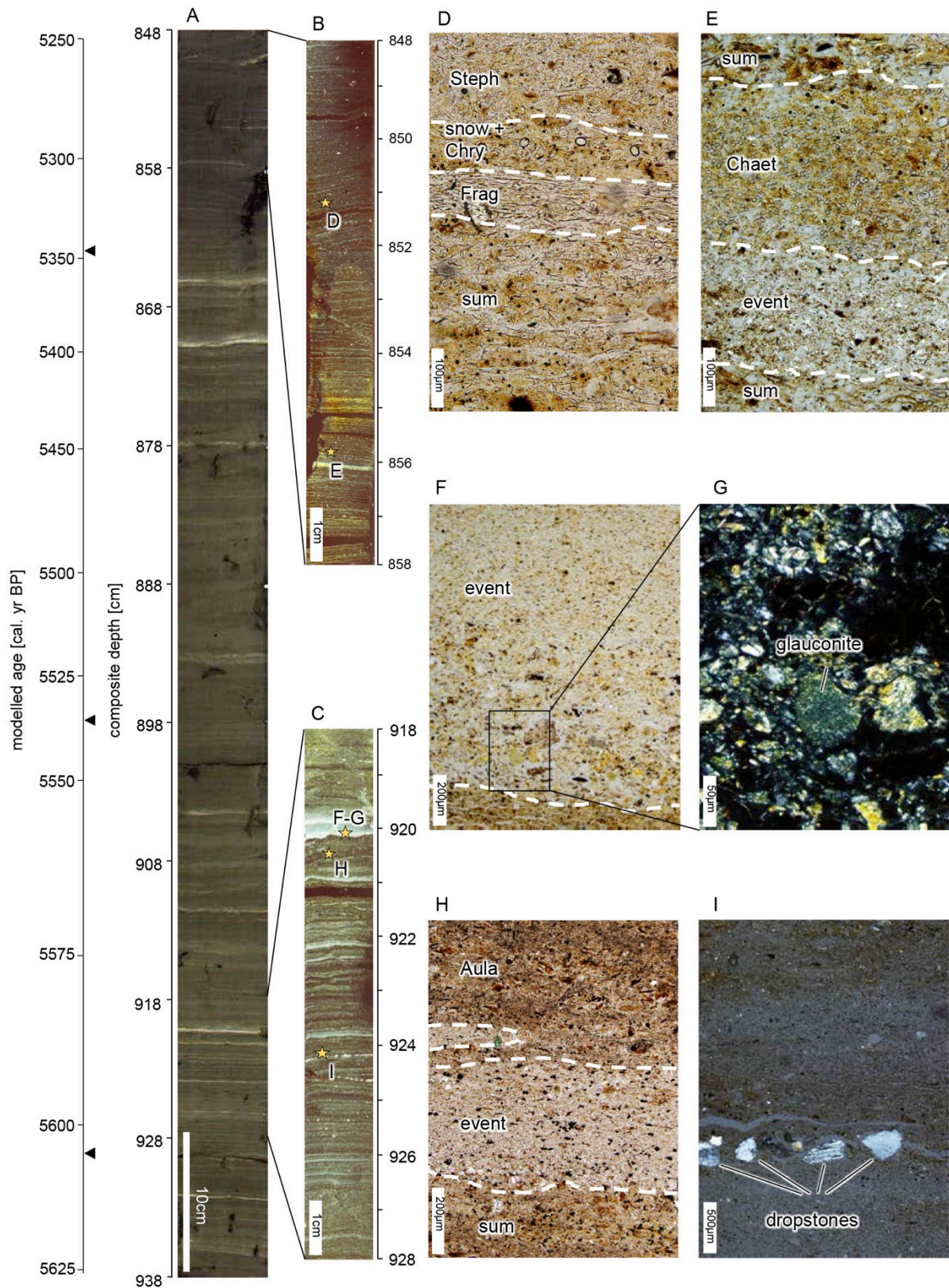


Figure 5.7: Images of the micro-facies analyses of section 9 showing (A) an overview photograph of the 90 cm section; (B-C) thin section images with yellow rectangles indicating the location of the microscopic images (D-I) with Aula - Aulacoseiraceae bloom, Chaet - Chaetocerotaceae resting spores, Chry - Chrysophyte cysts, Frag - Fragilariaceae - bloom, Steph - Stephanodiscaceae-bloom, snow - snowmelt layer, sum - summer layer, event - event layer.

5.6 Discussion

5.6.1 The Lake Kushu basin evolution since 16.6 cal. kyr BP

Schmidt et al. (2016) using only 10 diatom samples and 20 geochemical samples suggested three major phases: (i) marshy phase, (ii) brackish water lagoon phase and (iii) freshwater lake phase during the 16.6 kyr interval covered by the RK12 sedimentary record. Our current results help to verify and precise the findings of the pilot study. The multi-proxy analysis of the RK12 core allows for a continuous palaeoenvironmental reconstruction of Lake Kushu history despite the absence of diatoms in several zones (LDZ I; IIa; partly IIb and IIIc; Fig. 5.2A and 5.3). For these parts, the p-ED-XRF results serve as a robust method to differentiate facies types (Fig. 5.5). Limnological changes inferred by variations in the diatom assemblages can be supported by cluster groups and PCA from the p-Ed-XRF analysis that serve as integral tools for facies discrimination indicated by major shifts in PC-loadings. From the distribution of the attributes of each single analysis below and above these shifts we can also estimate their clearness. This enables us to identify transitions between different facies zones or stable conditions where these variations are lowest. Thus, the transition from the marshy phase (LDZ I) to the lagoon phase (LDZ II) can be slightly adjusted from 10 (1620 cm) to 9.3 cal. kyr BP (1600 cm) according to first diatom valves and the chemofacies classification of the p-ED-XRF data. The transition from the lagoon phase to the freshwater lake phase can be replaced from 6.6 cal. kyr BP (1160 cm) to 5.9 cal. kyr BP (1020 cm) delimited by the first appearance of planktonic freshwater *A. ambigua*, *A. granulata*, and *A. subarctica* and the decrease of marine Chaetocerotaceae resting spores and dinoflagellate cysts (Fig. 5.2). This transition is also visible in the cluster analysis of the elemental composition (Fig. 5.5).

Reasons for the lack of diatom valves are diverse. Typically, the majority of diatom silica is dissolved and recycled before only 5-20% of the valves are embedded in the lake sediments (Bootsma et al., 2003, Leng and Barker, 2006). Thus a longer sinking rate results in an increasing dissolution of frustules in the water column. Parts with non-laminated sediments suggest high turbulences induced by bioturbation and / or wind energy due to a flatten waterbody that prevent the frustules to settle down and therefore circulate in the alkaline water column (diatom assemblages indicate $\text{pH} > 7$; Fig. 5.3) until dissolution. It is also possible that the essential nutrients silica (Si), nitrogen (N) and phosphor (P) limited the growth of diatoms. Low Si/P and Si/N ratios in eutrophic lakes reduce diatom blooms for the benefit of other algal groups (Leng and Barker, 2006). A decrease in the diatom concentration (decreased productivity) also indicates a shorter duration of the growing season (Rioual et al., 2007). In shallow lakes, the growing season is a limiting factor for complex diatom succession to take place in the plankton. In addition, shallow lakes are strongly influenced by sediment infilling and therefore diatom records are often discontinuous (Rioual et al., 2007).

The lithology from 16.6-9.3 cal. kyr BP (LDZ I) shows sandy clays with pebbles likely indicating a fluvial depositional environment (Müller et al., 2016). Highest contents of Si, Fe and Ti (PC1) represent the terrestrial input at this stage, although a phase of high Fe contents (and simultaneously lower Ti-contents) at c. 1850 cm might be interpreted as pyrite formation and thus a phase with marine influence and reduced detrital input. An early, short interval was geochemically grouped as freshwater facies (c. 1600 cm) might also be interpreted as a layer with elevated Fe concentrations due to pyrite formation. Nevertheless, the stratigraphic position and the contemporary relative sea level fairly suggest an interpretation as detrital input. The semi-continuous p-ED-XRF data show a high compositional variability between 1930 and 1890 cm depth, which is geochemically similar to the freshwater facies (LDZ I). However, this group leads into a rather stable facies that is interpreted as a marshy environment from 1930 cm to a depth of 1600 cm. Diatoms are absent in the marshy phase, except of the lowermost sample (1930 cm) that contains several valves of *Diploneis subovalis* Cleve (78%), a common species in running waters (Krammer and Lange-Bertalot, 1997) and *Pinnularia viridis* (Nitzsch) Ehrenberg (15%), known from a stream-fed pond of several cm depth (Harper, 1976). A marshy environment with detrital sediment input is obvious.

LDZ IIa can be regarded as a transition zone with characteristics from the marshy phase and the lagoon phase. In the lower half of LDZ IIa first benthic freshwater diatoms indicate an early shallow freshwater lake that evolved around 9.3 cal. kyr BP, which might have been affected by the first marine influences due to the relative sea level rise (Chiba et al., 2016). This is shown by first appearance of marine diatoms (e.g. *Pinnunavis yarrensis* (Grunow) H. Okuno) and a slight increase of *P. brevistriata*, *P. elliptica* and *Staurosira pinnata* Ehrenberg, which can thrive in slightly brackish waters (Denys, 1990; Van Dam et al., 1994). The p-ED-XRF data confirm this assumption with a clear shift within the loading of PC1 towards more positive values (higher Fe-contents) and lower Si and Ti contents between 1601 and 1483 cm, reflecting reduced fluvial input into the shallow lake, although the geochemical variability is quite high. The lower PC1 sample scores are visible in the upper half of LDZ IIa (between 1483 - 1369 cm; 8.6 - 8.4 cal. kyr BP). This is regarded as a recurring phase of increased detrital input and thus represents a marshy phase with the absence of diatoms and a lithology similar to that in LDZ I.

Valves of marine *Cocconeis scutellum*, Chaetocerotaceae, Thalassiosiraceae and dinoflagellate cysts occur in LDZ IIb (c. 9.3-8.4 cal. kyr BP), when the marshy environment turned into a brackish water lagoon phase with tidal influences. The higher Cl-contents in the p-ED-XRF-data probably reflect the brackish water conditions because Cl in sediments is often used as an indicator for marine influence (Chagué-Goff, 2010). However, the interpretation of Cl is difficult due to its high solubility, which probably is reflected in the relatively large changes of the Cl-content within this part of the section. Our results for a brackish water lagoon phase with tidal influences correlate with the study from Kumano et al. (1990a) who, for the first time analyzed the marine

transgression on Rebus Island from a 1370 cm sediment core from the peat moor in the southern part of Lake Kushu. Whereas Kumano et al. (1990a) present only four ^{14}C dates from plant remains and organic material, we are able to date the timing of the marine transgression more accurately in this area to 8.4 to 5.9 cal. kyr BP (Fig. 5.2 and 5.3). This correlates with the global sea level rise during the Holocene transgression from 8.5 to 7.8 kyr BP that reached its maximum at 6.5 - 6.4 kyr BP (e.g. Bak, 2014; Chiba et al., 2016), possibly leading to a formation of the sand dune separating the former lagoon from the Funadomari Bay. The end of LDZ IIb is represented in the p-ED-XRF-data by fluctuating geochemical composition between 12.50 - 11.37 cm (8.3 to 7.5 cal. kyr BP), which is also reflected in the varying grouping results of this core section. Again, changes occur mainly within the Cl- and Ca-contents (PC2).

Freshwater conditions prevailed since 5.9 cal. kyr BP (LDZ IIIa) right after the maximum relative sea level was reached (Chiba et al., 2016). Planktonic freshwater *A. ambigua*, *A. granulata*, *A. islandica*, Stephanodiscaceae and benthic Epithemiaceae in LDZ dominate in LDZ IIIa (5.9 - 5.1 cal. Kyr BP) and indicate freshwater conditions with intermediate peaks of increased salinity implied by brackish taxa and two peaks of marine Chaetocerotaceae resting spores. This can be interpreted as a freshwater environment, which is regularly connected to the Funadomari Bay (e.g. fluctuating relative sea level) before the sand dune was build and separated the two systems from each other. The reconstructed water parameters (Fig. 5.3) illustrate the alternating changes of trophy, pH, P/B ratio and *Pediastrum* (Fig. 5.2B) in LDZ IIIa. The geochemical data supports the existence of short brackish phases, as well. It shows a high degree of variability of chemofacies groups between 8.3 - 5.8 cal. kyr BP (12.5 to 9.9 m depth, Fig. 5.5). The first appearance of the geochemical freshwater facies during the Holocene dates between 7.6 cal. kyr BP (12.50 m) and 6.4 cal. kyr BP (11.37 m), when Si decreases and Ti and Fe increase with decreasing depth. The cluster analysis of the elemental composition suggests alternating lagoon and freshwater characteristics between 6.4 and 5.8 cal. kyr BP, which supports the interpretation of the diatom data. This section will be discussed in detail in chapter 5.2.

In LDZ IIIb (5.1 - 2.2 cal. Kyr BP) and IIIc (2.2 - 0.3 cal. kyr BP) significant marine influence is not visible anymore and a meso- to eutrophic, alkaline water body existed. The P/B ratio implies a higher lake level compared to the lagoon phase (LDZ II). Loadings of PC1 of the geochemical data supports the interpretation of LDZ IIIb and IIIc as a freshwater phase, the trend of decreasing values of PC2 (increasing Ca-content and decreasing Cl-content) suggest decreasing lake levels towards recent times that is due to sediment infill and biomass accumulation to the lake basin (Schmidt et al., 2016).

Some climate variations can be inferred from the diatom assemblages from the stable freshwater lake phase (LDZ IIIb and IIIc). LDZ IIIb suggests a slight increase of temperature since c. 4.5 cal. kyr BP to present day shown by the decrease of *A. subarctica*, a cold-water diatom (Stoermer and Ladewski, 1976; Krammer and Lange-Bertalot, 2000) and the decrease of *S.*

hantzschii, a winter bloom diatom, whose decrease implies also a shortening winter time (Jung et al., 2009) and the increase of *A. islandica*, which prefers warmer temperatures (Solovieva et al., 2005). Koizumi (2008) postulated similar findings from diatom derived sea surface temperatures in the Tsugaru Street, a branch of the TWC (Fig. 5.1B). This supports the idea, that the Middle to Late Holocene climate in the western Hokkaido Region was mainly influenced by the TWC and EAWM right after the relative sea level rose during the Holocene transgression and the strengthening of the TWC (Leipe et al., 2013).

We aimed to contribute to a better understanding of human-environmental interaction in this region. The question of a certain human impact to Lake Kushu is still unknown. Due to the lack of diatom valves we are not able to reconstruct the limnology after first residential sites occurred between 4.9-4.4 cal. kyr BP (Middle Jomon, Inui, 2000; Müller et al., 2016) in detail. However, the green algae *Pediastrum* (Fig. 5.2B), indicative for nutrient enrichment (Fredskild, 1983), seems to correlate with the increasing number of sites during Middle to Final Jomon (4.4-3.2 cal. kyr BP) resulting in a peak of *Pediastrum* at c. 3.3 cal. kyr BP and a further increase in archaeological site numbers during the Epi Jomon, Okhotsk and Ainu periods (Abe et al., 2016) is parallel to highest values of *Pediastrum* (35%) between 2.3-0.1 cal. kyr BP. The noticeable deforestation of Rebun Island during Historic Ainu period (0.7-0.1 cal. kyr BP) suggested by the decline in arboreal pollen in the Lake Kushu sediment (Müller et al., 2016) might have led to increased drainage from the catchment and thus nutrient enrichment in Lake Kushu. Hence, the diatom assemblages in the uppermost samples of LDZ IIIc (c. 0.3 cal. kyr BP) show a slightly shift from meso- to eutrophic conditions. The chemofacies interpretation also shows a shift at this depth towards lower PC2 values that reflect higher Ca-, Ti-, and slightly higher Fe-contents but lower Cl-contents. This may reflect silting-up and an increasing terrestrial influence. The increasing number of *Myriophyllum* since 500 cal. yr BP might result from the deforestation (Müller et al. 2016) of the catchment area during Ainu period and thus increased drainage during rainfalls.

An important factor for hunter-gatherer migration remains the climate. Precession-forced enhancement of low-latitude solar insolation and strengthening of monsoonal systems are the main drivers of the Holocene Climate (e.g. Wanner et al., 2008). Multiple archaeological findings indicating a more permanent human occupation in this area are timed to the Holocene Climate Optimum (HCO; Müller et al., 2016; Schmidt et al., 2016). The HCO is reconstructed to the period of c. 8.7-5.2 cal. kyr BP in the Hokkaido Region (Igarashi et al., 2002; Igarashi, 2013; Leipe et al., 2015). Multiple Mid-Holocene pollen records in Hokkaido and adjacent regions of the Russian Far East (e.g. Sakhalin and Kuril Islands) reveal an increase of temperate broad-leaved taxon *Quercus* and a decrease of cold-tolerant *Larix* during the HCO (Sakaguchi, 1992; Igarashi et al., 2002; Igarashi et al., 2011). In addition, deglacial sea-level rise reactivated warm northward oceanic currents through the Sea of Japan potentially prolonging the northward extend of the HCO along the western Pacific coast (e.g. Tada et al., 1999; Watanabe et al., 2007; Chiba et al., 2016). We can

infer that Lake Kushu has been a freshwater lake since *c.* 5.9 cal. kyr BP that might have had positive effects on the permanent occupation of Holocene hunter-gatherers on Rebun Island.

5.6.2 Insights into the Lake Kushu ecosystem dynamics during the Mid-Holocene (5.6-5.2 cal. kyr BP)

The annual to seasonal analyses of section 9 (848-938 cm, 5637-5222 cal. yr BP) provides detailed insights to approximately 400 years of the Lake Kushu palaeolimnology during the Mid-Holocene. Its analysis is appropriate for the following reasons: (i) its limnology shows well-laminated sediments, which allows high-resolution analysis; (ii) it lays in the reconstructed LDZ IIIa of the freshwater lake phase, which consists of *A. ambigua*, *A. granulata* and *A. subarctica* as dominant freshwater species but of several brackish water taxa reaching up to 50%, as well, and therefore helps to decode the coexistence of freshwater and brackish taxa (Fig. 5.2); (iii) it shows the last significant evidence of brackish / marine influence after the Holocene transgression and corresponds to the strongest flow of the TWC (Nishida and Ikehara, 2013; Chiba et al., 2016; Leipe et al., 2013) and (iv) it reflects the final phase of the HCO, which was reconstructed to 8.7-5.2 cal. kyr BP in the Hokkaido Region, defined by slightly increased precipitation and temperatures, which corresponds to the spread of cool mixed and cool conifer forests in the Hokkaido Region (Igarashi et al., 2002, Igarashi 2013, Leipe et al., 2015), right after the climatic influence of large continental ice sheets or large mass reorganizations (high amount of meltwater from the ice sheets; Wanner et al., 2008).

The diatom and micro-facies analyses allowed the identification of typical seasonal layers (Fig. 5.6 and 5.7), of which the most prominent and frequent layer is the snowmelt layer ('snow'). It marks the beginning of an annual cycle in spring, after the EAWM brought high amount of moist and snow to the region. They often contain dropstones, which sank to the lake bottom after the ice cover melted (Fig. 5.7I). The organic-rich 'sum' layer with numerous diatom taxa probably represents accumulation during spring and summer. The diatom blooms (e.g. 'Steph' or 'Aula') occur irregularly and the main taxon varies throughout the section that implies limnological changes and divides the section to five diatom stages (DS).

DS A-I (*c.* 5637-5608 cal. yr BP) is a clear freshwater stage dominated by freshwater planktonic *A. ambigua* ($\leq 82\%$) and *A. granulata* taxa ($\leq 66\%$) that often co-occur because of similar ecological requirements. Both taxa prefer high light and temperate conditions, with blooms in summer and autumn, and are mainly found in shallow, alkaline lakes (Rioual et al., 2007). *A. ambigua* prefers meso- to eutrophic conditions (Reynolds, 1998; Rioual et al., 2007; Poister et al., 2012) whereas *A. granulata* occurs in eutrophic lakes and water temperatures excessively higher than 15°C (Shear et al., 1976). Both taxa require high optima for total phosphorous (TP) and silica concentrations (Rioual et al., 2007). The occurrence of *Pediastrum* in this stage may confirm warmer (Fredskild, 1983; Sarmaja-Korjonen et al., 2006) and rather nutrient-rich freshwater

conditions (oligo- to mesosaprobic; Komárek and Jankovská, 2001). Further, the occurrence of snowmelt layers with dropstones (Fig. 5.7) suggests regular snow-rich winters transporting nutrients from the catchment into the lake.

Micro-facies analysis of the laminated parts in DS Fr (5608-5584 cal. yr BP) reveal repeated clastic event layers including marine Chaetocerotaceae resting spores, which point to marine impacts caused by storm events. The resulting brackish water conditions also account for decreasing amounts of *Pediastrum* finds in this zone (Fig. 5.6). On the other hand, high percentages of freshwater *F. grunowii* (68%) and *D. tenuis* (58%), which were often found in cold, oxygen- and carbon-rich headwaters of streams (Patrick, 1977) and *Myriophyllum* (35%), a plant growing in the shallow areas in the southern peat near the Oshonnai River (personal observation) lead to the assumption that the storm events (typhoons) also might have been accompanied by intensive rainfall and thus short time lake level rises. This induces an enhanced water mixture and particularly increased drainage via the Oshonnai River (Fig. 5.1D) and results in higher abundances of Fragilariaceae, *Myriophyllum* and clastic layers in the sediment core.

DS A-II (c. 5584-5363 cal. yr BP) covers the largest part of the section. It reflects a relatively deeper freshwater lake indicated by a low P/B ratio and high percentages of planktonic *A. ambigua* and *A. granulata*.

The increase of *A. subarctica* from 5530 to 5500 cal. yr BP (26-93%) suggests a cooling period as it is common in shallow (Gibson et al., 2003), circumneutral (Rioual et al., 2007), nordic (Krammer and Lange-Bertalot, 2000) lakes with seasonal ice cover (Kilham et al., 1996; Interlandi et al., 1999; Gibson and Foy, 1988) that prefers cold-water conditions with favored temperatures about 4°C (Stoermer and Ladewski, 1976). These findings correspond with the 5.5 kyr climate deterioration event described by Koizumi and Yamamoto (2011) from diatom analysis reflecting cooler sea surface temperatures in the Sea of Japan. We relate the abundance of *A. subarctica* to cooler water temperatures and possibly extended ice cover in the winter period. The numerous clastic event layers can be explained by higher frequency of typhoons rather than changes in the EASM as this was discussed by Schlolaut et al. (2014) for Lake Suigetsu. The Hokkaido Region is affected by typhoons regularly with peak season in August and September resulting in lake level rise and flooding of the shores (Schlolaut et al., 2014; Schmidt et al., 2016).

Planktonic freshwater species such as *Aulacoseira* spp. disappear in DS St (c. 5363-5340 cal. yr BP) and indicate a decreasing water level. The micro-facies and limnology show fine to broad lamination and high amount of clastic event layers (Fig. 5.6) without marine diatoms those led to sediment infill. The presence of *D. tenuis*, *Myriophyllum* and clastic event layers indicate predominant terrestrial influence from the Oshonnai River and the surrounding area similar to DS Fr. The high impact of clastic material from the surrounding area led to nutrient enrichment and hence *S. hantzschii* blooms (Van Dam et al., 1994).

In DS Ch (c. 5340-5222 cal. yr BP) marine *Chaetoceros* resting spores and brackish / brackish-tolerant diatoms, e.g. *Epithemia* spp., *C. placentula* (Saunders et al., 2007) dominate the assemblages. The freshwater alga *Pediastrum* and freshwater diatoms decrease significantly. The marine impact seems higher compared to DS Fr. It is possible, that the marine impact increased due to intensified relative sea level fluctuations.

5.7 Conclusions

The high-resolution multi-proxy analysis of the RK12 sediment core allows for a continuous palaeolimnological reconstruction of Lake Kushu in the Late Glacial and Holocene time period. The accurate age model helps to precisely define the three lake basin development phases. (i) The marshy phase (16.6-9.3 cal. kyr BP) is characterized by sandy clayish sediments with pebbles, highest content of Si, Fe and Ti values and the absence of diatoms that indicate a riverine depositional environment. (ii) The lagoon phase (9.3-5.9 cal. kyr BP) can be divided into two subzones LDZ IIa and IIb. The former suggests a first lake phase with freshwater, brackish and marine diatoms and an elemental composition (lower Si and Ti values) that indicates a first marine influence to the environment after the relative sea level rose. The latter (LDZ IIb) shows highest marine impact with predominant marine diatoms, dinoflagellate cysts and highest values of Ca-Cl that point to a lagoonal system, when the relative sea level reached its maximum. (iii) The freshwater lake phase (5.9-0.3 cal. kyr BP) is characterized by highest percentages of freshwater Aulacoseiraceae valves and the occurrence of green algae that imply a meso- to eutrophic, alkaline lake with slightly decreasing water depth and eutrophication towards modern times. Our study shows that the combination of biogenic and geochemical methods complements each other. The elemental analysis represents the diatom zones well and serves as a robust method to bridge parts without diatoms.

The high environmental variability in LDZ IIIa has been analyzed from 90 cm thin sections (848-938 cm) of a well-laminated section 9 of RK12 to serve as an additional annual to seasonal tool to get insights into the Mid-Holocene lake evolution and to understand the high variability that has been uncovered by diatom and geochemical analyses. The micro-facies offered a high number of different short-term events that affected the lake: snowmelt, marine impacts (e.g. storm waves), terrestrial impacts (e.g. typhoons) and slight climatic changes (e.g. 5.5 kyr climate deterioration event).

We successfully combined biogenic, geochemical and sedimentological methods to reconstruct the Lake Kushu history in detail. The proofed existence of freshwater Lake Kushu since approximately 5000 yr BP, when the marine influence terminated, helps to understand the timing and background reasons of the hunter-gatherer human occupation on Rebus Island.

5.8 Acknowledgements

The present study is a contribution to the Baikal-Hokkaido Archaeology Project (BHAP) directed by Prof. Andrzej Weber (University of Alberta, Canada) and Prof. Hirofumi Kato (Hokkaido University, Japan). The palaeoenvironmental research (PI: P. Tarasov) on Rebun Island was initiated as part of the BHAP and financed via the Major Collaborative Research Initiative (MCRI) programme of the Social Sciences and Humanities Research Council of Canada, Japan Society for the Promotion of Science, and collaborating institutions, including the University of Alberta, the German Archaeological Institute (DAI), the Hokkaido University, and the Freie Universität Berlin (FUB). Coring of Lake Kushu and core transportation costs were covered by the Japanese MEXT-Japan Kakenhi research grant no. 21101002 held by H. Yonenobu. S. Müller acknowledges the support of H. Kato, T. Irino, and M. Yamamoto, who provided research facilities during her research stay at Hokkaido University. We greatly acknowledge various help and support to the project from local Ainu and fishermen communities and local governmental organizations. We thank T. Haraguchi (Osaka City University) for providing the bathymetry data of Lake Kushu, and A. Kossler (FUB) for initial work on the Rebun Island flora identification. Mareike Schmidt's work was financed via a BHAP PhD stipend (University of Alberta, 0424634401). We appreciate the financial support of the German Research Foundation (DFG Grants LE 3508/1-1, TA 540/5-1, and TA 540/5-2). We further thank Frank Kutz for technical support during semi-continuous p-ED-XRF analyses.

6. Conclusions

This doctoral thesis uses diatoms as bioindicators for palaeolimnological reconstructions and a combination of biogenic (pollen and NPP), bio- / geochemical (XRF, oxygen isotopes from water and frustules) and sedimentological (micro-facies) methods to reconstruct the palaeoenvironmental and climatic changes to contribute to our understanding of the migration dynamics of past hunter-gatherer populations within two different study regions (i.e. Middle Kahlari and Hokkaido Region). The Lake Palaeo-Makgadikgadi deposits contain a high number of well-preserved diatoms, but smaller diversity, whereas the Lake Kushu sediments show a higher number of taxa, but absence of valves and partly little valve concentrations. Nevertheless, the limnology of both lakes has been successfully reconstructed with diatom analysis and complementary methods. The final results can be described as the follows:

Lake Palaeo-Makgadikgadi

- First diatom-based evidence of a Late Pleistocene (MIS 5d-b) mega lake phase covering *c.* 1000 years is provided.
- Differential GPS-measured elevation of the deposits suggests a lake phase with a lake level at an altitude of *c.* 935-940 m a.s.l. that possibly covered at least 37,000 km² in the Makgadikgadi Basin.
- The diatom assemblages indicate a stable shallow, freshwater lake with alkaline and oligohaline conditions. Although the salinity is possibly not representative for the whole mega-lake because of the great distance to freshwater inflow from main rivers.
- $\delta^{18}\text{O}$ isotopic composition from diatom frustules indicates decadal to bi-decadal variability between warm-wet and cold-arid climate shifts and subsequent changes in the hydrologic balance (evaporation / precipitation).
- The existence of such a large lake during MIS 5 provides evidence that at least one short-term anomaly of higher humidity (e.g. Heinrich event-like climate period) occurred during a formerly postulated very dry period in southern Africa possibly triggered by North Atlantic iceberg discharges.
- The lake phase stands for favorable conditions and available potable water for hunter-gatherers (i.e. Khoisan-speaking groups). Together with archaeological finding it can be speculated that permanent human occupation in this region have been possible in the (semi-) arid environments since MIS 5

Lake Kushu

- The modern set of diatom samples and water chemistry from Lake Kushu (Rebun Island) environments represent a dimictic, mature shallow freshwater lake with massive green algal blooms in summer. Eutraphent to hypereutraphent taxa (e.g. *Stephanodiscus hantzschii*) indicate nature (silting basin) and human (deforestation, pollution) induced processes that lead to eutrophication.
- The 19.5 m long sediment core was successfully tested to serve as a multi-proxy archive for high-resolution environmental and climate reconstructions in the Hokkaido Region to improve the understanding of Holocene hunter-gatherer population dynamics.
- The very good correlation between the used methods (diatom, pollen and NPP and p-ED-XRF) and the accurate age model delimit three lake phases: (i) marshy phase (16.6-9.3 cal. kyr BP), (ii) lagoon phase (9.3-5.9 cal. kyr BP) and (iii) freshwater lake phase (5.9-0.3 cal. kyr BP).
- Diatom, aquatic plant and p-ED-XRF analyses highly correlate with each other and can provide valuable information of marine or terrestrial provenience of sediments. The marine impact in the lagoon phase can be correlated to the Holocene relative sea level rise that affected the lake between 8.4-5.9 kyr BP inferred from the occurrence of marine *Chaetocerotaceae* resting spores, dinoflagellate cysts and higher Cl-Ca contents.
- Micro-facies analysis serves as an additional tool to decipher high variability of limnology in LDZ IIIa and discovers marine and terrestrial clastic events that affected the lake between 5.6-5.2 cal. kyr BP after a sand barrier separated the lake from the Funadomari Bay.
- The modern diatom assemblages and personal observation show that the EAM influences the region with high precipitation in summer and winter including regular typhoons (with peaks in August-September). The micro-facies study mirrors similar effects in the Mid-Holocene (5.6-5.2 cal. kyr BP) by discovering numerous clastic event layers.
- The Mid- to Late Holocene freshwater phase is mainly characterized by the appearance of *Aulacoseira ambigua*, *A. granulata*, *A. islandica*, and *A. subarctica* reflecting meso- to eutrophic alkaline freshwater conditions.
- The existence of a stable freshwater lake since *c.* 5.9 cal. kyr BP correlates with the archaeological findings of permanent occupation of hunter-gatherers since 6000 years BP and helps to understand the human environmental interaction history on Rebun Island.

6.1 Outlook

The results demonstrate that diatom analysis provides detailed and valuable information about hydromorphological dynamics and palaeolimnology throughout a period of time. A Lake Palaeo-Makgadikgadi highstand is now characterized by its water parameters and marks a humid period (MIS 5) in southern Africa. To understand the complexity of the MOZB, further spatiotemporal studies are needed to decode the duration and extension of the suggested lake phases since the MIS 5 and to identify the triggers for these humid phases. It is eligible to investigate further lacustrine sediments from this lake phase in other places within the Makgadikgadi Basin and additionally to find deposits from another lake phase for comparison. However, diatom-rich deposits are rare in the Makgadikgadi Basin and little diatom research has been undertaken in this region. Our results represent only local water parameters and cannot stand for the total of 37,000 km² waterbody. Here, sediments need to be found and analyzed to resolve the limnology in all parts of the lake phase. It is still unknown, which (palaeo-) rivers were active at which time period and how much water inflow was necessary to fill the Makgadikgadi Basin. Studies to precise the period when the rivers were active are needed. The hydrologic situation depends on climate anomalies, which can be detected by multi-proxy studies of the lacustrine sediment in the Middle Kalahari. Most ages in the Middle Kalahari derive from OSL dating, which includes high uncertainties. Additional dating methods, e.g. radiocarbon dating from water organisms (e.g. molluscs) and organic-rich sediments might serve more accurate age models to decode the further humid periods younger than 50,000 years (technical limit of this method) and to connect the different highstands in the MOZB. Further investigations with differential GPS improve the determination of the elevation of lacustrine deposits and therefore, once again help to understand the complexity of the MOZB.

The Lake Kushu multi-proxy analysis provides continuous information of the last *c.* 16,600 years despite the absence of diatoms in some parts of the RK12 core. The small sample size of the analyzed material and relatively low diatom concentrations preclude any oxygen isotope analysis from frustules. Material accumulation for increasing the sample size (at the expense of resolution) might let to more information of the hydrologic balances.

Non-destructive μ XRF analysis can be used as an excellent tool to add information about the sedimentological provenience in the section 9 (Mid-Holocene) and to better distinguish marine from terrestrial impacts.

The Lake Kushu study provides a continuous record from 16,600 to 300 year BP. To close the gap of *c.* 300 years, the analysis of a short core from the upper sediment would be worthwhile. Especially, the last 300 years (upper 50 cm) between the top of the RK12 core and the modern lake bottom possibly yield new data about human environmental influences and reasons for eutrophication. A deepened combination and correlation of multi-proxy studies with archaeological investigations might provide a significant advance in reconstructing the Holocene history of climate and human development in the Hokkaido Region.

7. References

- Abe, C., Leipe, C., Tarasov, P.E., Müller, S. & Wagner, M., 2016. Spatio-temporal distribution of hunter-gatherer archaeological sites in the Hokkaido region (northern Japan): An overview. *THE HOLOCENE* 26 (10): 1–19.
- Adachi, N., Shinoda, K-I., Umetsu, K. & Matsumura, H., 2009. Mitochondrial DNA analysis of Jomon skeletons from the Funadomari site, Hokkaido, and its implication for the origins of Native American. *AMERICAN JOURNAL OF PHYSICAL ANTHROPOLOGY* 138 (3): 255–265.
- Aitchison, J., 1986. *The Statistical Analysis of Compositional Data*. Chapman and Hall, London, New York.
- Aitken, M.J., 1998. *An Introduction to Optical Dating: The Dating of Quaternary Sediments by the Use of Photon-Stimulated Luminescence*. Oxford University Press, Oxford.
- Alley, R.B. & Ágústsdóttir, A.M., 2005. The 8k event: cause and consequences of a major Holocene abrupt climate change. *QUATERNARY SCIENCE REVIEWS* 24: 1123–1149.
- Andersson, L., Gumbrecht, T., Hughes, D., Kniveton, D., Ringrose, S., Savenije, H., Todd, M., Wilk, J. & Wolski, P., 2003. Water flow dynamics in the Okavango River Basin and Delta: a prerequisite for the ecosystems of the Delta. *PHYSICS AND CHEMISTRY OF THE EARTH* 28: 1165–1172.
- Anonymous, DIN EN 13346, April 2001. Charakterisierung von Schlämmen – Bestimmung von Spurenelementen und Phosphor – Extraktionsverfahren mit Königswasser; Deutsche Fassung EN 13346: 2000, Beuth Verlag. (*in German*)
- Baillieu, T. A., 1979. Makgadikgadi pans complex of central Botswana: summary. *GEOLOGICAL SOCIETY OF AMERICA BULLETIN PART 1* 90: 133–136.
- Bak, Y.-S., 2014. Mid-Holocene sea-level fluctuation inferred from diatom analysis from sediments on the west coast of Korea. *QUATERNARY INTERNATIONAL* 384: 139–144.
- Balter, M., 2002. Becoming Human. What made humans modern? *SCIENCE* 295: 1219–1225.
- Batisani, N. & Yarnal, B., 2010. Rainfall variability and trends in semi-arid Botswana: Implications for climate change adaptation policy. *APPLIED GEOGRAPHY* 30: 483–489.
- Battarbee, R.W., 1988. The Use of Diatom Analysis in Archaeology: A Review. *JOURNAL OF ARCHAEOLOGICAL SCIENCE* 15: 621–644.
- Battarbee, R.W., Jones, V.J., Flower, R.J., Cameron, N.G., Bennion, H., Carvalho, L. & Juggins, S., 2001. Diatoms. In: Smol, J.P., Birks, H.J.B. & Last, W.M. (Eds.), *Tracking Environmental Change Using Lake Sediments, Terrestrial, Algal, and Siliceous Indicators*, Vol. 3. Kluwer Academic Publishers, Dordrecht, pp. 155–202.
- Battarbee, R.W., Charles, D.F., Dixit, S.S. & Renberg, I., 2010. Diatoms as indicators of surface water acidity. In: Smol, J.P. & Stoermer, E.F. (Eds.), *The Diatoms - Application for the Environmental and Earth Sciences*, 2nd Edition, Cambridge University Press, Cambridge, pp. 152–173.

- Beckhoff, B., Kanngießler, B., Langhoff, N., Wedell, R. & Wolff, H., 2006. Handbook of Practical X-Ray Fluorescence Analysis. Springer Verlag, Berlin, Heidelberg.
- Bennion, H., Juggins, S. & Anderson, N.J., 1996. Predicting epilimnetic phosphorus concentrations using an improved diatom-based transfer function and its application to Lake Eutrophication management. *ENVIRONMENTAL SCIENCE & TECHNOLOGY* 30: 2004–2007.
- Beug, H.-J., 2004. Leitfaden der Pollenbestimmung für Mitteleuropa und angrenzende Gebiete. Verlag Dr. Friedrich Pfeil, München. (*in German*)
- Bezrukova, E.V., Hildebrandt, S., Letunova, P.P., Ivanov, E.V., Orlova, L.A., Müller, S. & Tarasov, P.E., 2013. Vegetation dynamics around Lake Baikal since the middle Holocene reconstructed from the pollen and botanical composition analyses of peat sediments: Implication for paleoclimatic and archeological research. *QUATERNARY INTERNATIONAL* 290–291: 35–45.
- Binz, P., 1987. Oxygen-isotope analysis on recent and fossil diatoms from Lake Walen and Lake Zurich (Switzerland) and its application on paleoclimatic studies. PhD Thesis, Swiss Federal Institute of Technology, Zurich.
- Bond, G.C. & Lotti, R., 1995. Iceberg discharges into the North Atlantic on millennial time scales during the last glaciation. *SCIENCE* 267: 1005–1017.
- Bootsma, H.A., Hecky, R.E., Johnson, T.C., Kling, H.J. & Mwita, J., 2003. Inputs, outputs, and internal cycling of silica in a large, tropical lake. *JOURNAL OF GREAT LAKES RESEARCH* 29: 121–138.
- Bøtter-Jensen, L., 1997. Luminescence techniques: instrumentation and methods. *RADIATION MEASUREMENTS* 17: 749–768.
- Bøtter-Jensen, L., McKeever, S. & Wintle, A., 2003. Optically Stimulated Luminescence Dosimetry. Elsevier, Amsterdam.
- Bradshaw, E.G., Anderson, N.J., Jensen, J.P. & Jeppesen, E., 2002. Phosphorus dynamics in Danish lakes and the implications for diatom ecology and palaeoecology. *FRESHWATER BIOLOGY* 47: 1963–1975.
- Brauer, A. & Casanova, J., 2001. Chronology and depositional processes of the laminated sediment record from Lac d'Annecy, French Alps. *JOURNAL OF PALEOLIMNOLOGY* 25: 163–177.
- Breyer, B., 1982. Reconnaissance geomorphological terrain classification, lower Boteti region, northern Botswana. *ITC JOURNAL* 3: 317–323.
- Bronk Ramsey©, 2013. OxCal Program v4.2.4. Oxford: Radiocarbon Accelerator Unit, University of Oxford.
- Broecker, W.S., 2002. Massive ice berg discharges as triggers for global climate change. *NATURE* 372: 421–424.
- Bukhteeva, A.V. & Reimers, N.F., 1967. Vegetation map. In: Komsomol'skii, G.V. & Siryk, I.M. (Eds.), Atlas Sakhalinskoi Oblasti. Moscow: GUGK, pp. 106–107. (*in Russian*)

7. References

- Burrough, S.L., 2016. Late Quaternary Environmental Change and Human Occupation of the Southern African Interior. In: Jones, S.C., Stewart, B.A. (Eds.), *Africa from MIS 6-2: Population Dynamics and Palaeoenvironments, Vertebrate Paleobiology and Paleoanthropology*. Springer, Dordrecht, pp. 161–174.
- Burrough, S.L. & Thomas, D.S.G., 2009. Geomorphological contributions to palaeolimnology on the African continent. *GEOMORPHOLOGY* 103: 285–298.
- Burrough, S.L., Thomas, D.S.G., Bailey, R.M., 2009a. Mega-Lake in the Kalahari: A Late Pleistocene record of the Palaeolake Makgadikgadi system. *QUATERNARY SCIENCE REVIEWS* 28: 1392–1411.
- Burrough, S.L., Thomas, D.S.G. & Singarayer, J.S., 2009b. Late Quaternary hydrological dynamics in the Middle Kalahari: Forcing and feedbacks. *EARTH-SCIENCE REVIEWS* 96: 313–326.
- Burrough, S.L., Thomas, D.S.G., Shaw, P.A. & Bailey, R.M., 2007. Multiphase Quaternary highstands at Lake Ngami, Kalahari, northern Botswana. *PALAEOGEOGRAPHY PALAEOCLIMATOLOGY PALAEOECOLOGY* 253: 280–299.
- Caljon, A.G. & Cocquyt, C.Z., 1992. Diatoms from surface sediments of the northern part of Lake Tanganyika. *HYDROBIOLOGIA* 230: 135–156.
- Carto, S.L., Weaver, A.J., Hetherington, R., Lam, Y. & Wiebe, E.C., 2009. Out of Africa and into an ice age: on the role of global climate change in the late Pleistocene migration of early modern humans out of Africa. *JOURNAL OF HUMAN EVOLUTION* 56: 139–151.
- Chagué-Goff, C., 2010. Chemical signatures of palaeotsunamis: a forgotten proxy? *MARINE GEOLOGY* 271: 67–71.
- Chagué-Goff, C., Andrew, A., Szczuciński, W., Goff, J. & Nishimura, Y., 2012. Geochemical signatures up to the maximum inundation of the 2011 Tohoku-oki tsunami – Implications for the 869 AD Jogan and other palaeotsunamis. *SEDIMENTARY GEOLOGY* 282: 65–77.
- Chapligin, B., Leng, M.J., Webb, E., Alexandre, A., Dodd, J.P., Ijiri, A., Lücke, A., Shemesh, A., Abelmann, A., Herzschuh, U., Longstaffe, F.J., Meyer, H., Moschen, R., Okazaki, Y., Rees, N.H., Sharp, Z.D., Sloane, H.J., Sonzongi, C., Swann, G.E.A., Sylvestre, F., Tyler, J.J. & Yam, R., 2011. Inter-laboratory comparison of oxygen isotope compositions from biogenic silica. *GEOCHIMICA ET COSMOCHIMICA ACTA* 75: 7242–7256.
- Charlesworth, B., 2009. Effective population size and patterns of molecular evolution and variation. *NATURE REVIEWS GENETICS* 10: 195–205.
- Chase, B.M. & Meadows, M.E., 2007. Late Quaternary dynamics of southern Africa's winter rainfall zone. *EARTH-SCIENCE REVIEWS* 84: 103–138.
- Chase, B.M. & Brewer, S., 2009. Last Glacial Maximum dune activity in the Kalahari Desert of southern Africa: observations and simulations. *QUATERNARY SCIENCE REVIEWS* 28: 301–307.

- Chase, B.M., Scott, L., Meadows, M.E., Gil-Romera, G., Boom, A., Carr, A.S., Reimer, P.J., Truc, L., Valsecchi, V. & Quick, L.J., 2012. Rock hyrax middens: A palaeoenvironmental archive for southern African drylands. *QUATERNARY SCIENCE REVIEWS* 56: 107–125.
- Chiba, T., Siguhara, S., Matsushima, Y., Arai, Y. & Endo, K., 2016. Reconstruction of Holocene relative sea-level change and residual uplift in the Lake Inba area, Japan. *PALAEOGEOGRAPHY PALAEOCLIMATOLOGY PALAEOECOLOGY* 441: 982–996.
- Cholnoky, B.J., 1968. Die Ökologie der Diatomeen in Binnengewässern. J. Cramer, Lehre. (*in German*)
- Cohen, A.S., Stone, J.R., Beuning, K.R.M., Park, L.E., Reinthal, P.N., Dettman, D., Scholz, C.A., Johnson, T.C., King, J.W., Talbot, M.R., Brown, E.T. & Ivory, S.J., 2007. Ecological consequences of early Late Pleistocene megadroughts in tropical Africa. *PNAS* 104 (42): 16422–16427.
- Cook, G.T. & van der Plicht, J., 2007. Radiocarbon Dating. *ENCYCLOPEDIA OF QUATERNARY SCIENCE* 4: 2899–2911.
- Cooke, H.J., 1979. The Origin of the Makgadikgadi Pans. *BOTSWANA NOTES AND RECORDS* 11: 37–42.
- Cooke, H.J., 1980. Landform Evolution in the Context of Climatic Change and Neo-Tectonism in the Middle Kalahari of North-Central Botswana. *TRANSACTIONS OF THE INSTITUTE OF BRITISH GEOGRAPHERS* 5: 80–99.
- Cooke, H.J. & Verstappen, H.T., 1984. The landforms, and the western Makgadikgadi basin in northern Botswana, with a consideration of the chronology of the evolution of Lake Palaeo-Makgadikgadi. *ZEITSCHRIFT FÜR GEOMORPHOLOGIE* 28: 1–19.
- Cordier, S., Harmand, D., Lauer, T., Voinchet, P., Bahain, J.-J. & Frechen, M., 2012. Geochronological reconstruction of the Pleistocene evolution of the Sarre valley (France and Germany) using OSL and ESR dating techniques. *GEOMORPHOLOGY* 165–166: 91–106.
- Craig, H., 1961. Isotopic Variations in Meteoric Waters. *SCIENCE, NEW SERIES* 133: 1702–1703.
- Crawford, G.W., 1983. Paleoethnobotany of the Kameda Peninsula Jomon (Anthropological Papers, 73), Museum of Anthropology, University of Michigan, Ann Arbor, Michigan.
- Crawford, G.W., 1992. Prehistoric plant domestication in East Asia. In: Cowan, C.W. & Watson, P.J. (Eds.). *The Origins of Agriculture: An International Perspective*. Washington, D.C.: Smithsonian Institution Press, pp. 7–38.
- Crawford, G.W., 2011. Advances in understanding early agriculture in Japan. *CURRENT ANTHROPOLOGY* 52 (S4): S331–S345.
- Crawford, G.W. & Lee, G.A., 2003. Agricultural origins in the Korean peninsula. *ANTIQUITY* 77: 87–95.
- Crawford, G.W., Zhao, Z., Luan, F., 2005. Preliminary analysis of preserved plant remains unearthed from the Longshan culture site of Liangchengzhen. *KAOGU* 9: 73–80 (*in Chinese*).

7. References

- Cwynar, L.E., Burden, E. & McAndrews, J.H., 1979. An inexpensive sieving method for concentrating pollen and spores from fine grained sediments. *CANADIAN JOURNAL OF EARTH SCIENCES* 16: 1115–1120.
- Dai, F., Nevo, E., Wu, D., Comadran, J., Zhou, M., Qiu, L., Chen, Z., Beiles, A., Chen, G. & Zhang, G., 2012. Tibet is one of the centers of domestication of cultivated barley. *PROCEEDINGS OF THE NATIONAL ACADEMY OF SCIENCES OF THE UNITED STATES OF AMERICA* 109 (42): 16969–16973.
- D’Andrea, A.C., Crawford, G.W., Yoshizaki, M. & Kudo, T., 1995. Late Jomon cultigens in northeastern Japan. *ANTIQUITY* 69: 146–152.
- de Vries, J.J., Selaolo, E.T. & Beekman, H.E., 2000. Groundwater recharge in the Kalahari, with reference to paleo-hydrologic conditions. *JOURNAL OF HYDROLOGY* 238: 110–123.
- de Vries, J.L. & Vrebos, B.A.R., 2002. Quantification of infinitely thick specimens by XRF analysis. In: Van Grieken, R.E. & Markowicz, A.A. (Eds.), *Handbook of X-ray Spectrometry*, Second Edition. Marcel Dekker Inc., New York, Basel, pp. 341–406.
- Demske, D., Tarasov, P.E., Nakagawa, T. & Suigetsu 2006 Project Members, 2013. Atlas of pollen, spores and further nonpollen palynomorphs recorded in the glacial-interglacial late Quaternary sediments of Lake Suigetsu, central Japan. *QUATERNARY INTERNATIONAL* 290–291: 164–238.
- Denys, L., 1990. *Fragilaria* Blooms in the Holocene of the Western Coastal Plain of Belgia. In: Simola, H. (Ed.), *Proceedings of the Tenth International Diatom-Symposium – Joensuu, Finland 1988*. Koeltz-Scientific Books, Koenigstein, pp. 397–406.
- Deryugin, V.A., 2008. The metal ages and medieval period. *ARCHAEOLOGY, ETHNOLOGY, AND ANTHROPOLOGY OF EURASIA* 33: 58–66.
- Dolukhanov, P.M., Shukurov, A.M., Tarasov, P.E. & Zaitseva, G.I., 2002. Colonization of Northern Eurasia by Modern Humans: Radiocarbon Chronology and Environment. *JOURNAL OF ARCHAEOLOGICAL SCIENCE* 29: 593–606.
- Du Toit, A.L., 1933. Crustal movement as a factor in the geographical evolution of South Africa. *SOUTH AFRICAN GEOGRAPHICAL JOURNAL* 16: 3–20.
- Du Toit, A.L., 1937. *Our wandering continents - A hypothesis of continental drifting*, Oliver & Boyd: London.
- Ebert, J.I. & Hitchcock, R.K., 1978. Ancient Lake Makgadikgadi, Botswana: Mapping, Measurement and Palaeoclimate Significance. *PALAEOECOLOGY OF AFRICA* 10(11): 47–56.
- Eckardt, F.D., Bryant, R.G., McCulloch, G., Spiro, B. & Wood, W.W., 2008. The hydrochemistry of a semi-arid pan basin case study: Sua Pan, Makgadikgadi, Botswana. *APPLIED GEOCHEMISTRY* 23: 1563–1580.
- Einsele, G., 1992. *Sedimentary Basins – Evolution, Facies and Sediment Budget*. Springer Verlag, Berlin, Heidelberg.

- ESRI, 2014. ArcGIS Desktop: Release 10.2. Environmental Systems Research Institute, Redlands.
- Fægri, K., Kaland, P.E. & Krzywinski, K., 1989. Textbook of Pollen Analysis. 4th edition, John Wiley & Sons, Chichester.
- Fairhead, J.D. & Girdler, R.W., 1969. How far does the rift system extend through Africa? *NATURE* 221: 1018–1020.
- Filippov, A. & Riedel, F., 2009. The late Holocene mollusc fauna of the Aral Sea and its biogeographical and ecological interpretation. *LIMNOLOGICA* 39: 67–85.
- Fornace, K.L., Hughen, K.A., Shanahan, T.M., Fritz, S.C., Baker, P.A. & Sylvania, S.P., 2014. A 60,000-year record of hydrologic variability in the Central Andes from the hydrogen isotopic composition of leaf waxes in Lake Titicaca sediments. *EARTH PLANETARY SCIENCE LETTERS* 408: 263–271.
- Fredskild, B., 1983. The Holocene development of some low and high arctic Greenland lakes. *HYDROBIOLOGIA* 103: 217–224.
- Fuentes, A., 2009. Evolution of Human Behaviour. Oxford, Oxford University Press.
- Gabriel, K.R., 2002. Goodness of fit of biplots and correspondence analysis. *BIOMETRIKA* 89: 423–436.
- Ganopolski, A. & Rahmstorf, S., 2001. Rapid changes of glacial climate simulated in a coupled climate model. *NATURE* 409: 153–158.
- Gasse, F., 1986. East African Diatoms – Taxonomy, Ecological Distribution. Bibliotheca Diatomologica Series, Volume 11. J. Cramer, Berlin, Stuttgart.
- Gasse, F., Jugging, S. & Khelifa, L.B., 1995. Diatom-based transfer functions for inferring past hydrochemical characteristics of African lakes. *PALAEOGEOGRAPHY PALAEOCLIMATOLOGY PALAEOECOLOGY* 177: 31–54.
- Gasse, F., Fontes, J.C., Plaziat, J.C., Carbonel, P., Kaczmarska, I., De Dekker, P., Soulié-Marsche, I., Callot, Y. & Dupeuble, P.A., 1987. Biological remains, geochemistry and stable isotopes for the reconstruction of environmental and hydrological changes in the Holocene lakes from North Sahara. *PALAEOGEOGRAPHY PALAEOCLIMATOLOGY PALAEOECOLOGY* 60: 1–46.
- Gasse, F., Chalié, F., Vincens, A., Williams, M.A.J. & Williamson, D., 2008. Climatic patterns in equatorial and southern Africa from 30,000 to 10,000 years ago reconstructed from terrestrial and near-shore proxy data. *QUATERNARY SCIENCE REVIEWS* 27: 2316–2340.
- Genner, M.J., Seehausen, O., Lunt, D.H., Joyce, D.A., Shaw, P.W., Carvalho, G.R. & Turner, G.F., 2007. Age of cichlids: new dates for ancient fish radiations. *MOLECULAR BIOLOGY AND EVOLUTION* 24: 1269–1282.
- Geospatial Information Authority of Japan, 2012. Topographic map Funadomari 1:25,000.
- Geyh, M.A. & Heine, K., 2014. Several distinct wet periods since 420 ka in the Namib Desert inferred from U-series dates of speleothems. *QUATERNARY RESEARCH* 81(2): 381–391.

7. References

- Gibson, C.E. & Foy, R.H., 1988. The significance of growth rate and storage products for the ecology of *Melosira italica* ssp *subarctica* in Lough Neagh. In: Round, F.E. (Ed.), *Algae and the Aquatic Environment*. Biopress, Bristol, pp. 88–106.
- Gibson, C.E., Anderson, N.J. & Haworth, E., 2003. *Aulacoseira subarctica*: taxonomy, physiology, ecology and palaeoecology. *EUROPEAN JOURNAL OF PHYCOLOGY* 38: 83–101.
- Gill, D., Shomrony, A. & Fligelmann, H., 1993. Numerical zonation of log suites and logfacies recognition by multivariate clustering. *AMERICAN ASSOCIATION OF PETROLEUM GEOLOGISTS BULLETIN* 77: 1781–1791.
- Goff, J.R. & Chagué-Goff, C., 2001. Catastrophic events in New Zealand coastal environments. Conservation Advisory Science Notes No. 333, Department of Conservation, Wellington.
- Goff, J.R., Wells, A., Chagué-Goff, C., Nichol, S.L. & Devoy, R.J.N., 2004. The Elusive AD 1826 Tsunami, South Westland, New Zealand. *NEW ZEALAND GEOGRAPHER* 60 (2): 28–39.
- Göke, G., 1993. Einführung in die Präparation der Diatomeen. Naturwissenschaftliche Vereinigung Hagen e.V., Sonderheft SM 1. (in German)
- Gómez, N., Riera, J.L. & Sabater, S., 1995. Ecology and morphological variability of *Aulacoseira granulata* (Bacillariophyceae) in Spanish reservoirs. *JOURNAL OF PLANKTON RESEARCH* 17: 1–16.
- Goslar, T., van der Knaap W.O., Kamenik, C. & Van Leeuwen, J.F.N., 2009. Free-shape ¹⁴C age-depth modelling of an intensively dated modern peat profile. *JOURNAL OF QUATERNARY SCIENCE* 24: 481–499.
- Gotanda, K., Nakagawa, T., Tarasov, P.E., Kitagawa, J., Inoue, Y. & Yasuda, Y., 2002. Biome classification from Japanese pollen data: application to modern-day and Late Quaternary samples. *QUATERNARY SCIENCE REVIEWS* 21: 647–657.
- Gotanda, K., Nakagawa, T., Tarasov, P.E. & Yasuda, Y., 2008. Disturbed vegetation reconstruction using the biomization method from Japanese pollen data: Modern and Late Quaternary samples. *QUATERNARY INTERNATIONAL* 184: 56–74.
- Goto, Y. & McPhie, J., 1998. Endogenous growth of a Miocene submarine dacite cryptodome, Rebun Island, Hokkaido, Japan. *JOURNAL OF VOLCANOLOGY AND GEOTHERMAL RESEARCH* 84: 273–286.
- Grey, D.R.C. & Cooke, H.J., 1977. Some problems in the quaternary evolution of the landforms of northern Botswana. *CATENA* 4: 123–133.
- Grimm, E.C., 1987. CONISS: a FROTRAN 77 program for stratigraphically constrained cluster analysis by the method of incremental sum of squares. *COMPUTERS & GEOSCIENCES* 13: 13–55.
- Grimm, E.C., 1991–2011. Tilia[®] Version 1.7.16 (Computer Software) Illinois State Museum, Research and Collection Center, Springfield.

- Grove, A.T., 1969. Landforms and Climatic Change in the Kalahari and Ngamiland. *THE GEOGRAPHICAL JOURNAL* 135: 191–212.
- Guiry, M.D. & Guiry, G.M., 2017. AlgaeBase. World-wide Electronic Publication. National University of Ireland, Galway. URL <http://www.algaebase.org>.
- Gumbrecht, T., McCarthy, T.S. & Merry, C.L., 2001. The topography of the Okavango Delta, Botswana, and its tectonic and sedimentological implications. *SOUTH AFRICAN JOURNAL OF GEOLOGY* 104: 243–264.
- Habu, J., 2004. Ancient Jomon of Japan. Cambridge, Cambridge University Press.
- Haddon, I.G. & McCarthy, T.S., 2005. The Mesozoic–Cenozoic interior sag basins of Central Africa: The Late-Cretaceous–Cenozoic Kalahari and Okavango basins. *JOURNAL OF AFRICAN EARTH SCIENCES* 43: 316–333.
- Hall, R.I. & Smol, J.P., 2010. Diatoms as indicators of lake eutrophication. In: Smol, J.P. & Stoermer, E.F. (Eds.), *The Diatoms - Application for the Environmental and Earth Sciences*, 2nd Edition, Cambridge University Press, Cambridge, pp. 122–151.
- Hamano, Y., Maeda, Y., Matsumoto, Y. & Kumano, S., 1985. Holocene sedimentary history of some coastal plains in Hokkaido, Japan. III. Transition of diatom assemblages in Tokoro along the Okhotsk Sea. *JAPANESE JOURNAL OF ECOLOGY* 35: 307–316.
- Hanihara, K., 1991. Dual Structure Model for the Population History of the Japanese. *JAPAN REVIEW* 2: 1–33.
- Hanihara, T. & Ishida, H., 2009. Regional differences in craniofacial diversity and the population history of Jomon Japan. *AMERICAN JOURNAL OF PHYSICAL ANTHROPOLOGY* 139 (3): 311–322.
- Hanihara, T., Yoshida, K. & Ishida, H., 2008. Craniometric variation of the Ainu: an assessment of differential gene flow from northeast Asia into northern Japan, Hokkaido. *AMERICAN JOURNAL OF PHYSICAL ANTHROPOLOGY* 137 (3): 283–293.
- Harlan, J. & Zohary, D., 1966. Distribution of wild wheat and barley. *SCIENCE* 153: 1074–1080.
- Harper, M.A., 1976. Migration rhythm of the benthic diatom *Pinnularia viridis* on pond silt (note). *NEW ZEALAND JOURNAL OF MARINE AND FRESHWATER RESEARCH* 10 (2): 381–384.
- Haruki, M., Fujiwara, A., Matsuda, K., Natsume, S., Yajima, T., Namikawa, K. & Niiyama, K., 2004. Forest vegetation in Rishiri and Rebun Islands in Hokkaido, Japan. *RISHIRI STUDIES* 23: 57–91 (in Japanese).
- Hase, Y., Iwauchi, A., Uchikoshiyama, U., Noguchi, E. & Sasaki, N., 2012. Vegetation changes after the late period of the Last Glacial Age based on pollen analysis of the northern area of Aso Caldera in central Kyushu, Southwest Japan. *QUATERNARY INTERNATIONAL* 254: 107–117.
- Hashimoto, M., 1991. *Geology of Japan*. Terra Scientific Publishing Company, Kluwer Academic Publishers, Tokyo, Dordrecht, Boston, London.
- Hecky, R.E. & Kilham, P., 1973. Diatoms in alkaline, saline lakes: ecology and geochemical implications. *LIMNOLOGY AND OCEANOGRAPHY* 18: 53–71.

7. References

- Heine, K., 1981. Aride und pluviale Bedingungen während der letzten Kaltzeit in der Südwest-Kalahari (südliches Afrika): Ein Beitrag zur klimagenetischen Geomorphologie der Dünen, Pfannen und Täler. *ZEITSCHRIFT FÜR GEOMORPHOLOGIE (SUPPLEMENT)* 38: 1–37 (in German).
- Heine, K., 1982. The Main Stages of the Late Quaternary Evolution of the Kalahari Region, Southern Africa. *PALAEOECOLOGY OF AFRICA AND SURROUNDING ISLANDS* 15: 53–76.
- Heine, K., 1987. Zum Alter jungquartärer Seespiegelschwankungen in der Mittleren Kalahari, südliches Afrika. *PALAEOECOLOGY OF AFRICA AND SURROUNDING ISLANDS* 18: 73–101 (in German).
- Heine, K., 1988. Southern African Palaeoclimates 35–25 ka ago: A preliminary summary. *PALAEOECOLOGY OF AFRICA AND SURROUNDING ISLANDS* 19: 305–315.
- Henn, B.M., Gignoux, C.R., Jobin, M., Granka, J.M., Macpherson, J.M., Kidd, J.M., Rodríguez-Botigué, L., Ramachandran, S., Hon, L., Brisbin, A., Lin, A.A., Underhill, P.A., Comas, D., Kidd, K.K., Norman, P.J., Parham, P., Bustamante, C.D., Mountain, J.L. & Feldman, M.W., 2011. Hunter-gatherer genomic diversity suggests a southern African origin for modern humans. *PNAS* 108 (13): 5154–5162.
- Henshilwood, C.S., d’Errico, F., Yates, R., Jacobs, Z., Tribolo, C., Duller, G.A.T., Mercier, N., Sealy, J.C., Valladas, H., Watts, I. & Wintle, A.G., 2002. Emergence of Modern Human Behavior: Middle Stone Age Engravings from South Africa. *SCIENCE* 295: 1278–1280.
- Hijma, M.P. & Cohen, K.M., 2010. Timing and magnitude of the sea-level jump precluding the 8200 yr event. *GEOLOGY* 38 (3): 275–278.
- Hijmans, R.J., Cameron, S.E., Parra, J.L., Jones, P.G. & Jarvis, A., 2005. Very high resolution interpolated climate surface for global land areas. *INTERNATIONAL JOURNAL OF CLIMATOLOGY* 25 (15): 1965–1978.
- Hoelzmann, P., Schwalb, A., Roberts, N., Cooper, P. & Burgess, A., 2010. Hydrological response of an east-Saharan palaeolake (NW Sudan) to early-Holocene climate. *THE HOLOCENE* 20: 537–549.
- Hoelzmann, P., Klein, T., Kutz, F. & Schütt, B., 2017. A new device to mount portable energy-dispersive X-ray fluorescence spectrometers (p-ED-XRF) for semi-continuous analyses of split (sediment) cores and solid samples. *GEOSCIENTIFIC INSTRUMENTATION, METHODS AND DATA SYSTEMS* 6: 93–101.
- Holmgren, K., Karlén, W., Lauritzen, S.E., Lee-Thorp, J.A., Partridge, T.C., Piketh, S., Repinski, P., Stevenson, C., Svanered, O. & Tyson, P.D., 1999. A 3000-year high-resolution stalagmite-based record of palaeoclimate for northeastern South Africa. *THE HOLOCENE* 9: 295–309.
- Holmgren, K., Lee-Thorp, J.A., Cooper, G.R.J., Lundblad, K., Partridge, T.C., Scott, L., Sithaldeen, R., Talma, A.S. & Tyson, P.D., 2003. Persistent millennial-scale climatic variability over the past 25,000 years in Southern Africa. *QUATERNARY SCIENCE REVIEWS* 22: 2311–2326.

- Houk, V., Klee, R. & Tanaka, H., 2010. Atlas of freshwater diatoms with a Brief Key and Descriptions, Part III: Stephanodiscaceae A, *Cyclotella*, *Tertiarius*, *Discostella*. In: Pouličková, A. (Ed.), Fottea 10 (Supplement). Czech Phycological Society, Prague.
- Hudson, M.J., 1999. Ruins of Identity: Ethnogenesis in the Japanese Islands. University of Hawaii Press, Honolulu.
- Hudson, M.J., 2013. 28 Japan: Archaeology. In: Ness, I. (Ed.). The Encyclopedia of Global Human Migration. Blackwell Publishing Ltd, New York, pp. 224–229.
- Hürkamp, K., Raab, T. & Völkel, J., 2009. Two and three-dimensional quantification of lead contamination in alluvial soils of a historic mining area using field portable X-ray fluorescence (FPXRF) analysis. *Geomorphology* 110: 28–36.
- Hürkamp, K., Völkel, J., Heine, K., Bens, O., Leopold, M. & Winkelbauer, J., 2011. Late Quaternary environmental changes from aeolian and fluvial geoarchives in the southwestern Kalahari, South Africa: Implications for past African climate dynamics. *SOUTH AFRICAN JOURNAL OF GEOLOGY* 114: 459–474.
- IAEA, 2015. Global Network of Isotopes in Precipitation. The GNIP database. URL <http://www-naweb.iaea.org/napc/ih/index.html>.
- Igarashi, Y., 2008. Late Holocene vegetation history in Tanetomi wetland, Rishiri Island, Hokkaido. *RISHIRI STUDIES* 27: 1–7 (in Japanese).
- Igarashi, Y., 2013. Holocene vegetation and climate on Hokkaido Island, northern Japan. *QUATERNARY INTERNATIONAL* 290–291: 139–150.
- Igarashi, Y., 2016. Vegetation and climate during the LGM and the last deglaciation on Hokkaido and Sakhalin Islands in the northwest Pacific. *QUATERNARY INTERNATIONAL* 425: 28–37.
- Igarashi, Y. & Zharov, A.E., 2011. Climate and vegetation change during the late Pleistocene and early Holocene in Sakhalin and Hokkaido, northeast Asia. *QUATERNARY INTERNATIONAL* 237: 24–31.
- Igarashi, Y., Yamamoto, M. & Ikehara, K., 2011. Climate and vegetation in Hokkaido, northern Japan, since the LGM: Pollen records from core GH02-1030 off Tokashi in the northwestern Pacific. *JOURNAL OF ASIAN EARTH SCIENCES* 40 (6): 1102–1110.
- Igarashi, Y., Murayama, M., Igarashi, T., Higake, T. & Fukuda, M., 2002. History of *Larix* forest in Hokkaido and Sakhalin, northeast Asia since the last glacial. *ACTA PALAEONTOLOGICA SINICA* 41 (4): 524–533.
- Ihira, M., Maeda, Y., Matsumoto, E. & Kumano, S., 1985. Holocene sedimentary history of some coastal plains in Hokkaido, Japan. II. Diatom assemblages of the sediments from Kushiro Moor. *JAPANESE JOURNAL OF ECOLOGY* 35: 199–205.
- Ikeda, M., Fukusawa, H. & Okamura, M., 1998. Global climatic and sea-level fluctuations recorded from varved sediments – The paleoenvironmental changes during the past 2300 years

7. References

- in Lake Ogawara and Lake Jyusan, Aomori Prefecture, northeast Japan. *METEOROLOGICAL RESEARCH NOTES* 191: 35–58 (*in Japanese*).
- Imamura, K., 1996. Prehistoric Japan: New Perspectives on Insular East Asia. University of Hawaii Press, Honolulu.
- Ingman, M., Kaessmann, H., Pääbo, S. & Gyllensten, U., 2000. Mitochondrial genome variation and the origin of modern humans. *NATURE* 408: 708–713.
- Interlandi, S.J., Kilham, S.S. & Theriot, E.C., 1999. Responses of phytoplankton to varied resource availability in large lakes of the Greater Yellowstone Ecosystem. *LIMNOLOGY & OCEANOGRAPHY* 44: 668–682.
- Inui, T., 2000. Report on the Excavation at the Site of Funadomari. Rebun Cho Kyoiku Inikai, Rebun, pp. 5–10 (*in Japanese*).
- Itoh, S., 1987. Vegetation of Hokkaido. Hokkaido University Press, Sapporo. (*in Japanese*).
- Izuho, M. & Sato, H., 2007. Archaeological obsidian studies in Hokkaido, Japan: retrospect and prospect. *BULLETIN OF THE INDO-PACIFIC PREHISTORY ASSOCIATION* 27: 114–121.
- Izuho, M., Hayashi, K., Nakazawa, Y., Soda, T., Oda, N., Yamahara, T., Kitazawa, M. & Buvit, I., 2014. Investigating the eolian context of the Last Glacial Maximum occupation at Kawanishi-C, Hokkaido, Japan. *GEOARCHAEOLOGY* 29 (3): 202–220.
- Jacobs, Z. & Roberts, R.G., 2009. Catalysts for Stone Age innovations. *COMMUNICATIVE & INTEGRATIVE BIOLOGY* 2(2): 191–193.
- Jarvis, A., Reuter, H.I., Nelson, A. & Guevara, E., 2008. Hole-filled SRTM for the globe Version 4. URL <http://srtm.csi.cgiar.org>; CGIAR-CSI SRTM 90m Database.
- Jenkins, R., 1999. X-ray Fluorescence Spectrometry, Second Ed. Wiley & Sons, New York.
- Jolliffe, I.T., 1986. Principal Component Analysis. Springer, New York.
- Jouzel, J., Masson-Delmotte, V., Cattani, O., Dreyfus, G., Falourd, S., Hoffmann, G., Minster, B., Nouet, J., Barnola, J.M., Chappellaz, J., Fischer, H., Gallet, J.C., Johnsen, S., Leuenberger, M., Loulergue, L., Luethi, D., Oerter, H., Parrenin, F., Raisbeck, G., Raynaud, D., Schilt, A., Schwander, J., Selmo, E., Souchez, R., Spahni, R., Stauffer, B., Steffensen, J.P., Stenni, B., Stocker, T.F., Tison, J.L., Werner, M. & Wolff, E.W., 2007. Orbital and Millennial Antarctic Climate Variability over the Past 800,000 Years. *SCIENCE* 317: 793–796.
- Joyce, D.A., Lunt, D.H., Bills, R., Turner, G.F., Katongo, C., Duftner, N., Sturmbauer, C. & Seehausen, O., 2005. An extant cichlid fish radiation emerged in an extinct Pleistocene lake. *NATURE* 435: 90–95.
- Juggins, S., 2015. Rioja: analysis of Quaternary science data, R package version (0.9-5). URL <https://cran.r-project.org>.
- Jull, A.J.T., 2007. Radiocarbon Dating - AMS Method. *ENCYCLOPEDIA OF QUATERNARY SCIENCE* 4: 2911–2918.

- Jung, S.W., Know, O.Y., Lee, J.H. & Han, M.-S., 2009. Effects of Water Temperature and Silicate on the Winter Blooming Diatom *Stephanodiscus hantzschii* (Bacillariophyceae) Growing in Eutrophic Conditions in the Lower Han River. *SOUTH KOREAN JOURNAL OF FRESHWATER ECOLOGY* 24: 219–226.
- Kageyama, M., Peyron, O., Pinot, S., Tarasov, P.E., Guiot, J., Joussaume, S. & Ramstein, G., 2001. The Last Glacial Maximum climate over Europe and western Siberia: a PMIP comparison between models and data. *CLIMATE DYNAMICS* 17 (1): 23–43.
- Kalbe, L., 1980. Kieselalgen in Binnengewässern. Die neue Brehm-Bücherei, Wittenberg Lutherstadt. (in German).
- Kelly, M.G., Bennion, H., Cox, E.J., Goldsmith, B., Jamieson, J., Juggins, S., Mann, D.G. & Telford, R.J., 2005. Common freshwater diatoms of Britain and Ireland: An interactive identification key. Environment Agency, Bristol. URL <http://craticula.ncl.ac.uk/EADiatomKey/html/taxa.html>.
- Kelly, R.L., 1995. The Foraging Spectrum: Diversity in Hunter-Gatherer Lifeways. Smithsonian Institution Press, Washington, D.C.
- Kigoshi, T., Kumon, F., Hayashi, R., Kuriyama, M., Yamada, K. & Takemura, K., 2014. Climate changes for the past 52 ka clarified by total organic carbon concentrations and pollen composition in Lake Biwa, Japan. *QUATERNARY INTERNATIONAL* 333: 2–12.
- Kilham, S.S., Theriot, E.C. & Fritz, S.C., 1996. Linking planktonic diatoms and climate change in the large lakes of the Yellowstone ecosystem using resource theory. *LIMNOLOGY & OCEANOGRAPHY* 41: 1052–1062.
- Kimura, G., 1997. Cretaceous episodic growth of the Japanese Islands. *THE ISLAND ARC* 6: 52–68.
- Kinabo, B.D., Atekwana, E.A., Hogan, J.P., Modisi, M.P., Wheaton, D.D. & Kampunzu, A.B., 2007. Early structural development of the Okavango rift zone, NW Botswana. *JOURNAL OF AFRICAN EARTH SCIENCE* 48: 125–136.
- Kinabo, B.D., Hogan, J.P., Atekwana, E.A., Abdelsalam, M.G. & Modisi, M.P., 2008. Fault growth and propagation during incipient continental rifting: insights from a combined aeromagnetic and Shuttle Radar Topographic Mission digital elevation model investigation of the Okavango Rift Zone, northwest Botswana. *TECTONICS* 27: 1–16.
- Kleinen, T., Tarasov, P.E., Brovkin, V., Andreev, A. & Stebich, M., 2011. Comparison of modeled and reconstructed changes in forest cover through the past 8000 years: Eurasian perspective. *THE HOLOCENE* 5: 723–734.
- Kobayashi, T., Hudson, M. & Yamagata, M., 1992. Regional organization in the Jomon period. *ARCTIC ANTHROPOLOGY* 29 (1): 82–95.
- Kobayasi, H., Idei, M., Nagumo, T., Mayama, S. & Osada, K., 2006. H. Kobayasi's Atlas of Japanese Diatoms Based on Electron Microscopy, Vol. 1. Uchida Rokakuho Publishing Co., Ltd., Tokyo. (in Japanese).

7. References

- Koizumi, I., 2008. Diatom-derived SSTs (Td' ratio) indicate warm seas off Japan during the middle Holocene (8.2–3.3 kyr BP). *MARINE MICROPALAEONTOLOGY* 69: 263–281.
- Koizumi, I. & Yamamoto, H., 2011. Oceanographic variations over the last 150,000 yr in the Japan Sea and synchronous Holocene with the Northern Hemisphere. *JOURNAL OF ASIAN EARTH SCIENCES* 40: 1203–1213.
- Komárek, J. & Jankovská, V., 2001. Review of the Green Algae Genus *Pediastrum*; Implication for Pollen-analytical Research. Bibliotheca Phycologica Vol. 108, J. Cramer, Berlin, Stuttgart.
- Kossler, A., Tarasov, P.E., Schlolaut, G., Nakagawa, T., Marshall, M., Brauer, A., Staff, R., Bronk Ramsey, C., Bryant, C., Lamb, H., Demske, D., Gotanda, K., Haraguchi, T., Yokoyama, Y., Yonenobu, H., Tada, R. & Suigetsu 2006 Project Members, 2011. Onset and termination of the late-glacial climate reversal in the high-resolution diatom and sedimentary records from the annually laminated SG06 core from Lake Suigetsu, Japan. *PALAEOGEOGRAPHY PALAEOCLIMATOLOGY PALAEOECOLOGY* 306: 103–115.
- Kostrova, S.S., Meyer, H., Tarasov, P.E., Bezrukova, E.V., Chaplignin, B., Kossler, A., Pavlova, L. & Kuzmin, M.I., 2016. Oxygen isotope composition of diatoms from sediments of Lake Kotokel (Buryatia). *RUSSIAN GEOLOGY AND GEOPHYSICS* 57: 1239–1247.
- Krammer, K., 2002. Cymbella. In: Lange-Bertalot, H. (Ed.), Diatoms of Europe, Vol. 3. ARG Gantner Verlag KG, Ruggell.
- Krammer, K. & Lange-Bertalot, H., 1997. Bacillariophyceae. 1. Teil: Naviculaceae. In: Ettl, H., Gerloff, J., Heynig, H. & Mollenhauer, D. (Eds.), Süßwasserflora von Mitteleuropa 2/1. Spektrum Akademischer Verlag, Heidelberg. (*in German*).
- Krammer, K. & Lange-Bertalot, H., 1999. Bacillariophyceae. 2. Teil: Bacillariaceae, Epithemiaceae, Surirellaceae. In: Ettl, H., Gerloff, J., Heynig, H. & Mollenhauer, D. (Eds.), Süßwasserflora von Mitteleuropa 2/2. Spektrum Akademischer Verlag, Heidelberg. (*in German*).
- Krammer, K. & Lange-Bertalot, H., 2000. Bacillariophyceae. 3. Teil: Centrales, Fragilariaceae, Eunotiaceae. In: Ettl, H., Gerloff, J., Heynig, H. & Mollenhauer, D. (Eds.), Süßwasserflora von Mitteleuropa 2/3. Spektrum Akademischer Verlag, Heidelberg. (*in German*).
- Krammer, K. & Lange-Bertalot, H., 2004. Bacillariophyceae. 4. Teil: Achnanthes s. l., Navicula s. str., Gomphonema. In: Ettl, H., Gärtner, G., Heynig, H., Mollenhauer, D. (Eds.), Süßwasserflora von Mitteleuropa 2/4. Spektrum Akademischer Verlag, Heidelberg. (*in German*).
- Kulongoski, J.T., Hilton, D.R. & Selaolo, E.T., 2004. Climate variability in the Botswana Kalahari from the late Pleistocene to the present day. *GEOPHYSICAL RESEARCH LETTERS* 31: L10204, doi: [10.1029/2003GL019238](https://doi.org/10.1029/2003GL019238)

- Kumano, S., Sekiya, K. & Maeda, Y., 1984. Holocene sedimentary history of some coastal plains in Hokkaido, Japan I. Diatom assemblages of the sediments from Kutcharo Lake. *JAPANESE JOURNAL OF ECOLOGY* 34: 389–396.
- Kumano, S., Ihira, M., Kuromi, M., Maeda, Y., Matsumoto, E., Nakamura, T., Matsushima, Y., Sato, H. & Matsuda, I., 1990a. Holocene sedimentary history of some coastal Plains in Hokkaido, Japan V. Sedimentary History of Kushu Lake and Akkeshi. *ECOLOGICAL RESEARCH* 5: 277–289.
- Kumano, S., Ihira, M., Maeda, A., Yamauchi, M., Matsumoto, E. & Matsuda, I., 1990b. Holocene sedimentary history of some coastal plains in Hokkaido, Japan IV. Diatom Assemblages in the Sediments from Kushiro Moor (2). *ECOLOGICAL RESEARCH* 5: 221–235.
- Kuritani, T. & Nakamura, E., 2006. Elemental fractionation in lavas during post-eruptive degassing: Evidence from trachytic lavas, Rishiri Volcano, Japan. *JOURNAL OF VOLCANOLOGY AND GEOTHERMAL RESEARCH* 149: 124–138.
- Kusber, W.-H. & Cocquyt, C.Z., 2012. *Craticula elkab* (O. Müller ex O. Müller) Lange-Bertalot, Kusber & Cocquyt, comb. nov. – Typification and observations based on African sediment core material. *DIATOM RESEARCH* 22: 117–126.
- Kuzmin, Y.V., Glascock, M.D. & Sato, H., 2002. Sources of archaeological obsidian on Sakhalin Island (Russian Far East). *JOURNAL OF ARCHAEOLOGICAL SCIENCE* 29 (7): 741–749.
- Kuzmin, Y.V., Glascock, M.D. & Izuho, M., 2013. The geochemistry of the major sources of archaeological obsidian on Hokkaido Island (Japan): Shirataki and Oketo. *ARCHAOMETRY* 55(3): 355–369.
- Lancaster, I.N., 1978. The pans of the Southern Kalahari, Botswana. *THE GEOGRAPHICAL JOURNAL* 144 (1): 81–98.
- Lee, J.H., 2011. Algal Flora of Korea, Vol. 3, No. 5. Marine Diatoms I: Chrysophyta: Bacillariophyceae: Centrales: Biddulphiineae: Chaetoceraceae. National Institute of Biological Resources, Korea.
- Lee, J.H., 2012. Algal Flora of Korea, Vol. 3, No. 6. Marine Diatoms II: Chrysophyta: Bacillariophyceae: Centrales: Thalassiosiraceae: Rhizosoleniaceae. National Institute of Biological Resources, Korea.
- Lee, R.B. & Daly, R., 1999. *The Cambridge Encyclopedia of Hunters and Gatherers*. Cambridge University Press, Cambridge.
- Lee-Thorp, J.A., Holmgren, K., Lauritzen, S.E., Linge, H., Moberg, A., Partridge, T.C., Stevenson, C. & Tyson, P.D., 2001. Rapid climate shifts in the southern African interior throughout the mid to Late Holocene. *GEOPHYSICAL RESEARCH LETTERS* 28: 4507–4510.
- Leipe, C., Kito, N., Sakaguchi, Y. & Tarasov, P.E., 2013. Vegetation and climate history of northern Japan inferred from the 5500-year pollen record from the Oshima Peninsula, SW Hokkaido. *QUATERNARY INTERNATIONAL* 290–291: 151–163.

7. References

- Leipe, C., Demske, D., Tarasov, P.E., Wünnemann, B., Riedel, F. & HIMPAC Project Members, 2014a. Potential of pollen and non-pollen palynomorph records from Tso Moriri (Trans-Himalaya, NW India) for reconstructing Holocene limnology and human–environmental interactions. *QUATERNARY INTERNATIONAL* 348: 113–129.
- Leipe, C., Demske, D., Tarasov, P.E. & HIMPAC Project Members, 2014b. A Holocene pollen record from the northwestern Himalayan lake Tso Moriri: Implications for palaeoclimatic and archaeological research. *QUATERNARY INTERNATIONAL* 348: 93–112.
- Leipe, C., Nakagawa, T., Gotanda, K., Müller S. & Tarasov, P.E., 2015. Late Quaternary vegetation and climate dynamics at the northern limit of the East Asian summer monsoon and its regional and global-scale controls. *QUATERNARY SCIENCE REVIEWS* 116: 57–71.
- Leng, M.J. & Marshall, J.D., 2004. Palaeoclimate interpretation of stable isotope data from lake sediment archives. *QUATERNARY SCIENCE REVIEWS* 23: 811–831.
- Leng, M.J. & Barker, P.A., 2006. A review of the oxygen isotope composition of lacustrine diatom silica for palaeoclimate reconstruction. *EARTH-SCIENCE REVIEWS* 75: 5–27.
- Leng, M.J. & Sloane, H.J., 2008. Combined oxygen and silicon isotope analysis of biogenic silica. *JOURNAL OF QUATERNARY SCIENCE* 23: 313–319.
- Leng, M.J. & Henderson, A.C.G., 2013. Recent advances in isotopes as palaeolimnological proxies. *JOURNAL OF PALEOLIMNOLOGY* 49: 481–496.
- Levkov, Z., 2009. *Amphora* sensu lato. In: Lange-Bertalot, H. (Ed.), *Diatoms of Europe*, Vol. 5. A.R.G. Gantner K.G., Ruggell.
- Li, J.Z., Absher, D.M., Tang, H., Southwick, A.M., Casto, A.M., Ramachandran, S., Cann, H.M., Barsh, G.S., Feldman, M., Cavalli-Sforza, L.L. & Myers, R.M., 2008. Worldwide human relationships inferred from genome-wide patterns of variation. *SCIENCE* 319: 1100–1104.
- Lister, L.A., 1979. The geomorphic evolution of Zimbabwe-Rhodesia. *TRANSACTIONS OF THE GEOLOGICAL SOCIETY OF SOUTH AFRICA* 82: 363–370.
- Litt, T., Schölzel, C., Köhl, N. & Brauer, A., 2009. Vegetation and climate history in the Westeifel Volcanic Field (Germany) during the last 11,000 years based on annually laminated lacustrine sediments. *BOREAS* 38: 679–690.
- Livingstone, D., 1857. *Missionary travels and researches in South Africa*. Salzwasser Verlag, Bremen, 2010 (*reprint of original*).
- Lotter, A.F. & Birks, H.J.B., 1993. The impact of the Laacher See tephra on terrestrial and aquatic ecosystems in the Black Forest, southern Germany. *JOURNAL OF QUATERNARY SCIENCE* 8: 263–276.
- Lynch, J., 1990. Provisional elemental values for eight new geochemical lake sediment and stream sediment reference materials LKSD-1, LKSD-2, LKSD-3, LKSD-4, STSD-1, STSD-2, STSD-3 and STSD-4. *GEOSTANDARDS NEWSLETTER* 14 (1): 153–167.

- Mackay, A.W., Davidson, T., Wolski, P., Woodward, S., Mazebedi, R., Masamba, W.R.L. & Todd, M., 2012. Diatom sensitivity to hydrological and nutrient variability in a subtropical, flood-pulse wetland. *ECOHYDROLOGY* 5: 491–502.
- Mallick, D.I.J., Habgood, F., Skinner, A.C., 1981. A geological interpretation of Landsat imagery and air photography of Botswana. *OVERSEAS GEOLOGY AND MINERAL RESOURCES* 56: 1–35.
- Mandal, A.K., Zhang, J. & Asai, K., 2011. Stable isotopic and geochemical data for inferring sources of recharge and groundwater flow on the volcanic island of Rishiri, Japan. *APPLIED GEOCHEMISTRY* 26: 1741–1751.
- Marean, C.W., Bar-Matthews, M., Bernatchez, J., Fisher, E., Goldberg, P., Herries, A.I., Jacobs, Z., Jerardino, A., Karkanas, P., Minichillo, T., Nilssen, P.J., Thompson, E., Watts, I. & Williams, H.M., 2007. Early human use of marine resources and pigment in South Africa during the Middle Pleistocene. *NATURE* 449: 905–908.
- Matsumura, H. & Oxenham, M., 2013. 27 Eastern Asia and Japan: Human biology. In: Ness, I. (Ed.), *The Encyclopedia of Global Human Migration*. Blackwell Publishing Ltd., New York, pp. 217–223.
- McCarthy, T.S., Green, R.W. & Franey, N.J., 1993. The influence of neo-tectonics on water dispersal in the northeastern regions of the Okavango swamps, Botswana. *JOURNAL OF AFRICAN EARTH SCIENCES* 17: 23–32.
- McHugh, M. & Rogers, J.C., 2001. North Atlantic Oscillation influence on precipitation variability around the Southeast African Convergence Zone. *JOURNAL OF CLIMATE* 14: 3631–3642.
- McQuoid, M.R. & Hobson, L.A., 1996. Diatom resting stages. *JOURNAL OF PHYCOLOGY* 32: 889–902.
- Medlin, L.K., Gersonde, R., Kooistra, W.H.C.F. & Wellbrock, U., 1996. Evolution of the diatoms (Bacillariophyta). II Nuclear-encoded small-subunit rRNA sequence comparisons confirm a paraphyletic origin for the centric diatoms. *MOLECULAR BIOLOGY AND EVOLUTION* 13: 67–75.
- METI and NASA (Ministry of Economy, Trade and Industry, Japan, and National Aeronautics and Space Administration), 2011. Advanced Spaceborne Thermal Emission and Reflection Radiometer: Global Digital Elevation Model Version 2. URL <http://www.jspacesystems.or.jp/ersdac/GDEM/E/4.html>
- Meyer, H., Schönicke, L., Wand, U., Hubberten, H.-W. & Friedrichsen, H., 2000. Isotope studies of hydrogen and oxygen in ground ice – experiences with the equilibration technique. *ISOTOPES IN ENVIRONMENTAL AND HEALTH STUDIES* 36: 133–149.
- Mischke, S. & Wünnemann, B., 2006. The Holocene salinity history of Bosten Lake (Xinjiang, China) inferred from ostracod species assemblages and shell chemistry: Possible palaeoclimatic implications. *QUATERNARY INTERNATIONAL* 154–155: 100–112.

7. References

- Mitrofanova, E.Y., Sutchenkova, O.S. & Lovtskaya, O.V., 2016. Lake Teletskoye (Altai, Russia): reconstruction of the environment and prediction for its changes according to the composition and quantity of diatoms in the bottom sediments. *RUSSIAN GEOLOGY AND GEOPHYSICS* 57: 1321–1333.
- Miyoshi N., Fujiki, T. & Kimura, H., 2011. Pollen flora of Japan. Hokkaido University Press, Sapporo.
- Moiseyev, V.G., 2008. On the origin of the Okhotsk population of Northern and Eastern Hokkaido: cranial evidence. *ARCHAEOLOGY, ETHNOLOGY, ANTHROPOLOGY OF EURASIA* 33: 134–141.
- Mokhova, L., Tarasov, P.E., Bazarova, V. & Klimin, M., 2009. Quantitative biome reconstruction using modern and late Quaternary pollen data from the southern part of the Russian Far East. *QUATERNARY SCIENCE REVIEWS* 28: 2913–2926.
- Montero-Serrano, J.C., Palarea-Albaladejo, J., Martín-Fernández, J.A., Martínez-Santana, M. & Gutiérrez-Martín, J.V., 2010. Sedimentary chemofacies characterization by means of multivariate analysis. *SEDIMENTARY GEOLOGY* 228: 218–228.
- Moore, A.E. & Cotterill, F.P.D., 2010. Victoria Falls: Mosi-oa-Tunya – The Smoke That Thunders. In Migoń, P. (Ed.), *Geomorphological Landscapes of the World*. Springer Science + Business Media B.V., Dordrecht, pp. 143–153.
- Moore, A.E., Cotterill, F.P.D. & Eckardt, F.D., 2012. The evolution and ages of Makgadikgadi palaeo-lakes: Consilient evidence from Kalahari drainage Evolution, South-central Africa. *SOUTH AFRICAN JOURNAL OF GEOLOGY* 115: 385–413.
- Morales, E.A., Guerrero, J.M., Wetzel, C.E., Sala, S., Ector, L., 2013. Unraveling the identity of *Fragilaria pinnata* Ehrenberg and *Staurosira pinnata* Ehrenberg: Research in Progress on a Convuluted Story. *CRYPTOGAMIE, ALGOLOGIE* 34: 89–102.
- Morley, D.W., Leng, M.J., Mackay, A.W., Sloane, H.J., Rioual, P. & Battarbee, R.W., 2004. Cleaning of lake sediment samples for diatom oxygen isotope analysis. *JOURNAL OF PALEOLIMNOLOGY* 31: 391–401.
- Müller, S., Tarasov, P.E., Hoelzmann, P., Bezrukova, E.V., Kossler, A. & Krivonogov, S.K., 2014. Stable vegetation and environmental conditions during the Last Glacial Maximum: New results from Lake Kotokel (Lake Baikal region, southern Siberia, Russia). *QUATERNARY INTERNATIONAL* 348: 14–24.
- Müller, S., Schmidt, M., Kossler, A., Leipe, C., Irino, T., Yamamoto, M., Yonenobu, H., Goslar, T., Kato, H., Wagner, M., Weber, A.W. & Tarasov, P.E., 2016. Palaeobotanical records from Rebun Island and their potential for improving the chronological control and understanding human–environment interactions in the Hokkaido Region, Japan. *THE HOLOCENE* 26 (10): 1646–1660.
- Murray, A.S. & Wintle, A.G., 2000. Luminescence dating of quartz using an improved single-aliquot regenerative-dose protocol. *RADIATION MEASUREMENTS* 32: 57–73.

- Nakagawa, T., 2007. Double-L channel: an Amazingly Non-destructive Method of Continuous Sub-sampling from Sediment Cores. *QUATERNARY INTERNATIONAL* 167–168 (Suppl.): 298.
- Nakagawa, T., Tarasov, P.E., Nishida, K., Gotanda, K. & Yasuda, Y., 2002. Quantitative pollen-based climate reconstruction in central Japan: application to surface and Late Quaternary spectra. *QUATERNARY SCIENCE REVIEWS* 21: 2099–2113.
- Nakagawa, T., Kitagawa, H., Yasuda, Y., Tarasov, P.E., Gotanda, K. & Sawai, Y., 2005. Pollen/event stratigraphy of the varved sediment of Lake Suigetsu, central Japan from 15,701 to 10,217 SG vyr BP (Suigetsu varve years before present): Description, interpretation, and correlation with other regions. *QUATERNARY SCIENCE REVIEWS* 24: 1691–1701.
- Nakagawa, T., Gotanda, K., Haraguchi, T., Danhara, T., Yonenobu, H., Brauer, A., Yokoyama, Y., Tada, R., Takemura, K., Staff, R.A., Payne, R., Bronk Ramsey, C., Bryant, C., Brock, F., Scholaut, G., Marshall, M., Tarasov, P.E., Lamb, H. & Suigetsu 2006 Project Members, 2012. SG06, a fully continuous and varved sediment core from Lake Suigetsu, Japan: stratigraphy and potential for improving the radiocarbon calibration model and understanding of late Quaternary climate changes. *QUATERNARY SCIENCE REVIEWS* 36: 164–176.
- Nakamura, J., 1980a. Diagnostic characters of pollen grains of Japan, Part II. In: Osaka Museum of Natural History (Ed.), Special Publications from the Osaka Museum of Natural History, Vol. 12. Osaka Museum of Natural History, Osaka, pp. 1–157. (*in Japanese*)
- Nakamura, J., 1980b. Diagnostic characters of pollen grains of Japan, Part I. In: Osaka Museum of Natural History (Ed.), Special Publications from the Osaka Museum of Natural History, Vol. 13. Osaka Museum of Natural History, Osaka, pp. 1–91. (*in Japanese*)
- Nanayama, F., Furukawa, R., Shigeno, K., Makino, A., Soeda, Y. & Igarashi, Y., 2007. Nine unusually large tsunami deposits from the past 4000 years at Kiritappu marsh along the southern Kuril Trench. *SEDIMENTARY GEOLOGY* 200: 275–294.
- Nash, D.J. & McLaren, S.J., 2003. Kalahari valley calcretes: their nature, origins, and environmental significance. *QUATERNARY INTERNATIONAL* 111: 3–22.
- Nash, D.J., Shaw, P.A., & Thomas, D.S.G., 1994. Duricrust development and valley evolution: process-landform links in the Kalahari. *EARTH SURFACE PROCESSES AND LANDFORMS* 19: 299–317.
- Nikolaeva, A.S. & Shcherbakova, V.I., 1990. Physical map. In: Nikolaeva, A.S. & Shcherbakova, V.I. (Eds.), Geograficheskii Atlas SSSR. GUGK, Moscow, pp. 10–11. (*in Russian*)
- Nishida, N. & Ikehara, K., 2013. Holocene evolution of depositional processes off southwest Japan: Response to the Tsushima Warm Current and sea-level rise. *SEDIMENTARY GEOLOGY* 290: 138–148.
- Nomura, T. & Udagawa, H., 2006a. Shin Hokkaido no Kodai 1: Kyusekki/Jomon Bunka. The Hokkaido Shimbun Press, Sapporo. (*in Japanese*)

7. References

- Nomura, T. & Udagawa, H., 2006b. Shin Hokkaido no Kodai 2: Zoku-Jomon/Okhotsk Bunka. The Hokkaido Shimbun Press, Sapporo. (*in Japanese*)
- Nomura, T. & Udagawa, H., 2006c. Shin Hokkaido no Kodai 3: Satsumon/Ainu Bunka. The Hokkaido Shimbun Press, Sapporo. (*in Japanese*)
- Noshiro, S., Suzuki, M. & Sasaki, Y., 2007. Importance of *Rhus verniciflua* Stokes (lacquer tree) in prehistoric periods in Japan, deduced from identifications of its fossil woods. *VEGETATION HISTORY AND ARCHAEOBOTANY* 16: 405–411.
- Nugent, C., 1990. The Zambezi River: tectonism, climatic change and drainage evolution. *PALAEOGEOGRAPHY PALAEOCLIMATOLOGY PALAEOECOLOGY* 78: 55–69.
- Nugent, C., 1992. The Zambezi River: tectonism, climatic change and drainage evolution: reply to discussion. *PALAEOGEOGRAPHY PALAEOCLIMATOLOGY PALAEOECOLOGY* 91: 178–182.
- Ogi, M., Tachibana, Y. & Yamazaki, K., 2004. The Connectivity of the Winter North Atlantic Oscillation (NAO) and the Summer Okhotsk High. *JOURNAL OF THE METEOROLOGICAL SOCIETY OF JAPAN* 82: 905–913.
- Ohtsuka, T., 2002. Checklist and illustration of diatoms in the Hii River. *DIATOM* 18: 23–56.
- Ohyi, H., 1975. The Okhotsk culture, a maritime culture of the Southern Okhotsk Sea Region. In: Fitzhugh, W. (Ed.), *Prehistoric Maritime Adaptations of the Circumpolar Zone*. De Gruyter, Netherlands.
- Olympus Corporation, 2011. cellSens© Dimension: Release 1.5. Scientific Research Solution Group, Tokyo, Hamburg.
- Omoto, L. & Saitou, N., 1997. Genetic origins of the Japanese: A Partial Support for the Dual Structure Hypothesis. *AMERICAN JOURNAL OF PHYSICAL ANTHROPOLOGY* 102: 437–446.
- Omura, A. & Ikehara, K., 2010. Deep-sea sedimentation controlled by sea-level rise during the last deglaciation, an example from the Kumano Trough, Japan. *MARINE GEOLOGY* 274: 177–186.
- Palarea-Albaladejo, J. & Martín-Fernández, J.A., 2013. Values below detection limit in compositional chemical data. *ANALYTICA CHIMICA ACTA* 764: 32–43.
- Palarea-Albaladejo, J. & Martín-Fernández, J.A., 2015. zCompositions – R package for multivariate imputation of left-censored data under a compositional approach. *CHEMOMETRICS AND INTELLIGENT LABORATORY SYSTEMS* 143: 85–96.
- Passarge, S., 1904. Die Kalahari. Dietrich Reimer, Berlin. (*in German*).
- Patrick, R., 1977. The ecology of freshwater diatoms – diatom communities. In: Werner, D. (Ed.), *The biology of diatoms*. University of California Press, Berkeley, pp. 284–332.
- Peel, M.C., Finlayson, B.L. & McMahon, T.A., 2007. Updated world map of the Köppen–Geiger climate classification. *HYDROLOGY AND EARTH SYSTEM SCIENCES* 11: 1633–1644.
- Peltier, W.R. & Fairbanks, R.G., 2006. Global glacial ice volume and Last Glacial Maximum duration from an extended Barbados sea level record. *QUATERNARY SCIENCE REVIEWS* 25: 3322–3337.

- Plessen, B. & Helle, G., 2017. Vom Monitoring zum Klimaarchiv - Sauerstoffisotope in der Paläoklimatologie. *System Erde GFZ-Journal* 7 (1): 12–19. (in German)
- Podgorski, J.E., Green, A.G., Kgotlhang, L., Kinzelbach, W.K.H., Kalscheuer, T., Auken, E. & Ngwisanyi, T., 2013. Paleo-megalake and paleo-megafan in southern Africa. *GEOLOGY* 41: 1155–1158.
- Poister, D., Kurth, A., Farrell, A. & Gray, S., 2012. Seasonality of *Aulacoseira ambigua* abundance and filament length: biogeochemical implications. *PLANKTON & BENTHOS RESEARCH* 7: 55–63.
- Prescott, J.R. & Hutton, J.T., 1994. Cosmic ray contributions to dose rates for luminescence and ESR dating: Large depths and long-term time variations. *RADIATION MEASUREMENTS* 23: 497–500.
- R Core Team, 2013. R: A language and environment for statistical computing. R Foundation for Statistical Computing, Vienna, Austria. URL <http://www.R-project.org/>.
- Razjigaeva, N.G., Ganzey, L.A., Grebennikova, T.A., Belyanina, N.I., Mokhova, L.M., Arslanov, K.A. & Chernov, S.B., 2013. Holocene climatic changes and vegetation development in the Kuril Islands. *QUATERNARY INTERNATIONAL* 290–291: 126–138.
- Reille, M., 1992. Pollen et spores d'Europe et d'Afrique du nord. Laboratoire de Botanique historique et Palynologie, Marseille. (in French)
- Reille, M., 1995. Pollen et spores d'Europe et d'Afrique du nord, supplement 1. Laboratoire de Botanique historique et Palynologie, Marseille. (in French)
- Reille, M., 1998. Pollen et spores d'Europe et d'Afrique du nord, supplement 2. Laboratoire de Botanique historique et Palynologie, Marseille. (in French)
- Reimer, P.J., Bard, E., Bayliss, A., Beck, W.J., Blackwell, P.G., Bronk Ramsey, C., Buck, C.E., Cheng, H., Edwards, R.L., Friedrich, M., Grootes, P.M., Guilderson, T.P., Hafidason, H., Hajdas, I., Hatté, C., Heaton, T.J., Hoffmann, D.L., Hogg, A.G., Hughen, K.A., Kaiser, K.F., Kromer, B., Manning, S.W., Niu, M., Reimer, R.W., Richards, D.A., Scott, E.M., Southon, J.R., Staff, R.A., Turney, C.S.M. & van der Plicht, J., 2013. IntCal13 and Marine13 radiocarbon age calibration curves 0–50,000 years cal BP. *RADIOCARBON* 55 (4): 1869–1887.
- Reuter, H.I., Nelson, A. & Jarvis, A., 2007. An evaluation of void filling interpolation methods for SRTM data. *INTERNATIONAL JOURNAL OF GEOGRAPHICAL INFORMATION SCIENCE* 21: 983–1008.
- Reynolds, C.S., 1998. What factors influence the species composition of phytoplankton in lakes of different trophic status? *HYDROBIOLOGIA* 369: 11–26.
- Riedel, F., Erhardt, S., Chauke, C., Kossler, A., Shemang, E. & Tarasov, P., 2011. Evidence for a permanent lake in Sua Pan (Kalahari, Botswana) during the early centuries of the last millenium indicated by distribution of Baobab trees (*Adansonia digitata*) on “Kubu Island”. *QUATERNARY INTERNATIONAL* 253: 67–73.

7. References

- Riedel, F., Henderson, A.C.G., Heußner, K.-U., Kaufmann, G., Kossler, A., Leipe, C., Shemang, E. & Taft, L., 2014. Dynamics of a Kalahari long-lived mega-lake system: hydromorphological and limnological changes in the Makgadikgadi Basin (Botswana) during the terminal 50 ka. *HYDROBIOLOGIA* 739: 25–53.
- Ringrose, S., Downey, B., Genecke, D., Sefe, F. & Vink, B., 1999. Nature of calcareous deposits in the western Makgadikgadi basin, Botswana. *JOURNAL OF ARID ENVIRONMENTS* 43: 375–397.
- Ringrose, S., Huntsman-Mapila, P., Kampunzu, A.B., Downey, W., Coetzee, S., Vink, B., Matheson, W. & Vanderpost, C., 2005. Sedimentological and geochemical evidence for palaeo-environmental change in the Makgadikgadi subbasin, in relation to the MOZ rift depression, Botswana. *PALAEOGEOGRAPHY PALAEOCLIMATOLOGY PALAEOECOLOGY* 217: 265–287.
- Rioual, P., Andrieu-Ponel, V., de Beaulieu J.-L., Reille, M., Svobodova, H. & Battarbee, R.W., 2007. Diatom responses to limnological and climatic changes at Ribains Maar (French Massif Central) during the Eemian and Early Würm, *QUATERNARY SCIENCE REVIEWS* 26: 1557–1609.
- Rito, T., Richards, M.B., Fernandes, V., Alshamali, F., Cerny, V., Pereira, L. & Soares, P., 2013. The First Modern Human Dispersals across Africa. *PLOS ONE* 8 (11): e80031.
- Robbins, L.H., Brook, G.A., Murphy, M.L., Ivester, A.H. & Campbell, A.C., 2016. The Kalahari during MIS 6–2 (190–12 ka): Archaeology, Paleoenvironment, and Population Dynamics. In: Jones, S.C. & Stewart, B.A. (Eds.), *Africa from MIS 6–2: Population Dynamics and Palaeoenvironments: Vertebrate Paleobiology and Paleoanthropology Series*. Springer, Netherlands, pp. 175–193.
- Round, F.E., Crawford, R.M. & Mann, D.G., 1990. *The Diatoms, Biology & Morphology of the Genera*. Cambridge University Press, Cambridge.
- Rovira, L., Trobajo, R. & Ibáñez, C., 2012. The use of diatom assemblages as ecological indicators in highly stratified estuaries and evaluation of existing diatom indices. *MARINE POLLUTION BULLETIN* 64: 500–511.
- Rozanski, K., Araguás-Araguás, L. & Gonfiantini, R., 1993. Isotopic Patterns in Modern Global Precipitation. In: Swart, P.K., Lohman, K.C., McKenzie, J. & Savin, S. (Eds.), *Climate Change in Continental Isotopic Records*. AGU, Washington, D.C., pp. 1–36.
- Rozanski, K., Johnson, S.J., Schotterer, U. & Thomson, L.G., 1997. Reconstruction of past climates from stable isotope records of palaeo-precipitation preserved in continental archives. *HYDROLOGICAL SCIENCES JOURNAL* 42: 725–745.
- Sakaguchi, Y., 1992. Cooling of Hokkaido around 9000 BP caused by permafrost meltwater burst. *BULLETIN OF THE DEPARTMENT OF GEOGRAPHY, UNIVERSITY TOKYO* 24: 1–6.
- Sakaguchi, T., 2007a. Site Formation Processes and Long-Term Changes in Land Use among Maritime Hunter-Gatherers: A Case Study at the Hamanaka-2 site, Rebun Island, Hokkaido. *ARCTIC ANTHROPOLOGY* 44 (2): 31–50.

- Sakaguchi, T., 2007b. Refuse patterning and behavioral analysis in a pinniped hunting camp in the Late Jomon Period: A case study in layer V at the Hamanaka 2 site, Rebun Island, Hokkaido, Japan. *JOURNAL OF ANTHROPOLOGICAL ARCHAEOLOGY* 26(1): 28–46.
- Sarmaja-Korjonen, K., Seppänen, A., Bennike, O., 2006. *Pediastrum* algae from the classic late glacial Bølling Sø site, Denmark: Response of aquatic biota to climate change. *REVIEW OF PALAEOBOTANY & PALYNOLOGY* 138: 95–107.
- Sato, H., Kumano, S., Maeda, Y., Nakamura, T. & Matsuda, I., 1998. The Holocene development of Kushu Lake on Rebun Island in Hokkaido, Japan. *JOURNAL OF PALEOLIMNOLOGY* 20: 57–69.
- Sato, T., Amano, T., Ono, H., Ishida, H., Kodera, H., Matsumura, H., Yoneda, M. & Masuda, R., 2007. Origins and genetic features of the Okhotsk people, revealed by ancient mitochondrial DNA analysis. *JOURNAL OF HUMAN GENETICS* 52 (7): 618–627.
- Saunders, K.M., McMinn, A., Roberts, D., Hodgson, D.A. & Heijnis, H., 2007. Recent human-induced salinity changes in Ramsar-listed Orielton Lagoon, south-east Tasmania, Australia: a new approach for coastal lagoon conservation and management. *AQUATIC CONSERVATION* 17: 51–70.
- Sawada, H., Kondo, R., Satô, M. & Igarashi, Y., 2015. 3500-year Vegetation History of the Giboshi-Numa Wetland on the southeastern Slopes of Mt. Rishiri, Rishiri Island, Northern Hokkaido. *RISHIRI STUDIES* 34: 67–78 (*in Japanese*).
- Sawai, Y., 2002. Evidence for 17th-century tsunamis generated on the Kuril–Kamchatka subduction zone, Lake Tokotan, Hokkaido, Japan. *JOURNAL OF ASIAN EARTH SCIENCES* 20: 903–911.
- Schlolaut, G., Brauer, A., Marshall, M.H., Nakagawa, T., Staff, R.A., Ramsey, C.B., Lamb, H.F., Bryant, C.L., Naumann, R., Dulski, P., Brock, F., Yokoyama, Y., Tada, R., Haraguchi, T. & Suigetsu 2006 project members, 2014. Event layers in the Japanese Lake Suigetsu ‘SG06’ sediment core: description, interpretation and climatic implications. *QUATERNARY SCIENCE REVIEWS* 83: 157–170.
- Schlunbaum, G. & Baudler, H., 2001. Die Vielfalt innerer Küstengewässer an der südlichen Ostsee: Eine Übersicht von der Flensburger Förde bis zum Kurischen Haff, Teil 1: Entwicklungsgeschichte, Morphologie, Hydrologie und Hydrographie. *ROSTOCKER MEERESBIOLOGISCHE BEITRÄGE* 8: 5–61 (*in German*).
- Schmidt, M., Tarasov, P.E., Hoelzmann, P., Meyer, H. & Leipe, C., 2016. Diatoms from Lake Kushu: A pilot study to test the potential of a Late Quaternary palaeoenvironmental archive from Rebun Island (Hokkaido Region, Japan). *JOURNAL OF ASIAN EARTH SCIENCES* 122: 106–122.
- Schmidt, M., Fuchs, M., Henderson, A.C.G., Kossler, A., Leng, M.J., Mackay, A.W., Shemang, E. & Riedel, F., 2017. Paleolimnological features of a mega-lake phase in the Makgadikgadi

7. References

- Basin (Kalahari, Botswana) during Marine Isotope Stage 5 inferred from diatoms. *JOURNAL OF PALEOLIMNOLOGY* 58: 373–390.
- Scholz, C.A., Koczyński, T.A. & Hutchins, D.G., 1976. Evidence for incipient rifting in southern Africa. *GEOPHYSICAL JOURNAL OF THE ROYAL ASTRONOMICAL SOCIETY* 44: 135–144.
- Scholz, C.A., Johnson, T.C., Cohen, A.S., King, J.W., Peck, J.A., Overpeck, J.T., Talbot, M.R., Brown, E.T., Kalindekaffe, L., Amoako, P.Y.O., Lyons, R.P., Shanahan, T.M., Castañeda, I.S., Heil, C.W., Forman, S.L., McHargue, L.R., Beuning, K.R., Gomez, J. & Pierson, J., 2007. East African megadroughts between 135 and 75 thousand years ago and bearing on early-modern human origins. *PNAS* 104 (42): 16416–16421.
- Schönborn, W. & Risse-Buhl, U., 2013. Lehrbuch der Limnologie, 2. Edition, Schweizerbart, Stuttgart. (*in German*).
- Schultheiß, R., Van Bocxlaer, B., Riedel, F., von Rintelen, T. & Albrecht, C., 2014. Disjunct distributions of freshwater snails testify to a central role of the Congo system in shaping biogeographical patterns in Africa. *BMC EVOLUTIONARY BIOLOGY* 14: 42.
- Schuster, S.C., Miller, W., Ratan, A., Tomsho, L.P., Giardine, B., Kasson, L.R., Harris, R.S., Petersen, D.C., Zhao, F., Qi, J., Alkan, C., Kidd, J.M., Sun, Y., Drautz, D.I., Bouffard, P., Muzny, D.M., Reid, J.G., Nazareth, L.V., Wang, Q., Burhans, R., Riemer, C., Wittekindt, N.E., Moorjani, P., Tindall, E.A., Danko, C.G., Teo, W.S., Buboltz, A.M., Zhang, Z., Ma, Q., Oosthuisen, A., Steenkamp, A.W., Oosthuisen, H., Venter, P., Gajewski, J., Zhang, Y., Pugh, B.F., Makova, K.D., Nekrutenko, A., Mardis, E.R., Patterson, N., Pringle, T.H., Chiaromonte, F., Mullikin, J.C., Eichler, E.E., Hardison, R.C., Gibbs, R.A., Harkins, T.T. & Hayes, V.M., 2010. Complete Khoisan and Bantu genomes from southern Africa. *NATURE* 463: 943–947.
- Seidov, D. & Maslin, M., 2001. Atlantic ocean heat piracy and the bipolar climate see-saw during Heinrich and Dansgaard–Oeschger events. *JOURNAL OF QUATERNARY SCIENCE* 16: 321–328.
- Sharp, Z., 2007. Principles of Stable Isotope Geochemistry. Pearson Prentice Hall, New Jersey.
- Shaw, P.A. & Thomas, D.S.G., 1988. Lake Caprivi: a late Quaternary link between the Zambezi and middle Kalahari drainage systems. *ZEITSCHRIFT FÜR GEOMORPHOLOGIE, NEUE FOLGE* 32: 329–337.
- Shaw, P.A. & Thomas, D.S.G., 1992. Geomorphology, sedimentation, and tectonics in the Kalahari Rift. *ISRAEL JOURNAL OF EARTH SCIENCES* 41: 87–94.
- Shaw, P.A., Thomas, D.S.G. & Nash, D.J., 1992. Late Quaternary fluvial activity in the dry valleys (mekgacha) of the Middle and Southern Kalahari, southern Africa. *JOURNAL OF QUATERNARY SCIENCE* 7: 273–281.
- Shaw, P.A., Stokes, S., Thomas, D.S.G., Davies, F.B.M. & Holmgren, K., 1997. Palaeoecology and age of a Quaternary high lake level in the Makgadikgadi Basin of the Middle Kalahari, Botswana. *SOUTH AFRICAN JOURNAL OF SCIENCE* 93: 273–276.

- Shear, H., Nalewajko, C. & Bacchus, H.M., 1976. Some aspects of the ecology of *Melosira* ssp. in Ontario lakes. *HYDROBIOLOGIA* 50: 73–176.
- Shemang, E.M. & Molwalefhe, L.N., 2011. Geomorphic Landforms and Tectonism Along the Eastern Margin of the Okavango Rift Zone, North Western Botswana as Deduced from Geophysical Data in the Area. In: Sharkov, E.V. (Ed.), *New frontiers in Tectonic Research – General Problems, Sedimentary Basins and Island Arcs*. InTech, Rijeka, pp. 169–182.
- Shi, N., Schneider, R., Beug, H.-J. & Dupont, L.M., 2001. Southeast trade wind variations during the last 135 kyr: evidence from pollen spectra in eastern South Atlantic sediments. *EARTH AND PLANETARY SCIENCE LETTERS* 187: 311–321.
- Shimakura, M., 1973. Palynomorphs of Japanese plants. In: Osaka Museum of Natural History (Ed.), *Special Publications from the Osaka Museum of Natural History* (Osaka, Japan), pp. 1–60. (*in Japanese*)
- Smol, J.P. & Stoermer, E.F., 2010. *The Diatoms - Applications for the Environmental and Earth Sciences*, 2nd Edition, Cambridge University Press, Cambridge.
- Solovieva, N., Jones, V.J., Nazarova, L., Brooks, S.J., Birks, H.J.B., Grytnes, J.-A., Appleby, P.G., Kauppi, T., Kondratenok, B., Renberg, I., Ponomarev, V., 2005. Palaeolimnological evidence for recent climatic change in lakes from the northern Urals, arctic Russia. *JOURNAL OF PALEOLIMNOLOGY* 33: 463–482.
- Spengler, R.N. III, 2015. Agriculture in the Central Asian Bronze Age. *JOURNAL OF WORLD PREHISTORY* 28: 215–253.
- Stachura-Suchoples, K., 2001. Bioindicative values of dominant diatom species from the Gulf of Gdansk, Southern Baltic Sea, Poland. In: Jahn, R., Kociolek, J.P., Witkowski, A., Compère, P. (Eds.), *Lange-Bertalot Festschrift. ARG Gantner KG, Ruggell*, pp. 477–490.
- Stebich, M., Mingram, J., Han, J. & Liu, J., 2009. Late Pleistocene spread of (cool-)temperate forests in Northeast China and climate changes synchronous with the North Atlantic region. *GLOBAL AND PLANETARY CHANGE* 65: 56–70.
- Stebich, M., Rehfeld, K., Schlütz, F., Tarasov, P.E., Liu, J. & Mingram, J., 2015. Holocene vegetation and climate dynamics of NE China based on the pollen record from Sihailongwan Maar Lake. *QUATERNARY SCIENCE REVIEWS* 124: 275–289.
- Stockmarr, J., 1971. Tablets with spores used in absolute pollen analysis. *POLLEN ET SPORES* 13: 614–621.
- Stoermer, E.F. & Ladewski, T.B., 1976. *Apparent Optimal Temperatures for the Occurrence of Some Common Phytoplankton Species in Southern Lake Michigan*. Great Lakes research division, publication 18, The University of Michigan, Ann Arbor.
- Stoermer, E.F. & Smol, J.P., 1999. *The Diatoms: applications for the environmental and earth sciences*, Cambridge University Press: Cambridge.

7. References

- Stokes, S., 1999. Luminescence dating applications in geomorphological research. *GEOMORPHOLOGY* 29: 153–171.
- Stokes, S., Thomas, D.S.G. & Washington, R., 1997. Multiple episodes of aridity in southern Africa since the last interglacial period. *NATURE* 388: 154–158.
- Strauss, T. & von Maltitz, M.J., 2017. Generalizing Ward's Method for Use with Manhattan Distances. *PLoS ONE* 12(1), e0168288.
- Street, F.A. & Grove, A.T., 1976. Environmental and climatic implications of late Quaternary lake-level fluctuations in Africa. *NATURE* 261: 385–390.
- Stute, M. & Talma, A.S., 1998. Glacial temperatures and moisture transport regimes reconstructed from noble gases and $\delta^{18}\text{O}$, Stampriet aquifer, Namibia. Isotope techniques in the study of environmental change. International Atomic Energy Agency, Vienna, pp. 307–318.
- Stuut, J.-B.W., Prins, M.A., Schneider, R.R., Weltje, G.J., Jansen, J.H.F. & Postma, G., 2002. A 300-kyr record of aridity and wind strength in southwestern Africa: inferences from grain-size distributions of sediments on Walvis Ridge, SE Atlantic. *MARINE GEOLOGY* 180: 221–233.
- Summerfield, M.A., 1985a. Plate tectonics and landscape development on the African continent. In: Morisawa, M. & Hack, J.T. (Eds.): Tectonic geomorphology. The Binghamton Symposia in Geomorphology, Allen & Unwin: Boston, pp. 27–51.
- Summerfield, M.A., 1985b. Tectonic background to long-term landform development in tropical Africa. In: Douglas, I. & Spencer, T. (Eds.): Environmental change and tropical geomorphology. Allen & Unwin: London, pp. 281–291.
- Sun, B., Wagner, M., Zhao, Z., Li, G., Wu, X. & Tarasov, P.E., 2014. Archaeological discovery and research at Bianbiandong early Neolithic cave site, Shandong, China. *QUATERNARY INTERNATIONAL* 348: 169–182.
- Swann, G.E.A., Leng, M.J., Sloane, H.J., Maslin, M.A. & Onodera, J., 2007. Diatom oxygen isotopes: Evidence of a species effect in the sediment record. *GEOCHEMISTRY GEOPHYSICS GEOSYSTEMS* 8 (6): 1–10.
- Tada, R., Irino, T. & Koizumi, I., 1999. Land-ocean linkages over orbital and millennial timescales recorded in late Quaternary sediments of the Japan Sea. *PALEOCEANOGRAPHY* 14: 236–247.
- Tanaka, H., 2014. Atlas of Freshwater Fossil Diatoms in Japan – Including related Recent Taxa. Uchida Rokakuho Publishing Co., Ltd., Tokyo. (*in Japanese*).
- Tanaka, M., Cabrera, V.M., González, A.M., Larruga, J.M., Takeyasu, T., Fuku, N., Guo, L.-J., Hirose, R., Fujita, Y., Kurata, M., Shinoda, K-I., Umetsu, K., Yamada, Y., Oshida, Y., Sato, Y., Hattori, N., Mizuno, Y., Arai, Y., Hirose, N., Ohta, S., Ogawa, O., Tanaka, Y., Kawamori, R., Shamoto-Nagai, M., Maruyama, W., Shimokata, H., Suzuki, R. & Shimodaira, H., 2004. Mitochondrial Genome Variation in Eastern Asia and the Peopling of Japan. *GENOME RESEARCH* 14 (10A): 1832–1850.

- Tankard, A.J., Hobday, D.K., Jackson, M.P.A., Hunter, D.R., Eriksson, K.A. & Minter, W.E.L., 1982. Crustal evolution of southern Africa, 3.8 billion years of earth history, Springer Verlag: New York.
- Tarasov, P.E., White, D. & Weber, A.W., 2013. The Baikal-Hokkaido Archaeology Project: Environmental archives, proxies and reconstruction approaches. *QUATERNARY INTERNATIONAL* 290–291: 1–2.
- Tarasov, P.E., Bezrukova, E., Karabanov, E. et al., 2007. Vegetation and climate dynamics during the Holocene and Eemian interglacials derived from Lake Baikal pollen records. *PALAEOGEOGRAPHY PALAEOCLIMATOLOGY PALAEOECOLOGY* 252: 440–457.
- Tarasov, P.E., Nakagawa, T., Demske, D., Österle, H., Igarashi, Y., Kitagawa, J., Mokhova, L., Bazarova, V., Okuda, M., Gotanda, K., Miyoshi, N., Fujiki, T., Takemura, K., Yonenobu, H. & Fleck, A., 2011. Progress in the reconstruction of Quaternary climate dynamics in the Northwest Pacific: A new analogue reference dataset and its application to the 430-kyr pollen record from Lake Biwa. *EARTH-SCIENCE REVIEWS* 10: 64–79.
- Tarasov, P.E., Savelieva, L.A., Long, T. & Leipe, C., 2018. Postglacial vegetation and climate history and traces of early human impact and agriculture in the present-day cool mixed forest zone of European Russia. *QUATERNARY INTERNATIONAL* (in press). Doi: <https://doi.org/10.1016/j.quaint.2018.02.029>
- Taruno, H., 2010. The stages of land bridge formation between the Japanese Islands and the continent on the basis of faunal succession. *THE QUATERNARY RESEARCH* 49: 309–314.
- Templ, M., Filzmoser, P. & Reimann, C., 2008. Cluster analysis applied to regional geochemical data: Problems and possibilities. *APPLIED GEOCHEMISTRY* 23: 2198–2213.
- ter Braak, C.J.F. & Šmilauer, P., 2002. CANOCO Reference Manual and User's Guide to CANOCO for Windows: Software for Canonical Community Ordination Version 4.5. Microcomputer Power, Ithaca, New York.
- Terry, J.P. & Feng, C.-C., 2010. On quantifying the sinuosity of typhoon tracks in the western North Pacific basin. *APPLIED GEOGRAPHY* 30: 678–686.
- Thomas, A.D., Hoon, S.R. & Dougill, A.J., 2011. Soil respiration at five sites along the Kalahari transect: effects of temperature, precipitation pulses and biological soil crust cover. *GEODERMA* 167-168: 284–294.
- Thomas, D.S.G. & Shaw, P.A., 1991. The Kalahari environment. Cambridge University Press, Cambridge.
- Thomas, E.R., Wolff, E.W., Mulvaney, R., Steffensen, J.P., Johnsen, S.J., Arrowsmith, C., White, J.W.C., Vaughn, B. & Popp, T., 2007. The 8.2ka event from Greenland ice cores. *QUATERNARY SCIENCE REVIEWS* 26: 70–81.
- Tishkoff, S.A., Gonder, M.K., Henn, B.M., Mortensen, H., Knight, A., Gignoux, C., Fernandopulle, N., Lema, G., Nyambo, T.B., Ramakrishnan, U., Reed, F.A. & Mountain, J.L.,

7. References

2007. History of click-speaking populations of Africa inferred from mtDNA and Y chromosome genetic variation. *MOLECULAR BIOLOGY AND EVOLUTION* 24 (10): 2180–2195.
- Trobajo, R., Clavero, E., Chepurinov, V.A., Sabbe, K., Mann, D.G., Ishihara, S. & Cox, E.J., 2009. Morphological, genetic and mating diversity within the widespread bioindicator *Nitzschia palea* (Bacillariophyceae). *PHYCOLOGIA* 48: 443–459.
- Tuji, A., Kawashima, A., Julius, M.L. & Stoermer, E.F., 2003. *Stephanodiscus akanensis* sp. nov., a new species of extant diatom from Lake Akan, Hokkaido, Japan. *BULLETIN OF THE NATIONAL SCIENCE MUSEUM. SERIES B, BOTANY* 29: 1–8.
- Underhill, A.P. & Habu, J., 2006. Early communities in East Asia: Economic and Sociopolitical Organization at the Local and Regional Levels. In: Stark, M.T. (Ed.) *Archaeology of Asia*. Blackwell, Malden, pp. 121–148.
- Urrego, D.H., Sánchez Goñi, M.F., Daniau, A.-L., Lechevrel, S. & Hanquiez, V., 2015. Increased aridity in southwestern Africa during the warmest periods of the last interglacial. *CLIMATE OF THE PAST* 11: 1417–1431.
- Utagawa, Y., 2002. The world of the Okhotsk ‘bear festival’. In: Nishiaki, Y. & Utagawa, Y. (Eds.), *Another World of the North*. The University of Tokyo Press, Tokyo, pp. 106–113 (*in Japanese*).
- Van Dam, H., Mertens, A. & Sinkeldam, J., 1994. A coded checklist and ecological indicator values of freshwater diatoms from the Netherlands. *NETHERLANDS JOURNAL OF AQUATIC ECOLOGY* 28: 117–133.
- Van den Boogaart, K.G., Tolosana, R., Bren, M., 2014. *compositions: Compositional Data Analysis*.
- Van Zinderen Bakker, E.M., 1976. The evolution of Late-Quaternary palaeoclimates of southern Africa. *PALAEOECOLOGY OF AFRICA* 9:160–202.
- Velichko, A.A. & Nechaev, V.P., 2005. Methods of paleoclimate reconstruction. In: Velichko, A.A., & Nechaev, V.P. (Eds.), *Cenozoic climatic and environmental changes in Russia*. Geological Society of America, Special Paper 382, pp. 1–11.
- Verschuren, D., Sinninghe Damsté, S.J., Moernaut, J., Kristen, I., Blaauw, M., Fagot, M., Haug, G.H. & CHALLACEA project members, 2009. Half-precessional dynamics of monsoon rainfall near the East African Equator. *NATURE* 462: 637–641.
- Waelbroeck, C., Labeyrie, L., Michel, E., Duplessy, J.C., McManus, J.F., Lambeck, K., Balbon, E. & Labracherie, M., 2002. Sea-level and deep water temperature changes derived from benthic foraminifera isotopic records. *QUATERNARY SCIENCE REVIEWS* 21: 295–305.
- Walker, M., Johnsen, S., Rasmussen, S.O., Popp, T., Steffensen, J.-P., Gibbard, P., Hoek, W., Lowe, J., Andrews, J., Björck, S., Cwynar, L.C., Hughen, K., Kershaw, P., Kromer, B., Litt, T., Lowe, D.J., Nakagawa, T., Newnham, R. & Schwander, J., 2009. Formal definition and dating of the GSSP (Global Stratotype Section and Point) for the base of the Holocene using

- the Greenland NGRIP ice core, and selected auxiliary records. *JOURNAL OF QUATERNARY SCIENCE* 24: 3–17.
- Wallace, D.C., Brown, M.D. & Lott, M.T., 1999. Mitochondrial DNA variation in human evolution and disease. *GENE* 238: 211–230.
- Wan, Y.-Y., Lu, R., Du, Y.-M., Honda, T. & Miyakoshi, T., 2007. Does Donglan lacquer tree belong to *Rhus vernicifera* species? *INTERNATIONAL JOURNAL OF BIOLOGICAL MACROMOLECULES* 41: 497–503.
- Wanner, H., Beer, J., Bütikofer, J., Crowley, T.J., Cubasch, U., Flückiger, J., Goosse, H., Grosjean, M., Joos, F., Kaplan, J.O., Küttel, M., Müller, S.A., Prentice, I.C., Solomina, O., Stocker, T.F., Tarasov, P.E., Wagner, M. & Widmann, M., 2008. Mid- to Late Holocene climate change: an overview. *QUATERNARY SCIENCE REVIEWS* 27(19–20): 1791–1828.
- Watanabe, H., 1986. Community habitation and food gathering in prehistoric Japan: An ethnographic interpretation of the archaeological evidence. In: Pearson, R.J., Barnes, G.L. & Hutterer, K.L. (Eds.), *Windows on the Japanese past: Studies in Archaeology and Prehistory*. Centre for Japanese Studies, University of Michigan Press, Ann Arbor, pp. 229–254.
- Watanabe, S., Tada, R., Ikehara, K., Fujine, K. & Kido, Y., 2007. Sediment fabrics, oxygenation history, and circulation modes of Japan Sea during the Late Quaternary. *PALAEOGEOGRAPHY PALAEOCLIMATOLOGY PALAEOECOLOGY* 247: 50–64.
- Weber, A.W., Katzenberg, M.A. & Schurr, T., 2010. *Prehistoric Hunter-Gatherers of the Baikal Region, Siberia: Bioarchaeological Studies of past Life Ways*. University of Pennsylvania Museum of Archaeology and Anthropology, Philadelphia.
- Weber, A.W., Jordan, P. & Kato, H., 2013. Environmental change and cultural dynamics of Holocene hunter-gatherers in Northeast Asia: Comparative analyses and research potentials in Cis-Baikal (Siberia, Russia) and Hokkaido (Japan). *QUATERNARY INTERNATIONAL* 290–291: 3–20.
- White, D. & Bush, A., 2010. Holocene climate, environmental change, and Neolithic biocultural discontinuity in the Baikal region. In: Weber, A.W., Katzenberg, M.A. & Schurr, T. (Eds.), *Prehistoric Hunter-Gatherers of the Baikal Region, Siberia: Bioarchaeological Studies of past Life Ways*. University of Pennsylvania Museum of Archaeology and Anthropology, Philadelphia, pp. 1–26.
- White, K. & Eckardt, F., 2006. Geochemical mapping of carbonate sediments in the Makgadikgadi basin, Botswana, using moderate resolution remote sensing data. *EARTH SURFACE PROCESSES AND LANDFORMS* 31: 665–681.
- Wu, W.W., Wang, X.H., Wu, X.H., Jin, G.Y. & Tarasov, P.E., 2014. The early Holocene archaeobotanical record from the Zhangmatun site situated at the northern edge of the Shandong Highlands, China. *QUATERNARY INTERNATIONAL* 348: 183–193.

7. References

- Wufuer, R., Liu, Y., Mu, S., Song, W., Yang, X., Zhang, D. & Pan, X., 2014. Interaction of dissolved organic matter with Hg(II) along salinity gradient in Boston Lake. *GEOCHEMISTRY INTERNATIONAL* 52: 1072–1077.
- Yamada, G., 1996. The plants utilized during the Okhotsk cultural period. *BULLETIN OF THE HISTORICAL MUSEUM OF HOKKAIDO* 24: 49–66 (*in Japanese*).
- Yamada, G. & Tsubakisaka, A., 1995. The spread of cultivated crops from the mainland. In: Final Report on Research Project of the Historical and Cultural Exchange of the North, Historical Museum of Hokkaido, Sapporo, pp. 107–134 (*in Japanese*).
- Yamada, K., Kamite, M., Saito-Kato, M., Okuno, M., Shinozuka, Y. & Yasuda, Y., 2010. Late Holocene monsoonal-climate change inferred from Lakes Ni-no-Megata and San-no-Megata, northeastern Japan. *QUATERNARY INTERNATIONAL* 220: 122–132.
- Zolitschka, B., Francus, P., Ojala, A.E.K., & Schimmelmann, A., 2015. Varves in lake sediments - A review. *QUATERNARY SCIENCE REVIEWS* 117: 1–41.

8. Appendix

8.1 Supplementary material to the manuscripts

8.1.1 Diatoms from Lake Palaeo-Makgadikgadi

The diatom taxa list with the corresponding autecology regarding mode of living, pH, salinity and trophy is given in table 8.1. The percentage abundances are available in the Open Access information

system PANGAEA via the Digital Object Identifier (doi): <https://doi.pangaea.de/10.1594/PANGAEA.EA.889755>.

Table 8.1: Diatom taxa list of Lake Palaeo-Makgadikgadi samples with the corresponding autecology: B = benthic, P = planktonic, fresh = freshwater, oligo = oligohaline / oligotraphentic, meso = mesohaline / mesotraphentic, eu = eutraphentic.

<i>Genus species</i> Author Year	living	pH	salinity	trophy
<i>Achnanthes exigua</i> Grunow 1880	B	8-9	oligo	eu
<i>Amphora copulata</i> (Kützing) Schoemann & Archibald 1986	B	8-9	oligo	eu
<i>Amphora frickei</i> Reichelt 1904	B	-	-	-
<i>Anomoeoneis sphaerophora</i> E. Pfitzer 1871	B	8-9	meso	eu
<i>Aulacoseira ambigua</i> (Grunow) Simonsen 1979	P	7-8	oligo	eu
<i>Aulacoseira</i> sp. 1	P	-	-	-
<i>Campylodiscus clypeus</i> (Ehrenberg) Ehrenberg ex Kützing 1844	B	7-8	tolerant	eu
<i>Cocconeis placentula</i> Ehrenberg 1838	B	7-8	tolerant	eu
<i>Cocconeis</i> sp. 1	B	-	-	-
<i>Craticula</i> cf. <i>elkab</i> (O. Müller) Lange-Bertalot, Kusber & Cocquyt 2007	B	8-9	oligo	-
<i>Cyclotella meneghiniana</i> Kützing 1844	P	8-9	oligo	eu
<i>Cymatopleura solea</i> (Brébisson) W. Smith 1851	B	8-9	tolerant	eu
<i>Cymbella</i> cf. <i>lancettuliformis</i> Grunow 1875	B	-	fresh	-
<i>Cymbella cucumis</i> A. Schmidt 1875	B	7-8	-	-
<i>Cymbella cymbiformis</i> C. Agardh 1830	B	7-8	oligo	oligo
<i>Cymbella pusilla</i> Grunow 1875	B	7-8	tolerant	-
<i>Denticula kuetzingii</i> Grunow 1862	B	7-8	oligo	meso
<i>Discostella stelligera</i> (Cleve & Grunow) Houk & Klee 2004	P	tolerant	oligo	tolerant
<i>Discostella stelligeroides</i> (Hustedt) Houk & Klee 2004	P	-	-	tolerant
<i>Encyonema muelleri</i> (Hustedt) D.G. Mann 1990	B	8-9	fresh	-
<i>Epithemia sorex</i> Kützing 1844	B	8-9	oligo	eu
<i>Eunotia diodon</i> Ehrenberg 1837	B	<7	fresh	oligo
<i>Fragilaria</i> cf. <i>capucina</i> Desmazières 1825	P	7-8	oligo	tolerant
<i>Frustulia rhomboides</i> (Ehrenberg) De Toni 1891	B	<7	fresh	oligo
<i>Gomphonema angustatum</i> (Kützing) Rabenhorst 1864	B	7-8	oligo	oligo
<i>Gomphonema</i> cf. <i>clavatum</i> Ehrenberg 1832	B	8-9	fresh	oligo
<i>Halamphora thermalis</i> (Hustedt) Levkov 2009	B	8-9	oligo	-
<i>Halamphora veneta</i> (Kützing) Levkov 2009	B	8-9	oligo	eu

8. Appendix - 8.1 Supplementary material to the manuscripts

<i>Genus species</i> Author Year	living	pH	salinity	trophy
<i>Hantzschia amphioxys</i> (Ehrenberg) Grunow 1880	B	tolerant	oligo	tolerant
<i>Martyana martyi</i> (Héribaud-Joseph) Round 1990	B	8-9	oligo	tolerant
<i>Mastogloia elliptica</i> (C. Agardh) Cleve 1895	B	7-8	meso	-
<i>Navicula radiosa</i> Kützing 1844	B	<7	fresh	eu
<i>Navicula scutelloides</i> W. Smith 1843	B	8-9	fresh	eu
<i>Nitzschia cf. frustulum</i> (Kützing) Grunow 1880	B	8-9	meso	eu
<i>Nitzschia gracilis</i> Hantzsch 1860	B	tolerant	fresh	meso
<i>Nitzschia</i> sp. 1	B	-	-	-
<i>Nitzschia</i> sp. 2	B	-	-	-
<i>Pinnularia esox</i> Ehrenberg 1843	B	<7	fresh	meso
<i>Pinnularia microstauron</i> (Ehrenberg) Cleve 1891	B	<7	fresh	eu
<i>Placoneis gastrum</i> (Ehrenberg) Mereschkowsky 1903	B	7-8	oligo	eu
<i>Pseudostaurosira brevistriata</i> (Grunow) D.M. Williams & Round 1987	B	7-8	oligo	eu
<i>Rhopalodia gibba</i> (Ehrenberg) O. Müller 1895	B	tolerant	fresh	tolerant
<i>Rhopalodia gibberula</i> O. Müller 1895	B	tolerant	tolerant	tolerant
<i>Sellaphora pupula</i> (Kützing) Mereschkowsky 1902	B	tolerant	oligo	tolerant
<i>Stauroneis phoenicenteron</i> (Nitzsch) Ehrenberg 1843	B	<7	oligo	eu
<i>Staurosira construens</i> Ehrenberg 1843	B	8-9	oligo	eu
<i>Surirella engleri</i> O. Müller 1903	B	<7	fresh	-
<i>Surirella ovalis</i> Brébisson 1838	B	8-9	tolerant	eu
<i>Synedra</i> sp. 1	B	-	-	-
<i>Tryblionella cf. hungarica</i> (Grunow) Frenguelli 1942	B	8-9	meso	eu

8.1.2 Diatom taxa list of Lake Kushu sediment core

The diatom taxa list with the corresponding autecology regarding mode of living, pH, salinity and trophic is given in table 8.2. The percentage abundances are available in the Open Access information system PANGAEA via the Digital Object Identifier (doi): <https://doi.pangaea.de/10.1594/PANGAEA.8897784>.

Table 8.2: Diatom taxa list of Lake Palaeo-Makgadikgadi samples with the corresponding autecology: B = benthic, P = planktonic, fresh = freshwater, oligo = oligotraphentic, meso = mesotraphentic, eu = eutraphentic, hypereu = hypereutraphentic.

<i>Genus species</i> Author Year	living	pH	salinity	trophy
<i>Achnanthes brevipes</i> C. Agardh, nom. illeg. 1824	B	7-8	brackish	-
<i>Achnantheidium exiguum</i> (Grunow) Czarnecki 1994	B	8-9	fresh	tolerant
<i>Achnantheidium minutissimum</i> (Kützing) Czarnecki 1994	B	7-8	fresh	tolerant
<i>Actinoptychus senarius</i> (Ehrenberg) Ehrenberg 1843	P	8-9	marine	-
<i>Amphora birnirkiana</i> Patrick & Freese 1961	B	8-9	fresh	eu
<i>Amphora copulata</i> (Kützing) Schoeman & R.E.M. Archibald 1986	B	8-9	fresh	eu
<i>Amphora inariensis</i> Krammer 1980	B	-	fresh	oligo
<i>Amphora indistincta</i> Levkov 2009	B	-	fresh	oligo
<i>Aneumastus tuscula</i> (Ehrenberg) D.G. Mann & Stickle 1990	B	-	fresh	-
<i>Anomoeoneis sphaerophora</i> Pfitzer 1871	B	8-9	brackish	eu
<i>Asterionella formosa</i> Hassall 1850	P	-	fresh	eu
<i>Asteromphalus parvulus</i> Karsten 1905	P	8-9	marine	-
<i>Aulacoseira ambigua</i> (Grunow) Simonsen 1979	P	8-9	fresh	meso
<i>Aulacoseira granulata</i> (Ehrenberg) Simonsen 1979	P	8-9	fresh	eu
<i>Aulacoseira islandica</i> (O. Müller) Simonsen 1979	P	7-8	fresh	tolerant
<i>Aulacoseira subarctica</i> (O. Müller) E.Y. Haworth 1990	P	7-8	fresh	meso
<i>Bacillaria paxillifera</i> (O.F. Müller) T. Marsson 1901	B	7-8	marine	-
<i>Belonastrum berlinense</i> (Lemmermann) Round & Maidana 2001	B	-	fresh	eu
<i>Caloneis limosa</i> (Kützing) R.M. Patrick 1966	B	8-9	fresh	meso
<i>Campylodiscus imperialis</i> Greville 1860	B	8-9	marine	-
<i>Cavinula lacustris</i> (W. Gregory) D.G. Mann & Stickle 1990	B	7-8	fresh	oligo
<i>Cavinula scutelloides</i> (W. Smith) Lange-Bertalot 1996	B	8-9	fresh	eu
<i>Cavinula vincentii</i> Antoniadis & Hamilton 2008	B	8-9	fresh	oligo
<i>Chaetoceros diadema</i> (Ehrenberg) Gran 1897	P	8-9	marine	-
<i>Chaetoceros didymus</i> Ehrenberg 1845	P	8-9	marine	-
<i>Chaetoceros lorenzianus</i> Grunow 1863	P	8-9	marine	-
<i>Chaetoceros radicans</i> F. Schütt 1895	P	8-9	marine	-
<i>Chaetoceros</i> resting spores	P	8-9	marine	-
<i>Chaetoceros seiracanthus</i> Gran 1897	P	8-9	marine	-
<i>Cocconeis neothumensis</i> Krammer 1990	B	8-9	fresh	-
<i>Cocconeis placentula</i> Ehrenberg 1838	B	8-9	fresh	eu
<i>Cocconeis scutellum</i> Ehrenberg 1838	B	8-9	marine	-
<i>Conticribra guillardii</i> (Hasle) K. Stachura-Suchoples & D.M. Williams 2009	P	8-9	marine	-
<i>Coscinodiscus oculus-iridis</i> (Ehrenberg) Ehrenberg 1840	P	8-9	marine	-
<i>Coscinodiscus radiatus</i> Ehrenberg 1840	P	-	marine	-

8. Appendix - 8.1 Supplementary material to the manuscripts

<i>Genus species</i> Author Year	living	pH	salinity	trophy
<i>Craticula accomoda</i> (Hustedt) D.G. Mann 1990	B	8-9	fresh	eu
<i>Ctenophora pulchella</i> (Ralfs ex Kützing) D.M. Williams & Round 1986	B	-	brackish	eu
<i>Cyclostephanus dubius</i> (Hustedt) Round 1988	P	8-9	fresh	eu
<i>Cyclotella choctawhatcheeana</i> Prasad 1990	P	-	marine	tolerant
<i>Cyclotella meneghiniana</i> Kützing 1844	P	8-9	fresh	eu
<i>Cyclotella pseudostelligera</i> Hustedt 1939	P	7-8	fresh	eu
<i>Cymatopleura solea</i> (Brébisson) W. Smith 1851	B	-	fresh	eu
<i>Cymbella amoyensis</i> M. Voigt	B	8-9	fresh	-
<i>Cymbella aspera</i> (Ehrenberg) Cleve 1894	B	8-9	fresh	tolerant
<i>Cymbella cistula</i> (Ehrenberg) O. Kirchner 1878	B	8-9	fresh	eu
<i>Cymbella tumida</i> (Brébisson) van Heurck 1880	B	8-9	fresh	eu
<i>Cymbopleura anglica</i> (Lagerstedt) Krammer 2003	B	-	fresh	-
<i>Diatoma mesodon</i> (Ehrenberg) Kützing 1844	B	8-9	fresh	meso
<i>Diatoma tenue</i> C. Agardh 1812	P	8-9	fresh	eu
<i>Diploneis boldtiana</i> Cleve 1891	B	-	fresh	oligo
<i>Diploneis crabro</i> (Ehrenberg) Ehrenberg 1854	B	-	brackish	-
<i>Diploneis ovalis</i> (Hilse) Cleve 1891	B	8-9	fresh	-
<i>Diploneis parma</i> Cleve 1891	B	8-9	fresh	oligo
<i>Diploneis smithii</i> (Brébisson) Cleve 1894	B	-	brackish	-
<i>Diploneis suborbicularis</i> (W. Gregory) Cleve 1894	B	-	brackish	-
<i>Diploneis subovalis</i> Cleve 1894	B	-	fresh	-
<i>Discostella stelligera</i> (Cleve & Grunow) Houk & Klee 2004	P	-	fresh	-
<i>Ellerbeckia arenaria</i> (G. Moore ex Ralfs) R.M. Crawford 1988	B	-	fresh	-
<i>Encyonema caespitosum</i> Kützing 1849	B	-	fresh	eu
<i>Encyonema silesiacum</i> (Bleisch) D.G. Mann 1990	B	-	fresh	oligo
<i>Epithemia adnata</i> (Kützing) Brébisson 1838	B	8-9	fresh	eu
<i>Epithemia sorex</i> Kützing 1844	B	8-9	fresh	eu
<i>Epithemia turgida</i> (Ehrenberg) Kützing 1844	B	8-9	fresh	eu
<i>Eunotia bilunaris</i> (Ehrenberg) Schaarschmidt 1880	B	tolerant	fresh	tolerant
<i>Eunotia diodon</i> Ehrenberg 1837	B	<7	fresh	oligo
<i>Eunotia incisa</i> W. Smith ex W. Gregory 1854	B	<7	fresh	oligo
<i>Eunotia praerupta</i> Ehrenberg 1843	B	-	fresh	-
<i>Fallocia insociabilis</i> (Krasske) D.G. Mann 1990	B	7-8	fresh	meso
<i>Fragilaria construens</i> (Ehrenberg) Grunow 1862	B	8-9	fresh	eu
<i>Fragilaria grunowii</i> Lange-Bertalot & S. Ulrich 2014	P	tolerant	fresh	tolerant
<i>Fragilaria vaucheriae</i> (Kützing) J.B. Petersen 1938	B	8-9	fresh	eu
<i>Geissleria acceptata</i> (Hustedt) Lange-Bertalot & Metzeltin 1996	B	7-8	fresh	-
<i>Gomphonema acuminatum</i> Ehrenberg 1832	B	8-9	fresh	eu
<i>Gomphonema acuminatum</i> var. <i>brebissonii</i> (Kützing) Grunow 1880	B	7-8	fresh	-
<i>Gomphonema augur</i> Ehrenberg 1841	B	8-9	fresh	eu
<i>Gomphonema gracile</i> Ehrenberg 1838	B	7-8	fresh	meso
<i>Gomphonema grovei</i> var. <i>lingulatum</i> (Hustedt) Lange-Bertalot 1985	B	-	fresh	meso
<i>Gomphonema parvulum</i> (Kützing) Kützing 1849	B	7-8	fresh	eu
<i>Gomphonema truncatum</i> Ehrenberg 1832	B	8-9	fresh	eu
<i>Grammatophora hamulifera</i> Kützing 1844	B	-	marine	-
<i>Gyrosigma acuminatum</i> (Kützing) Rabenhorst 1853	B	-	brackish	-

8. Appendix - 8.1 Supplementary material to the manuscripts

Genus species Author Year	living	pH	salinity	trophy
<i>Halamphora subholsatica</i> (Krammer) Levkov 2009	B	-	brackish	-
<i>Halamphora subsalina</i> Levkov 2009	B	-	brackish	-
<i>Hannaea arcus</i> (Ehrenberg) R.M. Patrick 1966	B	8-9	fresh	oligo
<i>Hantzschia amphioxys</i> (Ehrenberg) Grunow 1880	B	7-8	fresh	eu
<i>Hippodonta capitata</i> (Ehrenberg) Lange-Bertalot, Metzeltin & Witkowski 1996	B	8-9	fresh	eu
<i>Hippodonta linearis</i> (Østrup) Lange-Bertalot, Metzeltin & Witkowski 1996	B	-	fresh	-
<i>Iconella tenera</i> (W. Gregory) Ruck & Nakov 2016	B	8-9	fresh	eu
<i>Karayevia clevei</i> (Grunow) Round & Bukhtiyarova 1999	B	8-9	fresh	eu
<i>Karayevia laterostrata</i> (Hustedt) Round & Bukhtiyarova 1999	B	-	fresh	-
<i>Lyrella atlantica</i> (Schmidt) D.G. Mann 1990	P	-	marine	-
<i>Martyana martyi</i> (Héribaud-Joseph) Round 1990	B	-	fresh	-
<i>Mastogloia elliptica</i> (C. Agardh) Cleve 1893	B	8-9	brackish	-
<i>Mastogloia pumila</i> (Grunow) Cleve 1985	B	8-9	brackish	-
<i>Mastogloia smithii</i> Thwaites ex W. Smith 1856	B	8-9	brackish	-
<i>Melosira arctica</i> Dickie 1852	P	8-9	marine	-
<i>Melosira undulata</i> (Ehrenberg) Kützing 1844	P	8-9	fresh	-
<i>Melosira varians</i> C. Agardh 1827	B	8-9	fresh	eu
<i>Meridion circulare</i> var. <i>constrictum</i> (Ralfs) van Heurck 1880	B	8-9	fresh	tolerant
<i>Navicula alpha</i> Cleve 1893	B	7-8	marine	-
<i>Navicula cryptocephala</i> Kützing 1844	B	7-8	fresh	tolerant
<i>Navicula cryptotenella</i> Lange-Bertalot 1985	B	8-9	fresh	tolerant
<i>Navicula directa</i> (W. Smith) Ralfs 1861	B	7-8	marine	-
<i>Navicula gregaria</i> Donkin 1861	B	8-9	brackish	eu
<i>Navicula lanceolata</i> Ehrenberg 1838	B	8-9	brackish	eu
<i>Navicula nipponica</i> (Skvortzov) Lange-Bertalot 1993	B	-	fresh	-
<i>Navicula notha</i> J.H. Wallace 1960	B	-	fresh	-
<i>Navicula oppugnata</i> Hustedt 1945	B	-	fresh	oligo
<i>Navicula perminuta</i> Grunow 1880	B	7-8	brackish	-
<i>Navicula radiosa</i> Kützing 1844	B	7-8	fresh	eu
<i>Navicula salinarum</i> Grunow 1880	B	7-8	marine	eu
<i>Navicula</i> sp. 1	B	-	-	-
<i>Navicula subconcentrica</i> Lange-Bertalot 2001	B	-	fresh	-
<i>Navicula subrostellata</i> Hustedt 1955	B	-	fresh	-
<i>Navicula vaneei</i> Lange-Bertalot 1998	B	-	brackish	-
<i>Navigeia decussis</i> (Østrup) Bukhtiyarova 2013	B	8-9	fresh	eu
<i>Neidium ampliatum</i> (Ehrenberg) Krammer 1985	B	-	fresh	-
<i>Nitzschia dissipata</i> (Kützing) Rabenhorst 1860	B	8-9	fresh	eu
<i>Nitzschia frustulum</i> (Kützing) Grunow 1880	B	7-8	brackish	eu
<i>Nitzschia lanceola</i> Grunow	B	7-8	marine	-
<i>Nitzschia palea</i> (Kützing) W. Smith 1856	B	7-8	fresh	hypereu
<i>Nitzschia paleacea</i> (Grunow) Grunow 1881	B	-	fresh	-
<i>Odontella aurita</i> (Lyngbye) C. Agardh 1832	P	8-9	marine	-
<i>Odontidium hyemale</i> (Roth) Kützing 1844	B	-	fresh	-
<i>Parlibellus crucicula</i> (W. Smith) Witkowski, Lange-Bertalot & Metzeltin 2000	B	7-8	marine	-

8. Appendix - 8.1 Supplementary material to the manuscripts

<i>Genus species</i> Author Year	living	pH	salinity	trophy
<i>Petronis marina</i> (Ralfs) D.G. Mann 1990	B	7-8	marine	-
<i>Pinnularia borealis</i> Ehrenberg 1843	B	7-8	fresh	eu
<i>Pinnularia elegans</i> (W. Smith) Krammer 1992	B	7-8	marine	-
<i>Pinnularia episcopalis</i> Cleve 1891	B	tolerant	fresh	tolerant
<i>Pinnularia mesolepta</i> (Ehrenberg) W. Smith 1853	B	8-9	fresh	-
<i>Pinnularia nobilis</i> (Ehrenberg) Ehrenberg 1843	B	<7	fresh	oligo
<i>Pinnularia oriunda</i> Krammer 1992	B	7-8	fresh	-
<i>Pinnularia similiformis</i> Krammer 1992	B	-	fresh	-
<i>Pinnularia sylvatica</i> Petersen	B	-	fresh	-
<i>Pinnularia viridis</i> (Nitzsch) Ehrenberg 1843	B	7-8	fresh	tolerant
<i>Pinnunavis yarrensensis</i> (Grunow) H. Okuno 1975	B	7-8	marine	-
<i>Placoneis clementis</i> (Grunow) E.J. Cox 1988	B	8-9	brackish	eu
<i>Placoneis clementis</i> var. <i>nipponica</i> (Skvortzov) T. Ohtsuka 2002	B	8-9	brackish	eu
<i>Placoneis placentula</i> (Ehrenberg) Mereschkowsky 1903	B	8-9	fresh	eu
<i>Placoneis undulata</i> (Østrup) Lange-Bertalot 2000	B	7-8	fresh	oligo
<i>Planothidium delicatulum</i> (Kützing) Round & Bukhtiyarova 1996	B	7-8	marine	-
<i>Planothidium joursacense</i> (Héribaud-Joseph) Lange-Bertalot 1999	B	8-9	fresh	oligo
<i>Planothidium lanceolatum</i> (Brébisson ex Kützing) Lange-Bertalot 1999	B	8-9	fresh	eu
<i>Planothidium rostratum</i> (Østrup) Lange-Bertalot 1999	B	-	fresh	oligo
<i>Pleurosigma elongatum</i> W. Smith 1852	B	-	brackish	-
<i>Psammodictyon panduriforme</i> (W. Gregory) D.G. Mann 1990	B	8-9	marine	-
<i>Pseudofallacia tenera</i> (Hustedt) Liu, Kociolek & Wang 2012	B	8-9	fresh	-
<i>Pseudostaurosira americana</i> E.A. Morales 2011	B	-	fresh	-
<i>Pseudostaurosira brevistriata</i> (Grunow) D.M. Williams & Round 1988	B	8-9	fresh	tolerant
<i>Pseudostaurosira elliptica</i> (Schumann) Edlund, Morales & Spaulding 2006	B	8-9	fresh	eu
<i>Rhabdonema arcuatum</i> (Lyngbye) Kützing 1844	B	-	marine	-
<i>Rhoicosphenia abbreviata</i> (C. Agardh) Lange-Bertalot 1980	B	8-9	fresh	eu
<i>Rhopalodia acuminata</i> Krammer 1987	B	-	brackish	-
<i>Rhopalodia brebissonii</i> Krammer 1987	B	8-9	fresh	-
<i>Rhopalodia gibba</i> (Ehrenberg) O. Müller 1895	B	8-9	fresh	eu
<i>Rossithidium anastasiae</i> (Kaczmarek) Potapova 2012	B	-	fresh	oligo
<i>Sellaphora laevis</i> (Kützing) D.G. Mann 1989	B	7-8	fresh	meso
<i>Sellaphora pupula</i> (Kützing) Mereschkovsky 1902	B	7-8	fresh	eu
<i>Seminavis robusta</i> D.B. Danielidis & D.G. Mann 2002	B	-	marine	-
<i>Stauroneis smithii</i> Grunow 1860	B	8-9	fresh	tolerant
<i>Staurophora brantii</i> L. Bahls 2012	B	8-9	brackish	meso
<i>Staurophora tackei</i> (Hustedt) L. Bahls 2012	B	-	fresh	-
<i>Staurosira construens</i> var. <i>binodis</i> (Ehrenberg) P.B. Hamilton 1992	B	8-9	fresh	eu
<i>Staurosirella pinnata</i> (Ehrenberg) D.M. Williams & Round 1988	B	8-9	brackish	tolerant
<i>Stephanodiscus hantzschii</i> Grunow 1880	P	8-9	fresh	hypereu
<i>Stephanopyxis</i> sp. 1	P	-	-	-
<i>Surirella fastuosa</i> (Ehrenberg) Ehrenberg 1843	B	-	brackish	-
<i>Surirella ovalis</i> Brébisson 1838	B	8-9	fresh	eu
<i>Tabellaria fenestrata</i> (Lyngbye) Kützing 1844	B	7-8	fresh	oligo

8. Appendix - 8.1 Supplementary material to the manuscripts

<i>Genus species</i> Author Year	living	pH	salinity	trophy
<i>Tabularia fasciculata</i> (C. Agardh) D.M. Williams & Round 1986	B	8-9	brackish	eu
<i>Thalassiosira allenii</i> Takano 1965	P	8-9	marine	-
<i>Thalassiosira angulata</i> (W. Gregory) Hasle 1978	P	8-9	marine	-
<i>Thalassiosira ferelineata</i> Hasle & G.A. Fryxell 1977	P	8-9	marine	-
<i>Trigonium</i> sp. 1	P	-	marine	-
<i>Tryblionella apiculata</i> W. Gregory 1857	B	7-8	marine	tolerant
<i>Tryblionella compressa</i> (J.W. Bailey) Poulin 1990	B	7-8	marine	-
<i>Tryblionella granulata</i> (Grunow) D.G. Mann 1990	B	7-8	marine	-
<i>Tryblionella persuadens</i> (Cholnoki) K.P. Cavalcante, P.I. Tremarin & T.A.V. Ludwig 2013	B	7-8	marine	-
<i>Tryblionella salinarum</i> (Grunow) Pelletan 1889	B	7-8	marine	eu
<i>Tryblionella scalaris</i> (Ehrenberg) Siver & P.B. Hamilton 2005	B	7-8	marine	-
<i>Ulnaria capitata</i> (Ehrenberg) Compère 2001	B	-	fresh	tolerant
<i>Ulnaria ulna</i> (Nitzsch) Compère 2001	B	8-9	fresh	eu

8. Appendix - 8.1 Supplementary material to the manuscripts

8.1.3 Diatom Taxa list of modern Lake Kushu

The diatom taxa list with the corresponding autecology regarding mode of living, pH, salinity and trophic is given in table 8.3. The percentage abundances are available in the Open Access information system PANGAEA via the Digital Object Identifier (doi): <https://doi.pangaea.de/10.1594/PANGAEA.8897788>.

Table 8.3: Diatom taxa list of Lake Palaeo-Makgadikgadi samples with the corresponding autecology: B = benthic, P = planktonic, fresh = freshwater, oligo = oligotraphentic, meso = mesotraphentic, eu = eutraphentic, hypereu = hypereutraphentic.

<i>Genus species</i>	Author	Year	living	pH	salinity	trophy
<i>Achnantheidium exiguum</i>	(Grunow) Czarnecki	1994	B	8-9	fresh	tolerant
<i>Achnantheidium minutissimum</i>	(Kützing) Czarnecki	1994	B	7-8	fresh	tolerant
<i>Amphora copulata</i>	(Kützing) Schoeman & R.E.M. Archibald	1986	B	8-9	fresh	eu
<i>Amphora inariensis</i>	Krammer	1980	B	-	fresh	oligo
<i>Amphora indistincta</i>	Levkov	2009	B	-	fresh	oligo
<i>Aneumastus tuscula</i>	(Ehrenberg) D.G. Mann & Stickle	1990	B	-	fresh	-
<i>Aulacoseira ambigua</i>	(Grunow) Simonsen	1979	P	8-9	fresh	meso
<i>Aulacoseira granulata</i>	(Ehrenberg) Simonsen	1979	P	8-9	fresh	eu
<i>Aulacoseira islandica</i>	(O. Müller) Simonsen	1979	P	7-8	fresh	tolerant
<i>Belonastrum berlinense</i>	(Lemmermann) Round & Maidana	2001	B	-	fresh	eu
<i>Caloneis limosa</i>	(Kützing) R.M. Patrick	1860	B	8-9	fresh	meso
<i>Cavinula vincentii</i>	(W. Smith) Lange-Bertalot	2008	B	8-9	fresh	oligo
<i>Cocconeis neothumensis</i>	Krammer	1990	B	8-9	fresh	-
<i>Cocconeis pediculus</i>	Ehrenberg	1838	B	8-9	brackish	eu
<i>Cocconeis placentula</i>	Ehrenberg	1838	B	8-9	fresh	eu
<i>Cyclotella choctawhatcheeana</i>	Prasad	1990	P	-	marine	tolerant
<i>Cyclotella meneghiniana</i>	Kützing	1844	P	8-9	fresh	eu
<i>Cymatopleura solea</i>	(Brébisson) W. Smith	1851	B	-	fresh	eu
<i>Cymbella amoyensis</i>	M. Voigt		B	8-9	fresh	-
<i>Cymbella cistula</i>	(Ehrenberg) O. Kirchner	1878	B	8-9	fresh	eu
<i>Diatoma mesodon</i>	(Ehrenberg) Kützing	1844	B	8-9	fresh	meso
<i>Diatoma tenuis</i>	C. Agardh	1812	P	8-9	fresh	eu
<i>Diploneis ovalis</i>	(Hilse) Cleve	1891	B	8-9	fresh	-
<i>Diploneis subovalis</i>	Cleve	1894	B	-	fresh	-
<i>Discostella pseudostelligera</i>	(Hustedt) Houk & Klee	2004	P	7-8	fresh	eu
<i>Discostella stelligera</i>	(Cleve & Grunow) Houk & Klee	2004	P	-	fresh	-
<i>Ellerbeckia arenaria</i>	(G. Moore ex Ralfs) R.M. Crawford	1988	B	-	fresh	-
<i>Encyonema caespitosum</i>	Kützing	1849	B	-	fresh	eu
<i>Encyonema silesiacum</i>	(Bleisch) D.G. Mann	1990	B	-	fresh	oligo
<i>Epithemia adnata</i>	(Kützing) Brébisson	1838	B	8-9	fresh	eu
<i>Epithemia sores</i>	Kützing	1844	B	8-9	fresh	eu
<i>Epithemia turgida</i>	(Ehrenberg) Kützing	1844	B	8-9	fresh	eu
<i>Eunotia bilunaris</i>	(Ehrenberg) Schaarschmidt	1880	B	tolerant	fresh	tolerant
<i>Eunotia diodon</i>	Ehrenberg	1837	B	<7	fresh	oligo
<i>Eunotia incisa</i>	W. Smith ex W. Gregory	1854	B	<7	fresh	oligo

8. Appendix - 8.1 Supplementary material to the manuscripts

Genus species Author Year	living	pH	salinity	trophy
<i>Fallocia insociabilis</i> (Krasske) D.G. Mann 1990	B	7-8	fresh	meso
<i>Fragilaria construens</i> (Ehrenberg) Grunow 1862	B	8-9	fresh	eu
<i>Fragilaria vaucheriae</i> (Kützing) J.B. Petersen 1938	B	8-9	fresh	eu
<i>Frustulia vulgaris</i> (Thwaites) De Toni 1891	B	8-9	fresh	eu
<i>Gomphoneis tetrastigmatum</i> Horikawa & Okuno 1944	B	-	fresh	-
<i>Gomphonema acuminatum</i> Ehrenberg 1832	B	8-9	fresh	eu
<i>Gomphonema acuminatum</i> var. <i>brebissonii</i> (Kützing) Grunow 1880	B	7-8	fresh	-
<i>Gomphonema augur</i> Ehrenberg 1841	B	8-9	fresh	eu
<i>Gomphonema gracile</i> Ehrenberg 1838	B	7-8	fresh	meso
<i>Gomphonema grovei</i> var. <i>lingulatum</i> (Hustedt) Lange-Bertalot 1985	B	-	fresh	meso
<i>Gomphonema parvulum</i> (Kützing) Kützing 1849	B	7-8	fresh	eu
<i>Gomphonema truncatum</i> Ehrenberg 1832	B	8-9	fresh	eu
<i>Hippodonta capitata</i> (Ehrenberg) Lange-Bertalot, Metzeltin & Witkowski 1996	B	8-9	fresh	eu
<i>Karayevia clevei</i> (Grunow) Round & Bukhtiyarova 1999	B	8-9	fresh	eu
<i>Melosira varians</i> C. Agardh 1827	B	8-9	fresh	eu
<i>Meridion circulare</i> var. <i>constrictum</i> (Ralfs) van Heurck 1880	B	8-9	fresh	tolerant
<i>Navicula gregaria</i> Donkin 1861	B	8-9	brackish	eu
<i>Navicula lanceolata</i> Ehrenberg 1838	B	8-9	brackish	eu
<i>Navicula nipponica</i> (Skvortzov) Lange-Bertalot 1993	B	-	fresh	-
<i>Navicula notha</i> J.H. Wallace 1960	B	-	fresh	-
<i>Navicula oppugnata</i> Hustedt 1945	B	-	fresh	oligo
<i>Navicula radiosa</i> Kützing 1844	B	7-8	fresh	eu
<i>Navicula</i> sp. 2	-	-	-	-
<i>Navicula vaneei</i> Lange-Bertalot 1998	B	-	brackish	-
<i>Navigeia decussis</i> (Østrup) Bukhtiyarova 2013	B	8-9	fresh	eu
<i>Navigeia ignota</i> (Krasske) Bukhtiyarova 2013	B	7-8	fresh	-
<i>Neidium ampliatum</i> (Ehrenberg) Krammer 1985	B	-	fresh	-
<i>Nitzschia dissipata</i> (Kützing) Rabenhorst 1860	B	8-9	fresh	eu
<i>Nitzschia frustulum</i> (Kützing) Grunow 1880	B	7-8	brackish	eu
<i>Nitzschia palea</i> (Kützing) W. Smith 1856	B	7-8	fresh	hypereu
<i>Nitzschia paleacea</i> (Grunow) Grunow 1881	B	-	fresh	-
<i>Pinnularia nobilis</i> (Ehrenberg) Ehrenberg 1843	B	<7	fresh	oligo
<i>Pinnularia similiformis</i> Krammer 1992	B	-	fresh	-
<i>Planothidium delicatulum</i> (Kützing) Round & Bukhtiyarova 1996	B	7-8	marine	-
<i>Planothidium joursacense</i> (Héribaud-Joseph) Lange-Bertalot 1999	B	8-9	fresh	oligo
<i>Planothidium lanceolatum</i> (Brébisson ex Kützing) Lange-Bertalot 1999	B	8-9	fresh	eu
<i>Planothidium rostratum</i> (Østrup) Lange-Bertalot 1999	B	-	fresh	oligo
<i>Platessa bahlsii</i> M. Potapova 2012	B	-	-	-
<i>Pseudostaurosira brevistriata</i> (Grunow) D.M. Williams & Round 1988	B	8-9	fresh	tolerant
<i>Rhoicosphenia abbreviata</i> (C. Agardh) Lange-Bertalot 1980	B	8-9	fresh	eu
<i>Rhopalodia gibba</i> (Ehrenberg) O. Müller 1985	B	8-9	fresh	eu
<i>Sellaphora laevisissima</i> (Kützing) D.G. Mann 1989	B	7-8	fresh	meso
<i>Sellaphora pupula</i> (Kützing) Mereschkovsky 1902	B	7-8	fresh	eu
<i>Staurosira construens</i> var. <i>binodis</i> (Ehrenberg) P.B. Hamilton 1992	B	8-9	fresh	eu

8. Appendix - 8.1 Supplementary material to the manuscripts

<i>Genus species</i> Author Year	living	pH	salinity	trophy
<i>Staurosirella pinnata</i> (Ehrenberg) D.M. Williams & Round 1988	B	8-9	brackish	tolerant
<i>Stephanodiscus hantzschii</i> Grunow 188ß	P	8-9	fresh	hypereu
<i>Surirella brébissonii</i> Krammer & Lange-Bertalot 1987	B	8-9	brackish	-
<i>Synedra</i> sp. 2	-	-	-	-
<i>Tabellaria fenestrata</i> (Lyngbye) Kützing 1844	B	7-8	fresh	oligo
<i>Tabularia fasciculata</i> (C. Agardh) D.M. Williams & Round 1986	B	8-9	brackish	eu
<i>Tryblionella littoralis</i> (Grunow) D.G. Mann 1990	B	-	marine	-
<i>Ulnaria delicatissima</i> (W. Smith) Aboal & P.C. Silva 2004	B	7-8	fresh	meso

8.2 List of publications

Journal articles:

Leipe, C., Müller, S., Hille, K., Kato, H., Kobe, F., Schmidt, M., Seyffert, K., Spengler, R., Wagner, M. & Tarasov, P.E., 2018. Vegetation change and human impacts on Rebun Island (Northwest Pacific) over the last 6000 years. *QUATERNARY SCIENCE REVIEWS* (accepted)

Schmidt, M., Becker, F., Hoelzmann, P., Leipe, C., Mingram, J., Müller, S., Tjallingii, R., Tarasov, P.E., 2018. A multi-proxy palaeolimnological record of the last ca. 16,600 years from coastal Lake Kushu in northern Japan. Ready for submission to *PALEOGEOGRAPHY PALEOCLIMATOLOGY PALEOECOLOGY*.

Müller, S., Schmidt, M., Kossler, A., Leipe, C., Irino, T., Yamamoto, M., Yonenobu, H., Goslar, T., Kato, H., Wagner, M., Weber, A.W. & Tarasov, P.E., 2016. Palaeobotanical records from Rebun Island and their potential for improving the chronological control and understanding human–environment interactions in the Hokkaido Region, Japan. *THE HOLOCENE* 26 (10): 1646-1660.

Schmidt, M., Tarasov, P.E., Hoelzmann, P., Meyer, H. & Leipe, C., 2016. Diatoms from Lake Kushu: A pilot study to test the potential of a Late Quaternary palaeoenvironmental archive from Rebun Island (Hokkaido Region, Japan). *JOURNAL OF ASIAN EARTH SCIENCES* 122: 106–122.

Schmidt, M., Fuchs, M., Henderson, A.C.G., Kossler, A., Melanie J. Leng, M.J., Mackay A.W., Shemang, E. & Riedel, F., 2017. Paleolimnological features of a mega-lake phase in the Makgadikgadi Basin (Kalahari, Botswana) during Marine Isotope Stage 5 inferred from diatoms. *JOURNAL OF PALEOLIMNOLOGY* 58 (3): 373-390.

Abstracts for Conference Presentations:

Schmidt, M., Tarasov, P.E., Hoelzmann, P., Meyer, H., 2015. A brief history of Lake Kushu throughout the Holocene. IPS2015; 13th International Paleolimnology Symposium, Lanzhou.

Schmidt, M., Tarasov, P., Hoelzmann, P., Meyer, H., 2015. Modern diatom assemblage from Rebun and Rishiri islands and its potential for interpretation of the high-resolution environmental archive of the last 17 kyr from Lake Kushu, Hokkaido Region, Japan. 9th Central European Diatom Meeting, Bremerhaven.

Hartmann, K., Riedel, F., Schmidt, M., Zhang, S., Shemang, E., 2014. Neotectonic formation of drainage patterns and their palaeohydrological implications for the Okwa River catchment, Botswana. European Geosciences Union, Vienna.

8. Appendix - 8.2 List of publications

Riedel, F., Fuchs, M., Henderson, A., Kossler, A., Leipe, C., Schmidt, M., Taft, L., 2012. Evolution of the mega-lake Palaeo-Makgadikgadi (Kalahari, Botswana) during the last 100 ka. Speciation in Ancient Lakes (SIAL) – 6, Bogor.

Schmidt, M., Kossler, A., Henderson, A.C.G., Shemang, E., Fuchs, M., Riedel, F., 2012. Late Pleistocene palaeolimnology of the megalake Palaeo-Makgadikgadi (Kalahari, Botswana) inferred from diatom assemblages, Centenary Meeting of the Paläontologische Gesellschaft, Berlin.

Schmidt, M., Henderson, A.C.G., Kossler, A., Fuchs, M., Shemang, E., Riedel, F., 2012. Diatom evidence for a MIS 5 mega lake highstand in the Kalahari (Botswana), IPS2012; 12th International Paleolimnology Symposium, Glasgow.

8.3 Curriculum Vitae

Due to data protection regulations, the curriculum vitae is not included in the online version of this doctoral thesis.

Due to data protection regulations, the curriculum vitae is not included in the online version of this doctoral thesis.

8.4 Declaration of Originality

Berlin, June 2018

Hereby I declare that I wrote this doctoral thesis by myself without sources other than those indicated in the text and related reference list. The work has not been previously submitted to the Freie Universität Berlin or any other university.

Mareike Schmidt